Title
REACTIONS OF FAST CARBON NUCLEI IN PHOTOGRAPHIC EMULSIONS

Author
Miller, James Fuller.

Publication Date
1952-07-01

6-618

UCRL- 1902

UNCLASSIFIED

R. Pyle
c. 2

UNIVERSITY OF CALIFORNIA — BERKELEY

RADIATION LABORATORY

DISCLAIMER

UCRL-1902
Unclassified-Physics Distribution

UNIVERSITY OF CALIFORNIA

Radiation Laboratory

Contract No. W-7405-eng-48

REACTIONS OF FAST CARBON NUCLEI IN PHOTOGRAPHIC EMULSIONS

James Fuller Miller

(Thesis)

July 1952

Berkeley, California

TABLE OF CONTENTS

PHOTOGRAPHS AND DRAWINGS

ABSTRACT

A study has been made of reactions produced in nuclear emulsions by the 112 Mev carbon^{12} and the 121 Mev carbon^{13} beams from the sixty-inch cyclotron at Crocker Laboratory of the University of California, Berkeley. The properties and expected behavior of carbon nuclei as bombarding particles are discussed in the light of the reactions observed.

An analysis is made of the salient features, both general and special, of 865 stars produced by 1,390,000 carbon^{12} ions and of 1114 stars produced by 1,845,540 carbon^{13} ions. The comparative reaction cross sections are discussed in some detail. The cross section is calculated for the total range as given by any initial energy and also for the differential range, as a function of the instantaneous energy. A further break-down is made for the cross section as it depends on the number of prongs. Three- and four-prong star cross sections are higher for carbon^{12} than for carbon^{13} and exhibit a detailed structure. Analysis shows the structure arises from impact disintegration and stripping of the carbon nucleus; these reactions account for the carbon^{12} ion having a larger cross section than the carbon^{13} ion has - 0.446 barns for 110 Mev carbon^{12} compared to 0.388 barns for 120 Mev carbon^{13}. The instantaneous cross section of carbon nuclei nearly equals the available geometric cross section for inelastic reactions until neutron evaporation events from silver and bromine reduce the number of charged particle stars.

The outstanding special type of reaction found is the impact disintegration

of the carbon nucleus into three alpha particles and the closely related stripping and capture of an alpha particle from the carbon nucleus by the target nucleus. These reactions are explicable on the basis of the modern alpha particle model of the carbon nucleus, the low energy required to break up the carbon nucleus, especially carbon^{12}, and the short de Broglie wave length of the carbon particle which permits a collision to be concentrated on a single alpha particle. A number of impact disintegration and strippings are analyzed in detail to bring out the interesting features of the reaction. Observations are made regarding beryllium^{8}, one of the fragments in the reaction before it breaks into two alpha particles.

Fission produced by carbon^{13} ions in bismuth-impregnated emulsions is discussed. Nine fission events were found from 1,702,600 tracks. The indicated cross section for fission is half the available reaction cross section.

Range-energy data for carbon ions have been obtained. Above 40 Mev, carbon and alpha particles are directly compared by passing them through slits. Below 40 Mev, data are obtained from knock-on protons. Comparisons are made of carbon ions with fission fragments and with light particles.

CHAPTER I

INTRODUCTION

The research described in this report had as its purpose a probing, both qualitative and quantitative, into the properties of 112 Mev C^{12} and 121 Mev C^{13} nuclei accelerated in the 60-inch Cyclotron at the Crocker Laboratory of the University of California. The deflected external beam was used in order to obtain a beam homogeneous in energy, and nuclear emulsions were employed to record the particle tracks. The use of nuclear emulsions permitted a detailed study of the nuclear reactions in which the carbon nuclei took part and of accurate registration of a range-energy curve. Emulsions have the advantage of integrating the beam so that beams too small for effective use by other techniques may be entirely adequate, and at the same time both individual and statistical data may be obtained, as contrasted to the usual statistical results. The external beam of $C^{12(6+)}$ ions is of the order of 10^6 particles per second, and the $C^{13(6+)}$ beam is about one-sixth as much when the gas used in the ion source is CO_2 with the carbon fraction enriched to 52.5 percent C^{13}.

Because of the limited beam current, the study and use of the carbon beam has been delayed far beyond what would be expected from the interest in it. Carbon nuclei were first accelerated in the cyclotron by Alvarez[1] in 1940. Subsequent work was interrupted by the war, after completion of

---

1. L. W. Alvarez, Phys. Rev. 58, 192 (1940).

research projects with the carbon beam by Tobias[2] and Condit.[3] After the war, attention was centered on obtaining a higher and more consistent beam, with special attention to development of an efficient ion source.[4] Although significant facts were uncovered, no single large step was made in increasing the beam current. The greatest single increase was at the end of 1951 when G. B. Rossi made an uncooled ion source out of graphite, exposed to the cyclotron radio-frequency field, and improved the beam by a factor of ten, bringing it to 10^6 $C^{12(6+)}$ per second externally, still too low for external bombardments.

After the development of a probe target mechanism for the 60-inch cyclotron in 1949, J. G. Hamilton proposed test bombardments of aluminum and gold with carbon ions in the internal beam to see if it were enough higher than the external beam to produce detectable activity. Internal to deflected ratios of about ten to one had been found with alpha particles, deuterons and protons. The first bombardment was in May, 1950. The results were surprising.[5] The reactions proposed to look for were $Al^{27}(C^{12}; \alpha, n)$ $Cl^{34}(\beta^+, 33$ min) and $Au^{197}(C^{12}; xn)$At (alpha decay). These were found in a quantity that indicated an internal beam 10^3 or 10^4 times higher than the external beam. The reason for the high ratio was found to be that the

---

2. C. A. Tobias, Ph.D. thesis, University of California, Berkeley (1942), Phys. Rev. 70, 89 (1946) and UCRL Report 1039 (1950).

3. R. I. Condit, Ph.D. thesis, University of California, Berkeley (1942) and Phys. Rev. 62, 301 (1942).

4. H. York, R. H. Hildebrand, T. M. Putnam and J. G. Hamilton, Phys. Rev. 70, 446 (1946).

5. J. F. Miller, J. G. Hamilton, T. M. Putnam, H. R. Haymond and G. B. Rossi, Phys. Rev. 80, 486 (1950).

carbon ions have a multitude of different orbits that require different magnet currents in order to be resonated to enter the deflector channel. There also exists an exponentially increasing beam, in the direction of lower energies, of carbon ions that would be unable to pass down the deflector channel at any magnet setting.

The internal beam has been developed, principally by A. Ghiorso and G. B. Rossi, into a useful tool for bombardments. A current measuring probe has permitted evaluation of the nature of the beam and of parameters that affect it. However, the great inhomogeneity of the internal beam has made precise experiments often impossible. In order to gain more definite information as to some properties of carbon ions, the external beam of homogeneous energy must be studied. The present study is for the purpose of considering such details as can be learned from nuclear emulsions.

There is a wide assortment of features that make carbon nuclei of interest as bombarding particles. Perhaps the most obvious is that, in one hit on a nucleus, there will be added twelve or thirteen nucleons. Naturally, then, any program to develop further transuranic elements would find carbon nuclei of interest.[6] The work with carbon ions by A. Ghiorso for the Chemistry Group of the University of California Radiation Laboratory has been primarily for this purpose. However, carbon nuclei, although they carry many nucleons into a reaction, carry too few neutrons to follow along the "Heisenberg valley" in any but the lighter-element portion of the nuclide chart. With the high excitation they produce, which will cause evaporation of more neutrons, they can be expected to produce

---

6. A. Ghiorso, S. G. Thompson, K. Street, and G. T. Seaborg, Phys. Rev. 81, 154 (1951).

fission, a process in strong or possibly prohibitive competition in producing transcalifornium elements.[7] The present study using emulsions has included some evaluation of the fission process, both in bismuth impregnated in emulsions, and in the elements normally present in the emulsion.

The ability of carbon nuclei to produce highly neutron deficient isotopes may be of positive interest in other regions, though it is of negative interest in the transuranic. For instance, the shell model of the nucleus predicts high stability of nuclides with closed proton or neutron shells according to the "magic numbers" 2,8,20,50,82 and 126. An isotope falling into a closed shell should accordingly have a greater release of energy than in the normal processes. On these premises, carbon nuclei should be efficient in producing radioactive alpha emitters falling into the 82 neutron shell. Such has been found to be the case by the Chemistry Group.[8] A similar possibility for an alpha active product in the region of the 50 neutron closed shell was considered. Apart from the present program, the writer made probe bombardments of zirconium, molybdenum, and niobium foils which were placed in scintillation and ionization chamber counters. Apparently positive results were invalidated by finding both types of counters would give counts from the intense beta-gamma activity of the neutron deficient isotopes produced by carbon ion bombardment. Later more refined and extensive experiments by R. W. Hoff and D. F. Martin of the Chemistry Group produced the same negative, but inconclusive, results. The use of

---

7. J. M. Hollander, UCRL Report 1396, July 1951.

8. J. O. Rasmussen, UCRL-1473 Rev. (Dec. 1951).

emulsions to see if alphas come from such foils has not been made but might be appropriate. In the case of reactions which might end in the 50 proton closed shell, the research described herein gives some fairly definite evidence.

Most of the questions on which evidence is sought in this emulsion study are of a general nature regarding the compound nucleus. For it is concerning the compound nucleus that almost all the visual information applies; the beta-gamma radioactivity of the product nucleus is not seen. We seek information on whether the reaction cross section using carbon nuclei is significantly higher or lower than with other bombarding particles and how the distribution of prongs in number and direction compares. Will the flow of a considerable number of nucleons at one moment into a nucleus produce any unusual features or increase the "sticking probability" in forming a compound nucleus? Will the processes in the compound nucleus be affected by the spatial correlation existing among the entering nucleons? Will the high angular momentum brought into an off-center collision by a carbon nucleus decrease the cross section for formation of a compound nucleus far below the geometric cross section? How will high angular momentum in a compound nucleus affect the particles it evaporates? Not all of these questions may find definite answers, especially if one effect tends to balance another. However, pieces of evidence can be expected regarding the model for the nucleus - the shell structure, statistical Fermi gas, liquid drop and alpha particle models.

Aside from statistical data and qualitative observations on the general nature of carbon-induced reactions, it is interesting to look for special types of reactions. It was a surprise not to find the anticipated

"hammer tracks" that would come from Li^8 (or B^8) ejected by the compound nucleus. A look-out was also kept for delayed proton or alpha emission from the product nucleus. The evidence in this respect is not conclusive.

The outstanding special reaction that showed up unmistakably and in striking quantity was the impact disintegration of the carbon nucleus into an alpha and Be^8, and the closely related stripping and capture of an alpha from the carbon nucleus, leaving Be^8. The evidence from these processes will be discussed in some detail in Chapter V.

Since a C^{13} beam was available, it was used as a foil with which to compare the C^{12} bombardments of emulsions. The differences, where they occur, are interesting. In impact disintegration and stripping, for example, one would expect rather different behavior from C^{12} and C^{13}.

In order to evaluate some of the data, it has been necessary to obtain a range-energy curve for carbon nuclei in emulsions. However, the data for such a curve are of interest in their own right, for the information they give and the considerations they involve regarding the mechanism of slowing down and stopping of the carbon ion. For instance, the nuclear collisions near the end of the carbon range could be important in a study of radiation damage. The type of Bragg ionization curve that should be produced by carbon ions is of interest to medical physics in studying the effect on cells of the ionization produced by heavy nuclei. A group under C. A. Tobias is currently engaged in such research with the external carbon beam.

CHAPTER II

EXPERIMENTAL CONDITIONS

In order to understand the limitations on the carbon beam, both as to size and homogeneity in energy, some background information might be pertinent concerning it.

Just how the completely stripped carbon nuclei are produced is unknown. The ionization potentials of the individual electrons in the carbon atom are:[9]

I	11.264 volts
II	24.376 volts
III	47.864 volts
IV	64.476 volts
V	391.986 volts
VI	489.84 volts

However, the potential drop across the arc in the ion source as shown by meters rarely exceeds 300 volts and may be as low as 200 volts. In comparison, when helium atoms are being stripped in the ion source, it is found that 250 to 300 volts is optimum, as would be expected in order to have about five times the ionization potential of the last electron to be stripped. A suggestion in the case of carbon is that plasma oscillations may supply the extra voltage needed by electrons to strip the last two electrons from the carbon. However, this speculation is belied, at least as any considerable mechanism, by good evidence that the carbon particles do not come from a line source (the ion source) but from the neighborhood around the ion source. Even before the internal beam was explored, there was

---

9. Atomic Energy Levels, Vol. I, Sec. I, Circular 467, Nat. Bur. Stds. (1949).

clear evidence as to the non-localized origin of the carbon beam. Since the 60-inch cyclotron is of fixed frequency and the magnetic field for resonance is $B = \frac{M}{Ze}\omega$, we should have $\frac{B_{C12(6+)}}{B_{He4(2+)}} = \frac{2.000096}{2.001396}$, using M/Z values for stripped nuclei derived from Mattauch and Flammersfeld's tables.[10] A magnetization curve for the 60-inch cyclotron shows that at alpha resonance (magnet field current = 290.45 amperes and magnet field at center = 15,279 oersteds, Jan. 10, 1952), dB/dI = 29.3 oersteds per ampere. These values imply that $C^{12(6+)}$ resonance should lie about 0.33 amperes below alpha resonance. Figure 1 shows an experimental resonance curve obtained from the set-up shown in Figs. 2, 3 and 4, using an ionization chamber connected through a pulse height discriminator to a counting rate meter. A single slit was used, open 0.15 inches at the cyclotron snout, to pass the full width of the resonance curve. The curve is suggestive rather than absolute since conditions may change with the cyclotron parameters such as the oscillator power used. The curve is so wide that it overlaps alphas, which, even though they are from residual helium in the tank and likely come principally from outside the ion cone, give quite a sharp resonance. In the tracks picked up on photographic plates there is further evidence of low carbon energies, spreading down to zero, and of their off-center orbits, unless proper precautions are taken to exclude them. These particles emerge from the gap between the dees (see Fig. 2) as shown by the fact that they persist when the deflector is turned down and that they can be cut out by a suitable blocking probe.

---

10. J. Mattauch and A. Flammersfeld: Isotopic Report. (1949) Tübingen.

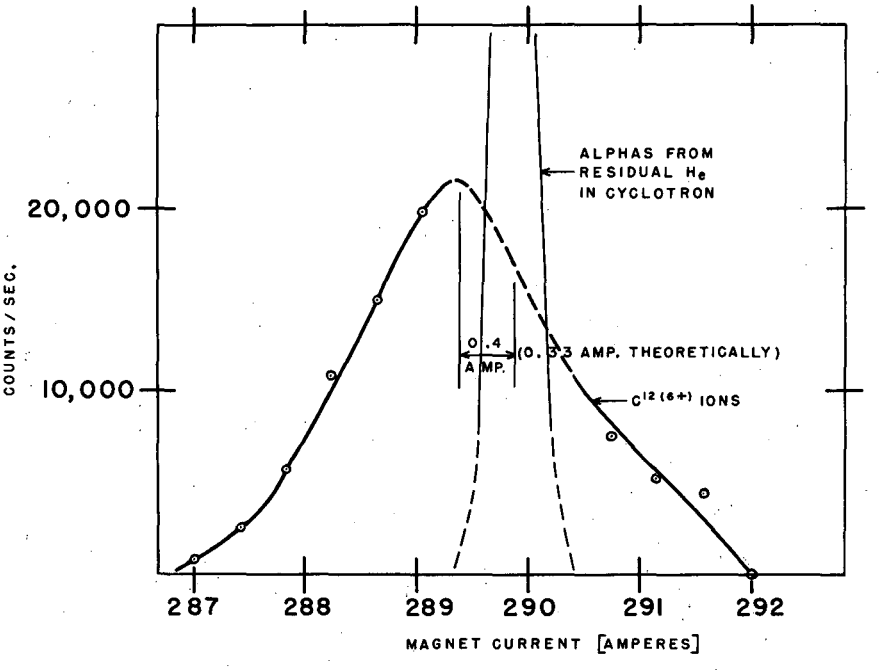

RESONANCE CURVE FOR EXTERNAL CARBON ION BEAM THROUGH ONE SLIT OPEN .15 INCHES

FIGURE I

MU 3794

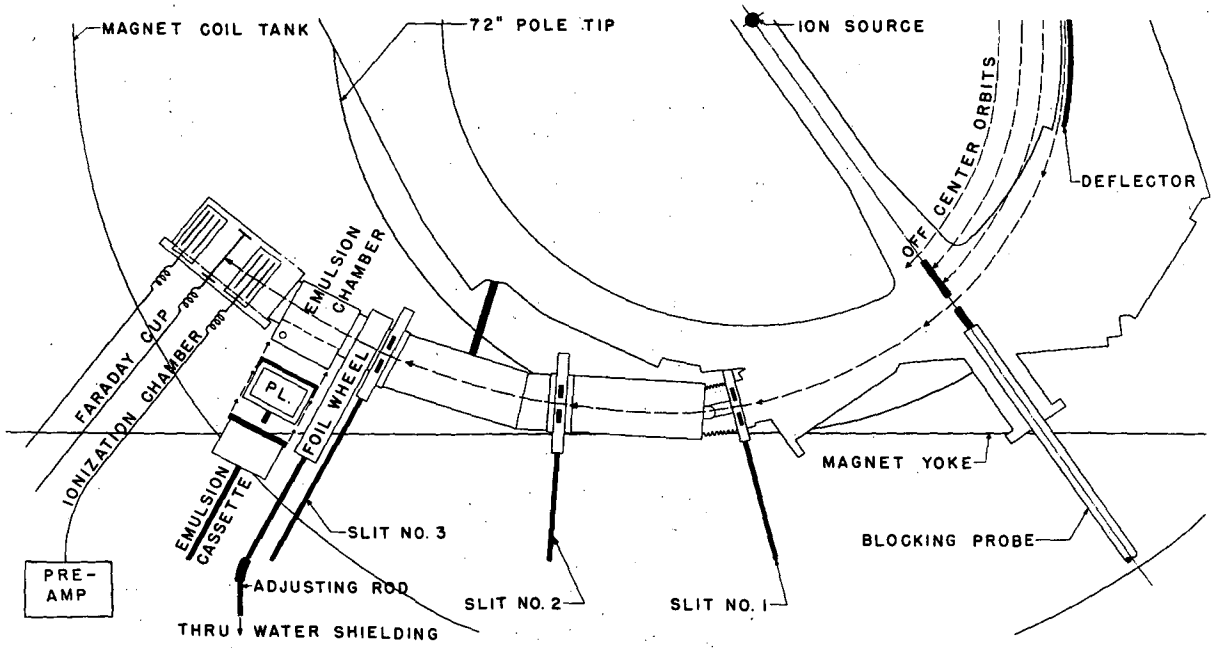

BEAM DETECTION AND PLATE EXPOSURE APPARATUS — FIGURE 2

FIGURE 3.

BEAM DETECTION AND EMULSION EXPOSURE APPARATUS

The beam enters through No. 1 slit at the right; No. 2 slit was inserted after this photograph was taken, near the weld seam; No. 3 slit is hidden by the foil wheel. The plate exposure chamber is to the left of the foil wheel, followed by the beam detection apparatus. In the foreground is the electrometer tube, at the end of a vacuum coaxial line.

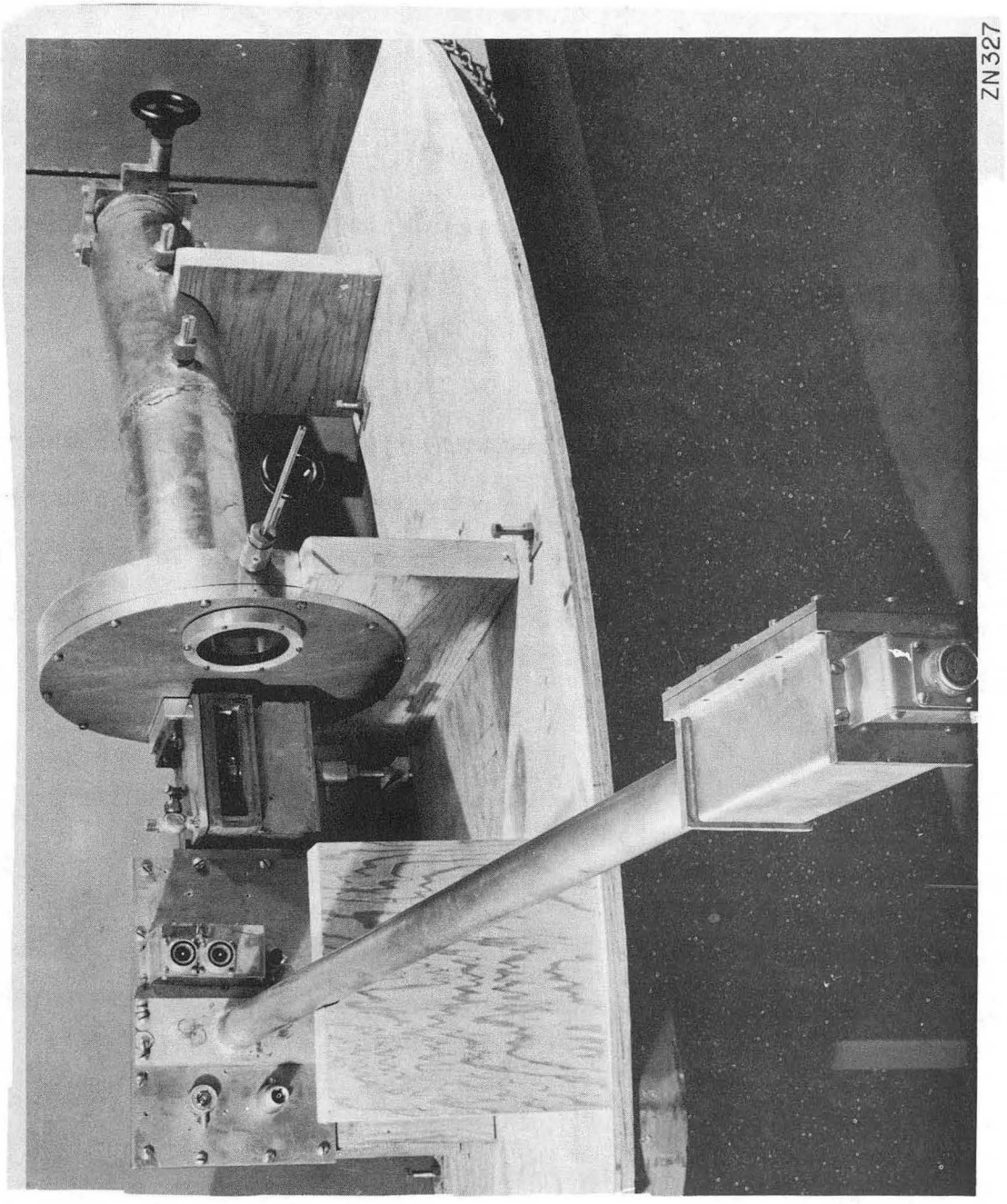

FIGURE 3

FIGURE 4.

BEAM DETECTION APPARATUS

The two ionization chambers are of drum type. Between them is the Faraday cup for collecting the carbon ion charge in vacuum.

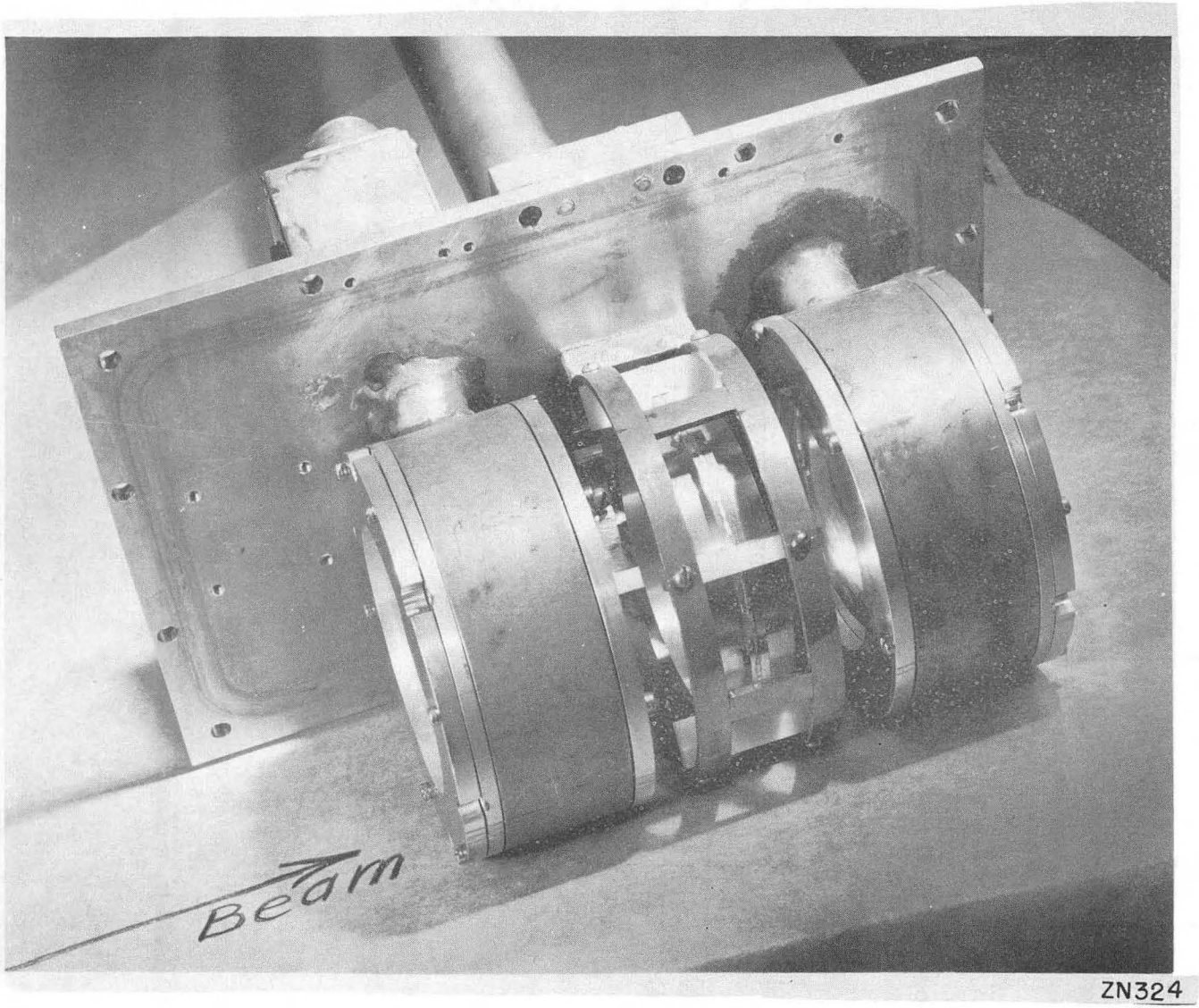

FIGURE 4

Two principal suggestions have been made to account for stripping outside the ion source. One is that the stripping is by a sheet of vertically oscillating electrons trapped in a potential well formed between the dees and an off-center ion source during each half cycle of the oscillator. The energies given these electrons can amount to a considerable fraction of the dee voltage. Such an electron sheet has been discussed by R. R. Wilson.[11] The other suggestion, by E. M. McMillan, is based on the fact that stripping can be produced by atomic collisions if once the velocity of the ions can be brought to match the "orbital" velocity of the electron to be stripped. The mechanism to achieve such a velocity for incompletely ionized carbon atoms is present. $C^{(2+)}$ can be resonance-accelerated with the cyclotron frequency the third harmonic of the ion's orbital frequency. Harmonic acceleration was noted by Lawrence and Livingston in 1932.[12] Orbital frequency, $\nu_{orbit} = \frac{1}{2\pi}\frac{q}{M} B$ where q is the ion charge. If q/M or B, or both, are adjusted so that the cyclotron frequency is an odd multiple of ion frequency, the ion will cross the dee gaps each revolution at the proper instant. Using his current measuring probe, A. Ghiorso has shown the presence of a beam of $C^{12(2+)}$ greater than 100 microamperes at the 23 inch radius. This beam, unlike the $C^{(6+)}$ beam, is sharply defined. Indeed the heating from it is a serious problem in probe bombardment. $C^{(2+)}$ will have one-ninth the energy of $C^{(6+)}$ when they are at the same radius. Hence, the energy at 25 inches would be about 12.5 Mev, while the velocity of the sixth electron corresponds to a C^{12} energy of 10.73 Mev. McMillan

---

11. R. R. Wilson, Phys. Rev. 56, 459 (1939).

12. E. O. Lawrence and M. S. Livingston, Phys. Rev. 40, 24 (1932).

suggests that the $C^{(2+)}$ ions may lose one or more electrons in collision either with gas atoms in the tank or with ions being circulated by the cyclotron. In the new state of ionization, the orbital radius of curvature will be different and the ion will not be in synchronism with the cyclotron frequency, unless it was completely stripped. Accordingly, as it crosses the dee gaps in its off-center orbit, it will sometimes be accelerated, sometimes decelerated. Its orbit will precess. Finally, it will undergo another collision. If the collision is with a beam particle, further ionization will be achieved more easily than if the collision is with a gas atom. Finally, $C^{(6+)}$ will be formed and, if its phase is correct, it will be accelerated by the cyclotron. Ghiorso has shown that the $C^{(2+)}$ beam can be reduced by increasing the tank pressure, but he has not been able to utilize the process to increase the $C^{(6+)}$ beam. It is interesting to notice that the external carbon beam, although it is very broad, is situated where it should be with respect to alphas. However, the internal carbon beam found by Ghiorso and Hollander (ref. 7, Fig. 2) is about four amperes below the alpha peak and the sharp $C^{(2+)}$ resonance is lower than the $C^{(6+)}$ peak, although, according to q/M value, it should be slightly higher.

The heterogeneity of the carbon ions in energy and in the direction at which they may emerge from the target snout, as well as the resonance curve coinciding near its peak with alphas, indicates that some care must be taken to select the beam for exposing nuclear plates. Accordingly, the apparatus shown in Figs. 2, 3 and 4 was built. The first part of it is an extension snout with three equally spaced slits over a distance of 26 inches.

These slits can be narrowed to select as narrow an energy spectrum as desired. The first slit is centered and adjustable only in width. The second and third slit are adjustable in width by rotating the rod leading through the Wilson seal and can be traversed by pushing this rod in or out by a screw mechanism. All the mechanical adjustments can be made while the beam is on by using an extension rod leading through the water tanks. The extension snout is followed by a foil wheel with twelve windows. The foils permit a study of the range of the ions selected by finding their Bragg curve or their extinction point using the first ionization chamber. Also, sufficient foils may be interposed to pass only alphas and permit determination of the alpha beam limits, which change with how recently the cyclotron was used to accelerate alphas. Thus can simply be found the magnet setting necessary to reduce alpha contamination on the nuclear plates to any desired level.

Each ionization chamber is built in the form of a drum with nitrogen at atmosphere pressure flowing slowly inside and with vacuum outside. The beam passes through the drum heads, which are of 1.4 mil dural, about the minimum which will hold atmospheric pressure over the unsupported diameter of 3-1/4 inches. Inside the chamber are three foils on rings insulated by teflon. The middle foil is the signal electrode and the outer two are high voltage plates with separate leads, so that they may be given the same or opposite polarity. As discussed by Rossi and Staub,[13] if the two plates have opposite polarity, a particle, say an alpha, passing all the way through, will give two pulses which nearly cancel each other. On the other

13. B. B. Rossi and H. H. Staub: Ionization Chambers and Counters, McGraw-Hill Book Co., New York (1949).

hand, if a particle, say a carbon ion, is stopped in the middle foil by interposing the correct foil in the foil wheel, it will give a pulse only in the front side of the chamber. This arrangement permitted studying the carbon beam when the alpha background was strong. However, at the peak of alphas the accumulation of imperfect cancelling was enough to overbalance the carbon beam. The drum type chamber has another good feature. Since the ions pass through the plates far from any edge, there is no edge effect to give different pip heights depending on how near the particle passes to one plate or the other. The pips seen on an oscilloscope from the drum chambers are of very uniform height if the energy is homogeneous. Thus, the effectiveness of the adjustments in getting rid of unwanted particles could be judged.

In the ionization chamber used here, the ions are collected directly along the line of the particle track, a condition enhancing recombination and, hence, reducing the pip heights. Since the amount of recombination will depend on the density of ionization, it cannot be expected that the pulse heights will correctly represent the Bragg ionization curve. Hence, a curve which was obtained using just the front half of the ionization chamber, with a sensitive region of 0.3 mil Al equivalent, should give a lower ratio of peak to initial ionization than the true one although, from the considerations to be discussed in Chapter VII, we expect a lower ratio for carbon nuclei than for alphas. It gave a ratio of 3.5 to 1, the lowest reading being taken after the minimum thickness of 2.0 mils Al equivalent necessary to enter the sensitive region. The range was about 53.5 mg/cm^2 Al for the carbon ions (of approximately 112 Mev energy). The recombination effect could be reduced, retaining the other good features of the chamber,

by tilting the drum so that collection is at an angle. Since the Medical Physics group studying ionization effects on cells plans a precise evaluation of the carbon particle ionization, modification and refinement of the equipment described here was not undertaken.

With a blank opening in the foil wheel, the carbon ion range is sufficient for the nuclei to pass completely through the first chamber before they reach the region of electron pickup. They are again in vacuum and their total charge will be collected by the electrometer Faraday cup. The bottom of this cup is sufficient to stop carbon ions but it will pass alphas unless foils are used to terminate the alpha range in the bottom of the cup. Since alphas normally pass through the cup, it has walls on both sides. These walls are shallow (half an inch high) since the cup is in a magnetic field of about 6000 oersteds. Because of the small beam at the time, precautions were taken that are not now required, such as the vacuum coaxial lead down the brass tube shown in Fig. 3 to the electrometer tube. L. K. Neher and K. D. Jenkins designed and built the electrometer circuits.

Beyond the Faraday cup was a second ionization chamber identical to the first. Its primary purpose was for use in case it was found desirable to obliterate the alpha beam background by using an anticoincidence circuit.

The time constant of the ionization chambers was made such that the pulses shown by the signal foil were due to electron collection, regardless of which direction the electrons actually traveled. The electron collection time was about one microsecond. The lead from the ionization chambers went to a UCRL standard preamplifier a few feet away where the magnetic field intensity was essentially zero. From there the signal went to a UCRL

standard linear amplifier and through a discriminator to either a scaler or a counting rate meter. Another lead from the linear amplifier went to an oscilloscope at the control room desk to permit maximizing the beam.

Prior to exposing a set of nuclear emulsion plates, the desired conditions were selected using narrow collimating slits. Leaving Number 2 slit full open, Numbers 1 and 3 slits were closed to a width of, say, 0.1 inch and Number 3 slit traversed to maximize the beam coming down the deflector channel. To center this beam for the nuclear plate, the apparatus as a whole was swung the measured displacement of Number 3 slit, which was then put back on center. Number 2 slit was now closed to the same width as the others and traversed to maximize the beam. If C^{12} were being used, an effective lower limit for alphas was found and the indicated magnet current held at the value for the exposure. The three slits were opened to half an inch each to give a desirable beam width on the plate. It was found that opening the slits to this value did not essentially increase the main gaussian energy distribution in the beam. The measurement of ranges on C^{12} plates, for example, shows consistently an average for the full energy particles of close to 170 microns with a maximum likelihood estimate of the standard deviation in the individual ranges of close to six microns. From the range-energy curve at 170 microns range, $\Delta E/\Delta R = 0.392$ Mev per micron. Therefore, the standard deviation in energy should be about 2.4 Mev, assuming that almost all this range dispersion is due to energy variation. The energy spread which can be passed by the three slits concerned here may be estimated from a calculation which was made for the three very narrow slits of the beam-energy measuring arm (shown in Fig. 44, Chapter VII). For a beam with a uniform distribution of energies and angles of incidence, passing through three evenly-spaced slits over a chord length of 25 inches in a magnet field of 6400

oersteds $\sigma\{E(\text{Mev})\} = 68.6\ W$, where W is the slit width (inches). In the present case, the field is not at all uniform, but its average value is not far from 6400 oersteds. Also, the slits cover 26 inches rather than 25 inches. But as an approximation we can use the value given above for $\sigma\{E\}$. We see that $\sigma = 2.4$ Mev requires a slit width of only 0.035 inches. Why, then, the low standard deviation with the slits open half an inch? The answer is that there is not a uniform distribution in energy and in angle of approach to the slits. The slits were maximized for the beam from the deflector, meaning that this group with relatively small spread in energy came through the slits at normal incidence. Particles of other energies had to come from a narrow angle prescribed by the gap between the dees. Consequently, the main group of particles from the deflector stands out alone, and its standard deviation is not larger than 2.4 Mev, no matter how wide the slits. Other tracks do appear on the plates but are well separated by the following characteristics: (1) Range measurements show effectively no tracks until a group is reached with range about 90-110 microns. Below it there are other apparent groupings becoming less distinct from each other. The blank between the 170 and 110 micron groups is evidently due to the blank region in energy and angle between the deflected beam and the beam escaping through the dee gaps with off-center orbits. (2) The photographic plate acts as a fourth slit. Although a particle of low energy may pass the three slits, it must fall on the inside edge of the beam at the plate. Consequently, it is simple to select a swath as a stopping point to cut off extraneous particles at a negligible level of significance.

After a probe port was constructed that permitted a probe to be inserted

on a radial line directly between the dees, it was possible to build a blocking probe to cut out the internal beam almost completely while letting the deflected beam pass through a slit in the probe. This probe is shown in position in Figure 2. It was used in exposing some of the later plates, and in all the range-energy measurements.

The photographic chamber was directly behind the foil wheel. The nuclear plates were brought up in a cassette which was butted up against the vacuum lock on the chamber, and the cassette was pumped down by a vacuum line at the lock. After the principal outgassing of the plates was over, in two or three minutes, the vacuum line was closed off and the vacuum lock gate slid down to permit shoving the plate on its tray into the exposure chamber. The tray normally held the plate at an angle of tilt of 4 degrees to the beam; if desired, the tray itself could be tilted to add 5 degrees more. Tilt is desirable to give easy distinction between surface scratches and tracks, to remove the main portion of tracks from any surface fog, to define a distinct point where a track enters the emulsion, and to give a higher probability for particles coming from a nuclear reaction to lie in the emulsion. Most of the plates were exposed at the 5 degree tilt. The 9 degree tilt was used principally for the bismuth-impregnated plates so that the two tracks from fission would have a better chance of lying in the emulsion.

With the usual beam intensities, exposure times were about 20 seconds for C^{12} beams and 2 minutes for C^{13} beams. These gave a density of tracks where almost all of the tracks were quite distinct from each other, but dense enough that events could be found without excessive travel and yet searching could be done with a dry objective, with its good depth of focus,

rather than with an immersion objective which would require continual focusing up and down while traversing.

Ilford nuclear emulsions were used. As a matter of personal preference the large plates, 3-1/4" x 4-1/4", were used rather than 1" x 3" plates. With the large plates, peeling at the edges was no problem such as it can be with small plates. Further, oil was less likely to run off large plates. A larger number of tracks could be surveyed, all produced at the same time, than on small plates.

The plates after exposure were sent to the nuclear emulsion group of the University of California Radiation Laboratory where they were given the standard processing. Almost all of the plates were free of surface fogging and had no troublesome background. In order not to change the track lengths, the plates were not scrubbed. There were a few extraneous tracks, mainly knock-on protons by neutrons and stars from naturally alpha-radioactive atoms scattered in the emulsion. These were mostly five-prong stars, which were usually in their characteristic grouping of three from one origin, followed by two more from an origin slightly removed due to the migration of the atom. These natural alpha stars were in all stages of fading of the latent image since some of the large plates used were several years old.

Both E-1 and D-1 emulsions were used and 100 microns was chosen as a suitable thickness to permit catching most of the emergent prongs and still to be easily processed. The D-1 emulsions were used only for study of fission. They are too insensitive for easy identification of tracks. With E-1 emulsions, identification is simple if the tracks are more than about ten microns long unless they are rising or digging steeply. In E-1 emulsions a carbon track could only be mistaken for an alpha very close to

the end of their tracks. The presence of a small amount of alpha contamination in the C^{12} beam was welcome since it gave a ready basis of comparison of an alpha track for any range up to 500 microns, and showed how, for example, an alpha deflected sharply downward might look. For identification of proton tracks there could always be found protons of various ranges, knocked-on by carbon ions or by alphas. No attempt was made to classify particles into sub-groups under singly-charged, doubly-charged and higher charged.

The E-1 emulsions give a solid track for carbon ions, with possibly a few gaps when the remaining range is under 15 microns (carbon nuclei pick up their inner two electrons at about 13 microns range). No study of gaps has been attempted in this research. A thorough study from counting gaps near the end of carbon tracks in D-1 emulsion has been made by P. C. Giles and W. H. Barkas.[14] Up to about 50 microns from its end in E-1 emulsion, the carbon track is covered with a "fur" of δ-rays (knock-on electrons), especially heavy in the first 50 microns and tapering down from there on. The δ-ray fur is familiar to those who have studied the heavy nuclei appearing in cosmic radiation. Where a great length of track is available to permit estimating velocity, the number of δ-rays lying between two selected energy values, per unit track length, has been used by Sörensen[15] to give quite an accurate estimate of the charge number, Z, of the particle, since for the same velocity the number of these δ's varies as Z^2. Sorensen estimates electron tracks should be long enough to be separately distinguishable (in electron-sensitive emulsions) if the energy is above 10 kilovolts,

---

14. P. C. Giles and W. H. Barkas, Phys. Rev. 85, 756 (1952).

15. S. O. C. Sörensen, Phil. Mag. 40, 947 (1949).

which implies that v/c is approximately 0.2. The maximum velocity that can be transferred to an electron is twice that of the nucleus colliding with it. A 112 Mev C^{12} ion has v/c = 0.141 and, hence, the maximum velocity an electron could acquire would give v/c = 0.282. The density of electron spurs above a given length along a track varies not only directly as Z^2 but inverseley as V^2. Consequently, for a very energetic particle, the spur density increases as the velocity decreases until a maximum is reached as the velocity falls below an efficient point for producing spurs of the selected length. Blau, Rudin and Lindenbaum,[16] from photodensitometer readings have guessed that this maximum occurs when the nucleus has approximately v/c = 0.3. On this basis, the density of δ-rays at the beginning of the tracks in this study is well below the maximum.

The E-1 emulsion is sensitive enough that an alpha track appears considerably heavier than a proton track except at the end where there would be a possibility of mistaking one for the other. In tracks of moderate length, the alpha is further distinguished from a proton by the rate of change of track density. It is true that alphas and protons of the same velocity have the same range (except for the small additive constant due to electron pickup by the alpha extending its range). And the dE/dX curves as a function of velocity are identical in shape for the two particles (except in about the last 6 microns of range). The magnitude of dE/dX is four times as great for the alpha as for the proton, since it varies as Z^2, but the alpha had four times the energy to lose. One would at first think the rate of increase of track density would be the same for the two

---

16. M. Blau, R. Rudin and S. Lindenbaum, Rev. Sci. Instr. 21, 978 (1950).

and such would be the case except for the nature of the photographic process. There is room for only about three grains per micron and, when one particle gives quite a dense track, the rate of increase in the number of grains per unit length, relative to the change in dE/dX per unit length, is less than would be the case for a more lightly ionizing particle. Blau[17] has put this fact into an equation which permits distinguishing between particles by grain counting. In addition to the effect just described, the proton track density peaks sharply in the last six microns compared to that of an alpha, due to the shape of the dE/dX curves there.

The microscopes used in the survey of the nuclear plates were two Zeiss Jena microscopes with laboratory-type stages (rectangular, with x- and y-coordinate scales). Each had apochromatic objective lenses and compensated eyepieces. They were equipped with 10 and 20 power dry objectives, 60 and 90 power oil-immersion objectives, and 7 and 10 power eyepieces. An additional magnification of 1.5 is built into the body tube.

In order to facilitate measuring track lengths exceeding the length of an eyepiece scale, a superstage micrometer was designed and built by Silge and Kuhne, San Francisco. It can measure any length in the x-direction up to 1 centimeter (far beyond the range required). The plate holder clamps were removed from the dove-tailed groove in which they lock and a sliding bar was fitted into this groove with the plate holder clamps fastened to it. No change was made in the position of the plate on the stage. The fixed part of the superstage was clamped at either end in the dove-tailed groove, with a reinforcing bar connecting the two ends. One end supplied

---

17. M. Blau, Phys. Rev. 75, 279 (1950).

a spring loading on the sliding bar while the other end contained a Zeiss precision screw of 1/2 mm pitch that made contact with the sliding bar through a small hardened steel ball. Thus, the sliding bar and the plate were moved on the superstage, independently of the x-coordinate coarse adjustment and in the same manner. The drum for the superstage is calibrated in 2 micron units. Lengths can be estimated to the nearest tenth of a unit but the accuracy of the screw is not expected to be better than about 1 micron. To permit holding small and large plates, an adjustable plate holder bracket was built of dural. To measure angles on the plates, a simple goniometer eyepiece was built. It should be accurate to about half a degree. A sketch of the superstage micrometer is shown in Fig. 7 and a photograph of the microscope stage, with a large plate in position, in Figure 6. A view of the laboratory arrangement of the microscopes is shown in Figure 5.

The technique used in searching plates was as follows: Scanning to locate events was done with 20X objective and 7X eyepieces (total magnification, 20 x 1.5 x 7 = 210), giving a field of view of 620 microns. The 10X objective was found inadequate for searching since tracks of protons could easily be missed. The oil-immersion 60X objective was required for scanning some of the denser bismuth-loaded plates, giving a field of view of 220 microns with 7X eyepieces. With the 620 micron field of view, swaths were overlapped by moving only 400 microns by the millimeter scale and vernier of the y-axis. With the 220 micron field of view, swaths were spaced 200 microns apart; failure to overlap was guarded against by observing that the field of view in a new swath actually overlapped the old field of view.

FIGURE 5.

LABORATORY ARRANGEMENT OF MICROSCOPES

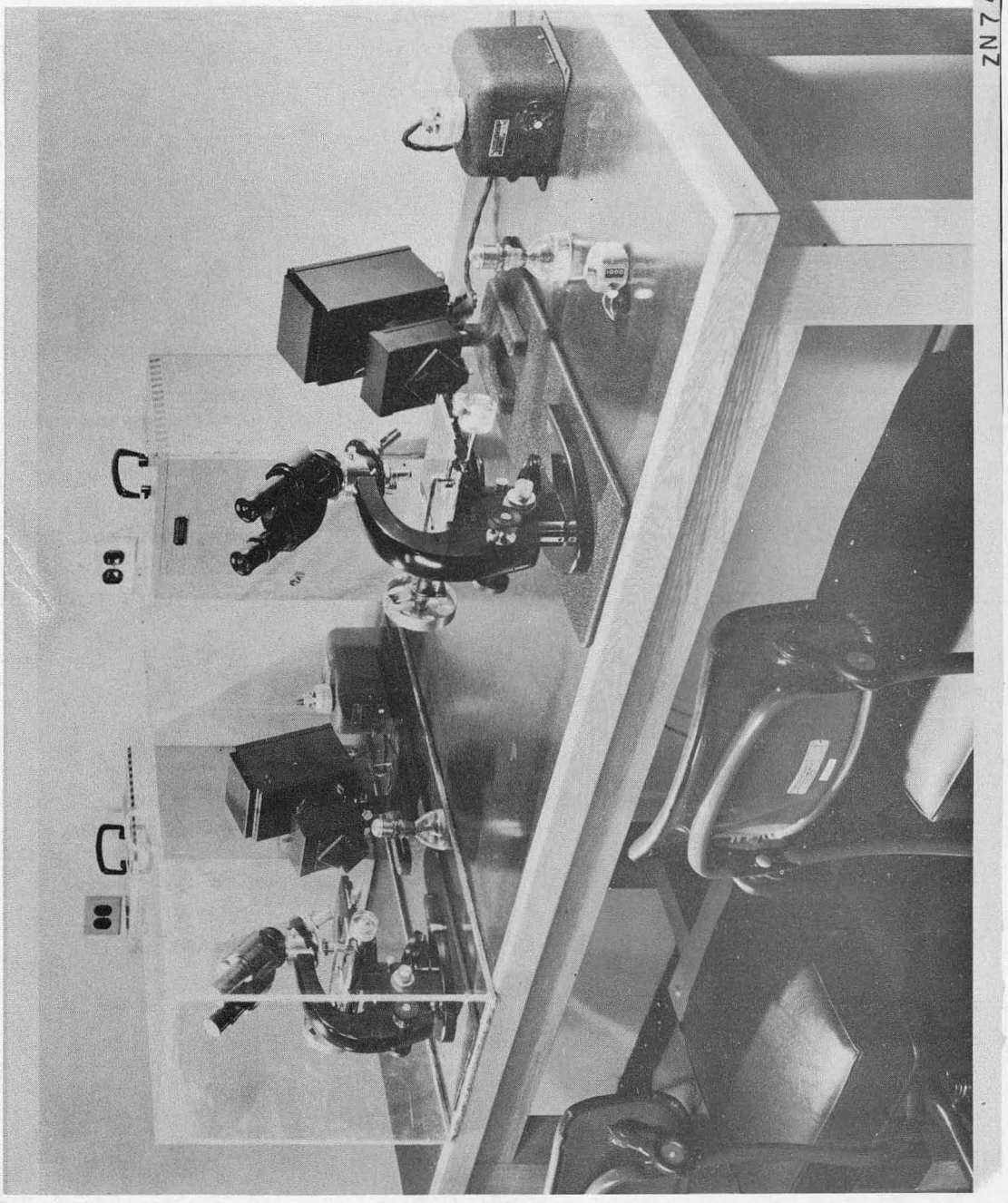

FIGURE 5

FIGURE 6.

MICROSCOPE STAGE

The independent superstage micrometer is shown and the modified bracket to hold large plates.

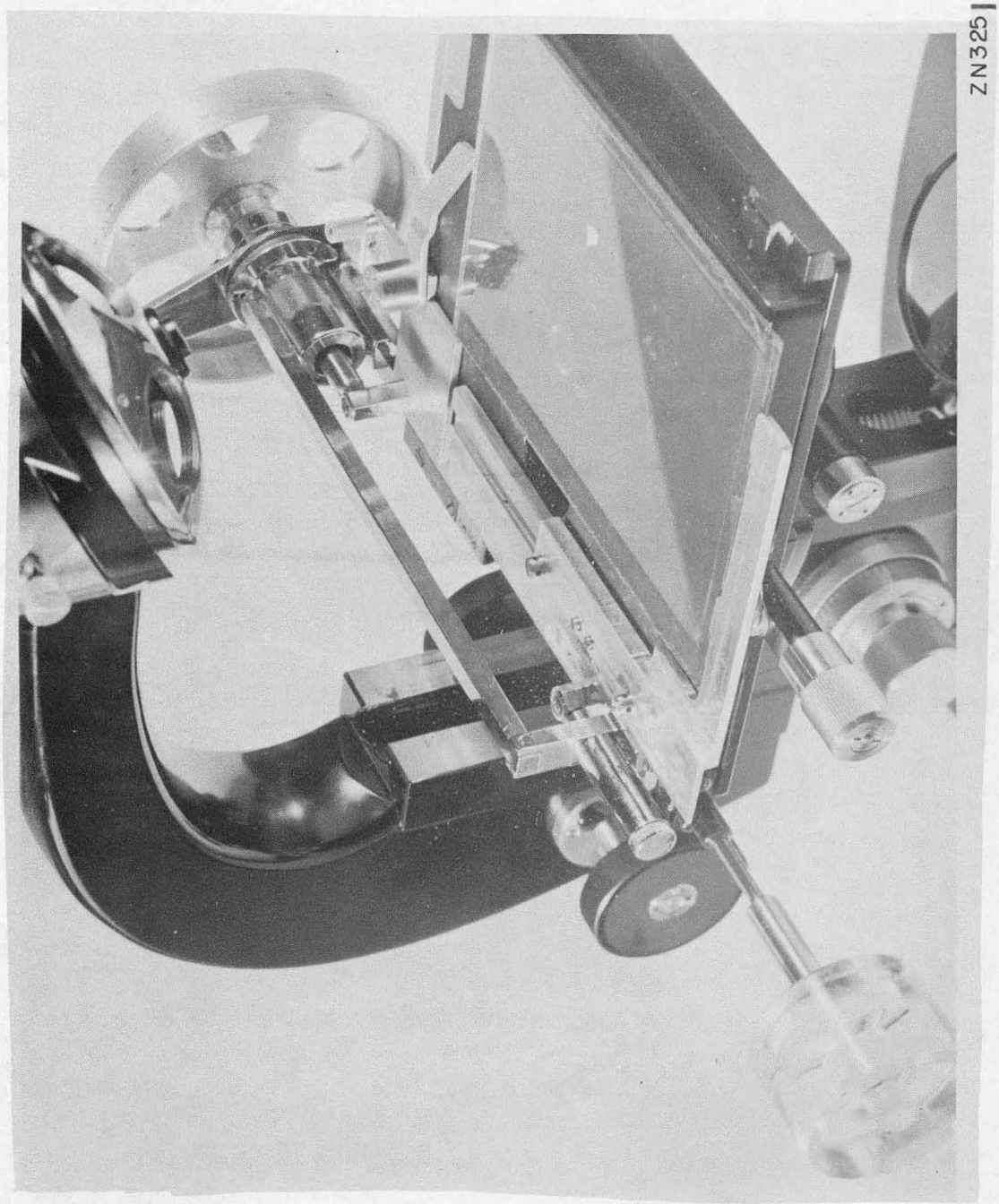

FIGURE 6

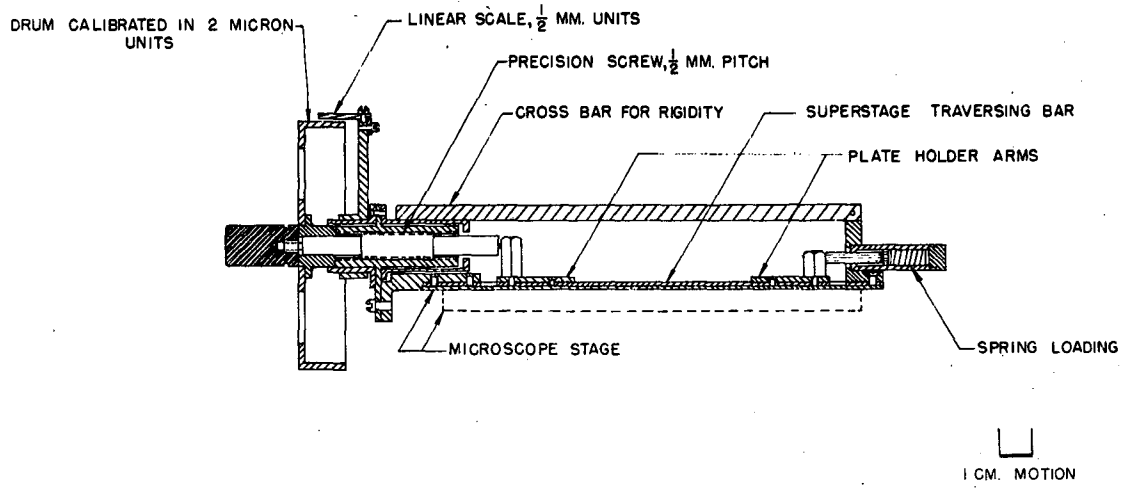

MICROSCOPE SUPERSTAGE

FIG. 7

MU 2272

FIGURE 7

It was soon found inefficient to search with a dry objective through a cover glass (to give the optically correct distance for which the lenses are designed), noting down coordinates of possible events and later going back to look at these under oil immersion. Instead, it was found better to apply a uniform layer of cedarwood oil on the region of the plate to be searched, using it as a sort of cover glass for the dry objective. It had the excellent feature of almost completely obliterating all surface scratches. When a possible event was seen, it was centered in the field of view and the 90X immersion objective rotated into position. Thus, everything on the plate that might be of interest could be examined with a minimum of trouble. The oil was kept from running off the plate during a search by wiping a small border of the emulsion with acetone, followed by wiping it with water. Enough water was left on the emulsion to form a boundary the oil did not pass.

One technician working over a period of about six months assisted in surveying the plates to locate events. The following data were taken for each event, or questionable event, located:

1) A sketch of the event, with coordinates.
2) The number of emergent prongs.
3) A tentative designation of prongs as protons, alphas, heavier than alpha, or product nucleus.
4) Distance from the beginning of the track to event.
5) Approximate ranges of the longer prongs.
6) Notation as to inclination of a prong in the emulsion and whether it went out the top or bottom.

7) Distribution of prongs by 60 degree sectors, with the forward sector centered in the direction of the entering carbon nucleus.

8) Special features of interest.

After the survey of a plate was completed, range measurements were made of 100 tracks, 25 in each of four areas spaced to give a true estimate of the mean range if the range should differ in different portions of the beam. No significant variation was found. To avoid any personal bias in selection of tracks to measure, the selection was prescribed: If the track beginning lay in the two middle reticule divisions and did not deviate by more than one reticule width in its range, it was to be measured unless it dipped or rose noticeably from its course. To avoid a chance of re-reading, the next track chosen was the first one after the end of the preceding track. Tracks that crossed or joined others were not read. Any small hook on the end of the track was straightened out visually and its extended length measured. In this respect the range would differ from that found by penetration of a foil but the correction would be small. Ranges of below normal energy carbon particles were read if they were over half the normal range. However, these were discarded in computing the mean and standard deviation in range on the usual criterion that, if their range was more than 5 standard deviations from the mean estimated with them included, they were not included. By virtue of the gap between the full energy and the lower energies, probably no particles coming from between the dees were included in computing the mean range.

Next, cross swaths were made at about six values of the x-coordinate, selected along the region surveyed. On these cross swaths a count was

made of all carbon tracks which had their beginning in the field of view. Cross counts were usually made under 60 x 1.5 x 7 magnification (field of view, 220 microns). Under this power there were not so many carbon tracks abreast as to cause confusion in counting, yet the field of view is considerably larger than the length of the anomalously short carbon tracks. Also, the magnification is adequate to detect whether a track has the fur of a "true" carbon at the beginning. Carbon tracks less than about half range could be unmistakably identified from their track beginnings and were excluded from the count. The question arose concerning the group of range about 100 to 110 microns. These have enough δ-rays that they might not be distinguished from full-range carbons unless the track were followed down in the emulsion to see its full range or outside the field of view, which was impractical. It was decided to count them as if they were full range. The error in doing so is on the conservative (low) side in calculating a reaction cross section. The error at most would be very small, since only a small fraction of the tracks in the area used is of this short length. The error is lessened by the fact that carbon particles of this range have a fair cross section for producing events. A few events (about six) were seen that seemed quite definitely not to come from full range carbon particles. Further, the purely statistical fluctuation in the number of events is enough to hide the effect of including the medium range particles as being of full range.

After the cross counts of a plate were completed, the values were plotted on graph paper at the proper abscissae, a smooth curve was drawn through the points and the area under the curve was measured with a

planimeter. When multiplied by the conversion factors, this area gave the total number of tracks in the area surveyed.

Since the emulsions were exposed in a vacuum, questions arise as to the effects of vacuum on the composition and thickness of emulsion. The emulsion contains a considerable percentage of water in solution in the gelatin and glycerin. In a vacuum some of this water should be pumped out, changing the percentages of the elements in the emulsion and, consequently, affecting the reaction cross section and the stopping power of the emulsion. Wilkins[18] has made a detailed study of the effect on stopping power and range of removing water from the emulsion. Ilford, in the technical leaflet accompanying the emulsions, gives the elemental composition based on a density of 3.915 gm/cm^3 (see Table 3.2, Chapter III). This density implies the presence of water in the emulsion since they quote a density for dry emulsion of 4.18 gm/cm^3, according to Wilkins. If we assume that water is absorbed by simple mixture, which has been confirmed by several experimenters, then it is simple to calculate the amount of water when the density is 3.915 gm/cm^3. If one cm^3 of dry emulsion of density ρ_o absorbs w grams of water, then the new volume of $(1 + w)$cm^3 will have a density ρ, given by $\rho = \frac{\rho_o + w}{1 + w}$. If $\rho_o = 4.18$ and $\rho = 3.915$, w must equal 0.09 gm of water/cm^3 of dry emulsion. From experimental data on w vs. relative humidity of the atmosphere in which the plate is in equilibrium, $w = 0.09$ corresponds to a relative humidity of about 30 percent. Under any condition where the absorbed water differs from that quoted, the stopping power of the emulsion should be corrected. Unfortunately, little

---

18. J. J. Wilkins, A.E.R.E. Report G/R. 664, Harwell, England (1951).

is known as to how to calculate accurately the change in water content when a plate is put in vacuum and Wilkins only points out the variety of conditions under which range-energy plates have been exposed. The matter has been discussed with A. J. Oliver[19], of the Film Group of the University of California Radiation Laboratory, who has made extensive studies of the properties of nuclear emulsions. He states that it must not be assumed that putting an emulsion under vacuum will remove all the water. An unprocessed 200 micron C-2 emulsion, in equilibrium at 38-40 percent relative humidity (R.H.), showed only about one percent shrinkage in thickness after being under vacuum for 45 hours. In contrast, plates brought from 40 percent R.H. to equilibrium at 10 percent R.H. showed a shrinkage of about 5 percent. On this basis, the 45 hours of pumping might correspond to a change in R.H. of about 6 percent. For the 100 micron emulsions used with carbon ions, the pumping of water would be faster than in the case of the 200 micron emulsions. It is quite apparent on first putting nuclear emulsions under vacuum that they are outgassing, which would include giving out water vapor. But after about five minutes, the outgassing rate has become negligible. When plates start at the fairly low relative humidity of 40 percent, probably the best representation of the true situation is the finding by Bradner, Smith, Barkas and Bishop[20] that no significant difference in stopping power could be detected between pumping times of six minutes and six hours. All the

---

19. A. J. Oliver, private communication.

20. H. Bradner, F. M. Smith, W. H. Barkas and A. S. Bishop, Phys. Rev. 77, 462 (1950).

plates in the present study were under vacuum for at least six minutes before bombardment and the range-energy plates were under vacuum for at least 20 minutes before using them. The completely "dry" emulsion Wilkins uses as a standard can probably not be prepared by evacuation but only by heating above the boiling point of water for some time.

Oliver has measured the density of some Ilford C-2 emulsions at 40 percent R.H. and found it to be only 3.82 gm/cm^3, with an error small enough to rule out its being as high as 3.915 gm/cm^3. This low density of his sample may have been due to manufacturing variations in the constituents of the dry emulsion. However, it points out the futility of trying to make a correction to stopping power for a small variation in water content unless the composition of the emulsion batch is precisely known and the effect of such factors as evacuation can be calculated accurately. Apparently the vacuum pumping on the 100 micron plates used in this study would give a smaller effect than the 45 hours of pumping on 200 micron plates. There the change of 6 percent in the R.H. value implied a decrease, Δw, of about 0.0084 gm of water per cm^3 of emulsion (see Fig. 1, ref. 18). If $\rho = 3.82$ gm/cm^3 to start with, $w = 0.1276$, and the pumping would bring it down to 0.119, which is still not lower than the water content calculated for the composition as Ilford gives it. The best approximation appears to be to use their composition without correction in the present case.

Information is required as to how to measure depth in emulsion after it is processed. The emulsion shrinks by a factor of about 2.3 during processing. The emulsion was exposed to the beam at virtually its full thickness, the one percent shrinkage observed by Oliver being negligible.

In calculating dip angles in emulsions, the depth of focus of a high power objective may be used. The 90X objective should permit depth measurements accurate to less than one micron of motion of the microscope lenses. This motion is read on a drum scale on the vertical adjustment and, for oil immersion objectives, equals the distance in the shrunken emulsion. To obtain the distance in the unprocessed emulsion, the depth read from the microscope should be multiplied by 2.3. For convenience, where the depth measurement was not critical, the readings were multiplied by 2.0 in this study rather than 2.3. It must be borne in mind that emulsions even after processing expand and shrink as the relative himidity changes, as the unprocessed emulsions do. Where a precise measure in depth is required, the relative humidity should be controlled.[21]

---

21. J. M. McAlister and D. W. Keam, Proc. Phys. Soc., London, A64, 91 (1951).

CHAPTER III

GENERALITIES ON REACTIONS.

The general properties of nuclear reactions from incident C^{12} and C^{13} particles follow quite closely what one would expect from a consideration of their nature as heavy, classical particles. Those used in this research have enough energy over the major part of their range to surmount any Coulomb barrier they meet and yet they are not in the region of relativistic velocities.

The velocity of carbon nuclei from the 60-inch Cyclotron is 4.24×10^9 cm/sec., giving $\beta = 0.141$ (for 112 Mev C^{12}). For this velocity they have a very short de Broglie wave length because of their large mass. $\lambda\!\!\!^{-} = \frac{\hbar}{Mv} = 1.248 \times 10^{-14}$ cm for the full velocity particle in the laboratory system. $\lambda\!\!\!^{-}$ is the de Broglie wave-length divided by 2π. This short quantum mechanical wave length means that a well defined wave packet can be formed to represent the carbon particle, and that we may follow it along a well-defined trajectory. The classical picture of a nuclear collision as one sphere striking another is in this case well justified by quantum mechanics, more so than would be the use of the Born approximation where a wave treatment is used to represent a random impact parameter and a weak interaction. The classical picture, is however, an approximation to the true and complete picture, which is more accurately portrayed by quantum mechanics if we used a solution free of approximations. The criteria for a classical treatment are discussed rather completely in Chapter VII.

In the present connection we may say that the criterion of a wave packet small with respect to the size of the struck particle is well satisfied: $\lambda\!\!\!^{-} \ll a$, where a is the nuclear radius. For Ag^{107}, $a = r_0 A^{1/3} = 6.5 \times 10^{-13}$ cm, (using $r_0 = 1.37 \times 10^{-13}$ cm) while $\lambda\!\!\!^{-}$ in the center of mass system, using the reduced mass, $\frac{M_c M_{Ag}}{M_c + M_{Ag}}$, and the relative velocity is: $\lambda\!\!\!^{-}_{C.M.} = (\lambda\!\!\!^{-}_{Lab})\left(\frac{M_c + M_{Ag}}{M_{Ag}}\right) = \frac{119}{107}\,\lambda\!\!\!^{-}_{Lab}$. Thus, a is approximately 47 times the wave length at full velocity. A consequence of this short wave length is that we may picture almost classically the orbital angular momentum carried into a nucleus by a carbon particle. Quantum mechanically, the magnitude of the orbital angular momentum vector is $\sqrt{L(L+1)}\,\hbar$ where L is the quantum number: 0,1,2,... Classically, angular momentum is given by $\mu v b$ where b denotes the impact parameter, namely the distance between the centers of the two nuclei measured perpendicular to their line of motion. We may write $\mu v b$ as $\frac{\hbar b}{\lambda\!\!\!^{-}_{C.M.}}$. Therefore, fairly accurately, $L \approx \frac{b}{\lambda\!\!\!^{-}_{C.M.}}$. The greatest value of b where a C^{12} nucleus surmounts the Coulomb and centrifugal potential barriers of the Ag^{107} nucleus will occur at the maximum velocity, and from a calculation such as that for Table 3.4, later in this chapter, is (for 110 Mev C^{12}) $b_{max} = 7.290 \times 10^{-13}$ cm. This value of b_{max} corresponds to $L \approx \frac{7.290 \times 10^{-13}}{\frac{119}{107}(1.248 \times 10^{-14})} = 52$. This is an extremely large angular momentum quantum number, and it is principally contributed to by the large mass of the carbon particle, though the size of the particle also enters.

A second criterion for the validity of an orbital treatment in following the details of a collision comes from the requirement that the uncertainty

in the original momentum of a particle must be much less than the momentum it transfers. Again, see Chapter VII. This criterion may be expressed as:

$$K \equiv \frac{2 z_1 z_2 e^2}{\hbar v} \gg 1$$

Z_1 is the charge number of the incident particle, Z_2 of the struck particle. In Chapter VII, since energy loss through electron collisions is being considered, $Z_2 = 1$, and in that case, for 120 Mev C^{12}, $K = 0.598$, so that the classical picture could not accurately be used until a low velocity was reached. However, in the present application to nuclear collisions, with the exception of collisions with hydrogen nuclei, Z_2 ranges from 6 to 47 and the classical picture is justified. It will be useful and accurate to calculate collision details using classical mechanics.

The use of carbon nuclei as bombarding particles is of considerable interest because they offer a means of introducing a large excitation energy into a nucleus without the use of the exceptionally high velocities necessary in the case of less massive particles. There should be no effect of nuclear transparency or of direct knock-on of imbedded individual nucleons in the target nucleus. The nuclear reactions from carbon particles should consequently give quite direct information as to the processes from compound nuclei at high excitation. There are two reservations: (1) Although an imbedded nucleon will not be knocked-on, the wave length is short enough that surface particles may be (more will be said of this later in discussing impact disintegration of C^{12}); (2) The high angular momentum that can be carried by carbon nuclei into the reaction may influence the outcome of the compound nucleus.

The excitation introduced into a compound nucleus by the bombarding particle is twofold - (1) from the discrepancy between the mass the compound nucleus should have for maximum stability and the sum of the masses of the bombarding and struck particles, and (2) from the kinetic energy in the center of mass system carried into the compound nucleus. The excitation from mass conversion into energy is shown in Table 3.1 for the principal constituents of the photographic emulsion. The mass excesses, M-A, for the lighter elements and compound nuclei are from Mattauch and Flammersfeld.[10] They give the mass excesses, evaluated from spectroscopic and reaction energy data principally, only up through argon. For the heavier atoms, the mass excesses are taken from masses calculated by N. Metropolis and G. Reitwiesner[22] using the Eniac digital computer to find the masses according to a semi-empirical formula given by Fermi. This formula, for the mass M of an atom of atomic number A and nuclear charge Z, is:

$$M(A,Z) = 1.01464A + 0.014A^{2/3} - 0.041905Z_A + \frac{0.041905}{Z_A}(Z-Z_A)^2 + \frac{0.036}{A^{3/4}}\lambda$$

$$\text{where } Z_A = \frac{A}{1.980670 + 0.0149624A^{2/3}}$$

$$\text{and } \lambda = \begin{cases} 1 \text{ for A even, Z odd} \\ -1 \text{ for A even, Z even} \\ 0 \text{ for A odd.} \end{cases}$$

The formula is quite accurate for medium and high masses but is badly in error for low masses in comparison with the values given by Mattauch and Flammersfeld.

---

22. N. Metropolis and G. Reitwiesner: Table of Atomic Masses. USAEC Report NP-1980 (1950).

TABLE 3.1

EXCITATION OF COMPOUND NUCLEUS FROM MASS DIFFERENCES.[10,22]
(M-A = Mass Excess, in milli mass units, mMU)
1 MU is equivalent to 931 Mev.

Target Nucleus	Target (M-A) [mMU]	Target + Incident (M-A) [mMU]	Compound Nucleus	Compound Nucleus (M-A) [mMU]	Δ MASS [mMU]	Excitation of compound nucleus E_x [Mev]
Incident Particle: $_6C^{12}$ (M-A = +3.855 ± 0.023 mMU)						
$_{47}Ag^{109}$	-51.83	-47.98	$_{53}I^{121}$	-45.08	-2.90	-2.70
Ag^{107}	-51.79	-47.94	I^{119}	-43.78	-4.16	-3.87
$_{35}Br^{81}$	-52.66	-48.81	$_{41}Nb^{93}$	-54.44	+5.63	+5.24
Br^{79}	-53.01	-49.16	Nb^{91}	-53.19	+4.03	+3.75
$_8O^{16}$	0.0000	+3.855±.023	$_{14}Si^{28}$	-14.55±.11	+18.40±.11	+17.12±.10
$_7N^{14}$	+7.540±.024	+11.395±.033	$_{13}Al^{26}$	-3.72±.26	+15.11±.26	+14.06±.24
$_6C^{12}$	+3.855±.023	+7.710±.032	$_{12}Mg^{24}$	-7.46±.08	+15.17±.09	+14.11±.08
$_1H^1$	+8.1297±.0032	+11.984±.023	$_7N^{13}$	+9.996±.028	+1.988±.037	+1.85±.03
Incident Particle: $_6C^{13}$ (M-A = +7.576±.023)						
Ag^{109}		-44.25	I^{122}	-44.34	+0.09	+0.08
Ag^{107}		-44.21	I^{120}	-43.57	-0.64	-0.60
Br^{81}		-45.08	Nb^{94}	-53.34	+8.26	+7.69
Br^{79}		-45.43	Nb^{92}	-52.78	+7.35	+6.84
O^{16}		+7.576	Si^{29}	-14.55	+22.13	+20.6
N^{14}		+15.116	Al^{27}	-10.26	+25.38	+23.6
C^{12}		+11.431	Mg^{25}	-6.29	+17.72	+16.5
$_1H^1$		+15.706	N^{14}	+7.540	+8.166	+7.6
$_{83}Bi^{209}$	+60.25	+67.83	$_{89}Ac^{222}$	+86.57	-18.74	-17.43

TABLE 3.2

CHARACTERISTIC PROPERTIES OF ILFORD EMULSIONS AT "NORMAL HUMIDITY".

Element	ρ (gm/cm^3)	Atom Percent	R (cm x 10^{13})	Area, S Percent	Coulomb V (mev)	$\frac{KE_{cm}}{KE_{lab}}$	KE_{lab} to exceed V Coul.	Residual range (μ)
C^{12} as the incident particle on non-loaded emulsions (C-2, E-1, E-1).								
Ag	1.85	12.766	9.657	26.78	42.00	.8999	46.67	46.5
Br	1.34	12.482	9.036	22.92	33.43	.8694	38.45	35.7
I	0.052	0.305	10.022	0.69	45.64	.9136	49.96	51.1
C	0.27	16.735	6.273	14.81	8.26	.5000	16.52	13.7
H	0.056	41.357	4.510	18.92	1.91	.0775	24.64	20.8
O	0.27	12.562	6.588	12.26	10.48	.5714	18.34	15.2
S	0.010	0.232	7.486	0.29	18.45	.7273	25.37	21.3
N	0.067	3.560	6.439	3.32	9.38	.5386	17.42	14.3
C^{13} as the incident particle on bismuth-loaded emulsions (D-1).								
Ag	1.39	9.530	9.743	20.09	41.63	.8924	46.65	
Br	1.01	9.348	9.120	17.27	33.12	.8601	38.51	
I	0.039	0.227	10.105	0.51	45.27	.9071	49.91	
C	0.33	20.323	6.357	18.24	8.15	.4802	16.97	
H	0.047	34.488	4.595	16.17	1.88	.0720	26.11	
O	0.43	19.878	6.673	19.66	10.35	.5517	18.76	
S	0.002	0.046	7.571	0.06	18.24	.7111	25.65	
N	0.062	3.274	6.522	3.09	9.26	.5187	17.85	
Na	0.06	1.930	7.117	2.17	13.34	.6388	20.88	
Bi	0.27	0.956	11.350	2.74	63.11	.9414	67.04	

$R = r_1 + r_2$ where subscript 1 denotes the incident particle (C^{12} or C^{13}) and 2 denotes the target nucleus.

$R = r_o (A_1^{1/3} + A_2^{1/3})$ $\qquad r_o = 1.37 \times 10^{-13}$ cm

Percent of the total nuclear area for the i^{th} element S_i is given by:

$$S_i = \frac{(\rho a)_i \ (A_i^{1/3} + A_C^{1/3})^2}{\sum (\rho a)_i \ (A_i^{1/3} + A_C^{1/3})^2} \times 100$$

$$V_{Coulomb} = \frac{Z_1 Z_2 e^2}{R}$$

$$\frac{KE_{cm}}{KE_{lab}} = \frac{M_2}{M_1 + M_2}$$

KE_{cm} means the kinetic energy of the carbon nucleus relative to the center of mass, and would more appropriately be written $KE_{C/cm}$.

The residual range given is that which the incident carbon has when it first fails to go over the Coulomb barrier in a head-on collision.

It is to be remarked that not in every case is energy liberated by the fusion of incident and target particle into a compound nucleus. In some cases additional energy must be supplied. Further, the excitations from adding C^{13} are in every case higher than those from C^{12}.

The excitation of the compound nucleus from the kinetic energy transported into it must be computed in the center of mass system, which means that the carbon nucleus can put almost all of its kinetic energy into excitation of the heavy nuclei, silver and bromine, but only 1/13th of the C^{12} kinetic energy into the compound nucleus formed in a collision with hydrogen. It must be remembered, too, that there is a "cut-off" energy below which neither kinetic energy nor mass conversion excitation can be added to the compound nucleus. The cut-off is determined, for S-type collisions (L=0), by the Coulomb barrier, and for collisions of non-zero angular momentum by the sum of the Coulomb and "centrifugal potential" barriers. In Table 3.2 the constituents of the emulsion are given, according to Ilford, for "normal humidity" (density=3.915 gm/cm^3), and the Coulomb barriers are calculated as well as the fraction of the kinetic energy available in the center of mass system to surmount the Coulomb barrier and excite the nucleus. The table is for the case L=0 only. Coulomb barriers are calculated using $r = r_{carbon} + r_{target}$ where the term on the right hand side is taken as $r_o A^{1/3}$ with $r_o = 1.37 \times 10^{-13}$ cm, from the work by Cook, McMillan, Peterson and Sewell[23] on the measurement of total cross sections for fast neutrons. See also the discussion by Fernbach,

---

23. L. J. Cook, E. M. McMillan, J. M. Peterson and D. C. Sewell, Phys. Rev. 75, 7 (1949).

Serber and Taylor.[24] This value for r_o will be used throughout this paper in preference to other values given. One reason for preferring it is that it is based on a separate consideration of the bombarding and target nuclei, while the value deduced from alpha radioactivity (for example, $r_o = 1.48 \times 10^{-13}$ given by Perlman, Ghiorso and Seaborg[25]) is based on the effective radius of the nucleus, considering the alpha particle as a point charge. Since the radius of the bombarding carbon nuclei must certainly be taken into account, the latter value of r_o is not used here despite its good fit for alpha emission in the heavy region of the nuclide chart.

In Table 3.2 the kinetic energy necessary to surmount the Coulomb barrier has been calculated as a lower limit beyond which reactions will not occur. We can explicitly neglect any effect of tunneling through the Coulomb barrier because of the large mass of the carbon particle which cuts the penetrability to the vanishing point. The transparency, G, of a potential energy barrier higher than the kinetic energy of a particle is given, in the W. K. B. approximation by:

$$G = \exp\left[-\frac{2}{\hbar}\int_a^b \sqrt{2\mu(U(r)-E)}\,dr\right]$$

where μ is the reduced mass of the bombarding and struck particles; $U(r)$ is the potential energy function, which is, in the case of a Coulomb barrier, $U(r)=\frac{Z_1 Z_2 e^2}{r}$; E is the initial energy of the incident particle; a is the value of r when $U = E$, and b is the radius at which Coulomb forces are overbalanced by the short-range nuclear forces. If, for example, we

---

24. S. Fernbach, R. Serber and T. B. Taylor, Phys. Rev. 75, 1352 (1949).

25. I. Perlman, A. Ghiorso, and G. T. Seaborg, Phys. Rev. 77, 26(1950).

compare the transparency for C^{12} and an alpha of the same initial velocity, we see that for C^{12}, $\mu = \frac{12\ M_2}{12+M_2}$ while for an alpha, $\mu = \frac{4\ M_2}{4+M_2}$, a ratio of close to 3 to 1. $U_C = 3U_\alpha$ and $E_C = 3\ E_\alpha$. The result is that quite closely $G_{C12} \approx G_\alpha^3$ where G_α is already a small number. Again the classical behavior of the carbon particle stands out.

One of the important sets of data in evaluating the nuclear reactions induced by a particle is the cross section. In the present study, conditions are favorable for obtaining details concerning the cross section in emulsion which might be difficult in experiments with other particles where the tracks are faint or excessively long or the energy ill-defined. A record was kept of the distance from the beginning of the track to each event. When subtracted from the average range for that plate, it gave the expected average residual range, which was converted into the energy at the time of the event by use of the experimental range-energy curve. For each plate a sampling gave the best estimate of the mean range and of the standard deviation of the individuals from this mean. In a typical case for C^{12}, the results were:

$$\mu \approx \bar{R} = \frac{\sum R_i}{n} = 172.06 \text{ microns (slant range)}$$

$$\sigma\{R\} \approx s = \sqrt{\frac{\sum (R_i - \bar{R})^2}{n-1}} = 6.11 \text{ microns}$$

where the terminology means (following Arley and Buch[26]): "The true (unknown) mean μ has the estimate $\bar{R}$, the average from the sample, and the

---

26. N. Arley and K. R. Buch: Introduction to the Theory of Probability and Statistics, (1950) John Wiley & Sons, New York.

true standard deviation of the individual values of R has the estimate s, obtained from the sample". Estimates can also be given for the standard deviation in $\overline{R}$ and in s.

$$\sigma\{R\} \approx \frac{s}{\sqrt{n}} = 0.52 \text{ microns}$$

$$\sigma\{s\} \approx \frac{s}{\sqrt{2(n-1)}} = 0.37 \text{ microns}$$

The mean and standard deviation of the initial range can be converted into a mean value and standard deviation of the energy at the time of the event as follows: Assume that at full energy, $\sigma\{E_o\} = k_o \sigma\{R_o\}$ where the subscript denotes the original values and k_o is the slope of the range-energy curve at that point. This conversion should be nearly correct. $\sigma\{R_o\} = 6.0$ microns fixes $\sigma\{E_o\}$ at about 2.4 Mev. It is true that with a monoenergetic beam there would be an appreciable $\sigma\{R_o\}$ arising from straggling and uncertainties in measurement. But for carbon particles, the straggling is only about 0.6 percent of the range (about 1.0 micron on the full range) and other contributions are similarly small. Since the sum of independent dispersions is given by the square root of the sum of their squares, it is apparent that nearly the whole contribution to $\sigma\{R_o\}$ must be that caused by a dispersion in initial energy. Now the residual range R at the time of the event has the expectation $\mathcal{E}\{R\} = \overline{R}_o - X$, where X is the distance to the event, and $\sigma\{R\} = \sigma\{R_o - X\} = \sqrt{\sigma^2\{R_o\} + \sigma^2\{X\}}$. $\sigma^2\{X\}$ is nearly zero, since X is quite precisely known. Therefore, $\sigma\{R\} \cong \sigma\{R_o\}$

wherever the event occurs along the track. Similarly, for the energy E at the time of the event, $\sigma\{E\} = \sqrt{\sigma^2\{E_o\} + \sigma^2\{\Delta E\}}$. $\sigma\{\Delta E\}$ is never greater than $\sigma\{E_o\}$ and usually is much smaller. Hence, $\sigma\{E\} \cong \sigma\{E_o\} = k_o \sigma\{R_o\}$. The standard deviation in the energy at the event is essentially constant at the value 2.4 Mev and the standard deviation in the residual range is that of the original range. $\sigma\{E\}$ is indicated at several points by the horizontal bar on the cross section curves of Figures 8, 9, and 10.

There are certain features which must be understood to interpret the cross section curves. First, the experimental cross section cannot include all inelastic reactions created by the bombarding particle but only those giving charged heavy particles. Neutrons, gamma rays and betas are not seen. Second, it is not possible to sort out the cross section of the different elements in the emulsion. Sometimes an event can be assigned fairly well to the lighter or the heavier elements of the emulsion but not well enough to permit computing individual cross sections from such data. Third, the acceptance of something seen in the emulsion as an inelastic nuclear event requires setting up certain criteria in cases that are not self-evident.

The bases on which events are accepted in this study are given below. To begin with, "zero" and one-prong stars are excluded. "Zero"-prong stars have been used by others as a classification under which to estimate stars missed in scanning and inelastic processes not classified as stars. Without doubt there must be a few stars missed in the areas surveyed in the E-1 plates exposed to carbon nuclei, but their number should be very

small in view of the clarity of the tracks and the low background. A larger number might be missed in the bismuth-loaded D-1 emulsions. There are special types of investigations at high velocities with different distinctions in classifying prongs where "zero" and one-prong stars are appropriate classifications.[27,28] In the present study, all prongs or spurs, regardless of length, are counted if they come from the star. Therefore, the product nucleus is counted as a prong, provided it is visible. In a small number of cases, no track of a product nucleus seemed to be present. Because of the dense ionization at the center of the star and the presence of δ-rays along the entering track, care must be taken not to count a δ-ray or a random alignment of a few grains as a true spur. δ-rays have tortuous paths while spurs from heavy ions are straight.

Also, spurs were excluded from counting if they definitely came from the entering track or the product nucleus at a detectable distance from the prong. One such case of a prong just preceding the event is shown in the photograph of Figure 34. A number of such prongs have been found on the product nucleus since it may be relatively heavy and of low velocity and, hence, in stopping may undergo many nuclear collisions giving rise to prongs nearly at 90 degrees. This behavior is discussed in Chapter VII. However, there are a number of stars where visible displacements appear between true prongs of the star. A displacement of the order of a micron (about the maximum) would correspond approximately to a time of the order

---

27. G. Bernardini, E. T. Booth, and S. J. Lindenbaum, Phys. Rev. 85, 826 (1952).

28. H. Fishman and A. M. Perry, Phys. Rev. 86, 167 (1952).

of 10^{-14} seconds.

The presence of cosmic ray stars, thorium stars, and cross tracks from protons knocked on by neutrons, can sometimes cause uncertainty as to whether a carbon-induced star is present. About half a dozen cosmic ray stars were definitely seen. They could not have been carbon stars since they were below the surface of the emulsion, with no entering carbon track. What, then, of a star on the surface with no detectable length of entering carbon track? If the forward collimation of the prongs was correct, these probably were carbon-induced, and the frequency of carbon stars versus cosmic ray stars would argue very strongly for the production by carbon particles. However, those where one or two microns of entering track could not be seen were rare (about six) and they were cast out. The error in doing so is almost eliminated in calculating the cross section curves by cutting off the calculation at the highest completely filled energy interval.

Stars from atoms decaying through the natural radioactive series often occur. Most of these are five-prong stars from the portion of the thorium series beginning with Th^{228}. Often there is a detectable displacement of the atom during the series of reactions but, in the cases where there is not, there will sometimes be a star with its center exactly on the carbon track. These can almost unmistakably be eliminated by the agreement in the lengths of the tracks with those from the thorium stars and by the fact that the carbon direction and energy are normal. Random proton tracks crossing a carbon track in perfect coincidence can similarly be excluded with reliability by the fact that neither the carbon nor the

proton seems to have been affected. Sometimes the proton direction can be seen by a variation in the density of grains.

The stars that must be examined most closely to distinguish between elastic and inelastic events are the two-prong stars. Elastic two-prong events can be classified rather closely. With C^{12} there is only one case where the angle between two elastic forks, in the laboratory system, can be less than 90 degrees. That is in the case where carbon knocks-on a proton. For elastic collisions of carbon with heavier nuclei than itself, the struck particle makes a short track nearly bisecting the external angle between the entering and leaving carbon tracks. The heavier the nucleus the more nearly the angle is bisected, because the struck nucleus acts more closely like a rigid wall, absorbing little energy from the carbon, and giving an angle of reflection equal to the angle of incidence both compared to the direction of the impulse. For C^{12} on C^{12}, the angle between the two prongs is always exactly 90 degrees. Such a collision is shown in Figure 22A. In the case of bombardments with C^{13}, elastic collisions with C^{12} can give an angle less than 90 degrees between the two prongs but the angle will not be much less. Any two-prong event, compatible in angle and energy with being elastic, was so classified.

For two-prong events where one prong is definitely an alpha particle, there is no question - the event is inelastic, because helium is not one of the emulsion constituents. When one prong is a proton, the inelastic events can be separated from the elastic collisions as follows:

(1) C^{12} can never be deflected more than $4^{\circ}48'$ by an elastic collision with a proton. This is seen by setting $\frac{d(\tan \theta)}{d \varphi} = 0$ in the

equation

$$\tan \theta = \frac{\sin 2\varphi}{\frac{M_1}{M_2} - \cos 2\varphi}$$

where θ is the deflection of the incident particle of mass M_1 in the laboratory system and φ is the laboratory angle the struck particle makes with the incident particle. The maximum θ occurs when

$$\cos 2\varphi = \frac{M_2}{M_1} \qquad \text{and if} \quad M_1 \gg M_2, \quad \theta_{max} \approx \frac{M_2}{M_1}$$

or in the present case, the precise $\tan \theta_{max} = \frac{1}{\sqrt{143}}$.

(2) If the proton track goes backward in the emulsion ($\varphi > 90°$), the event was classified as a star. If the event were from collision of C with H, it would be a (p,p') inelastic scattering from the proton's viewpoint. (3) There are, of course, inelastic scatterings of protons into forward angles by the carbon nucleus. Neither the angle nor the energy unbalance is generally enough to distinguish these from elastic events with any certainty. So far as is known, all of these were classified as elastic and no correction was made to compensate. (4) There is a case of a two-prong star with one prong a proton where the angle condition for an elastic knock-on is satisfied but there would be a gross discrepancy in the energy taken from the carbon nucleus if it were the heavy nucleus after the event. The discrepancy shows that there was not a collision with a proton, either elastic or inelastic, but with a heavier nucleus which emitted a single proton into a forward angle. Such events were, of course, classified as inelastic two-prong stars.

The cross sections of the aggregate of elements in the emulsion for production of stars by incident C^{12} and C^{13} are compared in Figure 8, from the data of Table 3.3. The cross section was computed by the formula:

$$\sigma(E_i) = \frac{n(E \leq E_i)}{N \rho_a R(E_i)} \qquad (3.1)$$

where n is the number of events produced by the N total incident particles when their energy was less than or equal to any selected energy, E_i, which one wishes to consider as the incident energy of the particles. E_i may be taken as the original energy from the cyclotron, E_o, or any arbitrary lesser value. $R(E_i)$ is their residual range at the energy E_i from the range-energy curves, and so is quite accurately known for a prescribed E_i. ρ_a is the atomic density in the emulsions.

$$\rho_a = \sum \rho_i \text{ (gm/cm}^3\text{)} \frac{6.023 \times 10^{23} \text{ (atoms/gm at wt)}}{M_i \text{ (gm/gm at wt)}}$$

The distinction should be noted that the cross sections in Fig. 8 are a function of the initial kinetic energy of the carbon ion, not of the instantaneous kinetic energy. Therefore, $\sigma(E_i)$ is an integral or average type of curve, a function of the upper limit of the integral and, hence, depending on all the energies lower than the particular E_i. The cross section as a function of the instantaneous energy is a differential curve which may be called the excitation function or the instantaneous cross section. For it we can write:

$$\sigma(E, E + \Delta E) = \frac{\Delta n (E, E + \Delta E)}{N \rho_a \Delta X(E, E + \Delta E)}, \text{ or } \sigma(E) = \frac{1}{N \rho_a} \frac{dn(E)}{dX} \qquad (3.2)$$

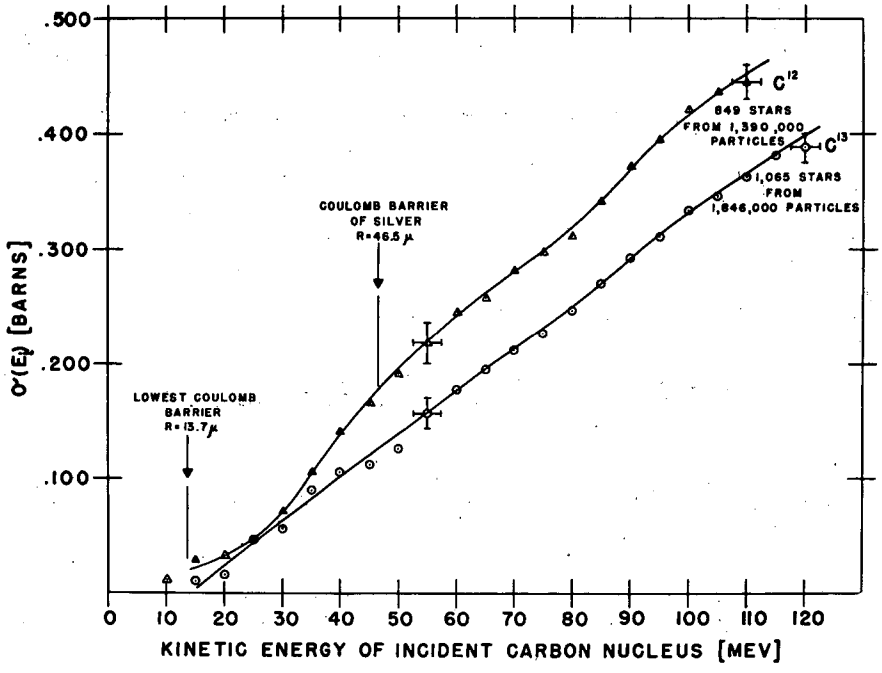

COMPARATIVE CROSS SECTION
FOR STAR PRODUCTION
BY INCIDENT C^{12} AND C^{13} NUCLEI

FIGURE 8

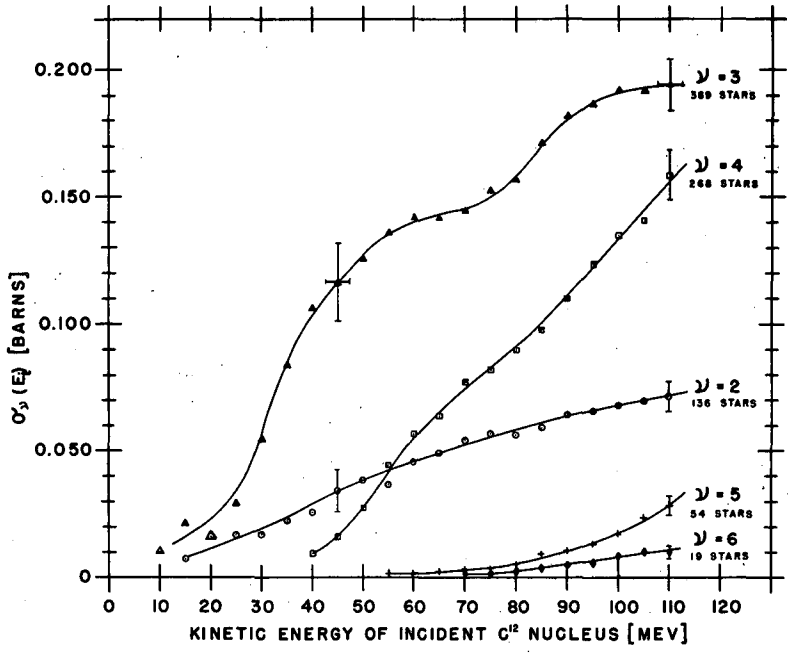

CROSS SECTION IN EMULSION
AS A FUNCTION OF ENERGY FOR REACTIONS
OF ν PRONGS PRODUCED BY
INCIDENT C^{12}

MU 3797

FIGURE 9

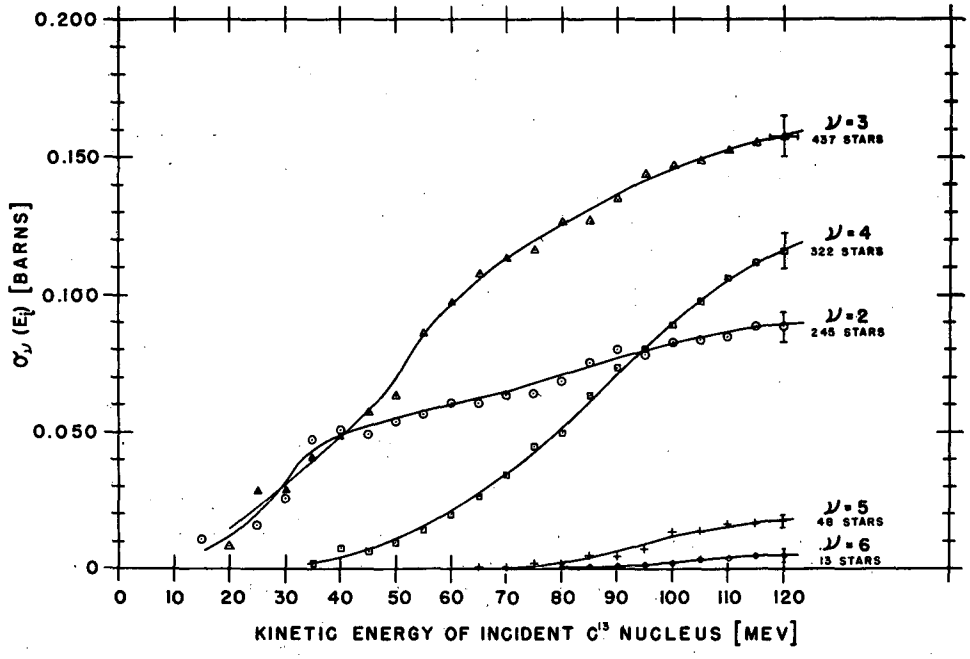

CROSS SECTION IN EMULSION AS A FUNCTION OF ENERGY FOR REACTIONS OF ν PRONGS PRODUCED BY INCIDENT C^{13} —

FIGURE 10

Since the $\sigma(E_i)$ curves in Fig. 8 appear to have some fine structure, especially in the case of the C^{12} curve, similar curves were plotted for each number of prongs, both for C^{12} and C^{13}. These are shown in Figs. 9 and 10 and are quite enlightening. The two-prong star curve is regular, (except for a step rise at the beginning in the C^{13} case) as are the five- and six-prong curves. The latter are rising slowly as is to be expected. The three-prong star curve, however, shows a complex structure. To a lesser extent, the four-prong curve appears to be similar. The causes for these deviations are quite certainly the stripping and impact disintegration of the C^{12} nucleus, as will be seen even more clearly in the instantaneous cross section curves of Figs. 12 and 13, which will be discussed later.

In calculating $n(E_i)$ from Eq. (3.1), the curve is smoothed by the fact that n cannot be precisely known as a function of E. We get $R(E_i)$ from the range-energy curve, but how can be know whether an event occurred when the residual range was less than $R(E_i)$? Only by measuring the distance X to the event and subtracting it from the average range for the plate. As we saw, because of the considerable standard deviation in R, nearly the same for each plate, we can only say that a definite X corresponds to an expected energy value with a $\sigma\{E\} \approx 2.4$ Mev. Since the cross section curve is an integral curve taking all events up to a given energy value, the uncertainty in E at the time of the event is of little importance except at the very low end of the curve and at the highest energy point of the curve.

For both C^{12} and C^{13}, the highest energy point is too low. Both curves were stopped with the last 5 Mev energy interval completely filled

on all the plates. (This accounts for only 849 C^{12} stars entering the calculation out of 865 found on the plates, and only 1065 C^{13} stars out of 1114 on the plates where the distance to the event was recorded. To speed up the search for bismuth fission, the data recorded were curtailed on later plates.) On some of the plates the last energy interval was barely filled. Consequently, there was not the contribution from the next higher interval that would normally occur as a result of the uncertainty in knowledge of the energy at the time of the event.

At the low energy end of the curve, the fluctuations are expected to be quite violent both because of the small number of events and of the uncertainty in energy. It will be noticed that there are perhaps more events at low energies than would be expected since the lowest Coulomb barrier requires 16.5 Mev kinetic energy. It would be the a priori logical conclusion that the very low energy tail was due to the carbon particles which initially had a greater than average energy and, hence, now have a longer residual range than is indicated. However, there is some evidence for the existence of reactions at low energies, possibly even lower than the lowest Coulomb barrier. The possibility and the evidence are discussed in Chapter V.

The standard deviation shown in the value of the cross section in Fig. 8 is solely that due to the statistical $\sqrt{n}$ fluctuation to be expected in the number of events on which the curve was based.

In the calculation of the cross section, $\sigma(E_i)$, all of the residual range of the carbon particle was used. This is the usual procedure for calculating the cross section in emulsion since the cut-off energy below

which a reaction cannot be produced varies with the different constituents. However, such a procedure prejudices the result in comparing a short range particle to a longer range one. The low energy cross section would be larger if we counted only the nuclei the particle met in the effective part of its range. The range occurs in the formula only for the purpose of giving the number of nuclei in the distance the particle penetrates.

Another factor that affects the value of the cross section found is what atoms are included in calculating the atomic density. When the bombarding particle is a proton or a neutron, it is evident that a star cannot be produced in a collision with hydrogen nucleus. Hence, the hydrogen atoms of the emulsion are excluded in calculating σ. The usual procedure is to do the same when the bombarding particle is a deuteron. However, with carbon particles the hydrogen nuclei can produce a star and, in the curves shown each hydrogen atom has been counted with exactly the same probability weight for creating a reaction as every other atom in the emulsion. Such a procedure is faulty in two respects: (1) The hydrogen nuclei should not be counted at a value higher than their comparative effective geometric cross section; (2) Reaction possibilities of carbon with hydrogen nuclei for producing stars are poor.

Regarding the latter, we may say that the carbon nucleus is able to get but a small fraction of its energy into a reaction with a proton. Let us consider C^{12}-induced reactions first, then those from C^{13}. Twelve-thirteenths of the kinetic energy of C^{12} remains as energy of motion of the entire system. The possible reactions of 112 Mev C^{12} on hydrogen are exactly those of 9.3 Mev protons on C^{12}. From Tables 3.1 and 3.2 the total

excitation of the compound nucleus even at full energy is (1/13)(112 Mev) + 1.85, or 10.53 Mev. There seems to be only one reaction from C^{12} at this energy with a charged particle coming out. That reaction is $C^{12}(p,p')C^{12}$. The (p,d) reaction, if it exists, and the (p,pn) reaction have too high thresholds. One might ask about a $C^{12}(p,\alpha)B^9$ reaction. Nothing appears to exist in the literature about this reaction, the compound nucleus seeming to decay by other means. The reaction would give a complete disintegration since B^9 is unstable to break-up into Be^8 + p by about 0.26 Mev[10] (or by 0.186 Mev)[29]. It breaks up in about 10^{-21} seconds. The resulting star would look like an impact disintegration plus a proton, with no trace of a product nucleus. No star fulfilling these specifications seems to be present. Therefore, the threshold must be too high. From mass excesses alone, the threshold for the reaction would be 7.53 Mev[10] in the center of mass system, with 10.53 Mev excitation available from 112 Mev C^{12}. However, the mass excesses are based on the ground state. In the ground state C^{12} has even parity and B^9 odd. Consequently, the proton cannot be captured in the s-state but must be in the p-state.

For C^{13} on hydrogen the reaction possibilities are better. Besides the (p,p') reaction, (p,d) and (p,α) reactions appear to be easily reached, requiring respectively a minimum of 2.70 Mev and 4.14 Mev[29]. This fact apparently accounts for the early sharp rise in the $\sigma(E_i)$ curve for two-prong stars from C^{13} and for its value being consistently higher than that from C^{12} (Figures 9 and 10). No routine analysis has been made of

---

29. W. F. Hornyak, T. Lauritsen, P. Morrison and W. A. Fowler, Rev. Mod. Phys. 22, 291 (1950).

two-prong stars containing an alpha to see if they were a (p,α) reaction, but a few cases (three or four) could not fail to be noticed since they occurred early enough, with low enough energy alpha emitted, that the sum of the distance traveled by the entering C^{13} and the product nucleus were noticeably longer than the range of C^{13} ions.

As a general feature of carbon reactions on hydrogen we notice that the cut-off energy determined by availability of kinetic energy in the center of mass system to cross the Coulomb barrier is not particularly low, since it is higher than that for reactions with carbon, nitrogen or oxygen. In compensation there is some possibility for a proton to tunnel through the barrier. Hydrogen atoms are by far the most numerous type in the emulsion - 41.3 percent of the total. If hydrogen were excluded in calculating the cross section, the C^{12} cross section at 110 Mev would go from 0.450 barns to $\frac{0.450}{1-.413}$ or 0.767 barns. This figure is not quoted with the idea that hydrogen should be excluded but rather to see the order of magnitude from such a modification.

A more reasonable modification, especially in view of the classical behavior of the carbon ion, would be to attribute reaction cross sections to the emulsion constituents in proportion to their geometric cross section, that is

$$\frac{\sigma_1}{(A_1^{1/3}+A_c^{1/3})^2} = \frac{\sigma_2}{(A_2^{1/3}+A_c^{1/3})^2} = \cdots$$

By definition of cross section: $\frac{n}{N} = \sum_i (\rho a)_i \sigma_i (R_{eff.})_i$

Here the effective range of the carbon ion for each constituent, $R_{eff.}$, has been inserted since an average or total range need no longer be used. $R_{eff.} = R$ (110 Mev) - $R_{residual}$ at Coulomb barrier from Table 3.2.

We may use Table 3.2 to get each $(\rho_a)_k \sigma_k$ in terms of a standard σ_j, say σ_{Ag}, since by our assumption

$$\sigma_k = \sigma_j \frac{(A_k^{1/3} + A_c^{1/3})^2}{(A_j^{1/3} + A_c^{1/3})^2} = \sigma_j \frac{S_k/\rho_k}{S_j/\rho_j}$$

or $$\rho_k \sigma_k = \rho_j \sigma_j \frac{S_k}{S_j}$$

The calculated cross sections, $\sigma_j(E_i)$, for reactions induced by 110 Mev C^{12}, are given below. The total number of reactions at 110 Mev was taken as that actually found, rather than making the correction for the unfilled adjacent energy interval.

Element	Ag	Br	I	C	H	O	S	N
$\sigma_j(E_i = 110$ Mev) (barns)	1.135	0.994	1.222	0.479	0.248	0.528	0.682	0.505

The reaction cross section in each case is 38.7 percent of the geometric area calculated by $\pi r_o^2 (A_j^{1/3} + A_c^{1/3})^2$.

On the same basis of assigning reaction cross sections according to geometric area, it is of interest to group the elements according to mass into three groups. The percent of the events attributable to

each group on an area basis is as follows:

(1) Ag, Br, I: 45.96 percent

(2) C,O,S,N: 33.96 percent

(3) H: 20.08 percent

An even closer and considerably more informative comparison of the experimental reaction cross section with the geometric one can be made from the following considerations. Like the experimental cross section, the available geometric reaction area varies with the energy of the incident particle, since the collision area which leads to penetration to the inner nuclear forces is limited by the Coulomb and centrifugal barriers. This geometric area will be called the "penetrability cross section", σ_p, after Heidmann and Bethe.[30] The best comparison of the experimental reaction cross section and the available geometric area will be from their values as functions of the instantaneous energy, E. Hence, from equation (3.2), the experimental $\sigma(E, E + \Delta E)$ has been computed (Table 3.3) for comparison with $\sigma_p(E)$ (Table 3.4). The latter was calculated only for C^{12}.

σ_p is (classically) zero below the kinetic energy necessary to cross the Coulomb barrier (given in Table 3.2). Above that energy it at first rises sharply, then more slowly, because of the "centrifugal potential" barrier, which is especially important in the case of a heavy, large incident particle. The centrifugal potential energy is a fictitious term that arises from taking a two-body collision problem in the center of mass system and, after converting to an equivalent one-body

---

30. J. Heidmann and H. A. Bethe, Phys. Rev. 84, 274 (1951).

TABLE 3.3

E_i (Mev)	$R(E_i)$ (μ)	Cumulative number of events for $E \leq E_i$ classified according to prongs							Cumulative totals	$\sigma(E_i)$ (barns)	$\sigma(E, E \pm \Delta E)$ (barns)	Aver. No. Prongs $\bar{n}(E, E \pm \Delta E)$
		2	3	4	5	6	7	8				
CARBON 12												
5	4.3	0	0						0	0.0000	0.000	0.00
10	8.5	0	1						1	0.0116	0.022	3.00
15	12.4	1	3						4	0.0287	0.068	2.67
20	16.6	3	3						6	0.0322	0.0423	2.00
25	21.2	4	7						11	0.0462	0.0967	2.80
30	26.0	5	16						21	0.0719	0.1854	2.90
35	31.8	8	30	0					38	0.1063	0.2610	2.82
40	37.7	11	45	4					60	0.1417	0.3320	3.05
45	44.3	17	58	8					83	0.1667	0.3102	2.91
50	51.1	22	72	16	0				110	0.1915	0.3534	3.11
55	58.2	24	89	29	1				143	0.2187	0.4135	3.39
60	65.9	34	105	42	1				182	0.2458	0.4510	3.08
65	74.0	41	118	53	2	0			214	0.2575	0.3516	3.19
70	83.1	51	135	72	3	2			263	0.2816	0.4790	3.35
75	92.2	59	158	85	4	2			308	0.2975	0.440	3.16
80	102.0	65	180	103	6	3	0		357	0.3114	0.445	3.39
85	112.3	75	216	123	12	5	1		432	0.3424	0.648	3.43
90	123.0	89	251	152	15	7	1	0	515	0.3726	0.690	3.33
95	134.0	99	281	186	20	9	1	1	597	0.3965	0.663	3.55
100	145.0	111	313	220	28	14	1	1	688	0.4220	0.736	3.58
105	157.0	123	338	248	42	18	1	1	771	0.4370	0.615	3.67
110	169.1	136	369	268	54	19	2	1	849	0.4465	0.574	3.49
CARBON 13												
5	4.3								0	0.0000	0.0000	0.00
10	8.4	0							0	0.0000	0.0000	0.00
15	12.5	2	0						2	0.0107	0.0327	2.00
20	16.5	2	2						4	0.0162	0.0333	3.00
25	21.0	5	9						14	0.0445	0.1498	2.70
30	25.7	10	11	0					21	0.0545	0.0983	2.29
35	31.1	22	19	1					42	0.0900	0.2593	2.48
40	37.0	28	27	4					59	0.1063	0.1922	2.82
45	43.3	32	37	4					73	0.1124	0.1482	2.71
50	49.6	40	47	7					94	0.1263	0.2223	2.76
55	56.5	48	73	12					133	0.1570	0.3770	2.92
60	63.7	58	93	19	0				170	0.1780	0.3425	2.92
65	71.4	65	115	28	1				209	0.1952	0.3380	3.10
70	79.6	76	135	41	1				253	0.2120	0.3575	3.05
75	88.4	85	154	59	3	0			301	0.2267	0.3634	3.27
80	97.5	100	185	72	3	1			361	0.2467	0.4395	3.02
85	107.3	121	204	102	8	1			436	0.2707	0.5100	3.25
90	117.3	141	237	129	8	1			516	0.2930	0.5330	3.09
95	127.5	150	275	153	14	2			594	0.3107	0.5100	3.38
100	138.7	172	305	185	28	4			694	0.3338	0.5950	3.44
105	149.8	188	334	219	31	7			779	0.3463	0.5105	3.39
110	161.0	205	368	256	39	9			877	0.3630	0.5835	3.43
115	173.0	230	402	290	43	12			977	0.3814	0.5555	3.26
120	185.3	245	437	322	48	13			1065	0.3880	0.4770	3.34

problem by using the reduced mass, ($\mu = \frac{M_1 M_2}{M_1+M_2}$) and relative coordinates, then changing from a two-dimensional problem to a one-dimensional one by making use of an integral of the motion, the constant angular momentum, L. In quantum mechanics, the angular momentum is quantized, and in analyzing collisions, each L value is treated separately and the result finally summed. The reader is referred to Heidmann and Bethe's article.[30] Because of the closely classical nature of collisions from carbon ions in nuclei of comparable or greater mass and because of the great number of L values that would be involved, the exact quantum mechanical treatment will be replaced here by the classical approximation, which will be closely correct except in the case of C on H, which is not of much importance. In the classical two-dimensional center of mass problem, $L = \mu v_o b$ where v_o is the relative velocity before encountering potentials.

The centrifugal potential energy term is: $V_{cf} = \frac{L^2}{2\mu r^2}$ where r is the distance between the particles at any time.

$$V_{cf} = \frac{1}{2}\mu v_o^2 \frac{b^2}{r^2}$$

When $b=0$, $V_{cf}=0$. If b should equal R (particles passing by, just touching), $V_{cf} = K E_{cm}$ where KE is the initial kinetic energy with respect to the center of mass. Therefore, in calculating b_{max}, the maximum impact parameter at which the particle can cross the fixed Coulomb barrier, we see that beginning at the point where $KE_{cm} = V_{coulomb}$, b_{max} rises sharply from zero and, as the KE_{cm} increases, b_{max} asymptotically approaches R. R denotes the distance necessary for a penetration to the inner nuclear

forces, namely, $R = r_0(A_1^{1/3} + A_2^{1/3})$. The penetrability cross section, or instantaneous geometric cross section for nuclear reaction, will, of course, be given by $\sigma_p = \pi b_{max}^2$. To find b_{max}: At closest elastic approach, $V_{Coul} + V_{cf} = (KE_{cm})_{initial}$ which gives

$$\frac{Z_1 Z_2 e^2}{R} + \frac{1}{2}\mu v_0^2 \frac{b_{max}^2}{R^2} = \frac{1}{2}\mu v_0^2$$

$$\sigma_p = \pi b_{max}^2 = \pi R^2 \left(1 - \frac{V_{coul}}{KE_{cm}}\right)$$

$(\sigma_p)_i$ for the collision of the i^{th} type of nucleus with carbon can be converted into the composite penetrability cross section, σ_p, by the definition of $\sigma(E, E + \Delta E)$:

$$\frac{\Delta n\,(E, E + \Delta E)}{N} = (\Delta X)\sum (\sigma_p)_i (\rho_a)_i = (\Delta X)(\sigma_p)\sum (\rho_a)_i$$

$$\sigma_p = \frac{\sum (\rho_a)_i (\sigma_p)_i}{\sum (\rho_a)_i} = \sum (\sigma_p)_{partial,\, i}$$

where $(\sigma_p)_{partial,\, i}$ is the contribution of $(\sigma_p)_i$ weighted according to the fractional number of the i^{th} nuclei to the total,

$$(\sigma_p)_{partial,\, i} = \frac{(\rho_a)_i (\sigma_p)_i}{\sum (\rho_a)_i}$$

The tabulated results of this calculation for C^{12} are given in Table 3.4.

TABLE 3.4

PENETRABILITY CROSS SECTIONS FOR NUCLEI IN EMULSION UNDER C^{12} BOMBARDMENT.

Element	Atom Percent	b_{max} (cm x 10^{13}) for Coulomb and centrifugal barrier penetration, for stated KE_{lab} of C^{12}. KE_{lab}(Mev)							
		20	30	40	50	60	80	100	120
Ag		0.000	0.000	0.000	2.492	4.551	6.233	7.052	7.549
Br		0.000	0.000	1.777	4.343	5.414	6.512	7.089	7.449
C		2.618	4.205	4.806	5.133	5.340	5.588	5.732	5.825
H		0.000	1.905	2.794	3.212	3.462	3.751	3.915	4.020
O		1.898	4.107	4.848	5.242	5.489	5.784	5.953	6.064
N		2.314	4.170	4.838	5.198	5.425	5.695	5.851	5.953
Classical Penetrability Cross Section, $\sigma_p = \pi b_{max}^2$ (barns)									
Ag		.0000	.0000	.0000	.1951	.6507	1.220	1.562	1.790
Br		.0000	.0000	.0992	.5926	.9208	1.332	1.579	1.743
C		.2151	.5555	.7256	.8277	.8958	0.981	1.032	1.066
H		.0000	.1140	.2452	.3241	.3765	0.442	0.482	0.508
O		.1131	.5299	.7384	.8633	.9465	1.051	1.113	1.155
N		.1683	.5463	.7353	.8488	.9246	1.019	1.076	1.113
$(\sigma_p)_{partial}$(barns) $= \frac{(\sigma_p)_i (P_a)_i}{\Sigma (P_a)_i}$									
Ag(+I)	13.071	.0000	.0000	.0000	.0255	.0850	.1595	.2042	.2340
Br	12.482	.0000	.0000	.0124	.0740	.1149	.1663	.1971	.2176
C	16.735	.0360	.0930	.1214	.1385	.1499	.1642	.1727	.1784
H	41.357	.0000	.0471	.1014	.1340	.1557	.1828	.1993	.2100
O(+S)	12.794	.0142	.0678	.0945	.1104	.1211	.1345	.1424	.1478
N	3.560	.0060	.0194	.0262	.0302	.0329	.0363	.0383	.0396
Total σ_p		.0562	.2273	.3559	.5126	.6595	.8436	.9540	1.0274

To reduce the amount of calculation, iodine and sulphur were not included until the final partial cross sections, when their atomic fractions were included as if they were respectively silver and oxygen.

Compare first the experimental instantaneous cross section for C^{12} and its penetrability cross section as given in Figure 11. Up to about 50 Mev, the curves agree quite well in magnitude. This is approximately the point where silver and bromine contributions to the cross section rise sharply. The geometric curve, although it has some detailed structure, does not seem to correspond in detail to that of the experimental curve. It should be borne in mind that while the experimental curve is for charged particle emission only, the geometric curve includes as well the reactions where only neutrons are emitted. Such reactions are according to theory[30,31] of appreciable quantity only with the heavier elements of the emulsion. This consideration should account for most of the difference between the two curves.

In order to make sure that the considerable diverging between the two curves in the region 50 to 75 Mev is not due to some phenomenon peculiar to C^{12} alone (such as its impact disintegration), the experimental cross section for C^{13} was plotted in the same figure (without showing the standard deviations). This curve shows at once that the effect is present for both C^{12} and C^{13} and is almost exactly the same in detail. Hence, ascribing the divergence to pure neutron stars is given greater credibility. Horning and Baumhoff[31] calculate that under deuteron bombardment at 35 Mev

---

31. W. Horning and L. Baumhoff, Phys. Rev. 75 370 (1949).

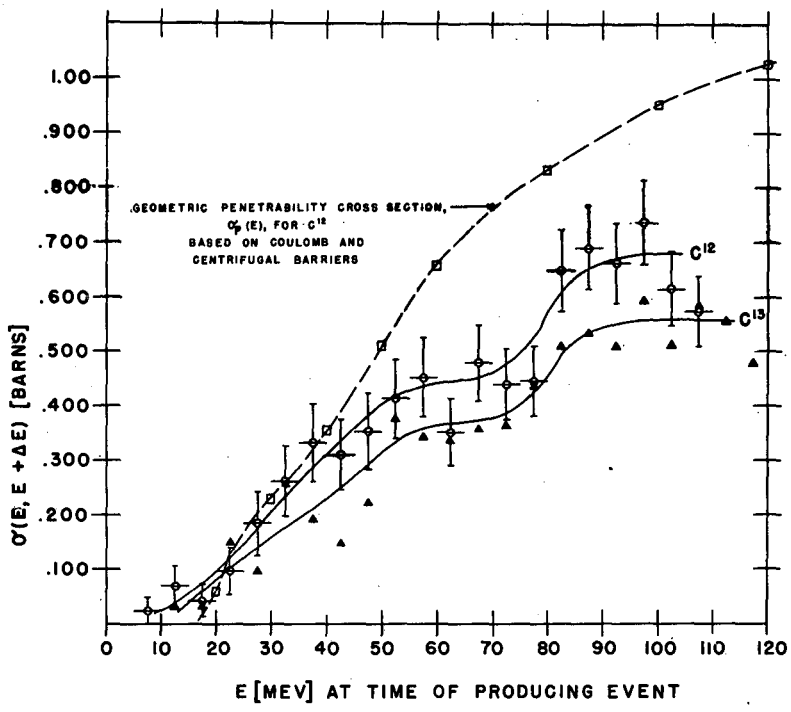

EXCITATION FUNCTION FOR
STAR PRODUCTION IN EMULSION BY C^{12} AND C^{13}

FIGURE II

MU 3799

incident energy, silver and bromine are almost certain to evaporate neutrons only. As the deuteron energy increases, the cross section for producing a charged-prong star rises rapidly, from about one-tenth the geometric cross section at 35 Mev to over nine-tenths at 190 Mev. Heidmann and Bethe, considering excitation from 17 Mev γ-rays, calculate that copper will evaporate about 83 percent neutrons and the percentage of neutrons increases rapidly with Z. At iodine, they say protons are absent and two-neutron emission begins to be possible. When bromine is the target nucleus in the present case of carbon ion bombardment, pure neutron stars should occur as predicted for deuteron or photon bombardment and, since the pure neutron stars favor low excitation, the effect on the experimental cross section is seen early. When it disappears, it does so rapidly, giving the sharp rise to the curve between 75 and 85 Mev. With silver as the target, the effect probably does not exist. The reason for this is that Ag + C gives, as compound nucleus, iodine isotopes which are already far neutron deficient. As a consequence, the production of pure neutron stars will be highly improbable. When bromine was the target of the carbon ions, the compound nucleus lay on or near the stability curve.

A factor which might cause a gradual divergence between the actual cross section and the penetrability cross section is that impact parameters corresponding to high angular momenta might prevent the occurrence of some reactions even after penetration of the barrier, and, hence, give a "sticking probability" less than one. An effect in the other direction, giving the experimental cross section an advantage over the geometric,

may be found in impact disintegration and stripping of the carbon nucleus, provided it can occur in cases where the carbon nucleus would have been unable to penetrate the barriers of the target nucleus. In Chapter V the question will be discussed.

Since the excitation curves of C^{12} and C^{13} for stars of all numbers of prongs showed a considerable similarity except for a greater rise at low energy for the C^{12} curve, it was thought of interest to see if the similarity could be seen in the three-prong and four-prong excitation functions individually. These are the cases where a divergence due to stripping and impact disintegration should appear. Figures 12 and 13 are plots for three-prong and four-prong stars respectively, with the statistical fluctuation of the points indicated for C^{12} only. The data can be obtained for Table 3.3. In judging the trends indicated by the plotted points, it must be borne in mind that the number of points per energy interval is inadequate to give a well-determined curve. Curves have been sketched in visually to give the best fit for the C^{12} and C^{13} points. However, no attempt has been made to pass an analytical curve through the data according to the theory of errors. The drawn curves are subjective; the reader may wish to draw curves emphasizing the similarity rather than the difference between the two particles. For instance, the C^{13} curve drawn has minimized some indication of a high energy hump such as C^{12} has. Further, on the high energy end of each curve, there is a falling-off which, since it occurs for both C^{12} and C^{13}, might be real. There is no reason why the unfilled interval beyond the last should have an effect reaching the next to the last interval.

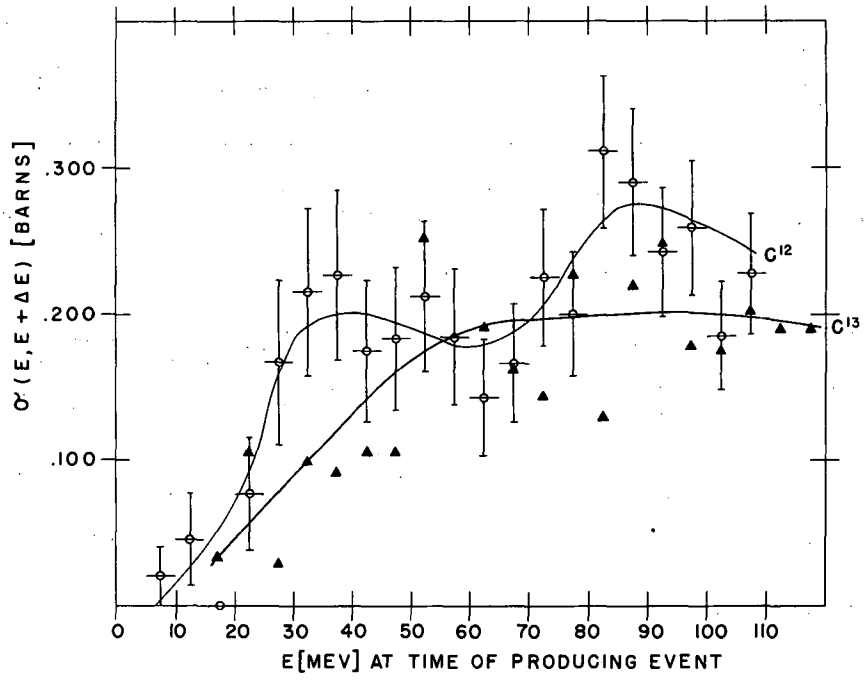

EXCITATION FUNCTION FOR
3 PRONG STARS
FROM BOMBARDMENT BY C^{12} AND C^{13}

MU3800

FIGURE 12

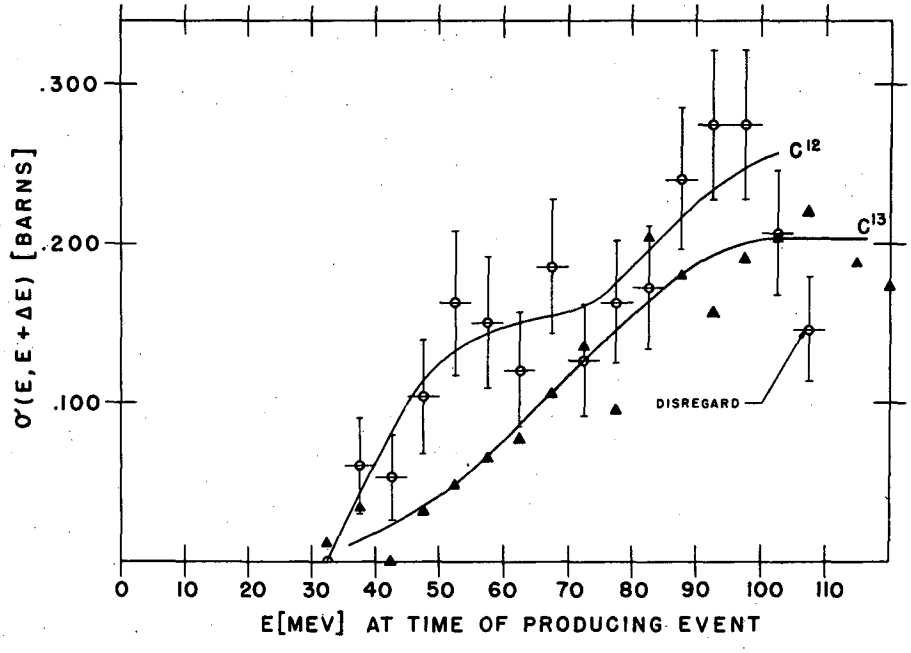

EXCITATION FUNCTION FOR
4 PRONG STARS
FROM BOMBARDMENT BY C^{12} AND C^{13}

FIGURE 13

MU3801

There are differences between the curves, however, which would be recognized by all observers. Especially in the three-prong star curves, there is a sharp rise in the excitation function for C^{12} at low energies which is not duplicated in the case of C^{13}. This is the "stripping hump". The preference of low energies by the stripping phenomenon will be discussed in Chapter V. For the four-prong star excitation function, there is a similar but smaller difference in the rise at the low energy end; the hump that is the difference between the two is caused by impact disintegration, which is greater for C^{12} than for C^{13}.

A point of interest regarding the magnitude of the cross section may be to compare it with the cross section in emulsion found for other particles. Considerable caution is required because of the different circumstances - differences in energy, type of incident particle, how the geometric cross section is computed, et cetera. A full discussion is not given here. The reader should consult the original article for the details of the calculations.

For protons, Germain[32] has measured the cross section at various energies from 95 to 340 Mev in sensitive emulsions (Ilford G-5). The cross section rises, not smoothly, from about 0.13 barn at 95 Mev to about 0.29 barn at 340 Mev. At 340 Mev, the mean free path is 73 cm. Hydrogen in the emulsion is, of course, excluded in calculating the number of atoms per unit volume. Bernardini, Booth, and Lindenbaum,[27] using protons of 350 to 400 Mev in G-5 emulsion and including all inelastic processes (stars of two or more prongs, one-prong stars, "zero"-prong

---

32. L. S. Germain, Phys. Rev. 82, 596 (1951).

stars, "stops" and inelastic scatterings greater than 10 degrees), got a mean free path of approximately 54 ± 9 cm and quote the mean free path based on geometric cross sections as 25 cm.

For deuterons, the study by Gardner and Peterson[33] gives no estimate of cross section since the plates were desensitized, which prevented counting the number of incident deuterons.

For alpha particles from 50 to 200 Mev in Eastman NTA emulsions, Gardner[34] found a cross section rising from 0.1 barn at 50 Mev to a maximum of 0.3 barn at 130 Mev and falling to about 0.15 barn at 200 Mev. All the elements of the emulsion were used in computing this cross section.

In the present study the cross section values, $\sigma(E_i)$, from carbon bombardment were still increasing with energy at the highest energies available. For C^{12} at 110 Mev, $\sigma(E_i) = 0.446$ barn, based on 849 stars. For C^{13} at 120 Mev (nearly the same velocity as 110 Mev C^{12}) $\sigma(E_i) = 0.388$ barn, based on 1065 stars. In the case of C^{12}, all the plates used were E-1, which is quite a sensitive emulsion. For instance, a proton with a range of 3000 microns (over 26 Mev) from a cosmic ray event was easily followed. Accordingly, it is unlikely that stars were missed because of invisibility of the prongs. The percentage of stars missed in scanning or misinterpreted as elastic is believed not large. Further, the estimate of the total number of tracks on a plate should not be off by more than about two percent. Hence, the main uncertainty in the cross section is the statistical fluctuation in the number of events, which is shown on the

---

33. E. Gardner and V. Peterson, Phys. Rev. 75, 364 (1949).

34. E. Gardner, Phys. Rev. 75, 379 (1949).

curves of Figure 8.

There is a real discrepancy between the cross sections from C^{12} and C^{13} bombardment. Several reasons for a difference between the two can be put forward. The first is that most of the C^{13} plates were Ilford D-1 loaded with bismuth, a much more insensitive emulsion than the E-1 used with C^{12}. Hence, events were more easily overlooked. There must be some truth in this. However, a partial check is available, since two plates of C^{13} on E-1 emulsion were read. They contained 238 stars in 382,000 tracks, giving a cross section of 0.409 ± 0.026 barn. This is higher than the average for the other C^{13} plates but is definitely below the C^{12} cross section. A second reason for the discrepancy can be found in the impact disintegration and stripping of C^{12}, a much more improbable process in the case of C^{13} bombardment. This is quite surely the main source of difference between the cross sections. A third factor that might produce a small difference between C^{12} and C^{13} is that the C^{13} carries an extra neutron into the compound nucleus, which consequently is less neutron deficient than in the C^{12} case and, hence, is likely to have more pure neutron stars. To conterbalance, C^{13} has more star reactions with hydrogen than C^{12} does.

The D-1 bismuth-loaded emulsions without doubt had an effect on the finding and classification of stars. In the D-1 emulsion, tracks of protons and alphas are more difficult to identify than in the E-1, and protons of moderate range can easily be missed. For instance, a proton of range 600 microns (about 10 Mev) would probably be missed unless the star had been located by a heavier prong and the region carefully searched.

Because of the great momentum carried into a reaction by a carbon ion, the forward velocity of evaporated particles may be considerable if the particle velocity in the center of mass system adds onto the center of mass motion. Accordingly, two-prong stars can easily be missed in D-1 emulsion.

In Fig. 14 is shown the distribution of stars from C^{12} and C^{13} according to the number of prongs per star. For comparison these curves have been normalized to a percentage basis. The number of stars on which each point is based is written in adjacent to the point. Regarding the prediction in the last paragraph that many two-prong stars from C^{13} will be missed, we notice that, on the contrary C^{13} shows a higher percentage of two-prong stars than does C^{12}. There are two evident reasons why. The first is the real contribution to the number of two-prong stars of of C^{13} by its reactions with hydrogen. The second is an apparent contribution to C^{13} two-prong stars which is actually a deficiency in the percentage of C^{12} two-prong stars because of the large number of three- and four-prong stars contributed by stripping and impact disintegration.

The general shape of the curves is similar to that for other bombarding particles. The most probable number of prongs for evaporation stars seems almost universally to be three. Horning and Baumhoff,[31] interpreting the data of Gardner and Peterson[33] on deuteron bombardment, have given a theoretical discussion of the number of prongs expected from a star. The average number of prongs is a better criterion than is the most probable number. For C^{12} of initial energy 110 Mev, the average number of prongs from the totality of stars is 3.36; for C^{13} of 120 Mev, it is 3.17. As

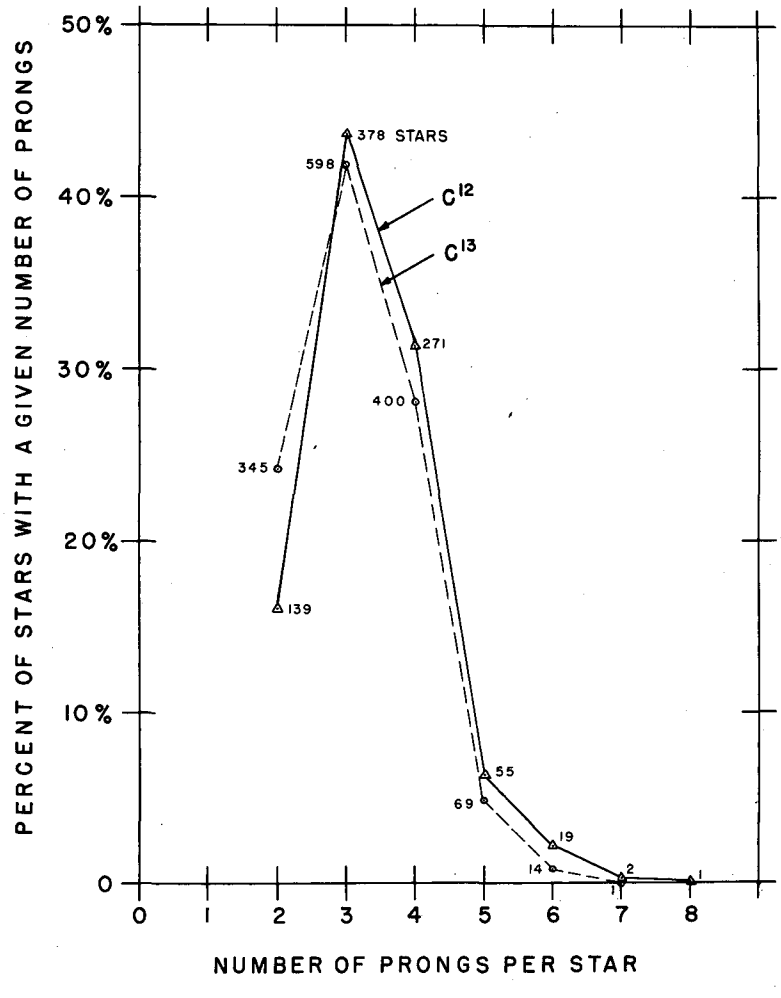

FIGURE 14

MU3802

with the cross section, the detail can be shown best by plotting the average number of prongs for stars produced in an energy interval, $n(E, E + \Delta E)$. Such a plot has been made in Fig. 15 and approximate curves sketched in. For both C^{12} and C^{13} the curves rise slowly as expected It is interesting that the C^{13} curve lies below that for C^{12}. Perhaps this is attributable in the low energy region to the three- and four-prong stars from stripping and impact disintegration of C^{12} compared to the greater prevalence of the two-prong stars from C^{13}. In the high energy region it may be due to four-prong stars from impact disintegration and possibly to cases of complete or partial double disintegration.

The concavity or convexity of the prong number distribution in Fig. 14 at four-prongs is a fair indication of the excitation of the compound nucleus. For instance, Gardner and Peterson found, for deuterons of 35 and 90 Mev, curves that were concave at four prongs but, at 130 and 190 Mev, curves that were convex. In the case of carbon ions the curves are convex at the four-prong point. The similarity of the prong-distribution curves for evaporation stars is that the history of a compound nucleus is independent of how it was formed for a given composition of neutrons and protons and a given excitation. The carbon ions will not give the direct knock-on of particles found in cosmic rays and in high velocity nucleon bombardments, but the subsequent de-excitation of the compound nucleus formed will be describable in the same terms. Carbon ions will, of course, tend to give compound nuclei of somewhat different composition (proton rich) than results from other particles. The silver and bromine nuclei are the only components in emulsion where the inelastic events can

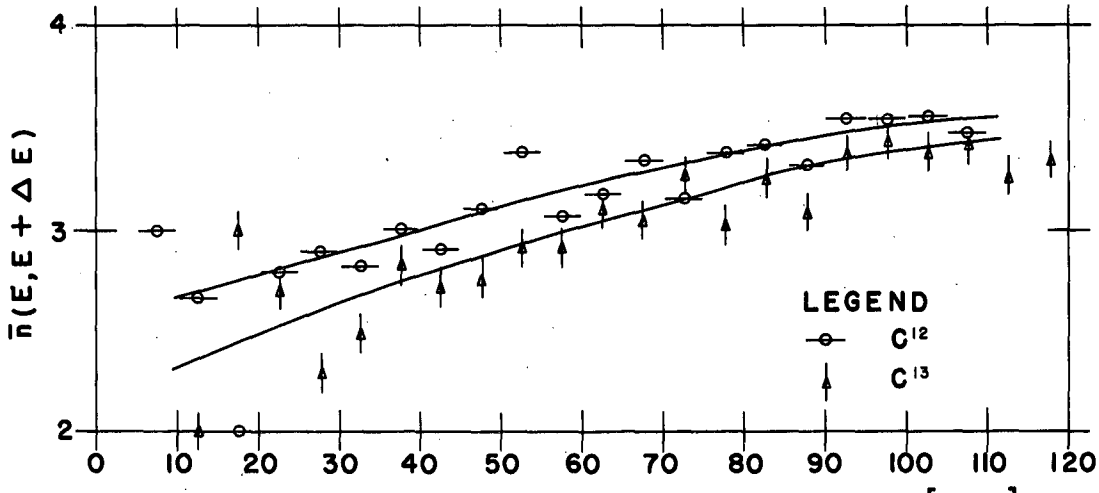

AVERAGE NUMBER OF PRONGS, $\bar{n}(E, E+\Delta E)$, FROM C^{12} AND C^{13} FOR STARS OCCURRING IN 5 MEV ENERGY INTERVALS

FIGURE 15

MU3803

well be described by the compound nucleus model. Carbon, oxygen, and nitrogen are too easily broken up directly into alphas and protons to be treated on the same basis.

A characterization of reactions that is not of great importance but that shows clearly the difference between bombarding particles is the distribution of prongs into sectors. Generally, sixty-degree sectors have been used, with the center lines of the sectors oriented with respect to the incident particle direction at 0°, 60°, 120° and 180 degrees. In the sectors at 60° and at 120°, the average for the right and left sectors is given. Figure 16 shows the distribution by sector from C^{12} and C^{13} bombardment compared with the distributions found by others for alphas, deuterons and neutrons of roughly comparable energy. The great difference is, of course, due to the momentum carried into the reaction. In the case of C^{12} and C^{13} the product nucleus almost always goes into the directly forward sector. As would be expected, C^{13} gives a little higher peak in the forward sector than does C^{12}. Table 3.5, giving the data for Figure 16, is below.

There is one feature of the distribution into sectors that is quite different from what one would naively expect and which gives some important information about the reactions. It shows up in the distribution by sectors only if such a distribution is plotted for various energies. For a given incident particle, the velocity of the system - target plus bombarding nucleus - with respect to the laboratory frame of reference, will vary with the incident velocity and the target mass, thus:

$$(M_1 + M_2)\ v\ \text{cm/Lab} = M_1\ v_1/\text{Lab}$$

TABLE 3.5

DISTRIBUTION OF STAR PRONGS BY 60 DEGREE SECTOR

Bombarding Particle	Percent in 60 degree sector			
	0°	$\pm 60^\circ$ Average	$\pm 120^\circ$ Average	180°
112 Mev C^{12}	59.60	14.00	4.56	3.34
121 Mev C^{13}	61.85	13.10	4.55	2.81
130 Mev deuterons[33]	33.66	19.35	10.50	6.62
50-200 Mev alphas[34]	∿43.00	∿21.50	∿5.00	∿3.00
∿150 Mev neutrons[35]	∿29.00	∿20.00	∿12.00	∿10.00

35. E. W. Titterton, Phil. Mag. 42, 109 (1951).

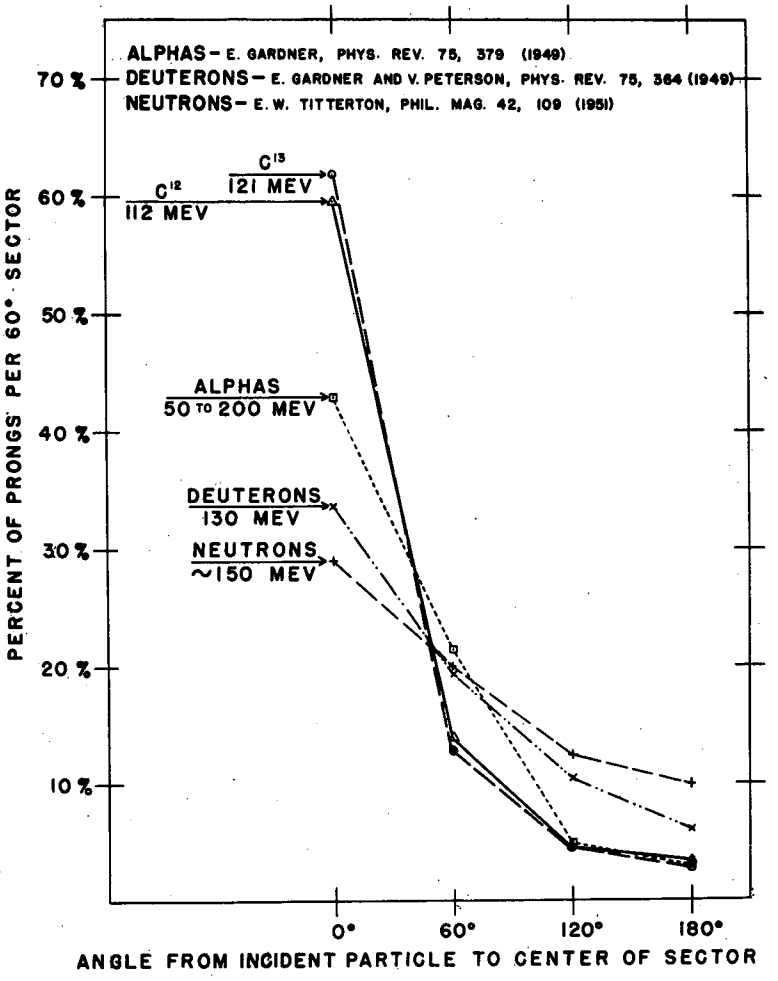

DISTRIBUTION OF PRONGS
INTO 60° SECTORS

MU3604

FIGURE 16

If we assume an isotropic distribution of prongs with respect to angle in the center of mass system, then the higher the velocity of the given incident particles, the more we expect the prongs in the emulsion - the laboratory frame of reference - to be directed forward. This relation should hold separately for each of the target particles. The reasoning is logically correct. But the observed data give just the opposite indication. Gardner and Peterson[33] in their Fig. 5 for angular distribution of prongs from deuterons of energies of 35, 90, 130 and 190 Mev, show that, as the incident energy increases, the proportion of prongs into the forward sector decreases.

The same result was observed for carbon ions, although it was recognized in a different way than by plotting the sector distribution versus energy. It possibly points out the effect a little more clearly. In analyzing the stars, a sequence on one plate was noticed where the ejection of a backward prong seemed to come preferentially when the distance to the event was short - that is, when the energy or momentum carried into the reaction was high. Qualitatively, these also appeared to be stars of a small number of prongs. It looked almost like a "splash" effect from the disruption of a considerable surface area by a forward moving plug of nucleons. To study the observation statistically, the measured distance to each event with one or more backward prongs was tabulated for the stars classed according to the number of their prongs and the average of these compared to the average for all stars of that class with and without backward prongs. Since the average range varies a little from plate to plate, the distance to each event was put in

terms of the fraction of the average range for that plate and finally a true fractional average was found for all plates, which was

$$\frac{\sum_i \sum_j \frac{X_{ij}}{\bar{R}_i}}{\sum n_i}$$

where i denotes the plate and j the event on it; X_{ij} is the distance to the event, $\bar{R}_i$ the average range of particles on that plate, and n_i the number of events of the given type on the plate. The data are summarized in Table 3.6 and plotted in Fig. 17 for C^{12} and C^{13}. Note the effect for C^{12}. For some plotted points the number of events averaged in (indicated alongside the point) is too small to be meaningful, but the other points are well determined. They indicate definitely that the higher the incident velocity for a given type of event, the less likely is the ejection of particles to be in the forward hemisphere in the emulsion. Especially marked is the effect for a small number of prongs - two- and three-prong stars. For two-prong stars, assuming the total mean range is about 171 microns, the average distance to all two-prong events is 70.6 microns, while the average to those with a backward prong is 58.4 microns. For three-prong stars, the average for all stars is 73.2 microns, while the average to events with one or more backward prongs is 62.2 microns, and to those with two or more backward prongs is 49.4 microns.

For C^{13}, oddly enough, the effect is not as distinct. The data indicate almost the same mean range for events with backward prongs as

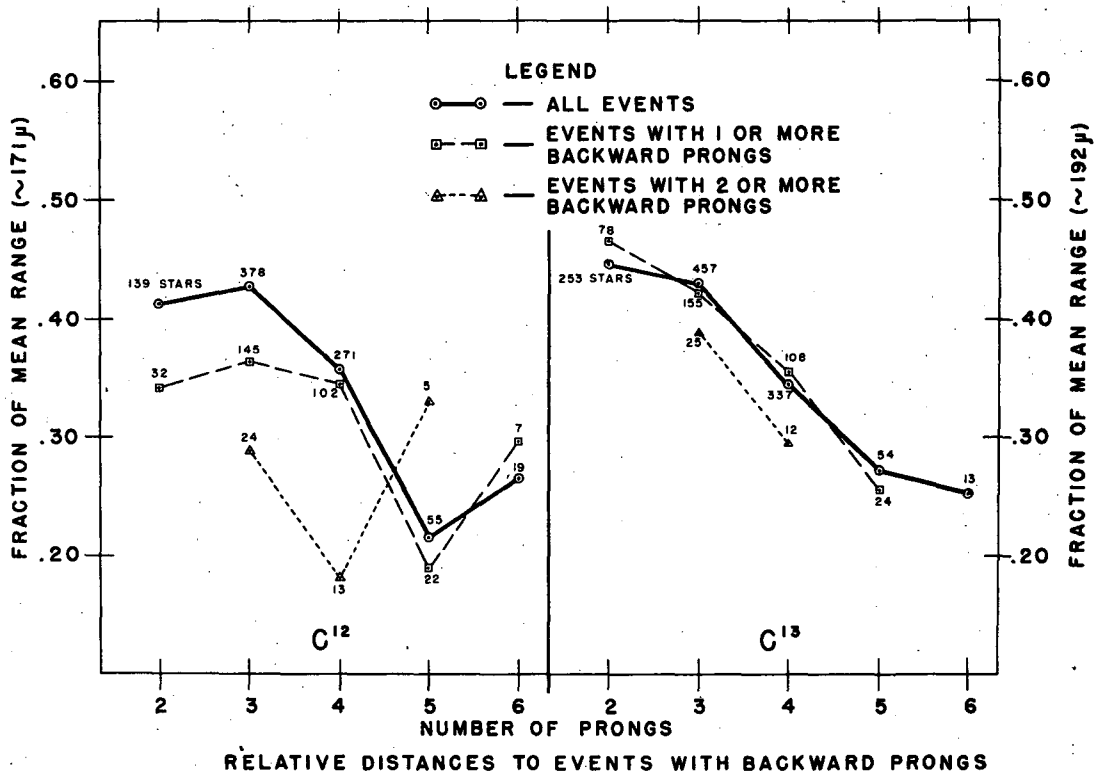

RELATIVE DISTANCES TO EVENTS WITH BACKWARD PRONGS

FIGURE 17

MU3805

TABLE 3.6

AVERAGE DISTANCE TO EVENTS WITH BACKWARD PRONGS COMPARED TO AVERAGE DISTANCE FOR ALL EVENTS.

Number of prongs	Number and fractional average distance for					
	All Events		Events with 1 or more prongs backward in laboratory		Events with 2 or more prongs backward in laboratory	
	Number	Distance	Number	Distance	Number	Distance
CARBON 12						
2	139	.4127	32	.3414	-	-
3	378	.4283	145	.3636	24	.2892
4	271	.3578	102	.3449	13	.1817
5	55	.2162	22	.1897	5	.3301
6	19	.2665	7	.2967	-	-
Possible and probable strippings and impact disintegrations						
3	155	.5199	36	.5080	4	.5911
4	103	.4089	28	.3975	1	.1470
C^{12} events after subtracting possible and probable stripping and impact disintegration						
3	223	.3647	109	.3159	20	.2288
4	168	.3264	74	.3250	12	.1846
CARBON 13						
2	253	.4467	78	.4659	-	-
3	457	.4293	155	.4218	25	.3890
4	337	.3446	108	.3537	12	.2943
5	54	.2716	24	.2553	-	-
6	13	.2526	-	-	-	-

for all events. Of course, the same average indicates the effect is present, because it would be expected that the probability of a backward prong in the emulsion would increase as the incident velocity decreased so that an isotropic distribution in the center of mass system was more nearly isotropic in the laboratory system. However, the effect is markedly less than for C^{12}. It will turn out that C^{13} is the anomalous case, not C^{12}.

In C^{12} the possibility existed that the observed results were due not so much to a short range for back ejection as to an unduly long range for forward ejection. The mechanism for such an effect was apparent - stripping and impact disintegration of the C^{12} nucleus. Accordingly, from the data in Chapter V, all possible and probable cases of stripping and impact disintegration were considered separately, as shown in Table 3.6. These cases did have a considerably longer than average range and a smaller percentage of backward prongs. However, the backward prongs occurred at a long range, too. The result was that, when these cases were subtracted out, the distance ratio of backward- prong events to the totality was hardly affected. The set of curves was merely displaced toward shorter ranges for three- and four-prong stars, to put them properly in line between the two- and five-prong stars.

To look at the effect in C^{12} in further detail, a histogram(Fig. 18) was plotted for the three-prong stars as a function of range intervals. The top part of the figures gives the number of all three-prong stars in the interval compared to the number with one or more prongs backward and two or more prongs backward. The lower half of Fig. 18 plots in histogram

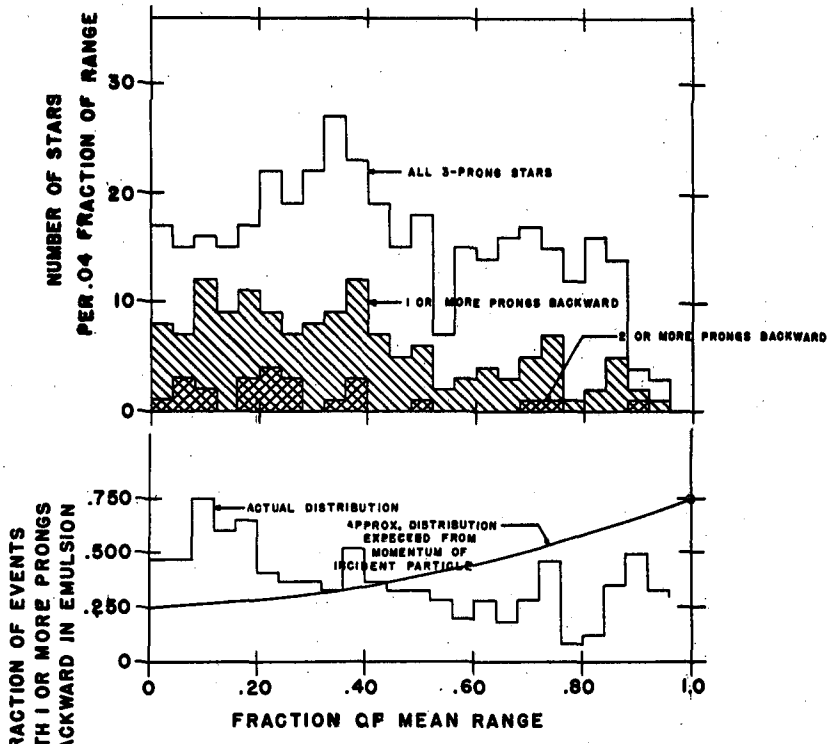

HISTOGRAM SHOWING BACKWARD PRONGS
AS A FUNCTION OF RANGE
3 PRONG STARS FROM C^{12}

FIGURE 18

MU 2806

form the percentage of the stars in the interval that have one or more prongs backward. Sketched in for comparison is an approximate curve of what distribution might possibly be expected from a consideration of the mass and velocity of the incident particle. The only determined point on this curve is the one at full range (zero velocity) where the laboratory and center of mass systems coincide. At that point the fraction with a backward prong should be 0.75 since a three-prong star in the emulsion is, nearly without exception, a two-prong star in the center of mass system, and the probability of neither of these two-prongs going backward is 0.25, if we assume a random distribution in angle. The curve has been extended to shorter ranges with an eye to making the total number of events with backward prongs as given by it equal to the total actually found. It has been curved to indicate somewhat the variation of incident velocity with range. The histogram, although it gives a little indication of a rise at low velocities, quite evidently runs almost counter to the curve drawn in.

The possible explanations of the observed effect are limited to a few quite definite causes. Three will be discussed, of which the third is the most probable.

(1) "Splash". When a particle with the spatial extent and the mass of a carbon ion hits a nucleus larger than itself, a mass motion of a "plug" of nucleons may likely be set up which persists for some distance into the nucleus, far enough that the entering surface is considerably indented or disrupted. It is true that the velocities of nucleons inside the target nucleus are comparable to the velocity of the carbon particle

but they have no net mass motion. The readjustment in the wake of the entering nucleons could produce the emission of one or more particles backward. This would occur in a frame of reference nearly at rest with respect to the laboratory system.

(2) Emitted particle velocity a steep function of excitation. It is evident that, with so heavy a bombarding particle as carbon, having a respectably high velocity, there will be considerable momentum of the center of mass system with respect to the laboratory. In the case of the lighter target elements, hydrogen, carbon, nitrogen and oxygen this momentum will imply a forward velocity which acts as a cut-off velocity for backward ejection of particles, especially when there is a considerable lateral component to the velocity. So we expect the forward ejection in the emulsion at high incident velocities to be even greater than in the case of bombardment with single nucleons of the same energy, although the carbon ion lacks the possibility of directly knocking out a nucleon. The forward velocity effect of the center of mass might be overbalanced if the velocity of the emitted particles were a steeper function of the excitation energy - that is, of the incident carbon velocity - than the velocity of the center of mass is. It is quite believable that such is the case. Then, there could result a more nearly isotropic laboratory distribution at a high velocity than at an intermediate velocity where the center of mass velocity gave the larger effect. The phenomenon would have to reverse again to give isotropy at the very low velocities. It seems quite unlikely that the emitted velocity as a function of excitation could be manipulated to give the magnitude of effect observed here.

(3) Excitation function steeper for heavy particles than for light particles. Because of the heavier mass of silver and bromine compared to that of the light components of the emulsion, the center of mass system in the case of collision with silver and bromine will be moving more slowly. If evaporation of particles from the compound nucleus is isotropic in the center of mass system, there will result a more nearly isotropic particle distribution in the emulsion from silver and bromine than from carbon, hydrogen, oxygen and nitrogen, for which the forward ejection is prominent. Nevertheless, it is true that for each type of target nucleus individually, the average distance to its stars with backward prongs should be longer than the average to all its stars. The factor which can invert the inequality in considering the aggregate of stars from all the target nuclei in the emulsion is for the heavy and the light nuclei to have quite different excitation functions, as they surely do have. This is the explanation that can account for the observed effect, probably in its entirety, without recourse to the other possibilities mentioned. In the case of the excitation function, it is not merely the Coulomb barrier penetration, since the barrier even of silver can be crossed at rather moderate velocities. It is rather the leveling off of the function for the lighter nuclei while it is still rising for the heavier nuclei. To a considerable extent the curves may be ascribed to the effect of the centrifugal potential. The geometric penetrability cross sections, based on Coulomb and centrifugal barrier penetration and the geometric size of the carbon and target nuclei, are shown for hydrogen, oxygen, bromine and silver in Fig. 19, taken from the data of Table 3.4.

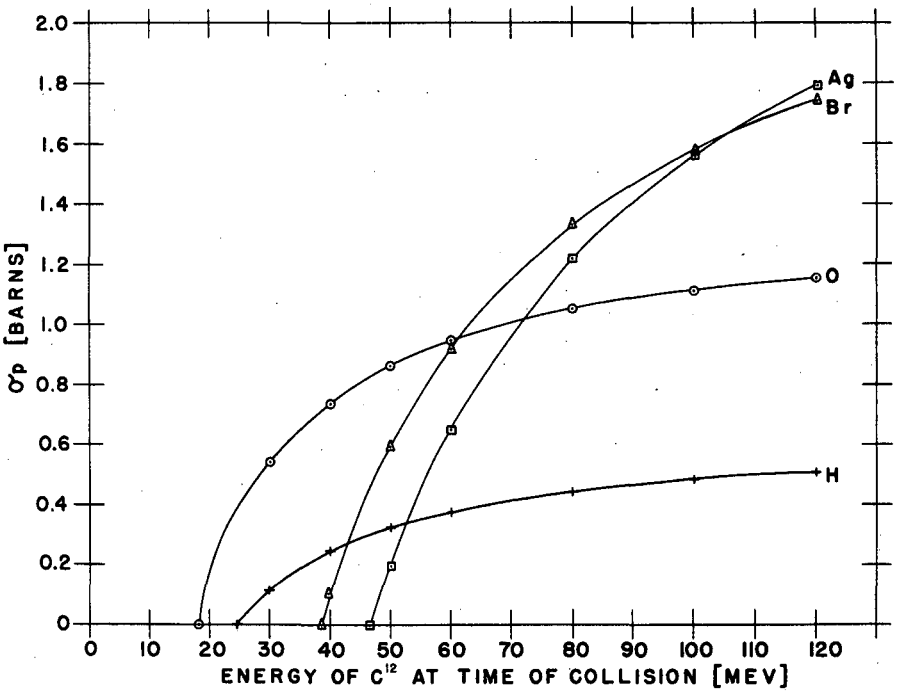

PENETRABILITY CROSS SECTIONS,
$\sigma_p(E)$, FOR C^{12} ON VARIOUS NUCLEI

FIGURE 19

MU3807

Horning and Baumhoff, interpreting the data of Gardner and Peterson on deuteron stars at various energies, arrived at the assignment of low deuteron energy stars to the lighter emulsion elements and of the high deuteron energy stars to the heavier elements by a consideration of the average number of prongs as a function of energy, rather than by considering the distribution by sector which Gardner and Peterson give. They point out that at low energies, the silver and bromine stars do not contribute prongs because of their high probability of giving pure neutron stars. They calculate that the mean number of visible prongs (excluding some high energy protons) due to evaporated charged particles (this excludes a prong formed by the product nucleus) will vary for silver and bromine from 1.1 at 35 Mev deuteron energy to 3.3 at 190 Mev, while the number of prongs from the light components of the emulsion will change very slowly since these elements can easily be broken up. Hence, to obtain the nearly constant average number of prongs actually found, they reason that the low energy stars must be nearly all due to carbon, nitrogen, oxygen and the high energy stars predominantly to silver and bromine. Others[27,36] have similarly ascribed the high energy stars to silver and bromine, even beyond their relative geometric areas when effects of nuclear transparency in the light elements enter.

The slope of the curves for the mean number of prongs with carbon bombardment indicates that the role played by silver and bromine at high energies is probably not quite as important as in the case of the lighter bombarding particles. For deuterons,[33] the mean number of prongs appears

---

36. M. Blau and A. R. Oliver, Bulletin, Amer. Phys. Soc., 27, No. 3, p. 6, (1952).

to be nearly constant from 90 to 190 Mev but lower at 35 Mev. One reason, of course, for the difference in the case of carbon is the absence of any transparency effect in the light target nuclei. Another is the high centrifugal potential which causes the penetrability cross section to rise more slowly for the heavy target nuclei. Another may be that, since the carbon particles introduce high excitation at a much less relative velocity than in the case of lighter particles, they are less apt to knock off a chip and more likely to break the target nuclei up into many particles.

The analysis of the backward prongs from C^{12} indicated the correctness of the original observation that the backward prongs at short distances come predominantly in cases where there is only one or two prongs other than the product nucleus. This is an indication both of the location of the effect in the rapid rise of the bromine and silver reaction cross sections and of the approximate number of charged prongs emitted by such particles at that excitation. Although silver is not inclined to evaporate many neutrons under carbon bombardment, there is a mechanism (the "magic" numbers of the closed shells) to limit the number of its charged particles and, at the same time, to make them more energetic. This is discussed in Chapter IV.

If the backward-prong behavior of C^{12} is normal, what can we say about the behavior of C^{13} which, by comparison, is anomalous? For the two-prong stars of C^{13}, where the distance to those with backward prongs is longer than the distance for all stars of the class, we can conclude that the data show the two-prong stars from hydrogen reactions, or from

lighter elements in general, overbalance the cases of single particle evaporation from silver and bromine. For three- and four-prong stars there is no immediate explanation for the failure of the silver and bromine excitation functions to show up. The three-prong stars, however, are nearly normal.

In the present study no analysis has been made of the range and consequent energy distribution of the evaporated prongs. The reason for the omission is that the large momentum imparted by carbon ions to the center of mass system with respect to the laboratory and the lack of knowledge as to what target nucleus was hit make it difficult to obtain any information that might show a discrepancy with theoretical energy distributions. The detailed energy distributions for neutrons and charged particles evaporated from the compound nucleus have been worked out theoretically[30,31,37,38,39,40] on the basis of the statistical gas model and would seem to be well grounded. Le Couteur[41] has made a small correction for very high excitations such as are found in cosmic ray stars to take account of a thermal expansion effect of the nucleus and a possible lowering of barriers for charged particle emission. The case of excitation from carbon particle bombardment barely borders on the lower

---

37. J. Frenkel, Phys. Zeits. Sowjetunion 9, 533 (1936)(In English).

38. V. F. Weisskopf, Phys. Rev. 52, 295(1937).

39. V. F. Weisskopf and D. H. Ewing, Phys. Rev. 57, 472 (1940).

40. V. F. Weisskopf in Lecture Series in Nuclear Physics, (MDDC 1175) US AEC (1947) (Los Alamos Lecture Notes).

41. K. J. Le Couteur, Proc. Phys. Soc., London, A63, 259 (1950).

edge of the effects he considers.

It may be of some interest to mention the longest range protons and alphas found from carbon bombardment even though the energy with respect to the center of mass is not known. From C^{12}-induced inelastic events, the longest proton track was 1780 microns (approximately 20 Mev) before it went out of the emulsion, the second longest was over 1350 microns (about 17 Mev). From there on down, the spacing in range is closer. These were forward ejections. The longest at approximately 90 degrees was 900 microns (about 13.2 Mev) and the longest almost directly backward was 725 microns (approximately 11.6 Mev) at 146 degrees. Another was 750 microns at 127 degrees. Alphas from C^{12} events ranged up to 896 microns ($E = 52.56$ Mev), projected directly forward. The next longest from C^{12} was 770 microns (48.12 Mev). These two alphas, and the first two below, are discussed in Chapter V.

From C^{13} bombardment the ranges are similar. Alphas of 898 microns and 793 microns occurred in four-prong events (two other alphas plus the struck nucleus) and an alpha of 800 microns (49.2 Mev) from a five-prong star.

Knock-on protons from both C^{12} and C^{13} were found which exceeded those from inelastic events by a small amount. From C^{12}, the longest knock-on seen was 1812 microns (nearly 20 Mev) and, from C^{13}, there was one which went out of the emulsion (E-1) after 1950 microns ($E > 20.7$ Mev). The range of knock-on protons is limited by the fact that, unless a particle be absorbed and re-emitted, it cannot acquire a velocity more than twice that of the heavy body striking it. This limitation would

permit protons up to nearly 37 Mev. However, a blow to give such a range cannot be delivered by the Coulomb field of the carbon nucleus as a whole and, if the interaction were between a proton of the nucleus and the struck proton, not more than 10 Mev could be delivered unless the momentum of the proton in the nucleus added on to the mass motion. Short-range nuclear forces could deliver the blow but presumably should be repulsive. Exchange forces in the nucleus are repulsive if the function of the interaction between the particles is anti-symmetric. This is partly so when the energy levels of the two particles are different. Parzen and Schiff[42] and Jastrow[43] have discussed the existence of short range repulsive forces in the nucleus.

From an excited compound nucleus the relative probabilities for emission of neutrons, protons and alphas have been discussed in the articles cited regarding the energy distribution of these particles. The assumption is made that the particles are emitted in succession, with intervening time adequate for several passages of particles across the nucleus to permit near equilibrium conditions to exist at each emission. Neutrons are most easily evaporated because they see no Coulomb barrier; hence, they need to be raised only from the top of the Fermi distribution to the top of the nuclear potential well (about 8 Mev). Protons and alphas see the Coulomb barrier in addition. Because of the penetrability function, protons can, in general, escape much more easily than alphas. If the binding energy of an alpha in the nucleus is less than that of a

---

42. G. Parzen and L. I. Schiff, Phys. Rev. 74, 1564 (1948).

43. R. Jastrow, Phys. Rev. 81, 165 (1951).

proton and, if Z is low or excitation high, the ratio of alphas to protons may be higher than normal. Heidmann and Bethe[30] find that for nuclei excited by 17 Mev gamma rays, the light elements evaporate protons in preference to neutrons (because the binding energy of a neutron is almost always higher than that of a proton in this region). However, there is practically no proton evaporation when the number of neutrons exceeds the number of protons. Up to nickel, protons occur in about equal numbers with neutrons. At copper, about 83 percent of the evaporated particles will be neutrons and, at iodine protons are practically missing.

Le Couteur,[41] studying high excitation (up to 600 Mev) in silver and bromine from cosmic rays, arrives at an expected ratio K for the number of alphas to the number of alphas and protons of about 0.27. This ratio was well verified experimentally by N. Page[44] for stars of more than six prongs, which presumably are attributable to silver and bromine target nuclei since carbon, nitrogen, and oxygen could not give stars of more than about five prongs. (Notice that with a composite incident nucleus, such as carbon, this limitation would not hold.) Her data indicate that carbon, nitrogen and oxygen may give approximately $K = 0.54$ (that is, roughly as many alphas as protons). Perkins[45] has verified these ratios from observing stars induced in the gelatin layers of a sandwich emulsion. For 27 stars observed originating in the gelatin, the numbers of alphas and protons were closely equal ($K=0.5$).

---

44. N. Page, Proc. Phys. Soc., London, A63, 250 (1950).

45. D. H. Perkins, Phil. Mag. 40, 601 (1949).

In bombardment with carbon nuclei we hardly expect a K as low as 0.27, or even 0.5, because of the alpha particle nature of the incident particle which, unless completely assimilated in the compound nucleus, would prejudice the result in favor of alphas. A phenomenon such as stripping or impact disintegration would, of course, badly upset the ratio.

Even when a compound nucleus is formed by penetration of C^{12} or C^{13}, there is reason to expect a large proportion of emitted alphas compared to protons (or neutrons). This reason is the higher angular momentum carried into the compound nucleus in a large percentage of the collisions. The angular momentum of a stable nucleus has an upper limit of about 9/2. An angular momentum of 50, such as carbon on silver or bromine might conceivably introduce, would be nearly the equivalent of having the spin of every nucleon lined up in the same direction.

The angular momentum will be reduced either by γ-radiation or by particle evaporation. Gamma emission cannot compete in speed with particle emission at high excitation energies. Therefore, until the excitation is at least below the Coulomb barriers, particles will have to carry off the excess angular momentum. This can be done most efficiently by heavy particles, namely, alphas rather than protons, because of their larger mass and because energy is available to evaporate only a limited number of particles to carry off angular momentum. Preston[46] has given a rigorous mathematical treatment of the case of alpha emission with $L \neq 0$. The angular momentum corresponds to a

---

46. M. A. Preston, Phys. Rev. 71, 865 (1947).

centrifugal potential, raising the resultant potential near the center of the nucleus and shifting the maxima of the internal wave functions farther out, giving a greater frequency of collision with the barrier and a greater probability of emission.

The high proportion of alphas to protons in the stars from carbon ions is at once evident. A limited study was made, taking just the stars from C^{12} bombardment with three identifiable prongs other than the product or knock-on nucleus. The 217 stars considered had 510 alphas and 141 protons ($K = 0.78$). The principal reason for such a high ratio was apparently the contribution from impact disintegration. Impact disintegration and angular momentum effects, though both contribute alphas, should differ in one respect. The former should give a non-random distribution with respect to the relative groupings of protons and alphas (favoring three alphas), while presumably the latter should give a random distribution. Hodgson[47] has given some tests for randomness in the distribution of the groupings of alphas and protons and for randomness in angle of emission. The latter could not be applied to the present data because of the impossibility of separating out the effect of the motion of the compound nucleus. The test regarding the distribution of groupings of alphas and protons is not a powerful one. It says nothing whatsoever as to why the ratio of the total numbers has a given value. It merely accepts this frequency ratio and uses it as the probability of emission. That is, the probability of emission of an alpha, $p_\alpha = K = .78$ and $p_p = .22$. In Fig. 20 is plotted the number of stars of each possible

47. P. E. Hodgson, Phil. Mag. 43, 190 (1952).

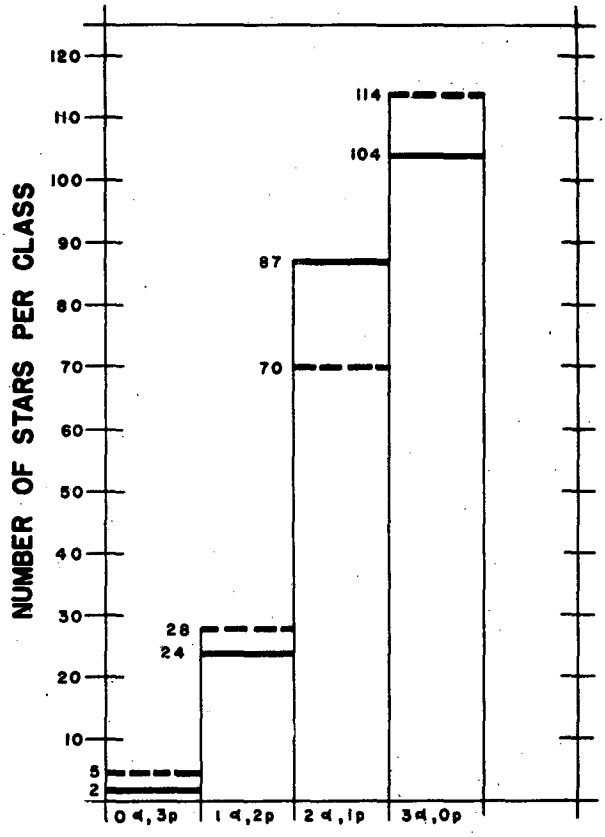

DISTRIBUTION OF ALPHAS AND PROTONS
FROM STARS WITH 3 IDENTIFIABLE PRONGS
OTHER THAN PRODUCT
(217 STARS)

FIGURE 20

MU 3809

type: 0 alphas, 3 protons; 1 alpha, 2 protons; 2 alphas, 1 proton; and 3 alphas, 0 proton. Now, if this distribution is random, it should agree with the binomial (or Bernoulli) distribution using p_α and p_p as given by the observed total frequency ratio. The probability of exactly m alphas and (m-n) protons (n=3) is given by:

$$p\left\{ m\alpha, (m-n)p \right\} = \frac{n!}{m!(n-m)!} p_\alpha^{m} (1-p_\alpha)^{n-m} .$$

The expectations based on these probabilities are also plotted in Figure 20. Now we can use the Chi-square test to see whether the observed data are a probable sample from the theoretical distribution. There are four groups or classes in the distribution. However, the number of degrees of freedom is less because, first, the total number of prongs is a constant and, second, we have estimated one of the parameters of the distribution, namely p_α, from the sample. This leaves two degrees of freedom, but we reduce it to one by combining the first two classes in order to get a class size where the fluctuation can be expected to be more nearly random. By definition, $\chi^2 = \sum \frac{s_i^2}{\sigma_i^2}$ where s_i is the actual deviation from the theoretical mean and σ_i is the standard deviation of the parent population. $\sigma_i = \sqrt{n}$. We get

$$\chi^2 = \frac{(33-26)^2}{26} + \frac{(17)^2}{87} + \frac{(10)^2}{104} = 6.17.$$

The tables of χ^2 then show that for one degree of freedom this value is significant at nearly the one percent level, which is called "highly significant". This indicates that the chance is about one percent that the actual sample came from a random distribution. From Fig. 20 it is

evident that the class of 2 alphas, 1 proton is deficient while the 3 alpha, 0 proton class is overfilled. It indicates quite definitely that the large ratio of alphas is not due entirely to an angular momentum effect.

At the end of this chapter are photographs of miscellaneous stars induced by C^{12} and C^{13}. Photographs of stars illustrating special features discussed later are included in Chapters IV, V, and VI.

FIGURE 21.

Relative track lengths of alpha particles, C^{13} and C^{12} ions, all accelerated by the cyclotron. The alpha and C^{12} are in the usual 100 micron Ilford E-1 emulsion; the C^{13} is in a trial plate of 50 micron E-1 emulsion that apparently had been desensitized until it was comparable in sensitivity to D-1 emulsion.

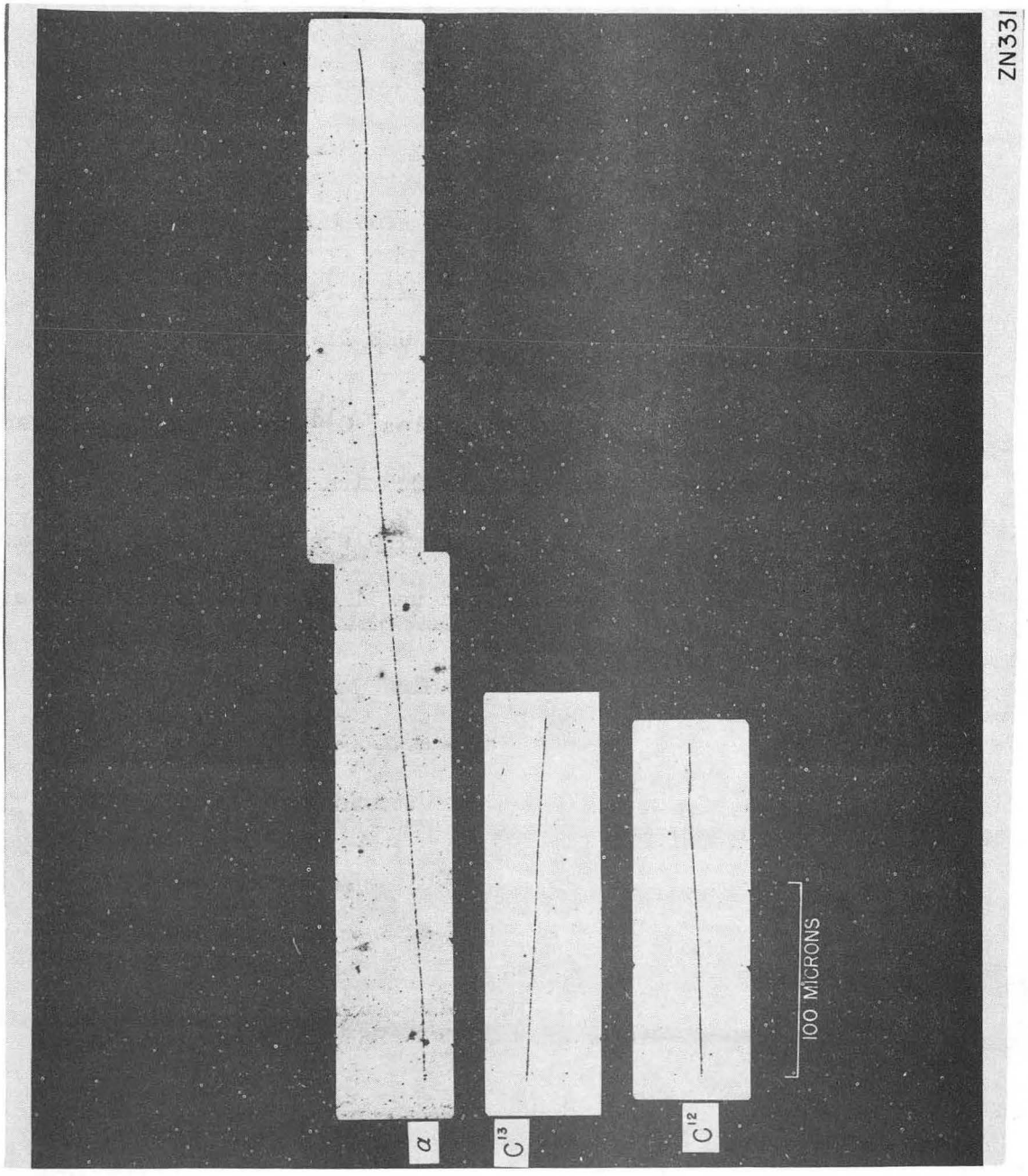

FIGURE 21

FIGURE 22A

An elastic collision of C^{12} with C^{12}. The angle between the two is always 90 degrees. In the case of C^{12}, few elastic collisions are seen more energetic than this one. However, in the case of C^{13} as the incident particle more violent elastic collisions are sometimes seen since C^{13} is harder to disintegrate than C^{12}. (The markers on the left of the picture indicate about 10 microns per unit.)

FIGURE 22B

A (C^{12},2α) reaction. The elastic nuclear collision of the product nucleus near the end of its track is typical of the heavier nuclei, and might well indicate that the event was produced by the C^{12} in a bromine or silver nucleus.

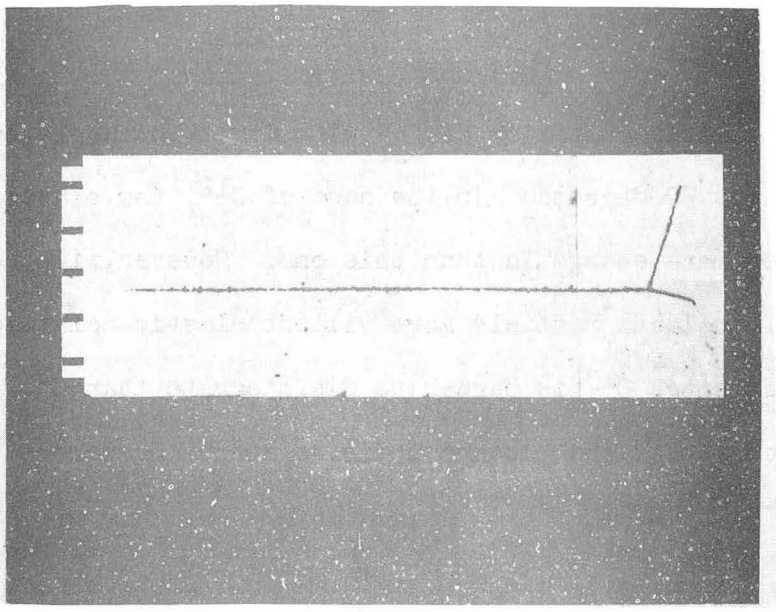

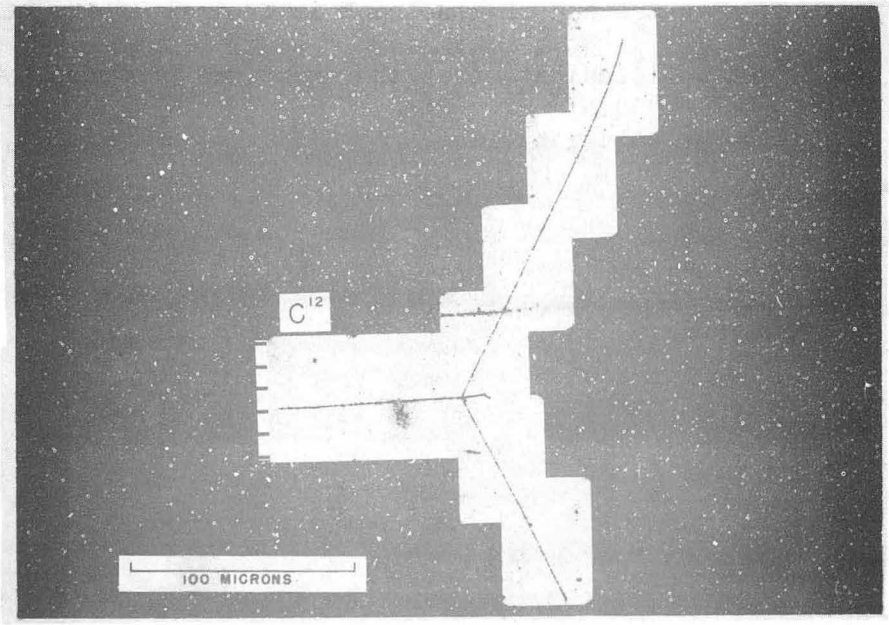

FIGURE 22

ZN319

FIGURE 23A

A (C^{12},2α) reaction. The length of the product nucleus track (between the two alphas) indicates that the nucleus struck was probably carbon, nitrogen, or oxygen. The shorter alpha track corresponds to an energy of only 1.5 Mev. This event indicates the difficulty that might arise in distinguishing a short alpha from a light product nucleus.

FIGURE 23B

A (C^{12}; α,p) reaction. Like the event in Figure 23A, this is a low energy reaction. The alpha had 3.5 Mev. energy, the proton 1.05 Mev. From the ranges, the nucleus struck was probably bromine or silver. If so, the energies of the evaporated particles are about the lowest that can be expected in view of the Coulomb barrier to be penetrated. See the discussion by Le Couteur.[41]

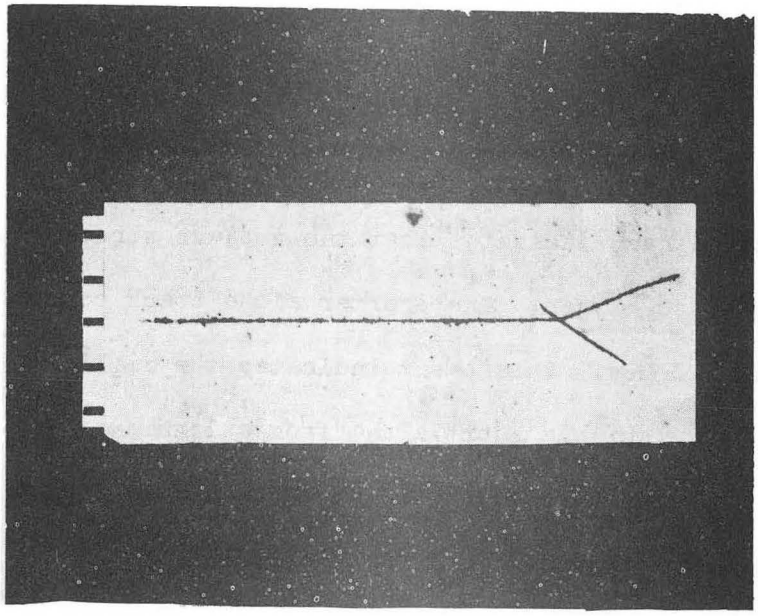

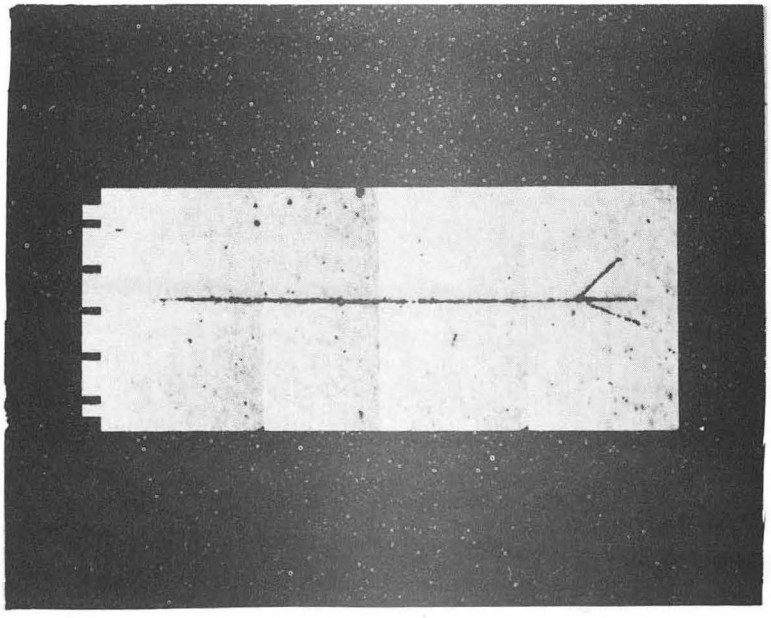

FIGURE 23

ZN320

FIGURE 24A

A (C^{12};2p, α) reaction. The alpha is heavier than normal because it is diving steeply. However, through the microscope, horizontal alphas and protons in E-1 emulsion are almost as easily distinguished.

FIGURE 24B

This five-prong star from C^{12} appears to be an incomplete double-disintegration, i.e., an impact disintegration of the incident nucleus and of the target nucleus. The impact disintegration origin for the star is given credence by the upper pair of alphas, which appears to have come from Be^8 in the ground state (See Chapter V).

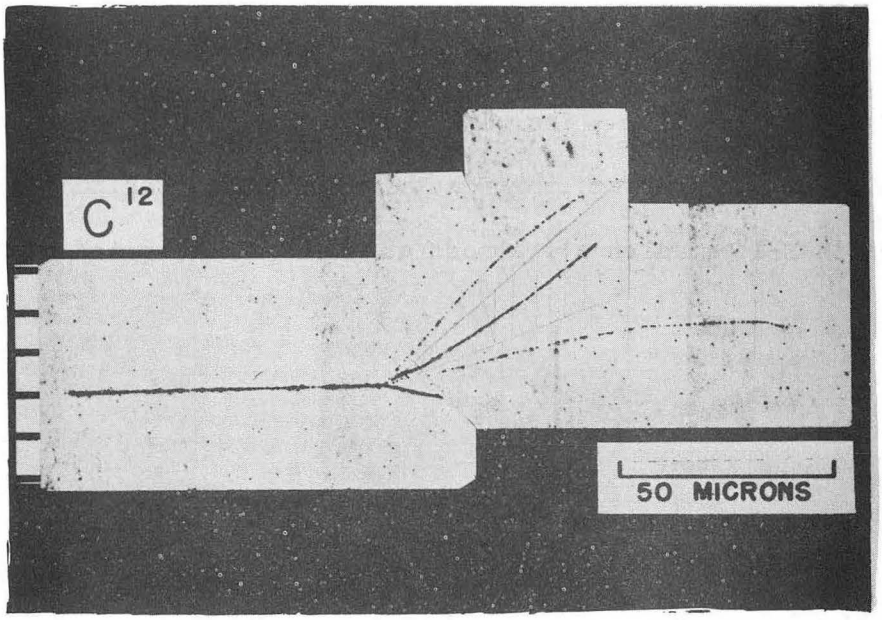

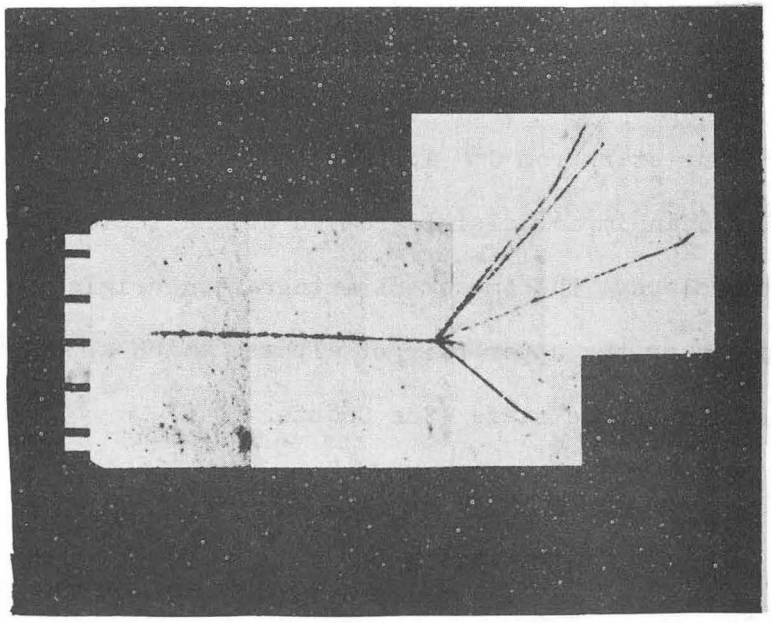

FIGURE 24

ZN 321

FIGURE 25A

A (C^{13},α) reaction, probably from silver or bromine target nucleus. Lighter target nuclei are less likely to give backward prongs because of the forward momentum from the entering C^{13}; a light product nucleus should give a longer track. The emulsion in this photograph, as in Figs. 25B, 26A and 26B, is an insensitive 50 micron E-1, of which only one plate was read.

FIGURE 25B

A five-prong star from C^{13}. The second from the bottom prong is the product nucleus. There are three alphas and one proton. The proton left almost no track in this insensitive emulsion at its beginning, although it was only about 600 microns long (about 10 Mev). The proton track was not noticed in making the mosaic. The C^{13} ion underwent an elastic collision before it hit the nucleus which produced the event. Notice the dense ionization at the star. This frequently occurs and sometimes makes it difficult to be certain as to whether another prong is present.

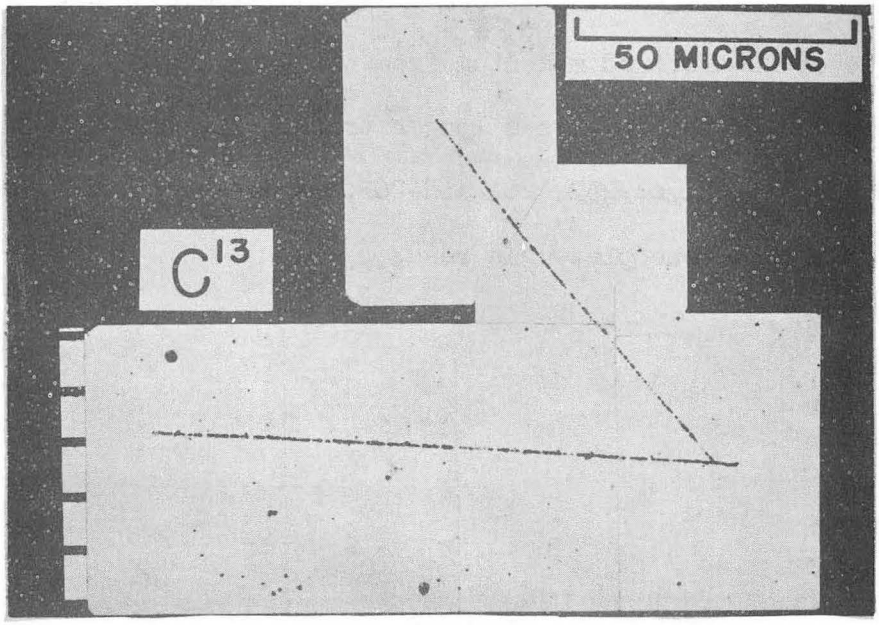

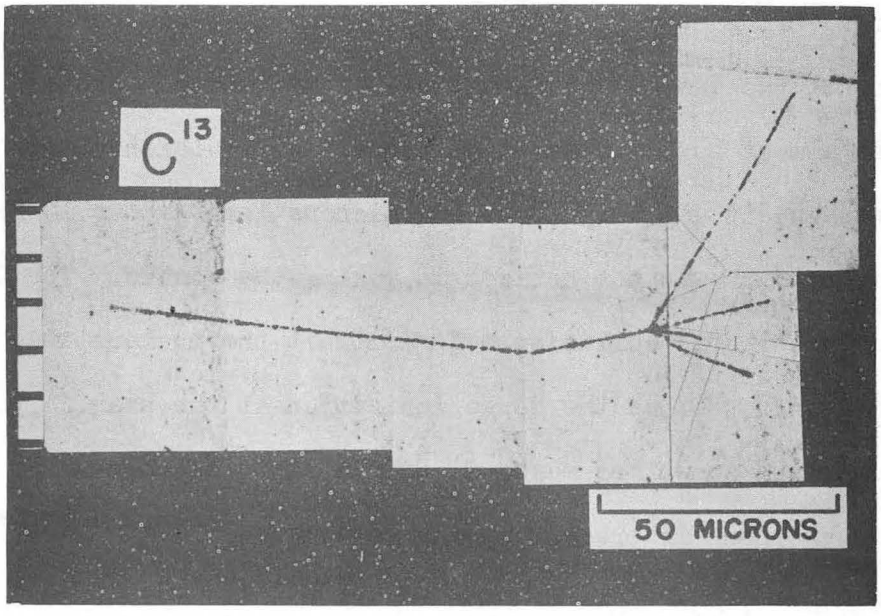

FIGURE 25

ZN322

FIGURE 26A

A C^{13} reaction with a heavy nucleus in the emulsion. The two long tracks are protons of approximately 6.2 and 7.5 Mev. The short track between them may be either an alpha or a proton. The emulsion is a 50 micron E-1 that perhaps had been desensitized.

FIGURE 26B

An (α,2p) evaporation from a compound nucleus formed by C^{13} with probably silver or bromine.

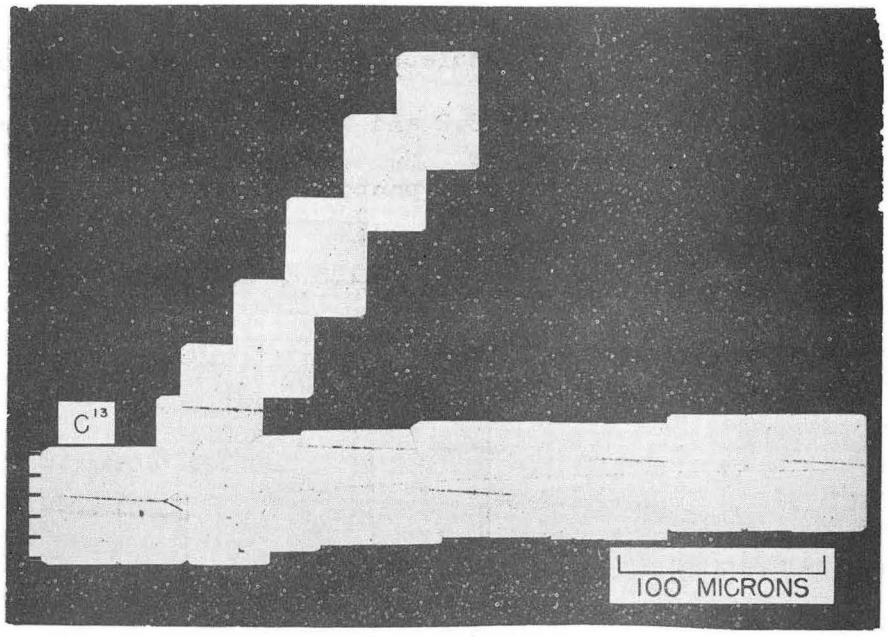

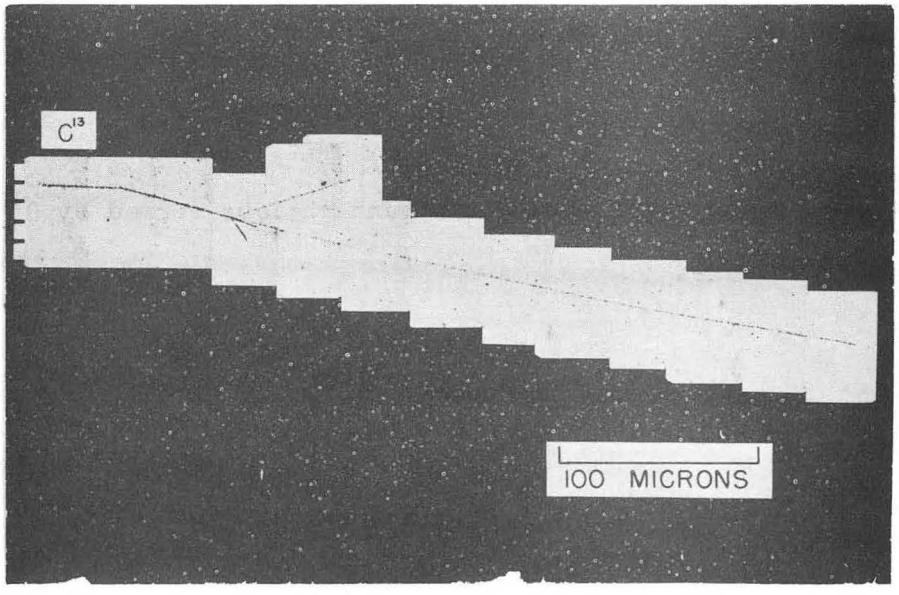

FIGURE 26

ZN323

FIGURE 27

A seven-prong star produced by C^{12} in 100 micron E-1 emulsion. The presence of the seventh prong is easily seen under the microscope and is indicated in the sequence of pictures at the right, taken at different depths. The four identifiable prongs are alphas. For comparison, the track of a C^{12} that was stopped by electron collisions, without an inelastic nuclear event, is shown at the left. On the average, only about one track out of 1600 produces an inelastic nuclear event. The short tracks on the emulsion surface are quite surely from $C^{12(2+)}$ ions that came from the gap between the dees or were scattered down the deflector channel. They do not have one-ninth the energy of the $C^{12(6+)}$ which they should have if they followed the same trajectory to the plate. As simple calculation shows, C^{2+} are over-deflected in the deflector electric field and, hence, cannot come out the channel unless they are scattered.

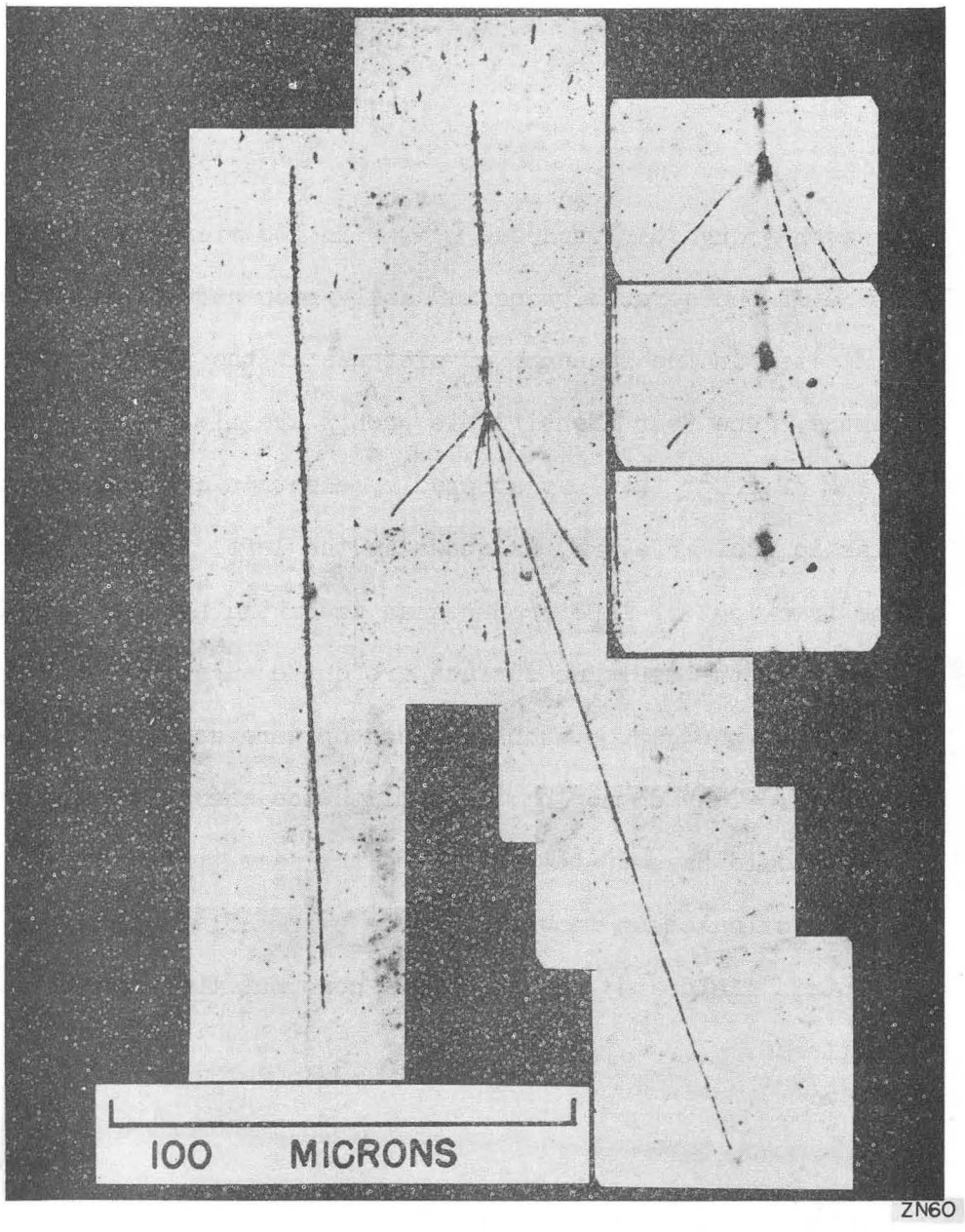

FIGURE 27

CHAPTER IV

SPECIAL REACTIONS

In this chapter will be considered a few special reactions other than stripping and impact disintegration, which will be discussed in Chapter V, and fission of bismuth, discussed in Chapter VI.

A question which naturally arises is: Can we expect to find particles heavier than alphas emitted in any of the carbon bombardment reactions? Such a particle might appear as the result of any of several different types of processes (for the moment, fission of the heavier components of the emulsion is excluded):

(1) As a residue from the nearly complete break-up of the incident carbon and light target nucleus;

(2) As an evaporated particle from a compound nucleus;

(3) Directly knocked out, or as a spallation fragment.

Fortunately, there is a means of identifying in the emulsion some of the products just heavier than an alpha. The most probable particle from the point of view of penetrating the Coulomb barrier is lithium. Li^6 and Li^7, which are stable, would be hard to recognize except that their trace should be $(3/2)^2$ as heavy as that of an alpha. However, Li^8 and Li^9 could easily be identified by the fact that at the end of their tracks would appear a "hammer" from a pair of nearly equal and opposite alphas. Li^9 is a so-called "delayed neutron emitter[48] in that

---

48. W. L. Gardner, N. Knable, and B. J. Moyer, Phys. Rev., 83, 1054 (1951).

it decays by β^- emission with a half-life of 0.168 seconds to an excited state of Be^9 which immediately gives off a neutron, becoming Be^8, which breaks up into the two alphas of the "hammer". Li^8 proceeds more directly to the same end by emitting a β^- (half-life, 0.88 seconds), thus falling to one of three excited states of Be^8- at 13, 10, or 3.0 Mev. These states are highly unstable, the Be^{8*} breaking into two alphas in about 10^{-21} seconds. Decay of Li^8 to the ground state of Be^8, which also is unstable to breaking up into two alphas, but which has a longer life (perhaps of the order of 10^{-16} seconds), is forbidden.

Two other detectable particles which are possible, but less probable because of their higher charge, are B^8 and C^9. B^8 is the mirror of Li^8; it gives off a β^+ (half-life, 0.65 ± 0.1 second)[49], decaying to an excited state of Be^8 as did Li^8. C^9, the mirror nucleus of Li^9 might be expected to be a "delayed proton emitter",[49] decaying by β^+ to an excited state of B^9 which would be unstable enough to emit a proton, thus becoming Be^8.

All these reactions would be recognizable by the fact that the parent particle would have come to rest before the β was emitted which permitted further decay to Be^8. The latter would then be recognized by the "hammer track" it makes - two equal and opposite alpha prongs of energy equal to that of the state of Be^8 involved. There might be a slight deviation from collinearity and from equality in range if the Be^8 breaks up before completing its recoil from the beta emission, or, in the case of Li^9 and C^9, from neutron and proton emission. In all cases

---

49. L. W. Alvarez, Phys. Rev. 80, 519 (1950).

except possibly Li^9 and C^9 the energy of the alphas would correspond to the 3.0 Mev or higher excited state of Be^8. With Li^9 and C^9 it seems possible that the decay could be to the ground state of Be^8, in which case the hammer would correspond to 0.1 Mev disintegration energy and, consequently, each alpha track would be less than one micron long.

Be^8 hammers, almost entirely ascribable to Li^8 because of its low charge, have been observed in photographic emulsion under many different types of bombardment. Franzinetti and Payne[50] found 28 such events in cosmic ray stars from direct hits or from mesons and neutrons. Of the 28, 13 seemed to be $C^{12} + n \rightarrow Li^8 + \alpha + p$. Adelman and Jones[51] found 11 Be^8 hammers in a study of 3000 negative pions from the 184-inch Cyclotron. Titterton[52] in 5000 stars from neutrons of about 170 Mev, found 21 hammer tracks. In only two of the 21 cases was B^8 the possible origin; one case seemed definitely to be from B^8. Titterton,[52] in research still under way with 170 Mev protons on emulsion, is finding approximately the same proportion of hammers. J. K. Bowker, continuing the work of E. Gardner on 300 Mev alphas at the University of California Radiation Laboratory, has found three hammers in about 1000 events (unpublished). In addition to these emulsion studies, Wright[53] has found Li^8 from ionization chamber bombardment of carbon, nitrogen, neon,

---

50. C. Franzinetti and R. M. Payne, Nature 161, 735 (1948).

51. F. L. Adelman and S. B. Jones, Science 111, 226 (1950).

52. E. W. Titterton, Phil. Mag. 42, 113 (1951).

53. S. C. Wright, Phys. Rev. 79, 838 (1950);

argon, krypton and xenon in gaseous form with 340 Mev protons and 190 Mev deuterons.

The wide variety of conditions under which the Be^8 hammer tracks have been found would lead one uncritically to expect them from carbon ion bombardment since the excitation from carbon ions can be nearly comparable to that in some of the cases cited above. However, in the 865 C^{12} stars and the 1427 C^{13} stars examined, there were no "hammer tracks". There was only one possible case and it was finally classified as probably the chance orientation of a three-prong star from a natural radioactive nucleus in the emulsion in such a manner than the end of one prong touched near the beginning of a short-range carbon, and the other two prongs were nearly, but not quite, opposite each other and not quite of the same length. It could have been an error to exclude this case, but the conclusion would be unchanged that Li^8 is of a lower order of probability than in the other cases cited. The reason was not hard to find. In most of the cases cited above the Li^8 was left as a residue from highly excited light nuclei which had evaporated alphas, protons and neutrons. Titterton discusses the possible reactions that agree with the stars he found. In each case carbon, nitrogen or oxygen was the target nucleus. Wright also ascribes his Li^8 from the light target elements, carbon, nitrogen and neon to being a residue. The difference in using carbon as a bombarding particle is that all the compound nuclei that can be formed are considerably heavier than in the cases above. They would have to evaporate a larger number of particles in order to leave Li^8. This fact, plus the lower excitation because of inability to get

more than about half its energy into excitation of a light nucleus, cut the "hammers" to the vanishing point. There are a number of stars in the emulsion (mostly six-prong) where there seems to have been a break-up of both the projected and target nuclei, but the break-up occurred along alpha-particle lines. As far as the necessary energy is concerned, Wright obtained excitation functions which show, for instance, that for 60 Mev deuterons on carbon, the cross section is only about 5×10^{-4} barns. This would be about one-thousandth the total cross section for star production by carbon particles. At 200 Mev it is nearly three times as large.

Another possibility for Li^8 to appear is as a directly evaporated particle from a compound nucleus, not as a residue. The Coulomb barriers are too high and the excitation too low from carbon ions to expect such an occurrence. Wright found a much lower yield of Li^8 from argon, krypton, xenon indicating a different mechanism from that present in the case of the lighter elements. He was able to get the correct order of magnitude using an evaporation model.

The production by a spallation process or direct knock-on has been postulated in high energy bombardment by light particles; such a process is most improbable, however, from carbon on heavy nuclei. Marquez and Perlman,[54] in bombardment of tin with 350 Mev protons and alpha particles, found iodine activities. To obtain these activities, more charge must have been introduced into the target than was carried by the bombarding particle. They thought the most probable mechanism was by secondary

---

54. L. Marquez and I. Perlman, Phys. Rev. 81, 953 (1951).

bombardment with lithium nuclei of masses 6,7,8 knocked out by the primary particle. They could not reconcile the lithium emission with evaporation, and so concluded the lithium was knocked out at high velocity, directly or by spallation. The threshold for the production of iodine seemed to be at about 50 Mev for both protons and alphas, but the yield was very low there; even at 340 Mev it was not higher than 5×10^{-5} barns. They also found that beryllium nuclei may come from reactions produced by 335 Mev protons on a variety of target nuclei.

Since the subject of delayed particle emitters has come up in connection with the identification of certain reaction products heavier than an alpha, it is convenient to discuss delayed particle emission a little more fully at this point. The interest now is in the delayed particle itself, not the nuclide left after its emission. Since only delayed protons and alphas would be detectable in the emulsion, delayed neutrons will not be mentioned. Alvarez[49] has pointed out that delayed proton or alpha emitters should occur on up the Heisenberg valley of the nuclides. In cases where the carbon nucleus does form a compound nucleus with a light target element we might get some of these.

An attractive prospect for proton emission is F^{17*}. The last proton in F^{17} in the ground state has a binding energy of only 0.6 Mev.[29] F^{17*} could be reached in the case of carbon bombardment by the following process:

$$C^{12} + C^{12} \longrightarrow {}_{12}Mg^{24} \longrightarrow {}_{10}Ne^{17} + \alpha + 3n$$

$${}_{10}Ne^{17} \longrightarrow {}_{9}F^{17*} + e^{+}$$

$$F^{17*} \longrightarrow {}_{8}O^{16} + {}_{1}H^{1}$$

(The $_{10}Ne^{17}$ would be called the delayed proton emitter). Two delayed alpha emitters which might occur from carbon bombardment are $_{11}Na^{20}$ and $_{13}Al^{24}$, by the following processes:

(1) $C^{12} + C^{12} \longrightarrow {}_{12}Mg^{24} \longrightarrow {}_{11}Na^{20} + p + 3n$

$${}_{11}Na^{20} \longrightarrow {}_{10}Ne^{20*} + e^{+}$$

$${}_{10}Ne^{20*} \longrightarrow {}_{8}O^{16} + \alpha$$

(2) $C^{12} + O^{16} \longrightarrow {}_{14}Si^{28} \longrightarrow {}_{13}Al^{24} + p + 3n$

$${}_{13}Al^{24} \longrightarrow {}_{12}Mg^{24*} + e^{+}$$

$${}_{12}Mg^{24*} \longrightarrow {}_{10}Ne^{20} + \alpha$$

The improbability of these processes is at once apparent. With an incident carbon of 100 Mev, say, only about 50 Mev could be put into the compound nucleus, plus about 15 Mev excitation from mass excess, which must suffice to evaporate four particles. The combination of three neutrons and one alpha or proton is quite improbable from so light a compound nucleus.

Similar processes with the heavy component of the emulsion, silver bromine and iodine, might have a higher probability though it would be difficult to predict which would be delayed proton and alpha emitters.

After eliminating a number of cases where an alpha or proton could have been knock-ons, there seems to be one reasonably definite case of delayed emission, probably of a proton. It was an event produced by

C^{12} and seems to belong to none of the above categories. The proton, of 28 microns range, comes off at a sharp angle from the very end of a heavy steeply diving track. Besides this prong, there is an alpha, and another prong heavier than an alpha that looks like the typical product nucleus from one of the light components of the emulsion.

The discussion now returns to heavy particles from nuclear reactions. A more rewarding study than looking for the special particles that would give a "hammer track" was to look for tracks from any particle with a charge definitely greater than that of an alpha.

Care and restraint must be exercised in judging the charge or mass of a particle by its track, particularly if there is any dip to the track. The shrinkage of the emulsion in thickness by a factor of about 2.3 during processing makes non-horizontal tracks appear unduly heavy. However, at fairly steep angles, a zigzag appearance of the track can usually be seen for a particle as light as an alpha. Sometimes, to be definite about the appearance of a dipping alpha, comparison was made with some of the cyclotron alphas in the C^{12} emulsions where one of these had been deflected steeply.

There were many doubtful cases found, from both C^{12} and C^{13}, where there appeared to be two prongs heavier than alphas (one such prong is nearly always present, from the product nucleus). But there were a number of cases where the conclusion was inescapable. Among the 865 C^{12} stars there are conservatively of the order of 20 such stars and with C^{13} the ratio is at least as high. In general, these are not two-prong stars; they usually have one additional prong.

We might tentatively classify such stars into two groups: (1) At least one particle is as light as carbon, or lighter, as seen from the ranges of one or both of the particles heavier than alpha; (2) Shorter range, and probably heavier, particles. The first group is the more numerous. It seems surprising that there should be rather frequent cases of particles heavier than alphas without some of these leading to Be^8 by way of the chains mentioned earlier. Perhaps the explanation may be as follows: Since it is improbable for heavy particles to be left by evaporation from a compound nucleus formed in carbon ion bombardment, then their origin may be ascribed to a knocking out of one or more particles from a light target nucleus, leaving a heavy particle, without the amalgamation of the carbon nucleus and the struck nucleus into a compound nucleus ever occurring. The wave length of the carbon ions is short enough to accomplish such a feat. The particles most easily knocked out are alphas and protons, both because they have a Coulomb field to knock on and because they normally lie farther out in the nucleus than do neutrons. Now it will be remarked that the nuclides leading through decay to Be^8 require that rather special combinations be knocked out of carbon, nitrogen or oxygen. The knocking out of a single alpha or proton or one of each will in none of these cases lead to a nucleus having a delayed emission and, hence, giving a hammer track from Be^8. In only one case will it lead directly to Be^8. This one direct case is the knocking out of an alpha from carbon, either as target or projectile (impact disintegration of C^{12}) or, alternatively, the capture of an alpha from the carbon nucleus by another nucleus (stripping).

When we see later how frequent these cases are, it will not seem quite so remarkable that we should find heavy fragments of various kinds apparently formed by knocking out an alpha or proton. Rather, we have to explain their infrequency by noting that knocking an alpha out of C^{12} requires much less of a blow than knocking it out of other nuclei.

Figure 28 is a photograph of a star with two prongs heavier than alpha particles. The incident particle was C^{12}, which traveled nine microns before the event. Since the average total range was 172 microns, the range-energy curve gives the probable energy at the time of the event as 107.5 Mev. The short track going upward in the picture is an alpha which went out the top of the emulsion after 11 microns. It looks a little heavier than the normal alpha probably because of extra sensitivity at the emulsion surface. It makes an angle of 83 degrees with the carbon track extended. The second particle clockwise, A, has a range of 43.1 microns and makes an angle of 24 degrees with the incident C^{12}. The third particle, B, has a range of 62.8 microns and makes an angle of 47.3 degrees. Neither A nor B is heavier than C^{12}. If both were C^{12}, the sum of their energies would be 102.3 Mev and, since the alpha had more than 3.1 Mev, the total does not leave enough energy for the separation of the alpha from the nucleus. Besides, conservation of y-momentum is not satisfied unless the alpha had 25 Mev energy. Therefore, the collision appears not to have been carbon on oxygen. It is not C^{12} on C^{12}, since we would get Be^{8} with its disintegration into alphas. But, if the event is C^{12} on N^{14}, all the data seem to fit. A would be C^{12} of energy 44.2 Mev and B would be B^{10} with 43.8 Mev (estimated by interpolation on the range-energy curve). To conserve y-momentum, the alpha must have had an energy of 9.0 Mev

FIGURE 28

The incident C^{12} knocks an alpha (headed upward in the photograph) from N^{14}, leaving it as B^{10} (bottom track). The C^{12} was not disintegrated (middle track) despite the low binding energy of the alpha in it.

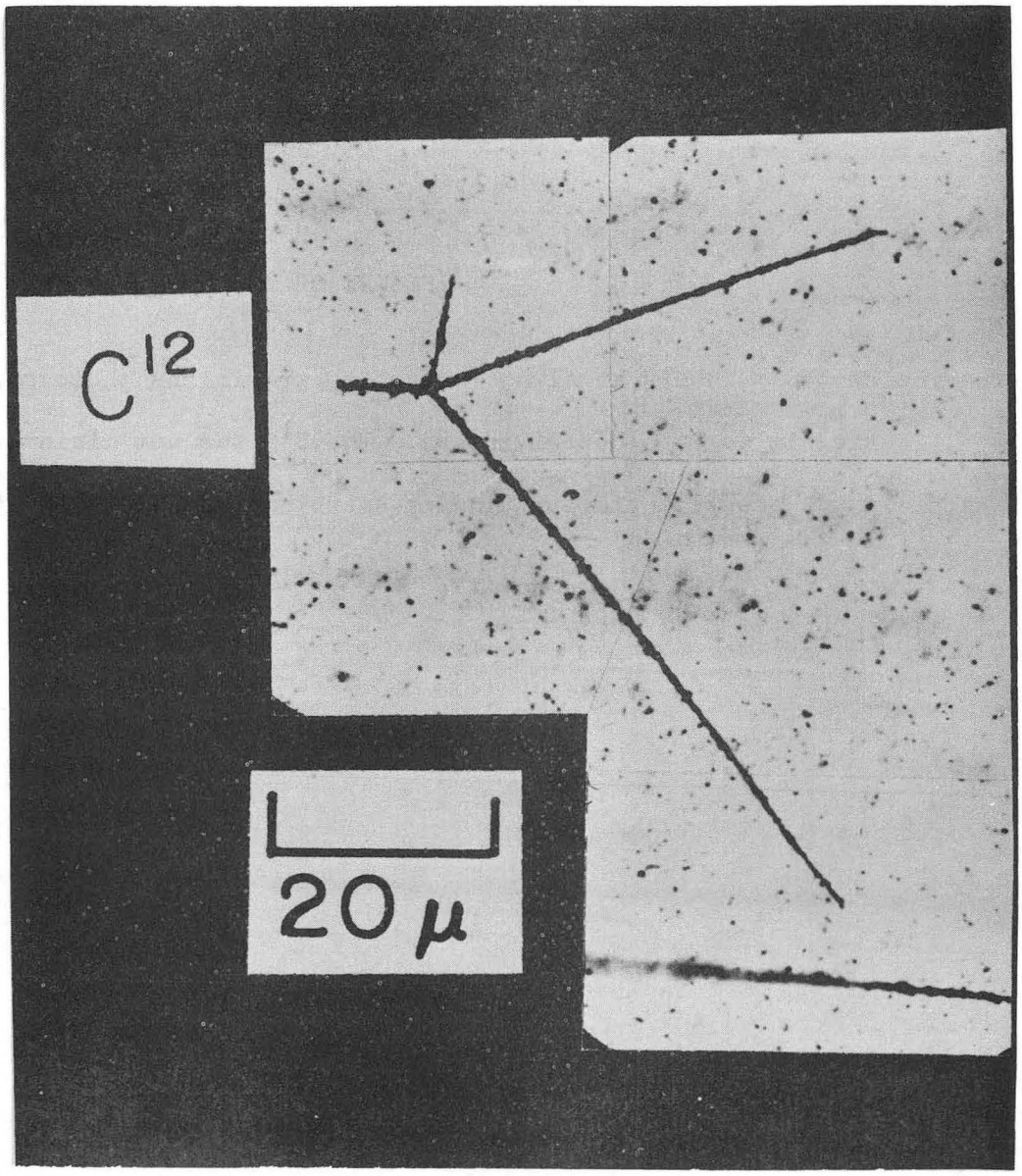

ZN334

FIGURE 25

(range of 57 microns). This gives a perfect fit also for conservation of x-momentum. The total prong energy is 97.0 Mev, leaving 10.5 Mev for separation energy. Hornyak, Lauritsen, Morrison and Fowler[29] give 11.7 Mev for the proper value. The C^{12} struck the N^{14} a little above center and to the left. It is odd that the C^{12} was not the particle which was broken up.

The second class of stars with two prongs heavier than alphas has prongs short enough that they might be heavier than carbon. The only possibilities are from silver, bromine and iodine of the emulsion, and the reaction apparently is one of fission of the compound nucleus. Because the effect may well be related to another effect, that of the closed shell structure of the nucleus, the latter will be mentioned first.

Silver nuclei bombarded with C^{12} or C^{13} ions give quite impressive visual evidence for the location of the compound nucleus with respect to the 50-proton closed shell of the nucleus. The initial reactions with C^{12} are:

$$_{47}Ag^{107} + {}_{6}C^{12} \longrightarrow {}_{53}I^{119}$$

and

$$_{47}Ag^{109} + {}_{6}C^{12} \longrightarrow {}_{53}I^{121}.$$

The 50-proton closed shell is reached by evaporation of an alpha and a proton from the compound nucleus. The cases where such events occurred are quite common and are distinguished by the great length of the proton and alpha tracks, often in the back hemisphere. The identification is rather clear that they came from a heavy nucleus from the appearance of the product nucleus track - short, and often with spurs and large angle deflections from nuclear collisions, as expected from a heavy particle.

In the case of bromine bombarded by C^{12} or C^{13} the compound nucleus formed is Nb. It can fall into the 50-neutron closed shell by evaporating one or more

neutrons, depending on the isotope involved. This reaction would not be seen in the photographic emulsion. However, the strong binding against removal of another neutron might dispose the nucleus toward charged particle emission, such as proton emission or fission.

The heavy tracks giving evidence for a fission type reaction in silver or bromine from carbon bombardment are not as unmistakable as the long range alphas and protons which give evidence for shell structure. In the first place, short tracks give poor evidence as to the mass of the particle, except in an insensitive emulsion such as D-1. In the second place, since the product nucleus from silver or bromine would be heavy, there will often be nuclear collisions in stopping and a fair percentage of the time these will be with carbon, nitrogen, oxygen or even heavier nuclei. A consequent appearance of forking of the product nucleus occurs in a large percentage of the silver and bromine stars. However, since there is apparently no reason for a fission reaction to be delayed, we can at once disregard all cases where an apparent splitting is separated from the star itself. This still leaves a few cases where two heavy particles come from a star, both from two-prong stars and from those with another particle, such as an alpha or proton.

A survey was made of the C^{13} plates to estimate the number of stars having two prongs heavy enough to indicate fission of the silver of bromine target nucleus. The C^{13} plates were used because most of them

are of D-1 emulsion, which records better than E-1 the difference between carbon and a heavier particle. Six quite certain cases were found from a total of 1114 stars. Others are possible but, from the length of the prongs, might be cases similar to that shown in Fig. 28, where carbon hit one of the lighter components of the emulsion.

There is no probability of confusing the fission of bromine or silver with that of bismuth since the angle between the prongs is much larger in the latter case. Rather, one must be sure that the collision could not be elastic, say C^{13} on C^{12}, since the angle between prongs may be near 90 degrees. The length of the prongs rules out an elastic collision, as does the density of the tracks.

Three of the stars considered to be fission had only two emergent particles. In two cases these were nearly symmetric, and in one case, quite asymmetric. The other three stars included a proton or alpha as well as two heavy particles. A remarkable feature was that the alpha or proton (identification not certain) was of short range, of the order of 20 microns for the two ending in the emulsion, while the third, which left the emulsion, appeared to be of comparable length.

The effect that the strong binding at the closed nuclear shells might have in inducing fission is not hard to see. The closed shell gives the possibility of energy release greater than could ordinarily be expected. If the short range particles observed were from transitions to a closed shell with lower energy release than expected on the average, then the remaining excitation would be particularly high.

The possibility of fission of Br or Ag is not entirely unexpected.

Batzel and Seaborg[55] found good evidence for a fission type process from 340 Mev proton bombardment of copper, bromine, silver, tin and barium. For instance, Cl^{38} from copper bombardment was found definitely beginning at 60 to 70 Mev proton energy, well below the threshold for its production by a spallation reaction having no particle heavier than an alpha. Ranges of the recoil fragments gave further evidence for the fission reaction. The yields are low - about 2×10^{-6} barns for the production of a particular nuclide, Na^{24}, from tin by 200 Mev protons.

It is known from mass calculations that for nuclides as low as $A \cong 83$ or $Z > 42$, symmetrical fission would be exothermic. For higher A or Z, asymmetric fission becomes exothermic.[56] Fission is prevented by the potential energy barrier. The threshold for fission is the difference between the barrier and the energy release from mass differences in the case of fission. For Br + C it is of the order of 40 Mev, for Ag + C, about 30 Mev.[57] For asymmetrical fission the threshold would be larger.

---

55. R. E. Batzel and G. T. Seaborg, Phys. Rev. 82, 607 (1951).

56. G. Gamow and C. L. Critchfield, Theory of Atomic Nucleus and Nuclear Energy-Sources, p. 147. Oxford: The Clarendon Press (1949).

57. D. Halliday, Introductory Nuclear Physics, p. 415. John Wiley and Sons, New York (1950).

CHAPTER V

IMPACT DISINTEGRATION AND STRIPPING OF CARBON NUCLEI

A. EXPERIMENTAL OBSERVATIONS

The phenomenon of impact disintegration of the C^{12} nucleus and the closely related stripping and capture of an alpha particle from C^{12} stand out strikingly. If an observer, unaware of the identity of the bombarding particle, viewed several hundred stars from incident C^{12} nuclei, he would arrive at the firm inference that the bombarding nucleus was composed of alpha particles and that the number of these alphas was three. Further, he would see the three-alpha nucleus frequently disintegrate into one alpha plus a closely correlated pair of alphas, the two of the pair having nearly the same range and only a small angular divergence (sometimes as low as 2 or 3 degrees). In many other cases, where the separation of the pair of alphas was more violent, a correlation could still be seen. Often, though not invariably, the collision that broke up the bombarding nucleus was so light as to barely produce a knock-on track. Sometimes it was rather a hard collision. Both the light and hard collisions seemed sometimes to produce only two alphas which, in the case of the gentle collision, went flying by as a pair, little deviated. It was apparent that, if a single bombarding particle had been used, these cases must represent the stripping off and capture of the third alpha. This process seemed not much more infrequent than the three-alpha process.

This is the general nature of the visual evidence. Knowing that

C^{12} nuclei were the bombarding particles, one can soon establish the true nature of the processes and identify the pair of alphas in the case of stripping, or the correlated pair in the case of impact disintegration, as Be^{8}, either in the ground state or in one of several excited states. The verification and the details of its occurrence need only be put into analytical terms. Fortunately, there are enough cases that an analysis can ascertain some of the more pertinent details concerning the process: (1) whether it is a low or high velocity process, (2) whether it can be produced by the Coulomb field (true electro-disintegration) or requires the high forces found only inside the nucleus, (3) whether or not it can occur with C^{13} bombardment (it can), (4) whether the target nuclei need be heavy or light, and (5) whether the energy may be partitioned in unusual ways. An analysis is made easier by the fact that impact disintegration and stripping have been rather extensively analyzed in the literature, particularly for the case of the deuteron. However, much of the analysis is applicable only to conditions not existing in the present case. Also in the literature is a considerable amount of research on the structure of the carbon nucleus and on the photodisintegration of C^{12}. Mention will be made of the theory of impact disintegration and stripping after the experimental evidence from the present study has been presented.

First, let us look briefly at the structure of the C^{12} nucleus and of Be^{8}. After the proposal about 1936 of the statistical models of the nucleus as a liquid drop or as a degenerate Fermi gas, the old alpha-particle model of the nucleus was abandoned. It had postulated

the permanent existence of the alpha particles in the nucleus, with the alphas interacting in accord with potential functions between them, and with the forces additive when several alphas were present. However, the alpha particle concept in connection with certain nuclei, especially those that are multiples of an alpha particle, was too much in accord with the behavior of these nuclei to be abandoned completely. J. A. Wheeler[58] in 1937 rephrased it in the form that is used today - that alpha particle structures and groupings of such structures form and reform in the nucleus, existing on the average for periods long relative to the oscillation and rotation periods of these groups before rearrangement occurs. The alpha structure determines the binding energies and imposes certain restrictions on the energy levels and properties of the nucleus which are observable. In 1938 Hafstad and Teller[59] extended the model to include nuclides with one nucleon above or below the multiple of an alpha particle. Their description applies, for instance, to Be^9 and to C^{13}. In C^{13} the extra neutron can interact with only one alpha particle at a time. See Gamow and Critchfield (Ref. 56, pp 102-106) and R. R. Haefner[60] for a survey of the alpha particle model. In C^{12} the alpha particle model is an equilateral triangle with three bonds, and a

---

58. J. A. Wheeler, Phys. Rev. 52, 1083 and 1107 (1937).

59. L. R. Hafstad and E. Teller, Phys. Rev. 54, 681 (1938).

60. R. R. Haefner, Rev. Mod. Phys. 23, 228 (1951).

binding of 2.59 milli-mass-units per bond. In Be^8 the model is a "dumbbell", with a single bond. From the considerations above, we see the factors favoring the disintegration of the carbon nucleus into alphas - the alpha particles already in existence, the low binding energy for disintegration, and further, a bombardment velocity corresponding to a de Broglie wave length short enough that the interaction can be localized approximately on a single alpha. The energy level diagrams given by Hornyak et al[29] show the disintegration possibilities for C^{12} and C^{13}. C^{12} can be broken up into Be^8 in the ground state plus an alpha with a minimum energy required of 7.39 Mev. Be^8 then spontaneously breaks up into two alphas in a time estimated to be shorter than 10^{-15} sec., with a separation energy of about 0.95 Mev. The lowest excited state of Be^8 that might be formed is at 2.9 Mev, with a width of 0.9 Mev and a correspondingly short life of about 10^{-21} seconds before disintegrating into two alphas. Because of the spacing between the ground state and first excited state, there will be little difficulty in recognizing ground state reactions in emulsions once the calculations for a few cases have been run through. We notice further that, although an alpha can quite easily be knocked out of C^{12}, such is not the case with a proton, neutron or deuteron, which require respectively a minimum energy of 15.96, 18.68, and 25.20 Mev. Collisions of C^{12} with hydrogen in the emulsion at the velocities present in this experiment definitely cannot produce disintegration, either by impact or by a reaction from the compound nucleus. The Coulomb barrier certainly is too low to deliver the necessary blow. The interior nuclear forces can deliver a sharper blow but,

even if the proton velocity in the center of mass system were reversed by a head-on blow, the energy transferred to an alpha particle in the nucleus would be too low to knock it out. Reactions from the compound nucleus to give three alphas, such as[48] $C^{12}(p,n)N^{12}$, followed by $N^{12} \xrightarrow{\beta^+} C^{12*} \longrightarrow \alpha + Be^8$, have too high a threshold (20.0 ± 0.1 Mev proton in the case cited). The case $C^{12}(p,\alpha)B^9$, with $B^9 \longrightarrow 2\alpha + p$ has not been observed.

In the case of disintegration of C^{13}, a minimum of 12.26 Mev is required to form $Be^8 + n + \alpha$. The probable processes and the evidence regarding disintegration of C^{13} will be discussed later in this chapter. Because of the extra energy required to disintegrate C^{13} in comparison with C^{12} and the decrease in probability with the amount of energy that must be transferred, especially if the transfer is to be made by the Coulomb field, we expect that if C^{13} is disintegrated at all it will be a much lower order process than for C^{12}.

The photodisintegration studies of C^{12} supply an excellent background of information on the disintegration process, although the photodisintegration process cannot be extended to the present case, as will be shown later. Wilkins, Goward and co-workers[61,62,63] in England have irradiated emulsions with bremsstrahlung of energy principally from 23 to 25.5 Mev.

---

61. F. K. Goward, V. L. Telegdi and J. J. Wilkins, Proc. Phys. Soc., London A63, 402 (1950).

62. J. J. Wilkins and F. K. Goward, Proc. Phys. Soc., London, A63, 1173 (1950).

63. J. J. Wilkins and F. K. Goward, Proc. Phys. Soc., London, A64, 201 (1951).

Up to February, 1951, 600 stars from photodisintegration of C^{12} had been studied. They find that in about 10 percent of the cases the process went by the ground state of Be^8 and, in the remaining cases, the 3 Mev excited level of Be^8 was predominant. (Notice that the carbon breaks into an alpha and Be^8, not directly into three alphas. The reason apparently is the improbability of a three-body process.) The ground state Be^8 stars form a background at all energies above the threshold, but the Be^{8*} stars show a sharp rise beginning at a photon energy of about 11.4 Mev, to a maximum at about 19 Mev, followed by an abrupt fall and a gradual re-increase. The large dip in the reaction seems ascribable to the incidence of (γ,n) and (γ,p) reactions. The peak cross section for the reaction is approximately 2.4×10^{-4} barns and might be re-evaluated to not more than twice this value.

Telegdi and Verde[64] have studied the reaction with gamma rays of about 18 Mev and discussed the results in the light of the alpha particle model. More recently, Eder and Telegdi[65] have used bremsstrahlung with a spectrum up to 32 Mev for photodisintegration of C^{12} in emulsion. They verify the ratio of 10 percent ground state to 90 percent excited state of Be^8, and they find the same abrupt dip and re-increase. They find that the ground state Be^8 stars do not experience the dip but they have a monotonely increasing cross section with energy.

In order to analyze the disintegration of C^{12} by impact, it fortunately is not necessary to know what nucleus was struck. If the

---

64. V. L. Telegdi and M. Verde, Helv. Phys. Acta 22, 380 (1949).

65. M. Eder and V. L. Telegdi, Helv. Phys. Acta 25, 55 (1952).

full length of the three alphas can be observed, all the important details of the event can be determined. From the range of each alpha, its initial energy in the laboratory system can be found. From the initial dip and azimuth of the alpha and the energy, the x, y and z components of momentum are obtained. The motion of the center of mass of the three alphas can then be determined and the energy and momentum of each with respect to this center of mass. The sum of these energies relative to the center of mass of the three alphas plus 7.39 Mev for disintegration into Be^8 and an alpha, minus 0.09 Mev for the energy release on the break of Be^8, gives the energy delivered to the C^{12} in the impact. Also, the angle between each pair of alphas in this center of mass system can be found from $\cos \theta_{ij} = \dfrac{\vec{p}\,\alpha_{i/CM} \cdot \vec{p}\,\alpha_{j/CM}}{\left|p\,\alpha_{i/CM}\right| \left|p\,\alpha_{j/CM}\right|}$ where

$p\,\alpha_{i/CM}$ is the momentum of the i^{th} alpha with respect to the center of mass of the three alphas. To test if any pair of alphas came from Be^8 we can make the assumption that it did and find the disintegration energy of the pair of alphas with respect to the parent Be^8 nucleus.[61] The diagram showing the situation in the center of mass system of the three alphas is as follows:

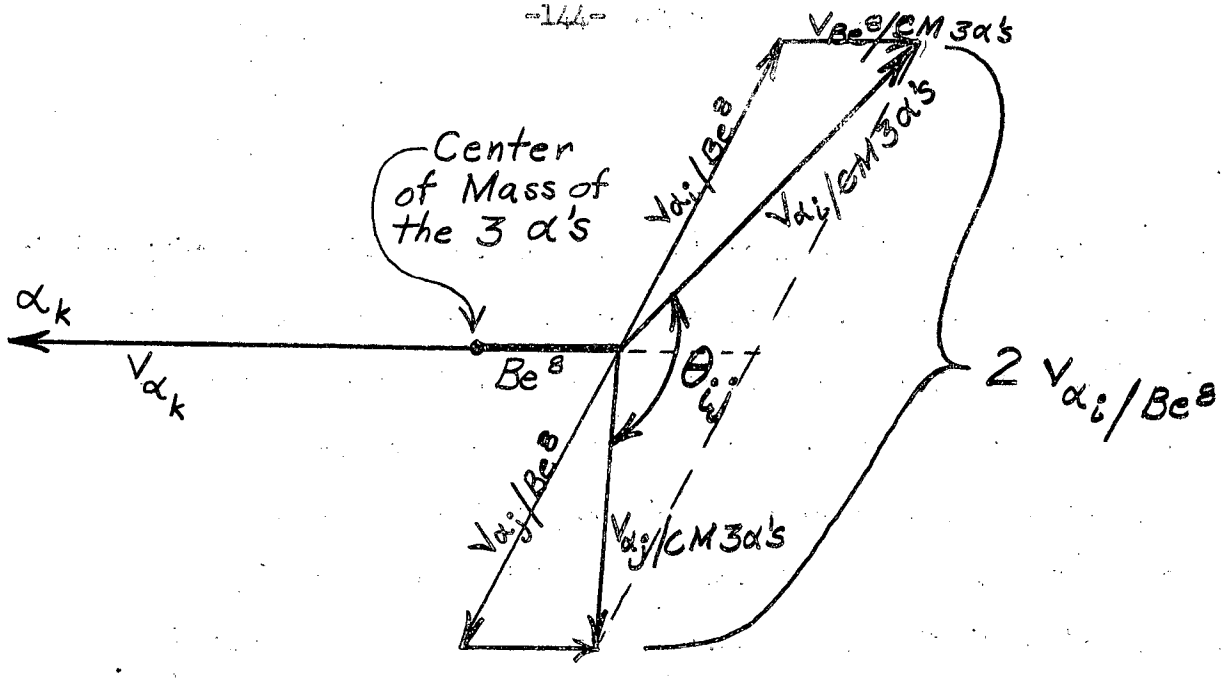

$$\left(2\,V_{\alpha_i/Be^8}\right)^2 = \left(V_{\alpha_i/CM\,3\alpha's}\right)^2 + \left(V_{\alpha_j/CM\,3\alpha's}\right)^2 - 2\left(V_{\alpha_i/CM\,3\alpha}\right)\left(V_{\alpha_j/CM\,3\alpha}\right)\cos\theta_{ij}$$

If we denote the separation energy of α_i and α_j with respect to the Be^8 nucleus as

$$E_{ij}{}^*/Be^8 = 1/2\,M_\alpha\,(V\,\alpha_{i/Be^8})^2 + 1/2\,M_\alpha\,(V\,\alpha_{j/Be^8})^2$$

and put the triangle relationship in terms of energy, we get:

$$E_{ij}{}^*/Be^8 = 1/2\,(E\,\alpha_{i/CM3\alpha's} + E_{\alpha_j/CM3\alpha's}) - (E\,\alpha_{i/CM}\,E\,\alpha_{j/CM})^{1/2}\cos\theta_{ij}\,.$$

All the quantities on the right hand side have been measured, permitting calculating of the Be^8 disintegration energy for each pair of alphas, assuming it had its origin as Be^8. Naturally, the result must be meaningless for two out of the three pairs. In the case of bombardment by carbon nuclei, sometimes three alphas will be evaporated by a compound nucleus, in which case all three separation energies are without meaning. The calculation can be used, however, to identify two alphas coming from

Be^8 in the ground state and, with enough carbon disintegrations, the higher states could also be recognized rather clearly.

To establish whether the high percentage of alphas and the non-random distribution in their grouping per star (discussed in Chapter III) came from the impact disintegration of C^{12} into an alpha plus Be^8, the analysis indicated above was carried out for stars produced by C^{12} bombardment. Every star was analyzed where there were three alphas ending in the emulsion and no other prong except the product or knock-on nucleus. The calculated data pertaining to Be^8 are tabulated in Table 5.1. In each case the Be^8 pair is starred if it is believed to exist. Sometimes the symmetry of the diagram in the center of mass system of the three alphas was an aid in showing which was probably the proper pair in the case of excited Be^8. The accuracy in the calculations in some places is not of a high order for the following reasons:

(1) A measurement of angle is difficult, particularly between alphas from Be^8 in the ground state. In such cases the tangent of the angle was measured using a reticule and hair-line but, even so, the proper setting was a guess. To some extent the difficulty was enhanced by an appearance that the two alphas diverged from a point some distance out from the star. When that was the case, the most probable separation point had to be guessed.

(2) E^*, a small quantity in many cases, is calculated from the difference between large quantities.

(3) Where some of the prongs dived rather steeply, an error is to be expected from the use of an emulsion shrinkage factor of 2.0 rather

TABLE 5.1

DATA REGARDING Be^8 FROM C^{12} DISINTEGRATION

Star No.	ΣE_{α_i} rel. to lab (Mev)	ΣE_{α_i} rel. to CM 3 α's (Mev)	Separation Energies (Mev) assuming Be^8 origin			Upper limit of Be^8 travel before disintegration (assuming there was travel)				Comments
			E^*_{12/Be^8}	E^*_{13/Be^8}	E^*_{23/Be^8}	A. Best estimate $d_{\alpha_i\alpha_j}$ (μ)	B. Extreme (μ)	$t = d/v$ (sec x 10^{13}) t_A	t_B	
1	105.9	0.567	0.154*	0.264	0.432	d_{12}= 3	5.0	0.74	1.23	Fig. 32
2	69.9	12.80	9.78	9.32	0.102*	d_{23}= 7	8.0	2.69	3.08	
3	69.3	2.34	1.84	1.49	0.183*	d_{23}= 3	4.0	0.85	1.14	
4	65.5	9.52	2.53	2.42	9.50*	d_{23}= $\frac{1}{2}$	1.0	0.17	0.34	Note d_{23}.
5	34.4	2.13	0.126*	1.90	1.16	d_{12}= 1	1.5	0.44	0.65	
6	17.9	11.3	2.44	10.22	4.31	0	0.0	-	-	I.D.?
7	28.4	16.79	6.81	11.21	7.16	0	0.0	-	-	I.D.?
8	55.7	5.22	0.344*	2.90	4.58	d_{12}= 1$\frac{1}{2}$	1.5	0.48	0.48	
9	72.9	7.40	0.072*	5.05	5.97	d_{12}= 2	3.0	0.56	0.84	
10	74.0	65.20	21.35	41.06	5.37*	d_{23}= 0	0.0	-	-	
11	48.8	0.533	0.423	0.243*	0.133	d_{13}= 4	5.0	1.42	1.77	‡
12	74.0	30.76	0.265*	23.55	22.31	d_{12}= 3	4.0	0.74	0.99	
13	17.6	3.86	2.58	3.16	0.046*	d_{23}= $\frac{1}{4}$	1.0	0.17	0.68	
14	81.6	37.5	0.149*	26.97	29.17	d_{12}= 3$\frac{1}{2}$	5.0	0.84	1.20	
15	36.1	16.8	7.47	10.29*	7.46	0	0.0	-	-	
16	12.16	5.89	0.679*	4.07	4.09	d_{12}= 0	0.5	0.00	0.33	
17	36.5	22.3	0.048*	17.4	15.9	d_{12}= 4	6.0	1.74	2.61	Fig. 35
18	22.1	5.36	2.69	4.62	0.726*	d_{23}= 0	0.5	0.00	0.27	
19	38.6	3.02	2.33	2.12	0.090*	d_{23}= 4	7.0	1.87	3.28	
20	41.5	15.7	8.88	10.22	4.39*	d_{23}= 1	1.0	0.42	0.42	Note d_{23}.
21	55.7	17.8	0.114*	14.50	12.07	d_{12}= 1$\frac{1}{2}$	5.0	0.46	1.53	
22	66.3	30.4	2.75*	27.60	15.2	0	0.0	-	-	
23	12.38	7.85	4.88	6.41	0.491*	d_{23}= 0	0.5	0.00	0.40	
24	52.3	1.36	0.083*	1.10	0.85	d_{12}= 4	5.0	1.26	1.57	
25	45.1	21.9	1.77	11.8	19.2	d_{12}= 0	2.0	-	-	I.D.?
26	79.4	14.26	0.052*	11.09	10.25	d_{12}= 1	3.0	0.24	0.73	
27	20.87	9.75	0.125*	7.57	6.92	d_{12}= 0	1.0	0.00	0.57	
28	61.2	17.9	4.82*	11.50	10.60	d_{12}= 0	0.5	0.00	0.19	
29	58.2	25.62	9.45	25.03	3.95	0	0.0	-	-	I.D.?
30	43.2	27.92	10.41	14.91	16.56	0	0.0	-	-	I.D.?
31	78.1	8.32	0.829	5.97	5.68	d_{12}= 0	1.0	-	-	I.D.?
32	31.46	9.73	5.76	3.24*	5.58	0	0.0	-	-	
33	10.60	1.63	0.874	1.47	0.096*	d_{13}= 1$\frac{1}{2}$	2.5	0.98	1.63	
34	26.44	5.14	0.206*	3.14	4.36	d_{12}= 3	5.0	1.22	2.03	
35	39.3	16.44	1.95	12.86	9.84	d_{12}= 0	0.5	-	-	I.D.?

‡ $\alpha_1\alpha_3$ appear to be Be^8 pair.

than the better value of 2.3.

Nevertheless, the data substantiates the visual evidence for impact disintegration and, in particular, for the existence of the ground state. Wherever the ground state could be distinguished visually without reservation, the analysis confirmed the assignment. Hence, both to establish the existence of ground state Be^8 in the case of stripping and to get additional data for a spectrum of the disintegration energies, the evident cases were analyzed from stripping and from stars where the third alpha went out of the emulsion. The data are in Table 5.2. The disintegration energies are grouped together to give the spectrum shown in Fig. 29 for the region below 1.0 Mev disintegration energy. The mean value is $E^* = 0.092$ Mev for the arbitrary group of 29 taken by excluding those above 0.154 Mev. (In Fig. 29, by error, a value of 0.134 was plotted for star No. 11 of Table 5.1, when the visual evidence is that the Be^8 pair of alphas was the pair which had a disintegration energy of 0.243 Mev). The average value of 0.092 Mev is, to some extent accidentally, in excellent agreement with the best values given for the disintegration energy of Be^8 in the ground state. Hemmendinger[66] got the value 0.103 ± 0.010 Mev, and Tollestrup, Fowler and Lauritsen[67] the value 0.089 ± 0.005 Mev. These values are in enough agreement with each other that it is doubtful if a better value could be obtained in the present case even from careful remeasurements and the setting up of criteria for acceptance. The main

---

66. A Hemmendinger, Phys. Rev. 73, 806 (1948) and revision, Phys. Rev. 75, 1267 (1949).

67. A. V. Tollestrup, W. A. Fowler and C.C. Lauritsen, Phys. Rev. 76, 428 (1949).

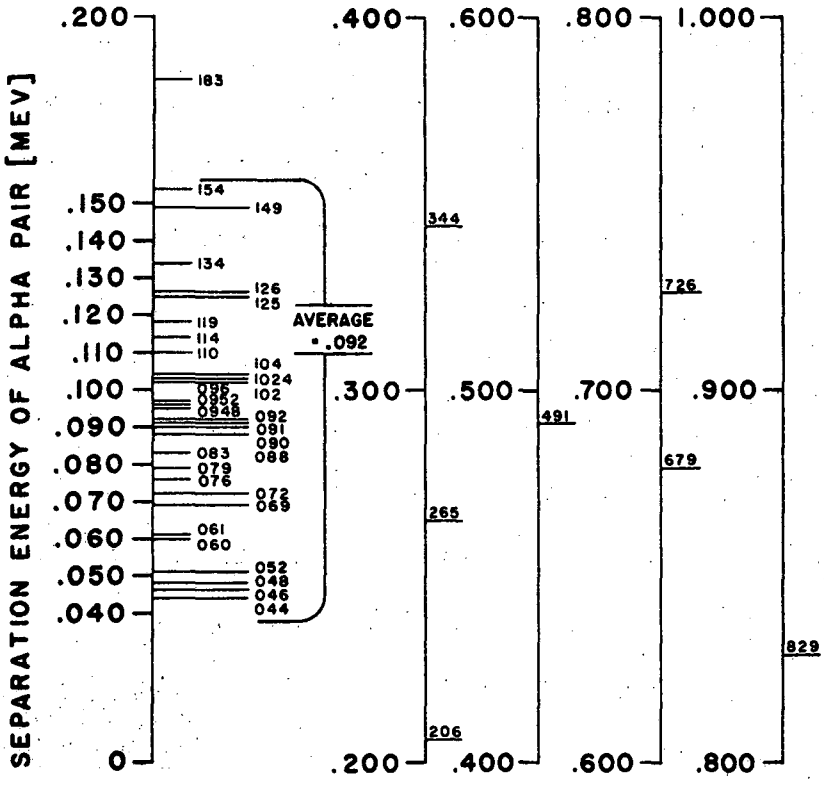

SPECTRAL DISTRIBUTION
OF BE^8 SEPARATION ENERGIES
BELOW I MEV

FIGURE 29

MU3808

TABLE 5.2

DATA REGARDING GROUND-STATE Be^8 FROM STRIPPING OF C^{12} AND FROM IMPACT DISINTEGRATION WITH THIRD ALPHA LEAVING THE EMULSION.

Star No.	E_{Be^8}/lab (Mev)	Disintegration Energy E*(Mev)	Upper limit of Be^8 travel before disintegration (assuming there was travel)				Comments
			A. Best estimate d (μ)	B. Extreme (μ)	$t = d/v$ (sec x 10^{13}) t_A	t_B	
36	78.5	.0598	3.0	4.5	0.69	1.04	Fig. 34
37	22.7	.0765	5.0	7.0	2.13	2.99	
38	37.2	.0908	2.5	3.0	0.84	1.00	
39	39.3	.0794	4.0	6.0	1.30	1.95	
40	76.5	.1042	3.0	4.0	0.70	0.93	
41	54.4	.1024	8.0	10.0	2.21	2.76	Fig. 36
42	68.0	.0612	3.5	5.0	0.86	1.24	Fig. 37
43	70.3	.0952	2.0	3.0	0.49	0.73	
44	46.2	.1186	3.5	4.0	1.05	1.20	
45	42.9	.0920	2.0	3.0	0.62	0.93	
46	55.8	.0688	6.0	12.0	1.50	2.99	
47	39.9	.0440	3.5	5.0	1.13	1.61	
48	50.8	.0948	3.0	7.0	0.86	2.00	
49	25.3	.1102	2.0	3.0	0.81	1.22	
50	27.1	.0882	5.0	8.5	1.96	3.33	

uncertainty would always be in the angle of divergence between the two alphas. Slightly improved accuracy would come from analyzing merely the Be^8 pair, as in the case of stripping. There the velocity of the center of mass of the Be^8 was found and the momentum and energy of either alpha with respect to this center of mass; this energy, when doubled, gives at once the disintegration energy.

The lifetime of Be^8 in the ground state is known only very roughly. Bethe[68] in 1937 calculated its lifetime on the basis of the systematics of alpha-radioactivity, using various values of the disintegration energy (then unknown) and of the effective radius. For 0.10 Mev disintegration energy he obtained a half-life of about 2×10^{-16} sec. for $R = 2.5 \times 10^{-13}$ cm and about 2.8×10^{-16} sec for $R = 5 \times 10^{-13}$ cm. These values are much longer than the 10^{-21} sec. half-life of Be^8 in the 2.9 Mev excited state and indicate a narrow energy level, which has never been detected by scattering. Bethe's estimate has only recently been questioned as the result of an analysis by Millar and Cameron[69] of the disintegration of O^{16} into four alphas by γ-rays up to 26.7 Mev. Of 303 such stars in Ilford E-1 emulsion, 119 had Be^8 as an intermediate product and 27 of these showed a measurable displacement of the Be^8 nucleus with respect to the other half of the O^{16} before disintegration of the Be^8. From their measurements they assigned to Be^8 in the ground state a half-life of $(5.3 \pm 1.1) \times 10^{-14}$ seconds. After this result was announced, Wilkins and Goward[70] reviewed

---

68. H. A. Bethe, Rev. Mod Phys. 9, 69 (1937) (p. 167).

69. C. H. Millar and A. G. W. Cameron, Phys. Rev. 81, 316 (1951).

70. J. J. Wilkins and F. K. Goward, Proc. Phys. Soc., London, A64, 849 (1951).

their stars from the photodisintegration of O^{16}. They found 280 stars with Be^8 in the ground state. They made a calculation of the limits of resolution on the point where the disintegration occurred, based on the Be^8 having about 2.5 Mev kinetic energy. They conclude that such a definite half-life as that given by Millar and Cameron cannot be obtained. However, their analysis indicates that 5×10^{14} sec. can be accepted as an upper limit of the half-life.

The impact disintegration of carbon in the present research gave some promise of shedding light on the lifetime of Be^8 since the displacement of the Be^8 in the emulsion before break-up would be considerably larger at the kinetic energies occurring here, which range up to about 70 Mev. To counterbalance, the angular resolution would be poorer. In some of the stars there did seem to be a definite intersection of the two alpha tracks beyond the star. Such an appearance could be deceiving since it might be due to small angle scattering. But it must be borne in mind that the disintegration energy determines a definite angle of separation for a given kinetic energy of the Be^8, and a late divergence of the alphas would have to mean that they were scattered towards each other before they were finally scattered apart. It might be hoped that travel as Be^8 would be detectable by the ionization density. Since the ionization varies as Z^2, the ionization from Be^8 would be twice that from two alphas. However, the response of the emulsion could hardly be expected to be linear if two particles were close enough to pass through the same crystals.

With the attitude that it would be virtually impossible to actually set the point of disintegration, data were taken on the upper limit for

that point. Two distances for each Be^8 in the ground state were recorded: (1) The best estimate of the upper limit under the assumption that the Be^8 did travel before disintegrating. This would be the distance of the solid track before it seemed to show any signs of widening. (2) The extreme upper limit. This would be the point, often still short of distinguishable double tracks, where the track definitely showed a thickening. The data are given in Tables 5.1 and 5.2. The times given by the best estimate of the upper limit have been grouped into intervals of 0.5×10^{-13} sec. and the resulting histogram plotted in Fig. 30 for the 36 cases of ground state Be^8 that have been analyzed. Except for a low number in the first time interval (which might be ascribed to the fact that the upper limit was estimated), the plot does seem to give some indication of a half-life of roughly 6×10^{-14} seconds. The inadequacy of the data must, of course, be kept in mind.

If such a long half-life is true, it may indicate, as pointed out by Sterns and McDaniel,[71] that the ground state of Be^8 has $J=2$, even parity, and that the 3-Mev level has $J = 0$, even.

A better determination of the half-life of Be^8 than can be obtained in photographic emulsion should be determinable from cloud chamber pictures, providing that turbulence can be eliminated and thin ionization tracks be obtained. In January, 1951, W. M. Powell and K. E. Relf, both of the University of California Radiation Laboratory, set up a large cloud chamber outside the magnetic field of the cyclotron. Carbon ions were piped to the cloud chamber through an iron extension snout on the

---

71. M. B. Stearns and B. D. McDaniel, Phys. Rev. 82, 450 (1951).

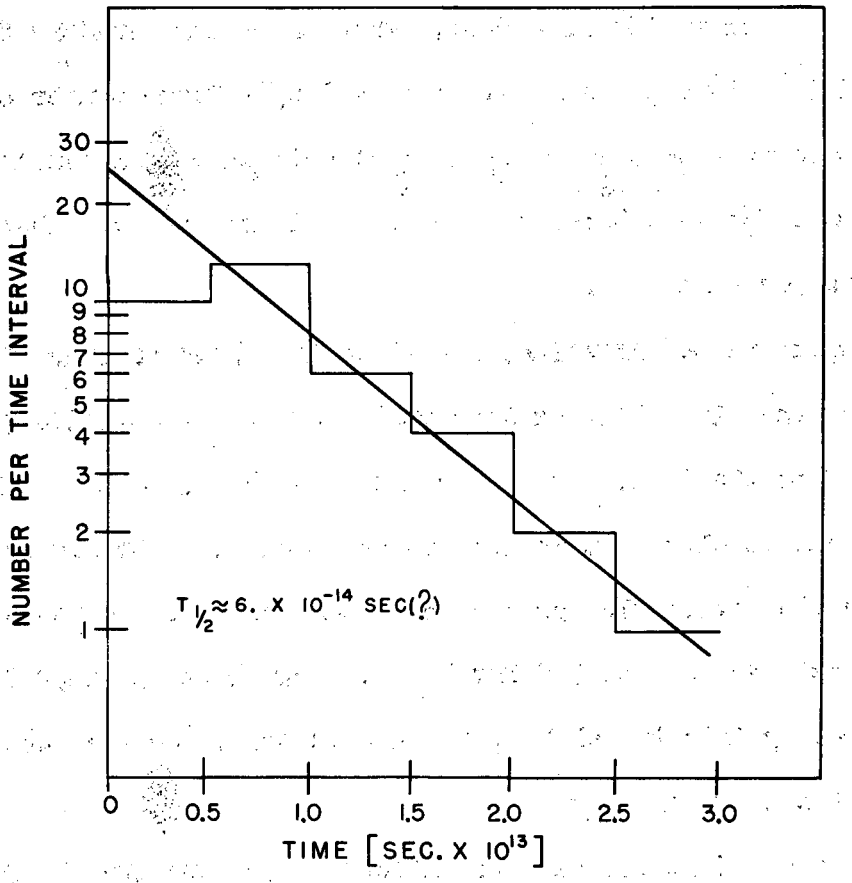

HISTOGRAM OF BEST ESTIMATE OF
UPPER LIMIT OF DISINTEGRATION TIME
OF Be^8 IN GROUND STATE
(36 EVENTS)

FIGURE 30

MU 383

cyclotron that acted as a magnetic shield, followed by a twelve-foot brass tube. The cloud chamber was filled with argon for the express purpose of detecting electro-disintegration of carbon nuclei. Elastic collisions were observed but no inelastic events. From the cross sections found in emulsion study, it is apparent that an exceedingly large number of pictures would have to be made to obtain significant data on carbon disintegration. The cloud chamber picture becomes confused if there are more than about a dozen tracks per expansion.

With respect to Be^8 lifetime, attention is called to stars No. 4 and 20, which are cases involving excited states of Be^8, respectively 9.5 Mev and 4.39 Mev from the data. These probably are the 9.8 and 4.9 Mev levels shown by Hornyak et al.[29] It is well established that the 4.9 Mev level must decay by the rather slow process of γ-emission before it can break into two alphas. As for the 9.8 Mev level, Hornyak et al show that it can break directly into two alphas; if this is true, the star observed must represent a different level.

What fraction of impact disintegrations of C^{12} involve the ground state of Be^8? A surprisingly large number do. Of the 35 stars from C^{12} with all three alphas ending in the emulsion, 21 or 22 have Be^8 in the ground state. Compare this to the 10 percent ground state figure found from γ-ray disintegration,[63,65] bearing in mind also that some of the stars in the present case, especially for higher values of the indicated disintegration energy, may not come from C^{12} disintegration but from a true compound nucleus. It must be admitted that the data above from carbon bombardment is unavoidably biased against the excited states of

Be^8 because the probability of finding three widely diverging alphas all ending in the emulsion is much less than when two of the alphas have almost the same direction and length. A better idea of the relative number of ground and excited states can be gained by an enumeration of all stars based on personal judgment as to whether or not impact disintegration was involved. Accordingly, Table 5.3 has been compiled. (It includes other data not pertinent at the moment - on stripping and on comparison with C^{13} bombardment.) To indicate to some degree the reliability to be placed on the assignment of stars, they were put into "probable" and "possible" classes. The assignment to "probable" is rather firm, especially if the easily recognizable ground state is present. For the "probable" excited states, the assignment must be based on such things as the symmetry of a pair of alphas or the reappearance of nearly all the incident energy in the three alphas. The "possible" classification is much more indefinite and includes nearly all stars where there appear to be three alphas and no other emitted particle. Of course, a considerable number of these will be evaporation stars from a compound nucleus. The table shows that the ratio of ground state to excited state was changed from 21/14 for stars with all prongs ending in the emulsion, to 41/53 for "probable" impact disintegrations, or to 50/78 for all "possible and probable". The lowest ratio corresponds to about 40 percent in the ground state. The reason for the disagreement with photodisintegration is not far to seek. As we shall see, often little energy is transferred to the carbon other than that to disintegrate it. The Be^8 is sheared off the C^{12} with hardly any effect on the Be^8. On the other hand in photodisintegration, since the

TABLE 5.3

STARS PROBABLY OR POSSIBLY INVOLVING IMPACT DISINTEGRATION OR STRIPPING.

Incident Particle:	C^{12}			C^{13}		
IMPACT DISINTEGRATION						
Probable:						
Ground state Be^8	41	94		21	48	
Excited state Be^8	53			27		
Possible:			128			75
Ground	9	34		3	27	
Excited	25			24		
STRIPPING						
Probable:						
Ground	11	59		12	38	
Excited	48			26		
Possible:			141			68
Ground	0	82		2	30	
Excited	82			28		
Total of all stars			865			1114

photon has almost no momentum, momentum must be conserved in the disintegration by equal and opposite impulses on the alpha and the Be^8. As a result, the Be^8 is often excited.

Another question we seek information on is whether impact disintegration is a high velocity or low velocity process. The distances from the track beginning to the events summarized in Table 5.3 were gathered for C^{12} and plotted in Figure 31. Since the data is not sufficient for precise analysis, no attempt was made to convert into energy terms, or even into fraction of the total range. In view of the fact that the average track length from plate to plate has a variation about equal to the standard deviation of the individual tracks on a plate (6 microns), the raw figure of distance to the event was plotted. In the case of impact disintegration, the ground state Be^8 "probable" cases are shown for comparison with the total of all "possible and probable, ground state and excited" cases. The latter distribution shows some indication of a double hump. If such is really the case, the first hump might be due to the shearing of Be^8 from C^{12} with large impact parameters, with the third alpha being kept out of the nucleus by the centrifugal barrier. The low velocity hump then would possibly be due to more nearly central collisions. The ground state Be^8 stars seem to show no preference for high or low velocity. It will be recalled from Chapter III in the discussion on backward prongs (Fig. 17 and Table 3.6) that four-prong stars have rather an early-range peak and that in comparison the cases of impact disintegration (which are nearly all included in the four-prong stars) have considerably longer average distance.

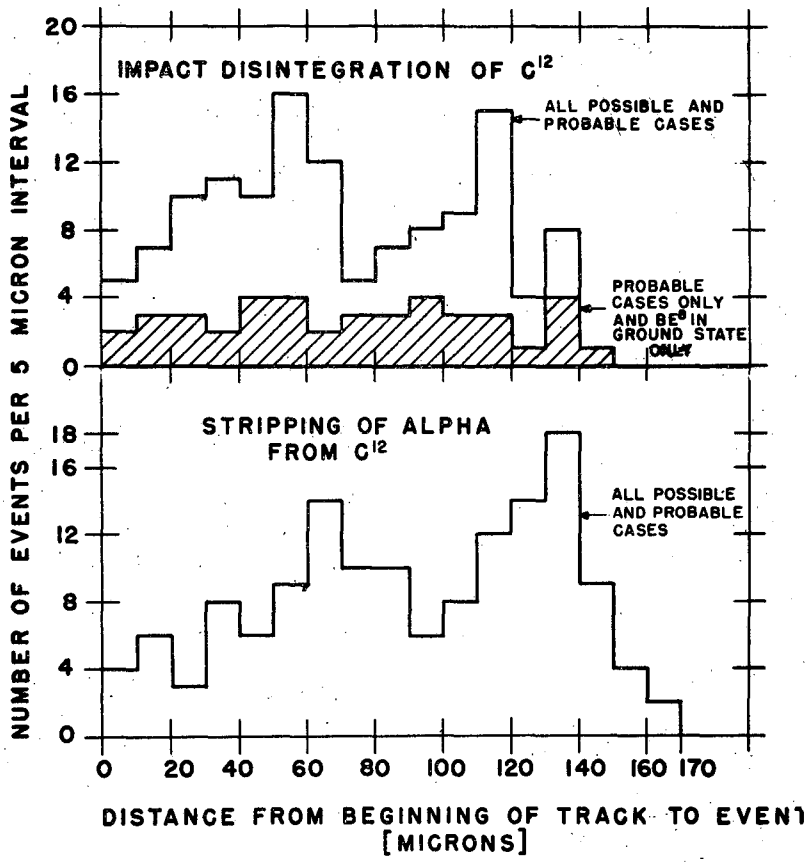

HISTOGRAM OF IMPACT DISINTEGRATION AND STRIPPING OF C^{12} NUCLEI

FIGURE 31

MU5810

There are some interesting features to the energy balances in the disintegration of C^{12}, given in Table 5.4 for the same set of stars considered in Table 5.1. For instance, we see how little energy was expended in some cases beyond that necessary to break up the carbon nucleus. In the first two stars, indeed, the energy comes out negative, due to the uncertainty in the energy of the particles in the carbon beam. Columns 3, 4 and 5 are considerably more accurate than is column 2. In some cases, e.g., stars 12 and 14, we see that considerable energy beyond the 7.39 Mev required was absorbed by the C^{12}, even though Be^8 in the ground state was involved.

Also light is shed on whether the struck nucleus was heavy or light from the following two considerations: (1) Comparison of the energy $E_{knock-on}$, delivered to the struck nucleus, with its range. Part of $E_{knock-on}$ could, of course, go into excitation rather than kinetic energy. $E_{knock-on}$ = (energy of C^{12} at time of event) - (energy of the three alphas with respect to the laboratory, plus the disintegration energy, 7.39 Mev, minus 0.09 Mev for energy release by Be^8). (2) Comparison of energy transferred to the struck nucleus, $E_{knock-on}$ with the energy that went into break-up of the C^{12}. The latter (shown in the table as $E_{C12_{break-up}}$) equals the sum of the alpha energies with respect to their center of mass, plus 7.39 Mev, minus 0.09 Mev.

If the energy delivered to the knock-on is comparable to that delivered to the C^{12}, then the struck nucleus probably was light. The collisions seem to be fairly evenly divided heavy and light target nuclei.

TABLE 5.4

ANALYSIS OF ENERGY IN IMPACT DISINTEGRATION OF C^{12}.

Star No.	Expected E_{C12} at event (±2.4 Mev s.d.)	$E_{3\alpha's}$ rel. to lab.	$E_{3\alpha's}$ rel. to lab. +7.39 - .09	E_{C12} break-up	Gd or *	$E_{knock-on}$ (Col 2-4)	Range of knock-on (μ)	Heavy or Light Target - Comments -
1	109.0	105.92	113.22	7.87	Gd	0.0	~0.7	Heavy? Fig. 32.
2	75.8	69.94	77.24	20.10	Gd	0.0	<2.0	Heavy
3	97.2	69.32	76.62	9.64	Gd	20.6	~0.7	Heavy
4	94.5	65.48	72.78	16.82	*	21.7	0.0	Heavy
5	56.2	34.42	41.72	9.43	Gd	14.5	17.5	Light (maybe C^{12})
6	72.0	17.94	25.24	18.62	ID?	46.8	25.2	Light (maybe C^{12})
7	58.9	28.38	35.68	24.08	ID?	23.2	28.6	Light (maybe C^{12})
8	73.2	55.68	62.98	12.52	Gd	10.2	8.5	Light
9	82.0	72.88	80.18	14.70	Gd	1.2	2.0	Heavy?
10	101.2	74.02	81.32	72.49	*	19.9	9.2	Light (1α of 898 μ)
11	90.0	48.76	56.06	7.83	Gd	34.0	~0.7	Heavy?
12	90.9	74.02	81.32	38.06	Gd	9.6	10.0	Light
13	38.4	17.56	24.86	11.16	Gd	13.5	7.5	Light
14	98.5	81.56	88.86	44.83	Gd	9.7	1.5	Heavy
15	101.0	36.10	43.40	24.11	*	57.6	30.2	Light (prob. oxygen)
16	44.0	12.16	19.46	13.19	Gd?	24.5	18.1	Light
17	74.4	36.51	43.81	29.56	Gd	30.6	24.8	Light(prob.C^{12})Fig.35
18	42.0	22.10	29.40	12.66	Gd?	12.6	4.0	Heavy?
19	46.3	38.60	45.90	10.32	Gd	0.4	1.4	Heavy?
20	52.8	41.48	48.78	22.96	*	4.0	4.0	Heavy?
21	68.5	55.72	63.02	25.09	Gd	5.5	4.5	Heavy?
22	80.9	66.26	73.56	37.68	*	7.3	10.0	Light
23	69.6	12.38	19.68	15.15	Gd?	50.0	45.6	Light (prob. C^{12})
24	65.2	52.32	59.62	8.66	Gd	5.6	2.0	Heavy?
25	62.3	45.12	52.42	29.17	ID?	9.9	4.5	Light?
26	87.7	79.36	86.66	21.56	Gd	1.1	2.5	Heavy?
27	53.5	20.87	28.17	17.05	Gd	25.3	13.0	Light
28	72.5	61.22	68.52	25.24	*	4.0	5.5	Heavy?
29	83.3	58.16	65.46	32.92	ID?	17.8	9.7	Light
30	73.1	43.19	50.49	35.22	ID?	22.6	13.8	Light
31	87.6	78.14	85.44	15.62	ID?	2.2	2.0	Heavy?
32	98.2	31.46	38.76	17.03	*	59.5	>25.5	Light
33	76.8	10.60	17.90	8.93	Gd	58.8	52.5	Light (prob. C^{12})
34	79.2	26.44	33.74	12.44	Gd	45.5	1.5	Heavy
35	51.4	39.26	46.56	23.74	ID?	4.8	5.0	Heavy?

E_{C12} break-up = $\sum_i E_{\alpha_i}$/CM of 3α's + 7.39 - 0.09

In some cases, such as stars 17, 23 and 33, the nucleus struck quite definitely was C^{12}. In such a case, because of the indistinguishability of like particles, it cannot be known which is the incident and which the struck particle. In star 33 the energy transfer was more than 50 Mev and yet one of the carbon nuclei was not disintegrated.

It is apparent from the energy transfers that in a number of cases, such as that shown in Fig. 35 (star 17), the necessary transfer could not have been effected by the Coulomb field alone. On the other hand, so little energy was transferred in certain other cases that there is no reason to think there was penetration beyond the Coulomb barrier (e.g. star No. 1, shown in Figure 32).

The partition of the energy between the Be^8 and the third alpha sometimes is quite interesting. There are a few cases where nearly all the kinetic energy of the C^{12} (except for the 7.39 Mev for disintegration) went into kinetic energy of the Be^8 and the alpha, and in some of these, such as stars 1 (Fig. 32) and 9, the energy was fairly well divided in the ratio 2 to 1. But there are other cases (and these are not confined to stars where nearly all the C^{12} kinetic energy reappeared) where an alpha got more than one-third of the C^{12} energy at the time of collision or a Be^8 in the ground state got more than two-thirds of the energy.

Some of the energetic alphas are quite striking. The alphas holding the range record are of this type - 896 microns from C^{12}, 898 microns from C^{13} disintegrations, while the range of cyclotron alphas is 500 microns. Table 5.5 gives the data on the cases that have been analyzed of a long alpha from impact disintegrations. Included are two cases from the C^{13}

TABLE 5.5

MORE THAN PROPORTIONATE ENERGY DISTRIBUTION IN IMPACT DISINTEGRATION AND STRIPPING OF CARBON NUCLEI.

Star No.	C^{12} or C^{13}	Be^8 Gd or *	KE_{carbon} entering event (±2.4 Mev)	Long range alpha from impact disintegration: Mass motion momentum p_{mm}	$\varphi = \cos^{-1}(\vec{p}_{mm}, \vec{p}_{act})$	Range (μ)	Actual energy	p_{actual}	$p_{actual} - (p_{mm}\cos\varphi)$	θ
2	C^{12}	Gd	75.8	10.60	19°15'	605	41.76	12.92	2.91	57°36'
10	C^{12}	*	101.2	11.61	1°30'	896	52.56	14.50	2.89	57°51'
-	C^{12}	*	89.5	10.92	13°30'	751	47.40	13.77	3.15	54°35'
-	C^{12}	Gd	92.6	11.18	5°45'	654	43.72	13.22	2.10	67°16'†
-	C^{13}	*	98.5	11.01	6°	898	55.20	14.86	3.91	44° 0'
-	C^{13}	*	99.6	11.07	4°	793	48.96	13.99	2.95	57° 8'
		ID or S			Be^8 in ground state (C^{12} stars only)					
12	C^{12}	ID	90.9	21.12	3°		68.23	23.36	2.27	
14	C^{12}	ID	98.5	22.93	5°		71.35	23.89	1.05	
26	C^{12}	ID	87.7	21.63	15°14'		70.55	23.76	2.89	
31	C^{12}	ID	87.6	21.61	0°		63.43	22.53	0.92‡	
36	C^{12}	ID	103.0	23.44	5°40'		78.51	25.06	1.73‡‡	
40	C^{12}	S	109.4	24.15	19°		76.47	24.73	1.89	
43	C^{12}	S	91.0	22.04	7°30'		70.31	23.72	1.87	

† Fig. 33.
‡ Gd state?
‡‡ Fig. 34.

Mass motion KE for alpha is 1/3 KE_{C12} or 4/13 KE_{C13}; for Be^8 it is 2/3 KE_{C12}.
All momenta (so-called) are $\sqrt{ME}$ with M=A, the mass number and E in Mev.
$p_{internal}$ is taken as $\sqrt{MI} = \sqrt{(4)(7.39)} = 5.436$.
Maximum possible momentum, $p_{max} = p_{mm}\cos\varphi + p_{internal}$.
Actual energy $Be^8 = E\alpha_1 + E\alpha_2 - 0.09$.

$$\theta = \cos^{-1}\frac{(p_{act} - p_{mm}\cos\varphi)}{p_{int}}$$

stars. The table does not include every case of more than proportionate energy division; therefore, no statistical conclusion regarding energy partition is to be drawn from it. It will be noticed that in most of the collisions producing a long alpha, the Be^8 was excited. Such an occurrence appears to be logical since the Be^8 was given a hard blow, partially stopping it, while the alpha went forward. In two cases, however, the Be^8 was left in the ground state. One such case (from an early plate not totaled into the present study) is shown in Figure 33. In order to show how large a component of the internal momentum of the alpha with respect to its nucleus added onto the incident momentum, the various columns of "momenta" have been calculated. For convenience, the "momentum" is given as $\sqrt{ME}$ with $M = A$, the mass number, and E in Mev. The proper fractional share of the incident momentum is called p_{mm} (mass motion momentum) and its component in the direction of the long range alpha is $p_{mm}\cos\varphi$. The internal momentum, p_{int}, is taken as $p_{int} = \sqrt{MI}$ where $I = 7.39$ Mev, the energy required to knock an alpha from the C^{12} nucleus. In using the value 7.39 Mev, we have taken an extreme upper limit for the internal momentum. It should be considered as a reference point, not as the true value. A more reasonable value of p_{int} might come from taking $I = (2/3)(7.39) = 4.93$ Mev since each alpha is held by two of the three alpha-alpha bonds. Another value might come from $\Delta p \Delta x \geq \hbar$ where for Δx we use $\sqrt{(x^2)_{av}}$ given by Wheeler (see later in this chapter). From this relation we get a momentum that corresponds to an energy of about 3.44 Mev. Either of these values will imply that the internal momentum lined up much more closely in the direction of the actual momentum than

is indicated by the angle θ in Table 5.5. In fact, for the C^{13} star that had an alpha of 898 microns range, the value $I = 3.44$ Mev is too small to give $\cos\theta \leq 1$.

The maximum possible momentum in the direction of the alpha would be $p_{mm}\cos\varphi + p_{int}$. The actual momentum, p_{act}, is calculated from the energy implied by the actual range of the alpha. A diagram of the momenta is below:

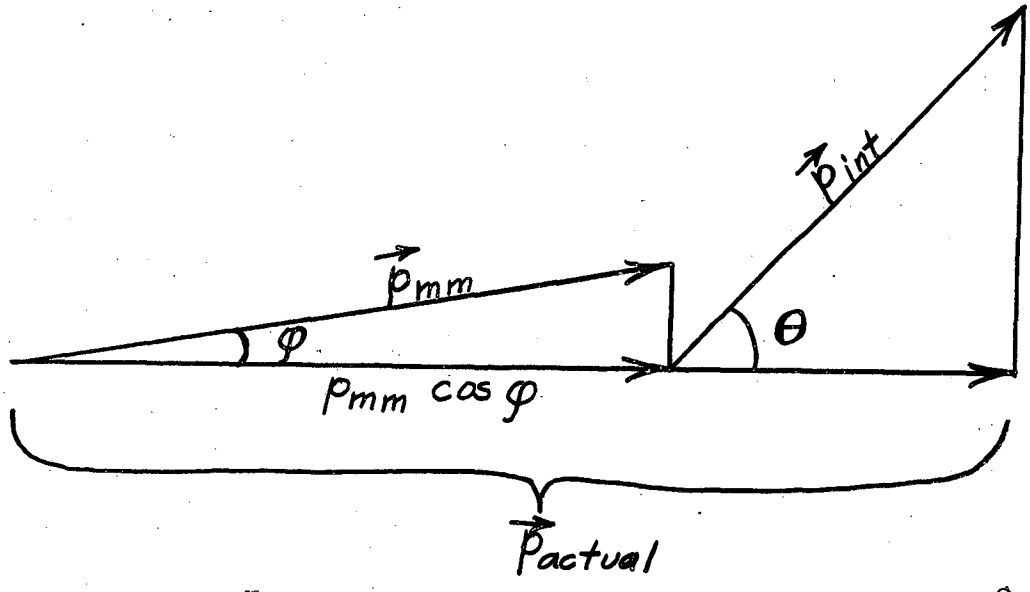

The second half of Table 5.5 gives cases of ground-state Be^8 from stripping and impact disintegration where the kinetic energy of the Be^8 was more than two-thirds of the entering C^{12} energy. Excited states of Be^8 were not included because of the difficulty in being sure of the classification. The internal motion of the Be^8 groups as a unit in the carbon nucleus shows up less impressively than did the internal alpha motion, yet can contribute an appreciable component of momentum, as

exemplified by stars 12 and 26. One of the Be^8 which got more than two-thirds of the C^{12} energy is shown in the impact disintegration of Figure 34 (star No. 36).

Until now impact disintegration has been discussed for C^{12}, with only bare reference to C^{13}. From the energy level and reaction diagrams,[29] it is evident that the disintegration of C^{13} into three alphas, plus a neutron, will be more difficult than breaking C^{12} into three alphas.

To knock out an alpha from C^{13}, leaving ground-state Be^9, requires at least 10.63 Mev. Be^9 is stable but, if Be^{9*} is formed, it can give Be^8 plus a neutron, with a minimum total energy requirement of 12.26 Mev. Another possibility might be to knock out He^5, leaving Be^8. This process requires a minimum of 13.0 Mev. The He^5 disintegrates in about 2.4×10^{-21} sec. into an alpha and neutron. A third possibility is to knock a neutron out of C^{13} (4.88 Mev minimum required) with the production of C^{12*} which, from its 9.7 Mev level or higher, may decay to $Be^8 + \alpha$. Despite the low energy for knocking out a neutron, it can easily be understood that the process will be much less favored in the case of carbon ion bombardment than is knocking out an alpha or He^5.

The bombardment of emulsion with C^{13} nuclei does not give unique evidence as to C^{13} disintegration because of the presence of C^{12} in the emulsion. In the center of mass system the bombardment could be considered to be by either C^{12} or C^{13}. In fact the C^{12} has the higher velocity. It was seen from the energy and range analysis of C^{12} impact disintegrations in Table 5.4 that C^{12} is frequently disintegrated by collisions with light

nuclei. Therefore, it is to be expected that many of the impact disintegration stars from C^{13} bombardment will be ascribable to C^{12}. On surveying the C^{13} plates, one is confronted with the evidence that such is indeed the case. On the C^{12}-bombarded plates the Be^{8} and alpha from impact disintegration are strongly directed forward and often have long ranges. On the C^{13} plates, however, it is at once noticeable that the average kinetic energy in the three alphas is much smaller and that their distribution is more nearly isotropic. The track of what would be called the knock-on nucleus in C^{12} bombardment is longer here, indicating that it is indeed the incident particle.

Not all the impact disintegrations from C^{13} follow the pattern described above. There is a considerable fraction with long range, forward-projected alphas and short knock-on tracks, not apparently different from disintegrations of incident C^{12} nuclei at high energy. These stars are assignable to the impact disintegration of the C^{13} itself.

It was not possible to determine what fraction of the disintegration stars on a C^{13}-bombarded plate is actually the disintegration of C^{13}. The distinction between disintegration of C^{12} and C^{13} may be far from clear-cut when the velocity has decreased appreciably. Table 5.3 gives a summary of impact disintegration of carbon from C^{13} bombardment without distinction between the two possible cases. The best index for comparison with C^{12} bombardment is the number of cases of stars with "probable" ground state Be^{8}. From C^{13} bombardment there are 21 of these out of 1114 stars of all types; from C^{12} there were 41 out of 865 stars, about two and a half times as many from C^{13} bombardment. In Table 3.2 of Chapter III is

shown the composition of the bismuth-loaded D-1 emulsions used in most of the C^{13} bombardments. In them the percentage of the total geometric nuclear area belonging to C^{12} is about 18.2 percent. Therefore, roughly, about (.182)(1114), or 203, stars are from collision of C^{13} on C^{12}. It is readily seen that 21 "probable" impact disintegrations with Be^8 in the ground state gives too high a ratio by a factor of two. The existence of impact disintegration of C^{13} is thus confirmed and roughly assigned half the disintegration stars. A visual examination would say this estimate is not unreasonable but perhaps a little high - that between a quarter and a half of the disintegrations are of C^{13}.

Since impact disintegration of C^{13} is possible, might not disintegration of O^{16} in the emulsion also occur? The energy level diagrams[29] show that it might be accomplished with an expenditure of about 16 Mev by knocking out an alpha to leave an excited state of C^{12} that could break up into Be^8 plus an alpha. A few stars with four alphas have been noticed that indeed appear to be disintegration of O^{16}.

All the experimental evidence discussed thus far has been on the subject of impact disintegration. However, the closely related phenomenon of stripping is nearly as frequent and hardly less striking. As used here, stripping includes those cases where the carbon nucleus was disintegrated into Be^8 and an alpha with the alpha being captured by the struck nucleus. The other possibility, of the Be^8 being captured and the alpha flying past, is not included for two reasons: (1) it would be hard to identify as stripping; (2) it does not occur with a probability comparable to that of the other case.

As in the case of impact disintegration where the impacts were sometimes hard, sometimes light, so it is with stripping, with perhaps a larger proportion of light impacts. A spur from the struck nucleus may be practically invisible, as in the stripping in Figure 36 (star No. 41) where only a small bump marks the spot where the event occurred. Such a bump would not be counted as a prong in the ordinary star. In the case of stripping, however, the uniform rule was adopted that they should be called three-prong stars even though a third prong could not be seen for certain.

The distances to "possible and probable" stripping events in C^{12} bombardment were gathered and plotted in histogram form in the lower part of Figure 31 for comparison with the same data from impact disintegrations. The two curves are not dissimilar though the stripping curve rather definitely seems to favor lower velocities. It should be mentioned that for events near the end of the carbon ion range there may be some confusion between stripping and impact disintegration since it often is impossible to tell whether the third track is of an alpha or of a light target nucleus.

In stripping, since an alpha is captured by the target nucleus there is the possibility of an (α, x) reaction. These have been observed to occur. They can be identified for certain only when the reaction is marked as stripping by the presence of Be^{8} in the ground state. An example of stripping plus an (α, p) reaction is shown in Figure 37. From the C^{12} plates the definite cases of stripping plus (α, x) reactions are: one of (α, p), one of (α, 2p), two of (α, αp). The case of an (α, α') reaction would of course be indistinguishable from impact

disintegration.

Stripping occurs in C^{13} bombardment, as did impact disintegration and apparently involves both the C^{12} in the emulsion and the incident C^{13}. Either He^5 or He^4 might be knocked out of the C^{13} nucleus and captured by the target nucleus.

The frequency of stripping, from both C^{12} and C^{13} bombardment, is indicated in Table 5.3. For the "probable" cases the number is seen to be about two-thirds of the corresponding number of impact disintegrations. The cases involving the ground state of Be^8 appear to be a significantly lower fraction of the total than in impact disintegration. The explanation may be that at the lower velocity the interaction with the Be^8 is stronger; possibly also the impact is more nearly central than with impact disintegration. In Table 5.3 the "possible" classification should be discounted severely, as mentioned before. The classification was included to give an upper limit for the process.

A comparative assessment of cross sections can now be made:

Impact Disintegration:

C^{12} bombardment:

$$\text{Lower limit} = \frac{(94)}{(865)}\ (0.446) = 0.049 \text{ barn (based on "probable" cases only)}$$

$$\text{Upper limit} = \frac{(128)}{(865)}\ (0.446) = 0.066 \text{ barn (based on all "possible and probable" cases).}$$

(0.446 is the cross section at 110 Mev for production of all types of stars).

Impact Disintegration: (cont'd)

C^{13} bombardment (Disintegration of C^{12} in emulsion and C^{13} are not separated):

$$\text{Lower limit} = \frac{(48)}{(1114)}(0.388) = 0.017 \text{ barn}$$

$$\text{Upper limit} = \frac{(75)}{(1114)}(0.388) = 0.026 \text{ barn}$$

Stripping:

C^{12} bombardment:

$$\text{Lower limit} = \frac{(59)}{(865)}(0.446) = 0.030 \text{ barn}$$

$$\text{Upper limit} = \frac{(141)}{(865)}(0.446) = 0.073 \text{ barn}$$

C^{13} bombardment:

$$\text{Lower limit} = \frac{(38)}{(1114)}(0.388) = 0.013 \text{ barn}$$

$$\text{Upper limit} = \frac{(68)}{(1114)}(0.388) = 0.024 \text{ barn}$$

There is one further piece of evidence regarding impact disintegration. A few five- and six-prong stars have a pair of alphas that look as if they had come from Be^8 in the ground state. An example is the star in Figure 24B. In addition, the composition of the six-prong stars, in particular, is remarkable. Few of them have a proton track, and about half of them seem definitely to have no prongs other than alphas. The indicated conclusion is that they represent a complete double disintegration of two

carbon nuclei. Correspondingly, some of the five-prong stars may represent partial double disintegration from collisions with carbon, nitrogen or oxygen in the emulsion. The conclusion is supported by the fact that under C^{12} bombardment there appears a higher percentage of five- and six-prong stars than from C^{13} bombardment, as shown in Figure 14.

B. THEORETICAL ASPECTS

No complete theoretical description of the impact disintegration and stripping of C^{12} and C^{13} will be given here. Instead, a discussion will be given of what method of treatment is applicable, and what is not, compared to other cases treated in the literature.

Disintegration by impact as a quantum mechanical problem was first discussed by Oppenheimer[72] in 1935 for the case of the deuteron. Since that time there have been many other treatments for the deuteron, both at low and high velocities, covering impact disintegration, stripping, and the Oppenheimer-Phillips process. The discussion of impact disintegration has been extended to particles other than the deuteron, especially for the case of very high velocities such as appear in cosmic rays. At high velocities the treatment can be made identical to that for photodisintegration by setting up the quantum mechanical description of the electric field from the passing particle.

Unfortunately, very little in the existing treatments can be applied to the present case of impact disintegration of carbon nuclei. The

---

72. J. R. Oppenheimer, Phys. Rev. 47, 845 (1935).

reason essentially is that the velocities here are rather low, but the interaction must be reasonably strong. C^{12} is fairly easy to disintegrate compared to most other nuclei since it requires only 7.39 Mev to knock out an alpha, but it is not as easy to break up as the deuteron where the binding is only 2.18 Mev.

We can rule out at once the photoelectric type of treatment[73,74,75,76] The treatment[74] essentially is a Fourier decomposition of the field of a passing charged particle from the frame of reference of the particle to be disintegrated. In this field there must be frequencies high enough to produce the disintegration; that is, $h\nu > 7.39$ Mev. Further, the relative velocity of the particles must be high enough that the exponential in the electric field term does not vary much during the collision time. This condition is: $2\pi\nu \ll \frac{v\gamma}{b}$ where $\gamma = \frac{1}{\sqrt{1-\beta^2}}$ and b is the impact parameter. In addition, the treatment is valid only for impact parameters greater than the sum of the radii of the particles. In the present case, from $2\pi\nu \ll \frac{v\gamma}{b}$ we see that in order to get a high enough frequency to disintegrate the C^{12} nucleus at the existing velocities, the value of b will be less than the sum of the nuclear radii.

There remains the possibility of using a treatment similar to that Bohr used in getting the energy loss of a heavy particle in collisions

---

73. C. F. v. Weiszacker, Zs. f. Phys. 88, 612 (1934).

74. E. J. Williams, Kgl. Danske Videnskabernes Selskab., Math-fys. Meddelelser, 13, No. 4 (1935).

75. B. d'Espagnat, C. R. Acad. Sci. Paris, 230, 1268 (1950) and 231, 38 (1950).

76. S. M. Dancoff, Phys. Rev. 72, 1017 (1947).

with electrons. In order to apply it, several features are to be noticed:

(1) The classical orbital treatment given by Bohr is to be used, not the Born approximation wave treatment by Bethe (see Chapter VII for more complete discussion on this point). The criterion determining that the orbital treatment is valid is that $K \equiv \frac{2Z_1Z_2e^2}{\hbar v} > 1$.

In collisions between C^{12} and other nuclei, $Z_2 \geq 6$ and $K > 1$ at all velocities present here, if we neglect collisions with hydrogen, which do not produce disintegrations.

(2) The de Broglie wave length is short enough that the incident particle can act on a single alpha particle in the C^{12} nucleus. Notice that the point of view has now been reversed so that the C^{12}, particle No. 1 in the formulae, is at rest and the other particle, No. 2, is in motion with respect to it. The problem is now one of the scattering of particle No. 2. If its scattering angle, $\theta_2 \gg \frac{\lambda}{\delta}$, where δ represents the dimensions of the cell occupied by the nuclear particle (here the alpha) then the action can be concentrated on that particle and will result in the excitation or disintegration of the nucleus.[77] Since $\lambda = \frac{\hbar}{Mv}$, the quantity $\frac{\lambda}{\delta}$ may be written as $\frac{\hbar/\delta}{Mv}$ where $\hbar/\delta$ is the characteristic momentum of the particle in the nucleus. θ may be written as $\frac{Mv\theta}{Mv}$, that is as the perpendicular component of momentum transferred over the total momentum. Therefore, the meaning of $\theta_2 \gg \frac{\lambda}{\delta}$ is that the momentum transferred is much greater than the characteristic momentum of the particle in the nucleus. Williams says that in such a

77. E. J. Williams, Proc. Roy. Soc., London, A169, 531 (1939).

collision the nuclear particle scatters as if it were "free" in the sense used by Bohr, and this scattering is over and above the elastic scattering.

(3) If the impact parameter b is greater than $r_1 + r_2$ not enough energy can be transferred to the C^{12} to disintegrate it. Therefore, the particles must collide in the classical sense of the word. Such a collision does not necessarily imply that the Coulomb barrier will be crossed. The particles may be deflected enough during the collision that there is no penetration.

In the light of these remarks, it is evident that knocking an alpha out of the carbon nucleus can be considered classically. We may use the Bohr concept of a "free" collision between the incident particle and the alpha, but the assumption is not as valid as the same assumption applied to an orbital electron.

There is one feature of the present problem that simplifies it. That is the alpha-particle model of the carbon nucleus, as proposed by Wheeler.[58] Most of the time the C^{12} nucleus is in the form of three alpha clusters, one at each corner of an equilateral triangle. The duration of the structure before breaking up and rearrangement of the clusters is long with respect to the rotational and vibrational periods of the alphas in the nucleus. The vibrational motion is principally of interest here. There are two fundamental modes of vibration: a non-degenerate mode that is an isotropic dilatation and contraction of the triangle (quantum number n_1), and a doubly degenerate mode (called "tipping") in which one side of the triangle shortens and at the same time moves farther from the opposite vertex (quantum number n_2).

Wheeler gives as the mean square displacement of an alpha from equilibrium,

$$(X^2)_{av} = (2n_1+1)(0.282)^2 + (2n_2+1)(0.336)^2$$

with the distance in units of $\frac{e^2}{mc^2} = 2.80 \times 10^{-13}$ cm.

For the ground state, $n_1 = 0$, $n_2 = 0$, the equation gives

$\sqrt{(X^2)_{av}} = 1.228 \times 10^{-13}$ cm. Since the radius of the C^{12} nucleus may be taken as 3.14×10^{-13} cm., we see that the alpha is relatively localized in the carbon nucleus. Consequently, the effective impact parameter is from the center of particle No. 2 to the center of the alpha rather than to the center of the carbon nucleus. More important yet, the possibility for the collision becoming adiabatic[78] is much lessened by the relatively fixed position and the rather weak oscillations (the binding energy per alpha-alpha bond is 2.46 Mev). If the alpha clusters moved freely in the carbon nucleus with a momentum corresponding to the 7.39 Mev disintegration energy, it would be nearly impossible to disintegrate the C^{12} nucleus at the velocities available.

Presumably the carbon nucleus may be disintegrated either by the Coulomb field or by the high, short-range, specifically nuclear forces. The energy analysis of the disintegrations observed indicated that many of them were produced by light blows. Consequently, it is of interest to make an estimate of the possibility of electro-disintegration, that is, of disintegration by the Coulomb field. Of course the Coulomb field may

---

78. Fermi: Orear, Rosenfeld, Schluter, Nuclear Physics, p. 29. University of Chicago Press (1950).

be the effective agent even after penetration of the barrier. However, the discussion here will consider penetration only to the top of the Coulomb barrier.

It is simple to compute an impact parameter, b_{min}, measured from the center of the carbon nucleus to the center of particle No. 2, such that the minimum distance of approach will be the sum of the radii of the two particles. From Chapter III,

$$b_{min} = R_{min}\left[1 - \frac{Z_1 Z_2 e^2}{R_{min}(\frac{1}{2}\mu v_o^2)}\right]^{1/2} \qquad \text{where } R_{min} = r_C + r_2.$$

The quantity here called b_{min}, the smallest impact parameter for which there is no penetration of the Coulomb barrier, was called b_{max} in Chapter III where penetration was being considered. For the application here, b_{max} will be defined as the maximum impact parameter at which 7.39 Mev can be delivered to the alpha. The equation will correspond exactly to that for b_{min}, with $R_{max} = r_C + r_2$ + (distance between their surfaces at perihelion). That is, R is the perihelion distance of particle No. 2 with respect to the carbon nucleus as a whole, whatever the condition of impact. The instantaneous cross section for electro-disintegration should be approximately proportional to $\pi (b_{max}^2 - b_{min}^2)$.

An approximation that should at least indicate the possibility of electro-disintegration and give its dependence on velocity is obtained by considering the alpha as a "free" particle and using the equation for energy transfer by momentum perpendicular to the trajectory:

$$W = \frac{p^2}{2M_\alpha}$$

where p may be written as

$$p = \frac{2Z_{\alpha} \; Z_2 e^2}{(R - r_C + r_{\alpha})v} \qquad \text{(Ref. 78, p. 28)}$$

($R - r_C + r_{\alpha}$ is the perihelion distance with respect to an alpha presumed to be lying in the carbon nucleus tangent to the point of nearest approach. In units of 10^{-13} cm, $R - r_C + r_{\alpha} = R - .96$)

Another expression for p is: $p = M_2 v \theta_2$ from Rutherford scattering theory, where θ_2 is the deflection of particle No. 2 in a system where the carbon nucleus initially was at rest. R_{max} can be found from:

$$\frac{R_{max} - r_C + r_{\alpha}}{R_{min} - r_C + r_{\alpha}} = \sqrt{\frac{W(R_{min})}{7.39}}$$

where $W(R_{min})$ is the energy transferred in Mev at R_{min}.

The calculation will be most nearly correct for the heavy target elements. Consider a collision with Ag^{107}. The C^{12} nucleus will be considered initially at rest and the Ag^{107} nucleus passing by. We find that the equation gives an upper limit of the kinetic energy of carbon nuclei beyond which electro-disintegration should not occur. This upper limit is at about 99 Mev for the C^{12} with respect to the laboratory; at that point b_{max} and b_{min} come together. As the velocity decreases, the gap between b_{max} and b_{min} widens until it reaches a maximum when $b_{min} = 0$. At 80 Mev, $b_{max} = 7.19$, $b_{min} = 7.20$ in units of 10^{-13} cm. At this value of b_{min}, $W = 9.13$ Mev transferred to the alpha. At 60 Mev, $b_{max} = 7.42$, $b_{min} = 4.515$

($W = 12.18$ Mev). At 46.9 Mev, $b_{max} = 7.3$, $b_{min} = 0$ ($W = 15.58$ Mev). For lower energies, b_{min} stays at zero, but b_{max} does not become zero until the energy is just under 25 Mev.

For the lighter elements of the emulsion, calculation shows a similar curve for b_{max} and b_{min}. However, the upper energy limit is lower (e.g. for collision with oxygen, it is at about 67.8 Mev kinetic energy of the C^{12} with respect to the laboratory). Also, the lower energy limit is lowered.

These calculations indicate that electro-disintegration is possible and that it prefers rather low velocities since energy transfer is more effective at low velocities. It has been tacitly assumed that there is no difficulty with the collisions becoming adiabatic at low velocities.

Another expression for the cross section for electro-disintegration besides $\sigma = k\pi (b_{max}^2 - b_{min}^2)$ is obtained by using the expression W for energy transfer per collision and from it setting up the expression $\frac{\Delta E}{\Delta x}$, the energy loss in collisions per unit distance.

Then $$\sigma = \frac{-\frac{\Delta E}{\Delta x}}{N k_1 \overline{W}}$$

where N is the number of nuclei per unit volume, k_1 is a constant and $\overline{W}$ is the average energy transferred to the C^{12} per disintegration. The poor feature of this equation is that experiment is the only way to determine $\overline{W}$; theory fails.

It is necessary to have a proportionality constant, k or k_1, in the

equations for the cross section because disintegration quite evidently will depend on the orientation of the equilateral triangle of alphas with respect to the target nucleus. Orientation probably accounts for the failure of strong blows in some cases to disintegrate the C^{12}.

If we drop the restriction of considering only electro-disintegration, we find the additional cases of disintegration by forces inside the Coulomb barrier. The forces are higher there, but also the probability of absorbing all or part of the carbon nucleus becomes important.

Stripping of an alpha from C^{12} or C^{13} appears to be not greatly different from stripping in the case of the deuteron.[79] The carbon nucleus is not as loosely bound as the deuteron nucleus, and the average separation between alpha clusters is relatively not as great as that between the proton and neutron in the deuteron. These factors reduce the cross section. In stripping of carbon there may be an effect analogous to the Oppenheimer-Phillips process.[80] In this effect, which occurs at low velocities, there is simple absorption of one particle (the neutron in the case of deuteron) while the other particle carries away the surplus energy and momentum.[81] In the case of carbon, certain orientations at fairly low velocities would tend to drive one alpha into the nucleus while the other two alphas were slowed down until they did not penetrate. The long-range alphas in impact disintegration illustrate the principle.

---

79. R. Serber, Phys. Rev. 72, 1008 (1947).

80. J. R. Oppenheimer and M. Phillips, Phys. Rev. 48, 500 (1935).

81. H. A. Bethe, Phys. Rev. 53, 39 (1938).

At high velocities it is possible that cases which would normally be stripping at lower velocities show up as impact disintegrations. This might be the case if the centrifugal potential acts to prevent amalgamation of the stripped alpha into the nucleus, or if it brings about an (α, α') reaction when the alpha does enter the nucleus. However, the importance of stripping plus an (α, α') reaction as a mode of impact disintegration should not be overestimated. If it were an important mechanism there should occur more stripping plus (α, p) reactions than do.

FIGURE 32

(Star No. 1 of Tables 5.1 and 5.4)

This star is an example of the impact disintegration of the incident C^{12} nucleus into three alphas with very little energy delivered to the C^{12} ($\sim$0.56 Mev) beyond the 7.39 Mev necessary to disintegrate it. The disintegration probably was a true electrodisintegration produced by the Coulomb field alone. The energy delivered to the struck nucleus cannot be measured accurately, but must have been very small. Its track is not over 3/4 micron long. The C^{12} nucleus had traveled five microns before the collision and presumably had 109.2 Mev energy remaining ($\pm$2.4 Mev s.d. from the energy spread of the beam). The ranges of the alphas are (from top to bottom) 389 microns (32.20 Mev), 476 microns (36.32 Mev) and 500 microns (37.50 Mev). The last alpha may have gone out the bottom of the emulsion near the end of its range. The sum of the alpha energies plus the 7.39 Mev to disintegrate the C^{12} minus 0.09 Mev released by the Be^{8} totals 113.22 Mev, more than would have been available unless the C^{12} had had more than the average energy by nearly two standard deviations. The top pair of alphas appears to be the pair that came from Be^{8} in the ground state. A disintegration energy analysis confirms the assignment and gives the disintegration energy as 0.154 Mev.

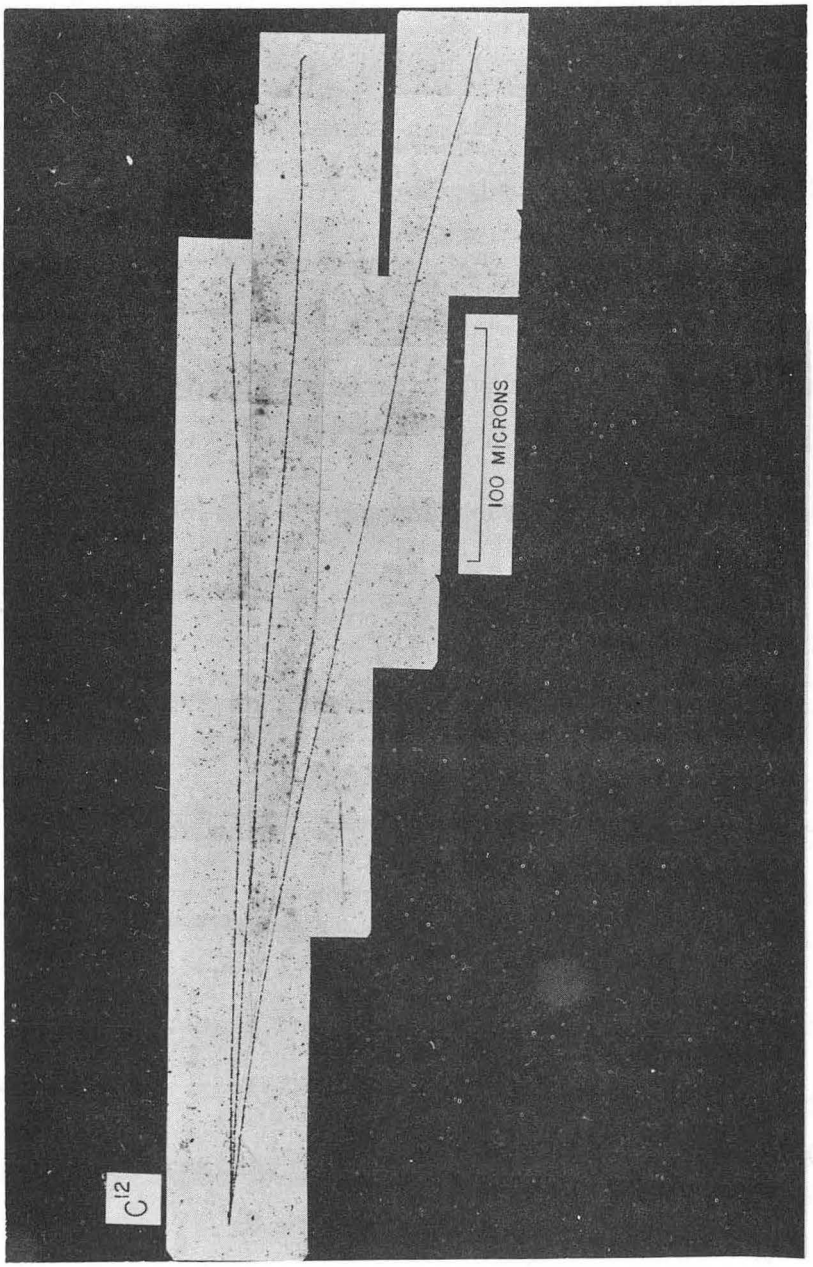

ZN 339

FIGURE 32

FIGURE 33.

This case of impact disintegration of C^{12} is an example of the internal momentum adding on a component to the mass motion momentum of the alpha to give a longer range than would be expected on the basis of assigning to the alpha one-third the linear momentum of the C^{12} at the time of collision. The C^{12} had traveled 34.3 microns before disintegrating. The average range of carbon ions on the plate was 163.0 microns. Therefore, the expected energy at the time of the event was 92.6 Mev. The long alpha had a range of 654 microns and energy of 43.7 Mev., nearly half the energy of the C^{12}.

The other pair of alphas is from Be^{8} in the ground state. The knock-on nucleus gave a track 11 microns long just below the long alpha. The energy that went to the knock-on nucleus has an expected value of 11.7 Mev. From the range and energy, the struck nucleus must have been light. The short spur at five o'clock is definitely present and could even be a double track. More probably it is not a real track but was caused by the intense ionization at the point of collision.

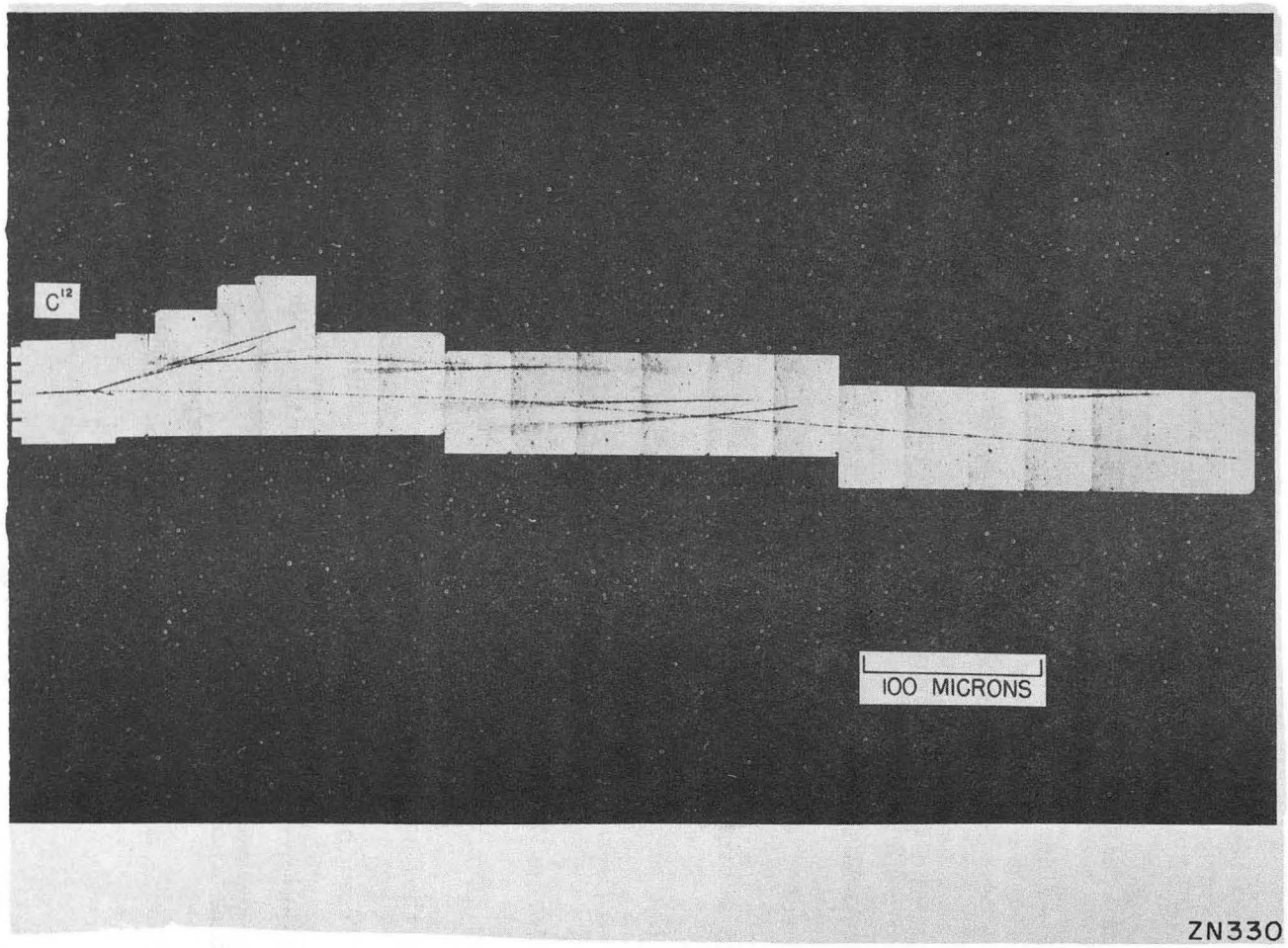

FIGURE 33

FIGURE 34

(Star No. 36 in Tables 5.2 and 5.5)

This star is an impact disintegration of C^{12} with more than two-thirds the linear momentum going to the ground state Be^{8}, which broke into the long pair of alphas. The third alpha is the short prong at twelve o'clock. It went out the top of the emulsion. The Be^{8} pair of alphas had ranges of 553 microns (39.40 Mev) and 543 microns (39.20 Mev). The latter track appears slightly longer in the mosaic. Actually it dipped down, then back up and went out the top surface of the emulsion near the end of its range. Therefore, the sum of the energies, 78.60 Mev, is slightly less than the correct value. The energy of the C^{12} at collision was 103 Mev. The struck nucleus is at four o'clock. It is twelve microns long and is going down in the emulsion at an angle of 45 degrees.

Delta rays can be seen quite clearly on the C^{12} track. There is also a straight spur at eleven o'clock just ahead of the event. What caused it is not known. It may be a very short proton track from an elastic collision just before the event.

The heavy dark bar over halfway down the alpha tracks is a flaw on the surface of the emulsion.

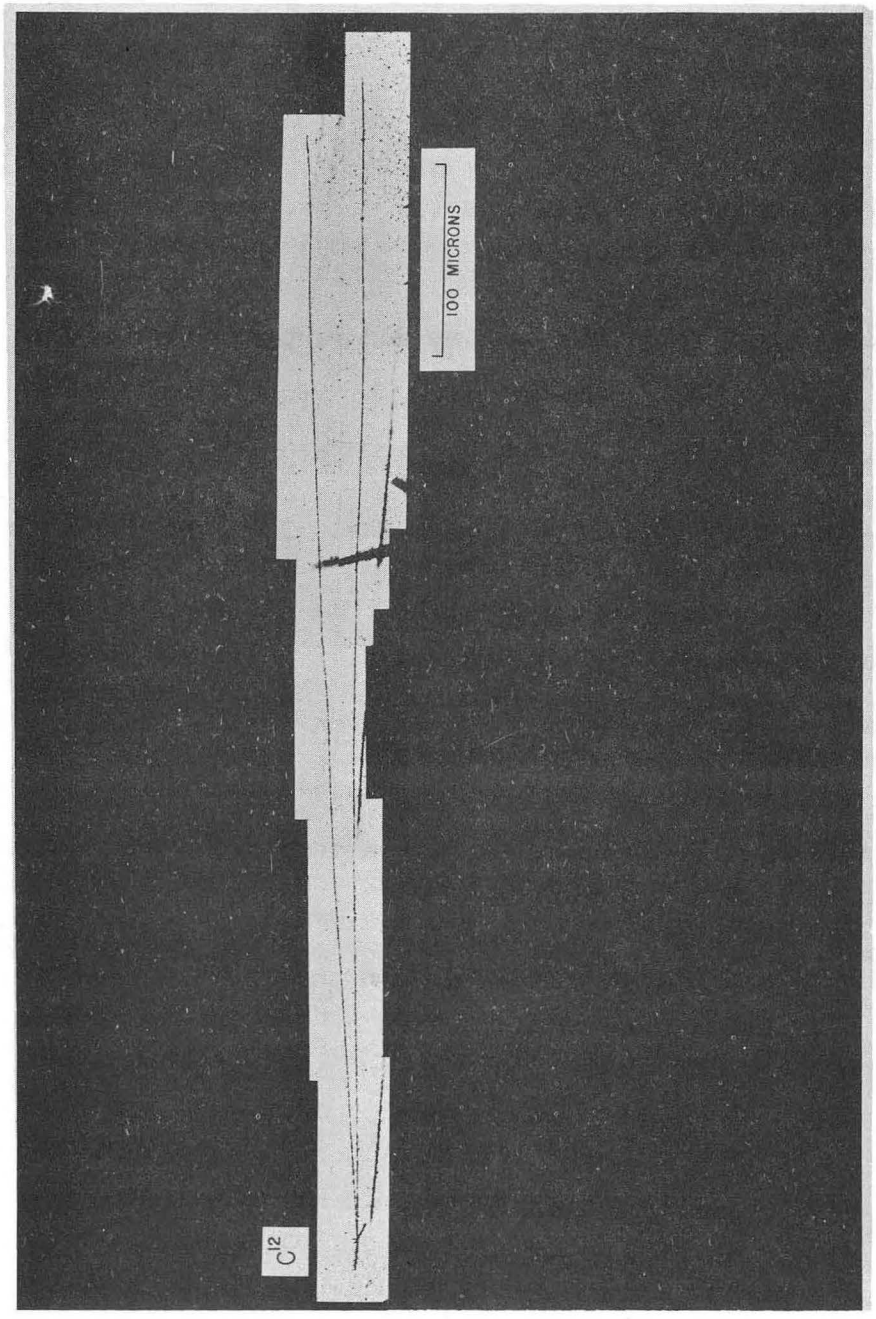

ZN336

FIGURE 34

FIGURE 35.

(STAR NO. 17 in TABLES 5.1 and 5.4)

This impact disintegration of C^{12} is one that could not have been produced by the Coulomb field alone but must have required the sharp specifically nuclear forces.

The incident C^{12} traveled 85 microns before the event occurred. Its expected residual energy was 74.4 Mev. The top pair of alphas is from Be^{8} in the ground state, and gives a disintegration energy of 0.048 Mev. The upper alpha appears to have knocked-on a proton right at the end of its range.

The three alphas (top to bottom) had kinetic energies of 11.64, 10.44 and 14.43 Mev., respectively. In the center of mass system the three alphas had 22.26 Mev. With the 7.30 Mev. (= 7.39 - 0.09) to disintegrate the C^{12}, this means that 29.56 Mev. was the break-up energy delivered. The best value for the energy remaining for the knock-on particle is 74.4 - (11.64+10.44+14.43+7.30), or 30.6 Mev. Its range is 28.9 microns. These values of range and energy, and the near equality in the energy delivered to each of the two colliding particles, indicate the struck particle also was C^{12}. If so, then it is impossible to say which was the incident particle. The orientations at collision must play a considerable role in determining whether or not a C^{12} will be disintegrated.

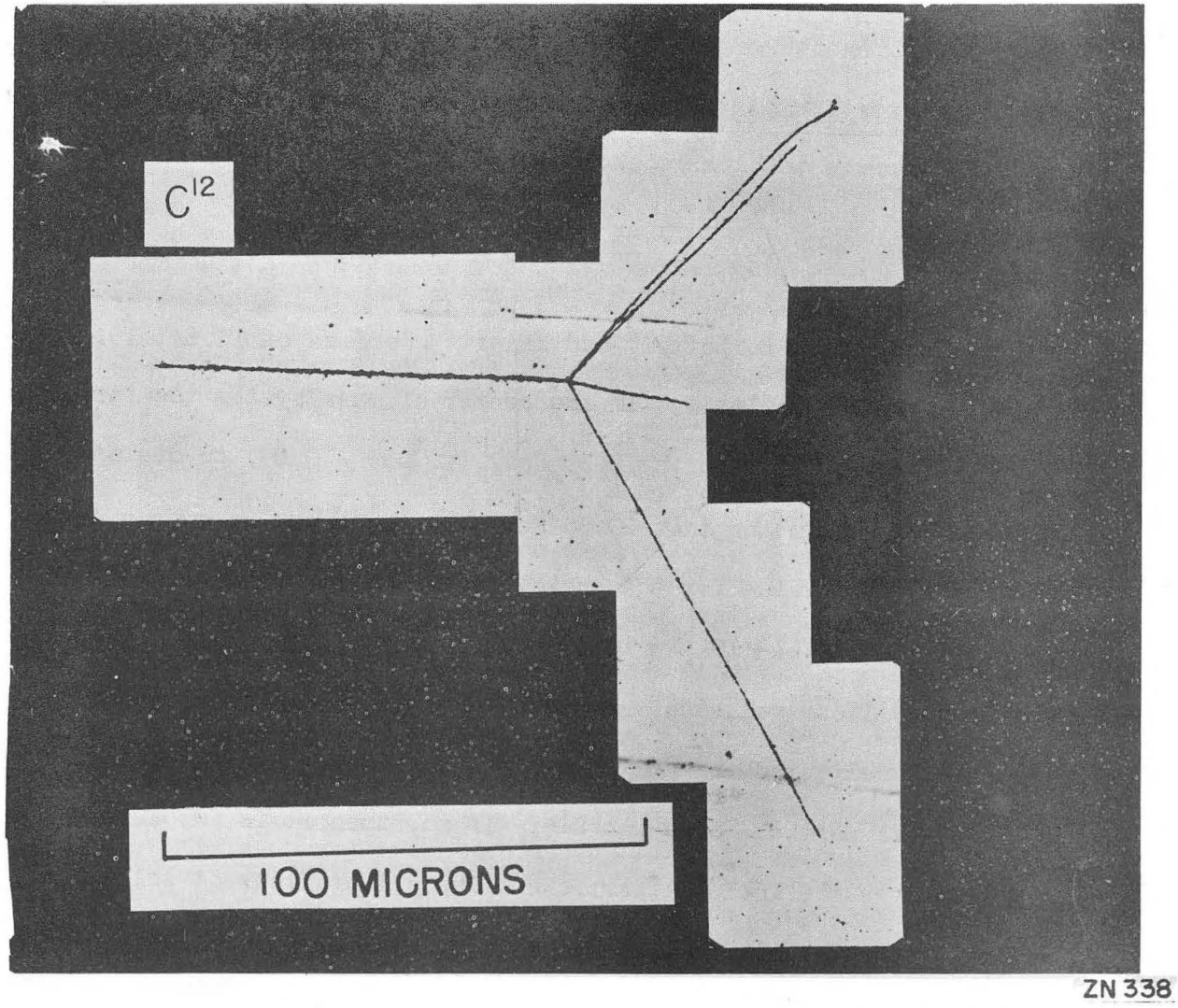

FIGURE 35

FIGURE 36.

(STAR NO. 41 of TABLE 5.2)

This star is an example of the stripping and capture of one alpha from the incident C^{12} by the struck nucleus. In the case shown, the Be^{8} was left in the ground state. The nucleus which absorbed the third alpha apparently was heavy. Its track is a barly detectable hump at the point of bending.

The C^{12} had traveled 66 microns before the event occurred. Its expected residual energy was 81.6 Mev. The two alphas had 25.76 and 28.72 Mev., giving a total exactly two-thirds of the C^{12} energy. The disintegration energy of the Be^{8} was 0.102 Mev. This star shows how difficult it may be to decide on the diverging point of the two alphas in order to measure the angle which determines the separation energy, or to measure the distance the Be^{8} traveled before disintegrating.

Cases of stripping with the Be^{8} left in an excited state often occur. They are easily identified in the rather rare cases when no third track can be seen, by the fact that the C^{12} suddenly breaks into two alphas tracks diverging at a wide angle. The star of Figure 22B is a possible, but not probable, stripping. The energy of the two alphas there is too low, compared to the C^{12} energy, for it to be "probable".

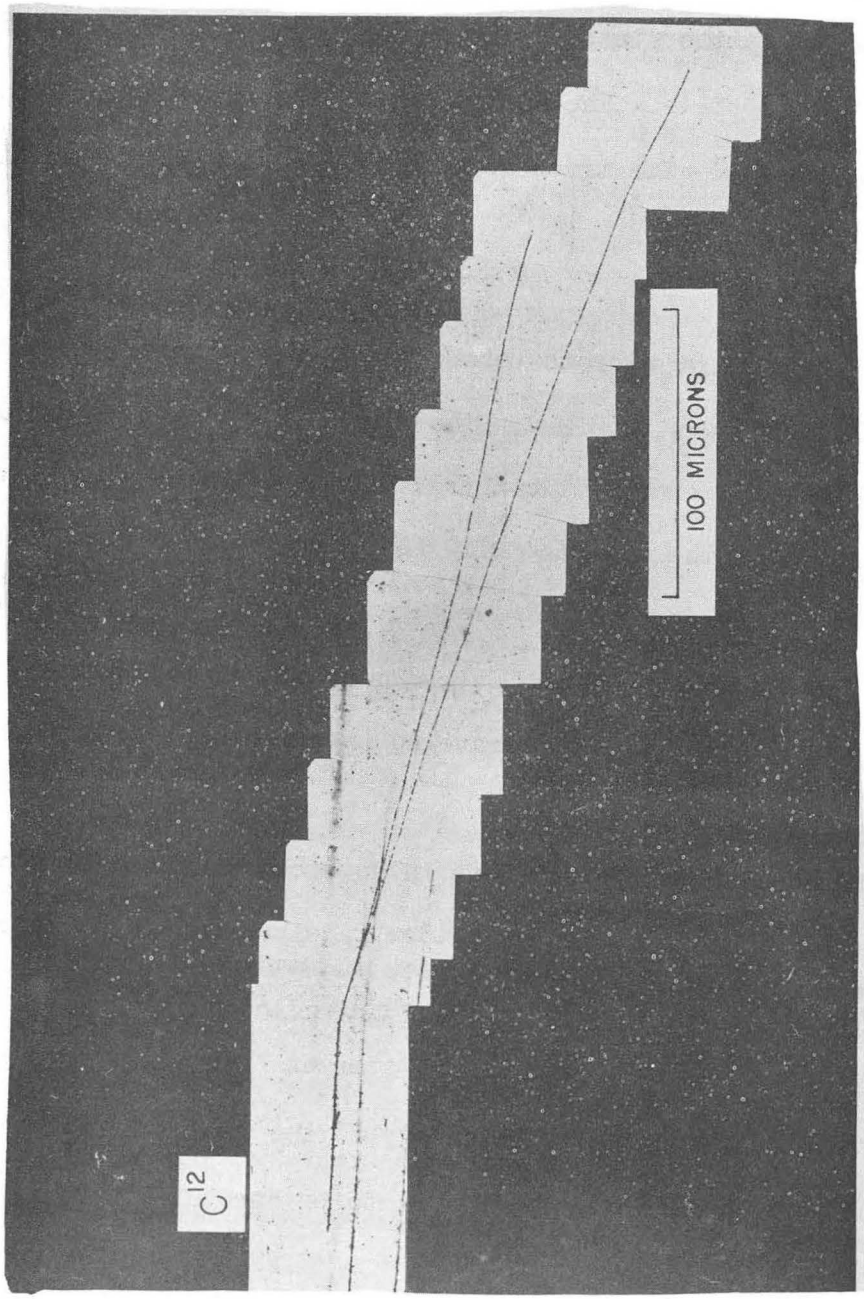

ZN333

FIGURE 36

FIGURE 37

(Star No. 42 of Table 5.2)

This star is a case of the stripping and capture of an alpha from the incident C^{12} nucleus, followed by an (α,p) reaction in the struck nucleus.

The fact that it is a stripping is verified by the ground state Be^{8} pair of alphas and by the failure of a charge as great as the C^{12} charge to appear in prongs. The light track is definitely a proton. It went out the top of the emulsion after 28 microns. It appeared to be of medium range, say of the order of 100 microns.

The C^{12} traveled 28 microns before the event. Its residual energy should have been 99.4 Mev. Of this the two alphas got 68.06 Mev, slightly more than their share. The energy of the alpha, therefore, was 99.4 - (68.06 + 7.30), or 24.0 Mev.

The disintegration energy of the Be^{8} comes out as 0.061 Mev.

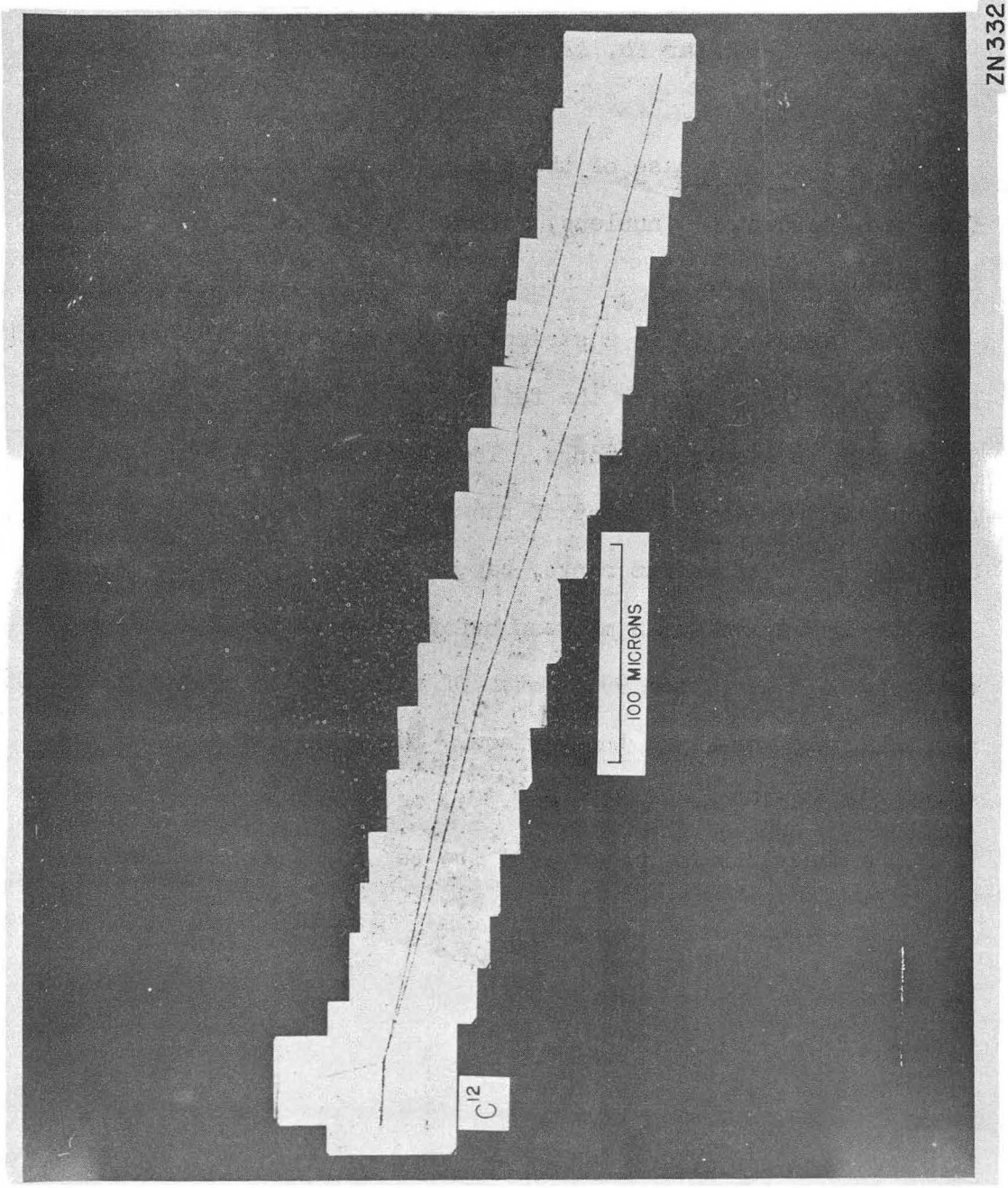

FIGURE 37

CHAPTER VI

FISSION OF BISMUTH

Fission provides serious competition to other types of nuclear reactions in the heavy elements even with moderate excitation. The fissionability parameter Z^2/A falls off rapidly with decreasing Z, but increases with decreasing A. Therefore, neutron deficient nuclides are especially subject to fission. The compound nuclei formed in carbon ion bombardment of heavy elements are already neutron deficient and they will evaporate still more neutrons because of their excitation.

Both for the sake of getting a general idea regarding fission in carbon ion bombardment and for obtaining information which might be applicable in evaluating the competition[7] of fission in trying to produce trans-californium elements, J. G. Hamilton proposed that bismuth-impregnated emulsions be bombarded by C^{13} ions. Bismuth was selected for the target material for several reasons: (1) It is stable, has a single isotope, and is high enough in the list of elements that the nuclides formed by carbon bombardment should have appreciable fission cross sections. The object was not to see how far down the list an element could be made to undergo fission. Such a program would give no statistical data because of the extreme rarity of occurrence, based principally on the amount of loading that can be put in an emulsion. Further, fission appears to be possible throughout the nuclide chart. As it was, the frequency of fission was about one per 200,000 tracks, for which the survey time ran about 30 hours. (2) Fission is expected not

to be the predominant reaction in bismuth bombardment as it might be with heavier elements. The fission cross section should still be rising sharply. Data regarding the rising part of the curve should be of more use than data taken somewhere on a nearly level plateau. (3) Emulsions are commercially available with bismuth loading.

It is desirable to have an insensitive emulsion, such as Ilford D-1, to search for fission fragments, in order to get good contrast between these fragments and carbon ions. On the other hand in D-1 emulsion, if C^{12} ions rather than C^{13} were used, there might arise the possibility of confusing an incident alpha and a C^{12} ion. In order to avoid this possibility, it was proposed that C^{13} ions be used. Their use fit in well with the general program since comparison studies of C^{12} and C^{13} bombardments were desirable.

The emulsion used was Ilford D-1, 100 microns thick. The loading is 0.27 gm/cm^3 of bismuth at "normal humidity". That is, one atom out of every 104 is bismuth. In reply to an inquiry, Mr. C. Waller of Ilford Limited, stated that "...the bismuth is included in the emulsion in the form of a water-soluble salt which will be more or less uniformly distributed. Lack of uniformity may result from migration of the salt when the emulsion is dried, but this effect would be small." The nature of the bismuth salt is not stated. (Dr. Harry Foreman, of this laboratory, prepared a bismuth salt by a chelation action of ethylene diamine tetra-acetate on bismuth subnitrate. Two atoms of bismuth could be put on each molecule, permitting a heavy loading. Emulsions loaded by soaking in this

solution were prepared, but all the emulsions studied were those loaded by Ilford, since there seemed to be a better guarantee of the amount and uniformity of loading.)

The batch of Ilford bismuth-loaded emulsions obtained had a considerable number of random specks as if from foreign matter, and the size of the silver-bromide crystals was far from uniform. These defects sometimes interfered seriously with interpretation of other stars but never of the fission reactions. Mr. Waller, who examined the emulsion batch, expressed the belief that the silver had become aggregated in some way.

The question arose as to whether fission events observed in the emulsion might come from carbon ions on uranium or thorium in the emulsion. Mr. Waller states that, "We have previously been asked whether the bismuth salt we are using may be contaminated with a very small amount (e.g., 1 in 100 million) of a radioactive element, but we have been unable to obtain this information". For an approximate evaluation of uranium content, 4.2 grams of emulsion (containing 0.313 grams of bismuth) were stripped off and, after ashing in a crucible, were analyzed spectrographically by Conway and Tuttle of the University of California Radiation Laboratory. They found strong silver lines, moderate (1 to 10 percent content) bismuth lines, but could not detect uranium lines. The upper limit for non-detection is about 0.1 percent since uranium lines are not strong. This evidence, weak though it is, would rule out uranium fission. Unless the uranium (or other element) loading were greater than about one-fifth the bismuth loading, which is heavy, the cross section would have to be larger than the geometric cross

section. Observation of decay stars from naturally radioactive atoms in the emulsion indicates the limit of radioactive impurities is not higher than in ordinary emulsion.

Plates were exposed at the maximum tilt of $8^{o}51'$ to increase the probability of both fission fragments ending in the emulsion. Eleven plates were examined. The last two plates have tracks of greater range than the others because the beam energy had been increased to about 130 Mev, from 120 Mev, by balancing the dee voltages and increasing the frequency.

Nine cases of fission were found in 1,702,600 tracks that produced a total of 1121 events of all kinds. All the cases of fission were unquestionable and it is doubtful if any were missed. There was one case of fission where a third particle, presumed to be an alpha, but not identified certainly, appears. Photographs of two of the fission events are shown in Figures 38 and 39. In Fig. 40, there is a projection tracing of each of the events with the pertinent data alongside. X is the distance to the event, $\bar{R}$ the average range of tracks on the plate, E is the kinetic energy of the C^{13} with respect to the laboratory at the time of the event, and E_x is the excitation of the compound nucleus. The angles given are the opening angle between the two fragments and the angle between one prong and the entering carbon track. The track length of each fragment is given. In cases where there was a nuclear collision, the length is based on a guess as to which particle was the fragment.

The radius for collision of C^{13} with Bi^{209} is 11.350×10^{-13} cm, corresponding to a Coulomb barrier of 63.11 Mev. To cross this barrier, the C^{13} nucleus must have 67.04 Mev with respect to the laboratory since only 0.9414 of its energy is available in the center of the mass system.

We may now calculate the cross section for fission,

$$\sigma_f = \frac{n}{\rho_{Bi} \sum_i N_i (\bar{R}_i - R_B)} \qquad 6.1$$

where $n = 9$, $\rho_{Bi} = 0.778 \times 10^{21}$ atoms/cm^3, the density of bismuth atoms in the emulsion, N_i is the number of tracks on the i^{th} plate, with average range $\bar{R}_i$, and $R_B = 74.6$ microns, the residual range at the Coulomb barrier of 67.04 Mev. The calculation gives $\sigma_f = 0.538$ barn. The uncertainty in this value is $\pm$ 33 percent from the expected statistical fluctuations.

The geometric cross section, $\pi R^2 = 4.050$ barns. However, not all the geometric cross section is available for reactions because of the centrifugal barrier. The penetrability cross section $\sigma_p = \pi R^2 \left(1 - \frac{V_{coul.}}{KE_{Cl3}/\ C.M.}\right)$ is given below:

KE_{Cl3}/Lab (Mev)	130	120	110	100	90	80	70	67.04
σ_p (barns)	1.961	1.785	1.580	1.337	1.032	0.656	0.174	0
Residual Range (μ)	211.5	185.7	161.5	139.0	117.4	97.5	79.5	74.6

It is not fair to compare these instantaneous cross sections directly with the average cross section given by equation (6.1). An average value of

σ_p with respect to range is required as a function of the initial energy, E_i. The equation is:

$$\sigma_p(E_i) = \frac{\int_{E_B}^{E_i} \sigma_p(R)\, dX}{\int_{R_{13}}^{R_i} dX} \qquad 6.2$$

where σ_p as a function of range is given by the table above. $\sigma_p(R)$ corresponds to $\frac{1}{N \rho_a} \frac{dn}{dX}$ of the usual excitation function, and equation (6.2) converts this value to the cross section as a function of the initial energy. From a plot of σ_p vs. R, an approximate value of $\sigma_p(E_i)$ was obtained by taking a value of 200 microns ($E_i = 125.6$ Mev) for R_i for all the plates. The result was that $\sigma_p(E_i = 125.6 \text{ Mev}) \cong 1.16$ barns. The value of σ_f found is almost exactly half the corresponding penetrability cross section, implying that about 50 percent, perhaps more, of all nuclear reactions (excluding impact disintegration of the C^{13} nucleus) are fission events.

Calling the reaction "fission of bismuth" is somewhat a misnomer. In almost every case the nucleus which fissions will be $_{89}Ac$. There will be no single isotope responsible for all the events, but the most probable nucleus is $_{89}Ac^{215}$ because it has the closed shell of 126 neutrons, giving strong binding of the last neutron and making removal of one more neutron difficult. It would be produced by a (C^{13}, 7n) reaction, which one would

guess to be one of the most probable reactions in view of the large yield[7] of 4n and 6n reactions from the rather low energy internal C^{12} beam on gold.

An estimate can be obtained as follows of the most probable number of neutrons evaporated before fission. (The assumption, to be discussed later, is made that neutron evaporation precedes fission.) The excitation of the compound nucleus is the sum of the kinetic energy of the C^{13} in the center of mass system and of the mass excitation, which is negative, 17.43 Mev.

KE of C^{13}/lab (Mev)	130	120	67.04
E_x of Ac^{222} (Mev)	104.9	95.5	45.7

(For comparison, we notice that the cases of fission observed had a spectrum of excitation energies of the compound nucleus extending from 66.6 Mev to 93.5 Mev (Fig. 40). The lowest value is well above the theoretical lower limit.) Corresponding to any excitation a temperature may be assigned to the nucleus, considering it as a degenerate Fermi gas. $E_x = a(kT)^2$, neglecting higher terms in T. The value of a is not well known. Weisskopf[40] gives the equation:

$$a = \frac{3.35}{4} (A - 40)^{1/2} \text{ (Mev)}^{-1}$$

where E_x and kT are both measured in Mev. For $A = 222$, this equation gives $a = 11.33$. In a later estimate,[82] Blatt and Weisskopf give the value $a = 10$ for odd values of A in the neighborhood of $A = 201$. Nuclei with even A

82. J. M. Blatt and V. F. Weisskopf, The Theory of Nuclear Reactions. (A forthcoming book, issued in part as ONR Technical Report No. 42, and AEC Report NP-1587, Laboratory for Nuclear Science and Engineering, Mass. Inst. of Technology, 1950).

probably have smaller energy level densities and consequently smaller values of a. The approximate nuclear temperatures, kT, calculated with a = 10 for a few values of excitation are:

E_x(Mev)	104.9	93.5	66.6	45.7
kT(Mev)	3.24	3.06	2.58	2.14

The two outside values are the extremes of initial temperature for 130 Mev C^{13} bombardment; the two inner are the extremes in observed fission. Weisskopf[40] states that each neutron evaporated will have a most probable kinetic energy of 2kT where kT is the temperature of the nucleus after emission. For the first neutron evaporated, $2kT \cong 6.0$ Mev and the binding energy is 6.5 Mev. The binding energy is higher for odd A, where there is an even number of neutrons. The average value for even and odd nuclei is initially about 7.0 Mev. It rises slowly to about 8.0 Mev as A decreases to A = 212. Meanwhile, the excitation has decreased rapidly with each neutron evaporated and the temperature had fallen correspondingly. The number of neutrons evaporated in the observed cases of fission probably was between six and ten. A more accurate estimate could be made along the lines of the calculation in Ref. 78, p. 163.

The cases of fission produced by carbon ion bombardment are "fast fission", that is, the initial excitation is high. In such cases the fission fragment yield curve has been observed to have a single hump in contrast to the double-hump curve found in low energy fission such as that from U^{235} plus thermal neutrons. In the single-hump curve, symmetric

fission is more prominent than any other single partition, but slight asymmetry is the rule. Jungerman and Wright[83] found that in the case of neutron bombardment of heavy elements, the double-peaked curve began to appear when the energy was lowered to 45 Mev.

The single-hump curve gives evidence that evaporation of most or all of the neutrons energetically possible comes before fission. For fission fragments from bombardment of bismuth with 190 Mev.deuterons, Goeckermann and Perlman[84] found a single-hump curve with its maximum point corresponding to the evaporation of about 12 neutrons before fission. This displacement must have preceded fission since there were the appropriate number of β^+ emitters in the fission fragments, under the assumption that Z and A split proportionally.

Further evidence was found by Jungerman and Wright, who measured the energy in individual fission pulses. They obtained quite closely the same average energy for various values of incident neutron energy. They conclude that the actual fission must occur when the nucleus is in a relatively unexcited state and that the energy of the fragments is from the energy released by splitting alone.

On the other hand, if it were nearly an exclusive rule that evaporation of neutrons proceeded until the excitation was reduced below the binding energy of the next neutron before fission occurs, then there would hardly be reason to expect other than the asymmetric fission characteristic

---

83. J. Jungerman and S. C. Wright, Phys. Rev. 76, 1112 (1949).

84. R. H. Goeckermann and I. Perlman, Phys. Rev. 76, 628 (1949).

of such excitations. Asymmetric fission gives the greatest fraction of the total energy release in the fission pulse itself; that is, the minimum of energy is spent in subsequent de-excitation by beta and gamma emission. For symmetric fission pulses to exhibit nearly the same energy, the nuclei must have undergone fission when they had more excitation than if all possible neutrons had been evaporated. Further, evidence of fission in the middle of the nuclide chart, where the fission threshold may be of the order of 30 Mev, shows that fission may compete in speed with neutron emission.

Despite reservations, it may be accepted as a fairly accurate rule that large yields in fission will occur only when the fission threshold is lower than the binding energy of the last neutron that can be evaporated. The importance of fission compared to other methods of de-excitation such as gamma-emission then will depend approximately on the gap between neutron binding energy and fission threshold compared to the gap between the fission threshold and zero excitation. Fission does not, however, become important immediately at its threshold. The curve sketched below shows the relative gaps in the present case.

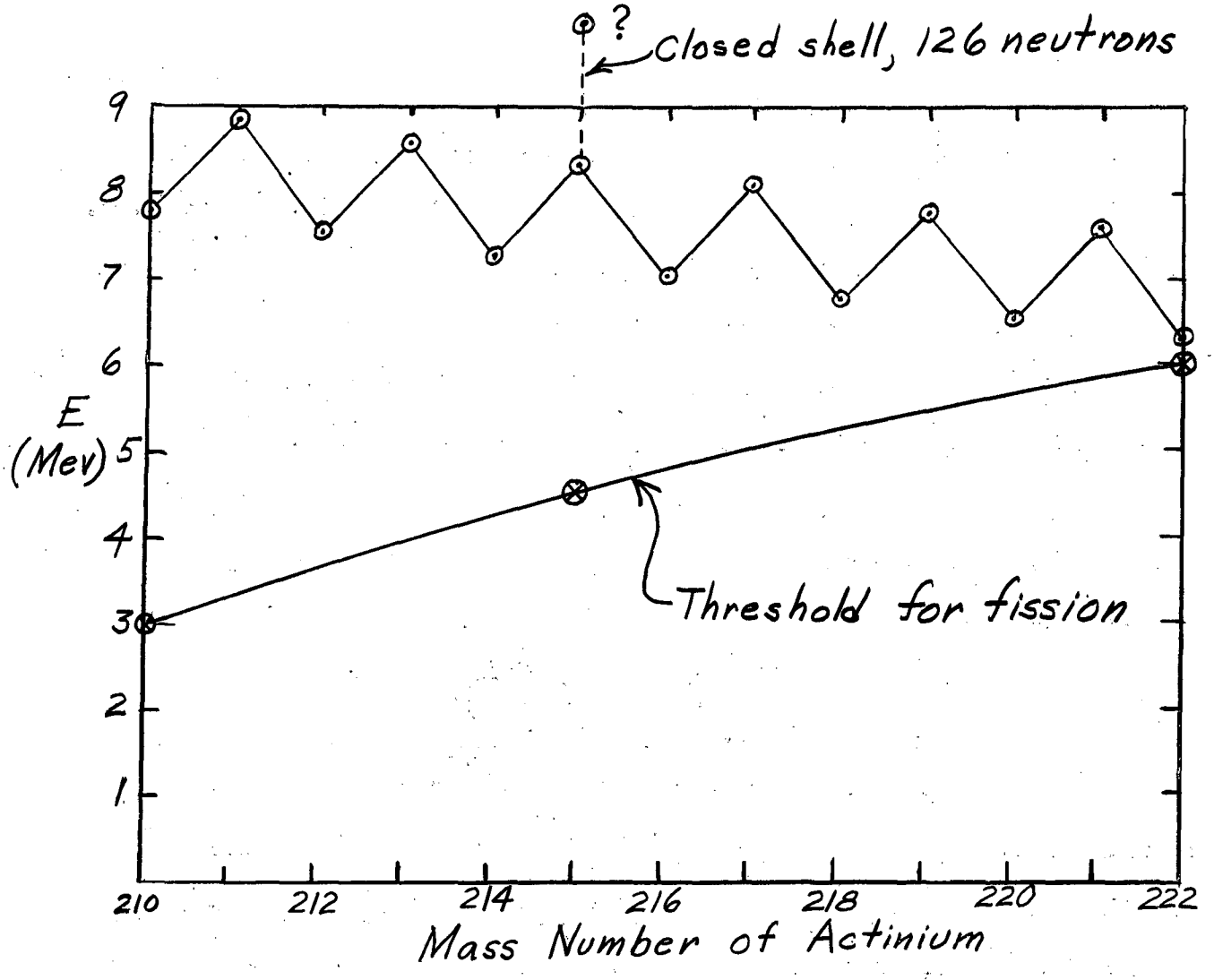

The upper curve is the binding energy for removal of a neutron from actinium of the mass number shown. It is calculated from the tables[22] of N. Metropolis and G. Reitwiesner, using the value M-A = 8.939 mMU for the neutron, given by Mattauch and Flammersfeld.[10] The calculated values do not take into consideration the effect of the closed neutron shell on binding. For Ac^{215} the binding will be higher by an unknown amount. Also sketched in is the threshold for fission, based on Z^2/A, calculated by Frankel and Metropolis[85] on the Eniac. Even at Ac^{222} fission is possible. Its Z^2/A is 35.67, almost exactly the same as that of U^{238}. For Ac^{215}, $Z^2/A = 36.8$. The thresholds for photo-fission

---

85. S. Frankel and N. Metropolis, Phys. Rev. 72, 914 (1947).

are: for Ac^{222}, approximately 6 Mev; for Ac^{215}, approximately 4.5 Mev; for Ac^{210}, approximately 3 Mev.

It is interesting to calculate in detail the mechanics of one of the fission events to see how it agrees with theory. Consider the fission in Figure 38. The excitation was 66.6 Mev. In order to study symmetric fission, assume 6 neutrons were evaporated before fission and that in evaporation they carried away essentially all the excitation but no net momentum (a fairly accurate assumption). The fission reaction was $_{89}Ac^{216} \xrightarrow{f} {}_{44}Ru^{108} + {}_{45}Rh^{108}$. The relation between momenta of the fission fragments in the center of mass system and the laboratory system is sketched below.

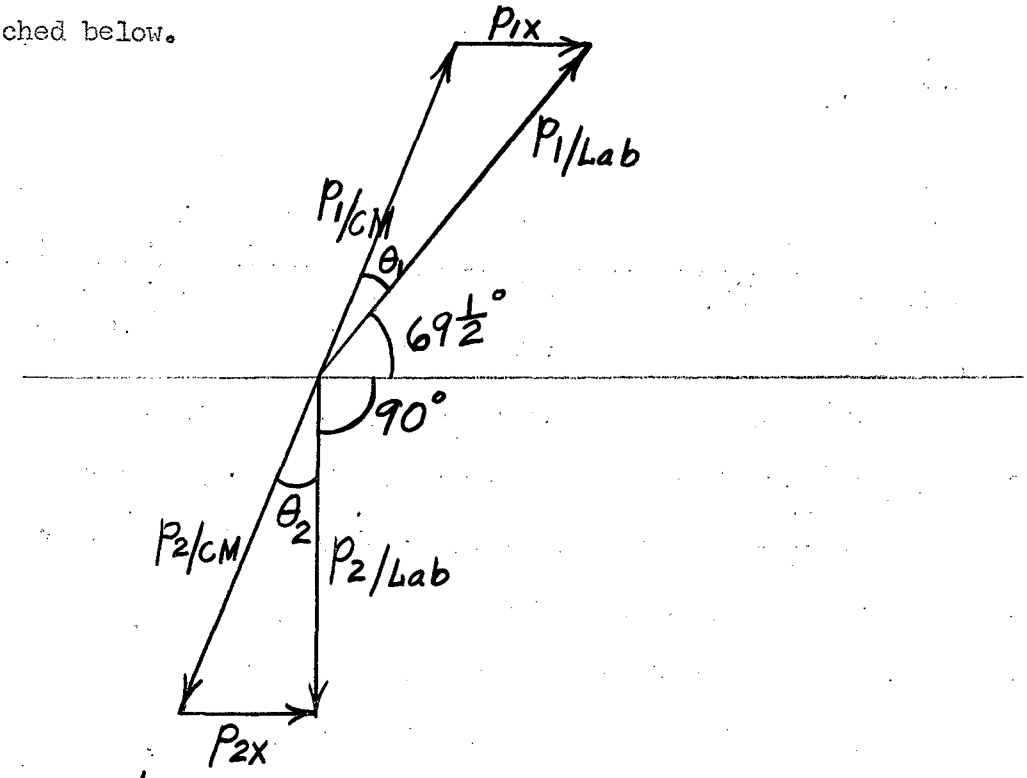

The equations are:

1) $\frac{P_{1x}}{\sin\theta_1} = \frac{P_{1/CM}}{\sin 69\frac{1}{2}^\circ}$

2) $\frac{P_{2x}}{\sin\theta_2} = \frac{P_{2/CM}}{\sin 90^\circ}$

3) $P_{1/CM} = P_{2/CM}$

4) $P_{1x} = P_{2x}$

5) $\theta_1 + \theta_2 + 159\frac{1}{2}^\circ = 180^\circ$

6) $P_{1x} (= P_{2x}) = \frac{P_{C^{13}}}{2}$ (an assumption)

FIGURE 38.

Fission of bismuth by C^{13}. The data for this star are given in Fig. 40 and the event is analyzed in the text. This fission event had the least excitation of any found, namely 66.6 Mev. The initial compound nucleus, Ac^{222}, probably evaporated 6 or 7 neutrons before fission. The fission seems to have been symmetrical or nearly so. Both fragment tracks are horizontal in the emulsion. The length of the track at 6 o'clock is 11.5 μ; of the other, 12.3 μ (to include the two detached grains).

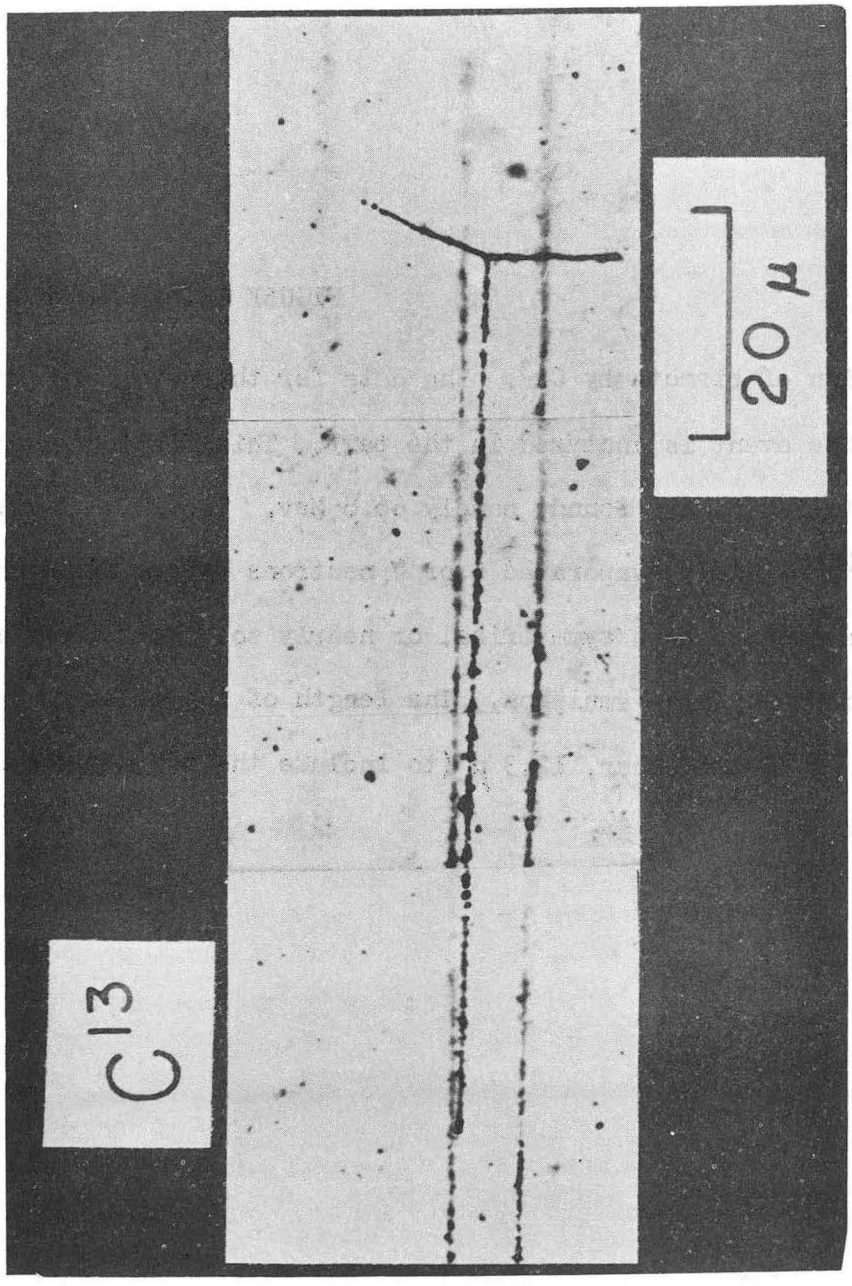

ZN335

FIGURE 38

The solution of these equations gives:

$$\theta = 9^{\circ}54', \quad \theta_2 = 10^{\circ}36'$$

and the energy of each fragment in the center of mass system is 79 Mev. The energy of fission calculated from the masses is 163.3 Mev. (Mass of $_{89}Ac^{216}$ = 216.07925 Mass Units, mass of Ru^{108} = 107.95265, mass of Rh^{108} = 107.95111). The agreement is good.

It might be well to calculate the minimum angle between prongs in symmetric fission. The minimum angle occurs when the break-up in the center of mass system is exactly perpendicular to the entering momentum, and when the latter is a maximum (130 Mev C^{13}). Assume 10 neutrons evaporated before fission. The energy release from mass differences will be 166.5 Mev. The minimum angle comes out as 155° 20'.

No estimates have been made from ranges of the fragments as to whether the actual fission is symmetric. The ranges are so short in emulsion, the "hard" collisions so frequent, andthe range-energy relation so imperfectly known, that it appeared little information could be gained. Consideration of the momenta, as above, indicates that a single-hump fission yield curve seems compatible with the observed fragments.

From the tracings of Fig. 40, notice how many of the fission fragments had branching due to elastic nuclear collisions. The high frequency is explained by the theory of the stopping of fission fragments. See Chapter VII.

The fission event with an alpha (presumed) also emitted (shown

in Fig. 39), cannot of course, be taken as an indication of the frequency of such an event. Nevertheless, for highly neutron-deficient nuclides such as are formed, it is not highly improbable that a charged particle should be evaporated, either from the parent nucleus or from one of the excited fragments. Alpha emission in fission of nuclides such as U^{235} and Pu^{239} by slow neutrons is well established.[86,87,88] The frequency is low - about one in 250 events for U^{235}. Alpha emission does not seem to occur with comparable frequency in fission by fast neutrons, an indication that the alpha comes from the compound nucleus, not from one of the fragments, and that alpha emission is discriminated against by the speed of the reaction. However, the case is not one of highly neutron-deficient nuclides such as carbon bombardment produces.

---

86. G. Farwell, E. Segrè, and C. Wiegand, Phys. Rev. 71, 327 (1947).

87. L. Marshall, Phys. Rev. 75, 1339 (1949).

88. K. W. Allen and J. T. Dewan, Phys. Rev. 80, 181 (1950).

FIGURE 39.

Fission of bismuth by C^{13} with an alpha emitted in addition. The event occurred after 30.9 microns. The excitation of the compound nucleus was 93.5 Mev. The identification of the third particle as an alpha is not certain, but its presence is. It shows up better under the microscope than in the mosaic. Its range cannot be stated since it went out the top of the emulsion after 6.5 microns. The fragment track at 8 o'clock is 10.0 microns long, the one in the forward direction is 13.5 microns. The fission fragments probably get most of the forward momentum of the C^{13} ion but very little of its kinetic energy.

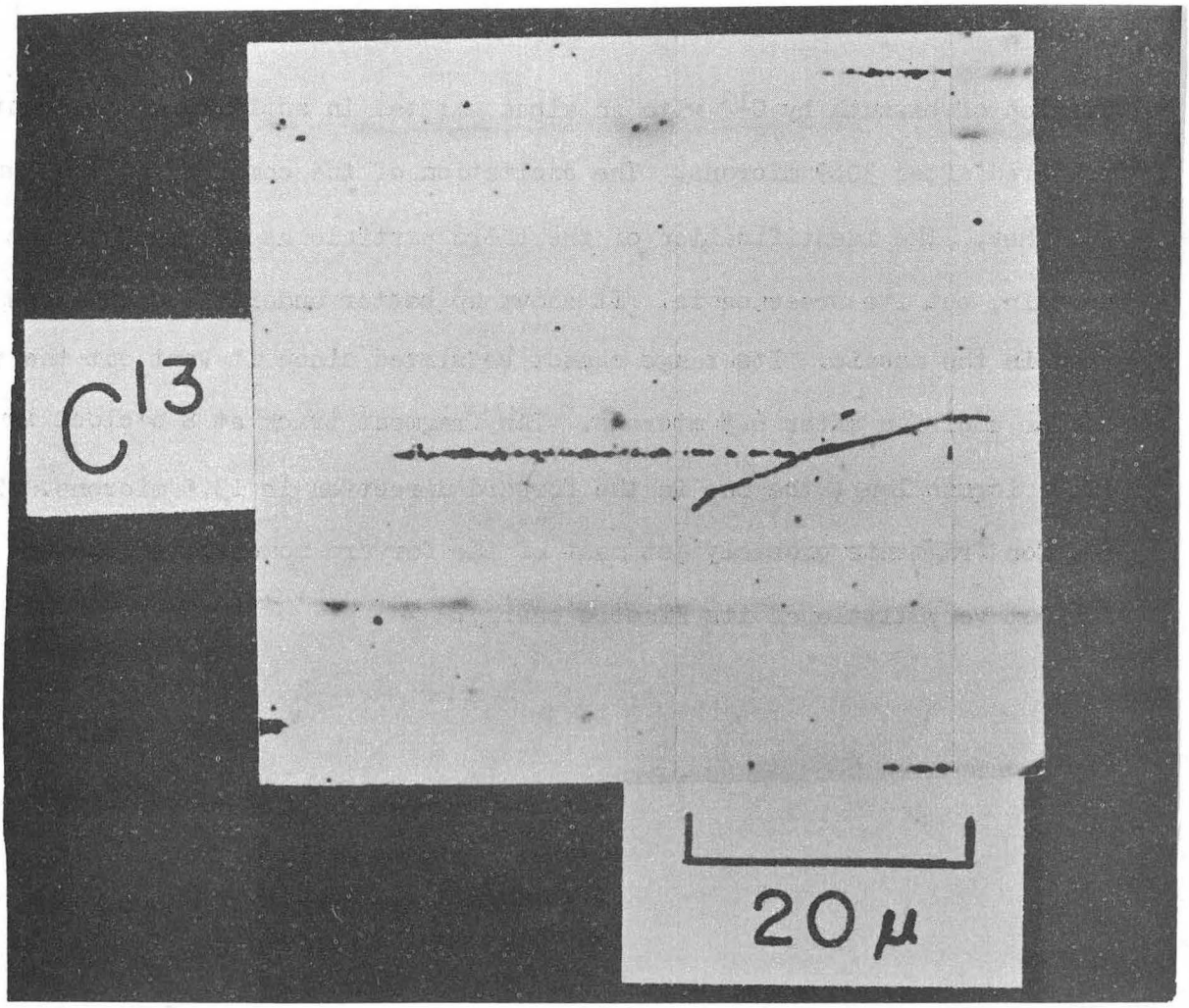

ZN337

FIGURE 39

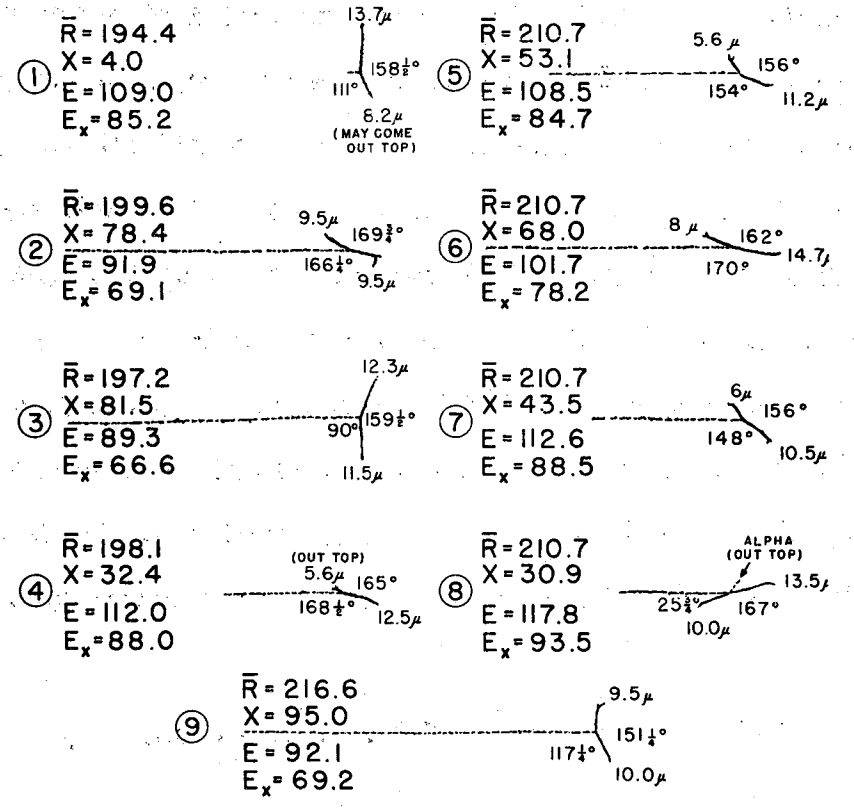

HORIZONTAL PROJECTION TRACINGS
OF ALL OBSERVED FISSIONS OF BISMUTH
BY C^{13}

FIGURE 40

MU3933

CHAPTER VII

RANGE - ENERGY RELATION FOR CARBON NUCLEI

A. THEORY

A range-energy relation for carbon nuclei is of interest not only for its practical use in calculations--for example, in finding the energy that a carbon nucleus carries into a nuclear reaction - but also for its theoretical aspects, in that carbon occupies an intermediate position between light fast nuclei and fission fragments, two classes in which different types of stopping effects play the major role. Carbon lies, of course, much nearer to the light fast nuclei - protons, deuterons, alphas.

For the light and heavy incident nuclei, the energy loss per unit path length may be written as the sum of two terms, the first giving the loss in electron encounters, the second in elastic nuclear collisions.

$$-dE/dx = \frac{2\pi N(Z_1^*)^2 e^4}{mv^2} B_\epsilon + \frac{2\pi N Z_1^2 Z_2^2 e^4}{M_2 v^2} B_\nu \qquad 7.1$$

This equation corresponds to that given by Bohr.[89] The subscript 1 denotes the incident particle, 2 the target atom. The first term contains the electron mass, m, but not the incident particle mass. It depends on the square of the effective charge, Z_1^*, of the incident particle. N is the

---

89. N. Bohr: The Penetration of Atomic Particles through Matter. Kgl. Danske Videnskabernes Selskab., (Math-fys. Meddelelser) 18, No. 8 (1948) p. 124.

number of target atoms per unit volume, and it is multiplied by Z_2, (included in B_ε) to give the number of electrons per unit volume. B_ε is a logarithmic term, which may be called the "stopping number"; ε denotes that it is for electronic collisions. It will be discussed below.

The second term is analogous to the first but concerns collisions with target nuclei. Hence, the single electron charge is replaced by Z_2 and the electron mass by M_2. N is the number of nuclei per unit volume and B_ν is the logarithmic term pertaining to nuclear collisions. Notice that Z_1^* has been replaced by Z_1.

It is at once evident (ref. 89,p. 124) that because of the appearance of the electron mass in the denominator in the first term, M/Z_2 compared to M_2/Z_2 in the second term, (there is a Z_2 included in B_ε of the first term) the energy loss to electrons is much greater than the loss to target nuclei except when the incident velocity becomes so low that the incident nucleus picks up electrons, making Z_1^* enough lower than Z_1 to reverse the relative magnitude of the terms. Indeed the first term is the important one even for fission fragments over the large part of their range.

Fission fragments always carry some electrons about their nuclei, giving a Z_1^* less than Z_1. There is an approximate criterion, but a reliable one, given by Bohr (ref. 89,p. 116) that when the speed of a nucleus exceeds that of the electron in a given "orbit", the nucleus in interaction with matter will lose that electron. This is a statistical criterion, the atom alternating between losing and capturing an electron in the particular state, but we may be quite sure that for the larger part of the time a nucleus of velocity greater than that of the electron

in its 1S -orbit will be completely stripped. Hence, beyond this velocity Z_1^* becomes Z_1. The domain where this is true is generally considerable for light nuclei. To discuss their energy loss, it is advantageous to break the electronic stopping term into two parts, one where $Z_1^* = Z_1$ and the other with $Z_1^* < Z_1$. These will be discussed successively.

1. dE/dx when $Z_1^* = Z_1$ (stripped nucleus):

Quantum mechanics should give the complete solution, but in the practical solution of problems, it has been necessary to use approximations which apply only under specific circumstances. These circumstances, or criteria, will be discussed here since they delimit the zones where carbon nuclei behave differently from lighter, or from heavier, nuclei. The distinction between the different treatments can most easily be shown by discussing them in their historical order.

After the discovery of the nuclear atom by Rutherford, early attempts were made to account for the quite definite range of alpha-particles as being due to the cumulative effect of a large number of small energy loses to electrons bound around the nuclei in the target atoms. J.J.Thomson and C. G. Darwin gave separate treatments, considering the binding of the electron to the nucleus. N. Bohr[90] in 1913 gave an equation for the rate of energy loss to electrons in which the treatment was classical, the essential contribution being in his demonstration that the energy transfer to the electron through the interaction of its Coulomb field with that of the incident nucleus did not involve the binding of the electron to the parent nucleus if the time of collision, τ, was much shorter than the period, T, of the electron in its orbit. These may be called "free"

90. N. Bohr, Phil. Mag. (6) 25, 10 (1913).

collisions. If we specify the impact parameter, b, as the perpendicular distance from the center of the target atom to the incident path of the nucleus, then $\tau \approx \frac{b}{v}$, v being the incident velocity. $T = \frac{1}{\nu} \approx \frac{d}{u}$ if d is the orbital size and u the "orbital velocity". Hence, to have $\tau \ll T$, we must have the impact parameter b less than $b_{max} = \frac{v}{\nu}$ or $\frac{v}{u} d$. For $b > b_{max}$, adiabatic conditions begin to set in; the energy transfer is no longer independent of the binding to the nucleus, and as b increases further, the possible energy transfer falls off as e^{-b} (Ref. 77, p 29).

The Bohr equation may easily be derived (Ref. 77) by considering the incident nucleus as having a well-defined impact parameter with respect to the target atom and considering the energy transferred through impulses for $b_{min} < b < b_{max}$, where an approximate b_{min} is given by the fact that not more energy can be delivered to an electron than $1/2\ m(2v)^2$. $b_{min} = \frac{Z_1 e^2}{m v^2}$. The resulting equation is:

$$-dE/dx = \frac{4\pi Z_1^2 e^4 N}{m v^2} B_\varepsilon \qquad 7.2$$

where the stopping number, $B_\varepsilon = Z_2 \ln \frac{b_{max}}{b_{min}} = Z_2 \ln \left(\frac{m v^3}{\nu Z_1 e^2} \right)$.

Now $\frac{e^2}{\hbar} = v_o$, the orbital velocity of an electron in the 1s-orbit in the hydrogen atom, and $h\nu = I$, the ionization energy for a given electron. In practice, for an average over all the electrons, we must replace I by $\bar{I}$. $\bar{I}$ must come from experiment since attempts to derive it

theoretically have been unsuccessful (Ref 89, pp 97-99). We get

$$\frac{b_{max}}{b_{min}} = \frac{2\pi m v^3}{\bar{I} Z_1 v_o}.$$

After Heisenberg formulated the uncertainty principle, and Schrödinger the wave mechanics, in 1924 and 1925, the implications in the assumptions under the derivation of the Bohr equation could be seen more clearly. In the first place, in order to have a definite impact parameter, we must be able to describe the incident particle by a wave packet with dimensions small with respect to atomic dimensions, a. That is, the de Broglie wave length, divided by 2π, $\lambda\!\!\!^{-}_{de\ B}$, must satisfy the requirement: $\lambda\!\!\!^{-}_{de\ B} << a$. (If the uncertainty in the impact parameter, Δx, were of the order of a, then from $\Delta p\ \Delta x \geq \hbar$ we get $\Delta p \approx \frac{\hbar}{a}$. But we must have $\Delta p << p = M_1 v$. Hence $\frac{\hbar}{a} << M_1 v$ or $\frac{\hbar}{M_1 v} (= \lambda\!\!\!^{-}_{de\ B}) << a$.)

A further condition is found from the fact that to calculate the impulse transferred we must have the uncertainty in the original momentum much less than the change in momentum of the incident particle during the collision, which is the transferred momentum. The perpendicular impulse is approximately $\frac{2 Z_1 e^2}{v b}$ (Ref. 77, p. 28) or $\frac{V}{v}$ where V is the potential energy of the electron in the incident particle's field. $\Delta p << p$ transferred gives $\frac{\hbar}{a} << \frac{V}{v}$. In a Coulomb field, this becomes, using the same distance element on both sides, $\frac{Z_1 e^2}{\hbar v} >> 1$ or, more closely, $\frac{2 Z_1 e^2}{\hbar v} >> 1$.

For further reference we define

$$K \equiv \frac{2 Z_1 e^2}{\hbar v}.$$

The criteria for Bohr's energy-loss equation thus are:

$$\text{(a)} \quad \tau \ll T$$

$$\text{(b)} \quad \lambda\!\!\!^{-}_{\text{de B}} \ll a \qquad 7.3$$

$$\text{(c)} \quad K \gg 1$$

These conditions mean that the equation requires a well-defined orbit throughout and a strong interaction. It is, therefore, entirely classical.

It is illuminating to notice that the energy loss through collisions may be derived from the Rutherford scattering law. Williams[91] has given an especially good discussion of this derivation. Since the incident heavy particle is deflected through a very small angle, its momentum transfer to the electron is closely $M_1 v \theta$, measured in the laboratory frame of reference, and the energy transfer is $\frac{(M_1 v \theta)^2}{2 m}$. If this term be multiplied by the Rutherford scattering law which gives the probable distribution in θ, and by the number of collisions per unit distance, NZ_2, and the whole integrated from θ_{min} to θ_{max}, the result should be the Bohr energy-loss equation.

---

91. E. J. Williams, Rev. Mod. Phys. 17, 217 (1945).

$$-dE/dx = \int_{\theta_{min}}^{\theta_{max}} N Z_2 \frac{(M_1 v \theta)^2}{2m} \frac{d\sigma}{d\omega} d\omega$$

where $\frac{d\sigma}{d\omega} = \frac{1}{4} \frac{e^2 Z_1 Z^2}{M_1 v^2} \frac{1}{\sin^4 \frac{\theta}{2}}$ and $d\omega = 2\pi \sin\theta \, d\theta$

In $\frac{d\sigma}{d\omega}$, $Z_1 = 1$ since the deflection is due to an electron.

Sin $\theta \approx \theta$, while $\theta_{max} \approx \frac{m}{M_1}$, and θ_{min} is found from the momentum transfer at b_{max}:

$$M_1 v \theta_{min} = \frac{2 Z_1 e^2}{v b_{max}}, \quad \text{or } \theta_{min} = \frac{2 Z_1 e^2 \nu}{M_1 v^3}.$$

We get

$$-dE/dx = \int_{\theta_{min}}^{\theta_{max}} \left(\frac{4\pi N Z_1^2 e^4}{m v^2} \right) Z_2 \frac{d\theta}{\theta} = k B_\varepsilon$$

where $B_\varepsilon = Z_2 \ln \frac{\theta_{max}}{\theta_{min}} = Z_2 \ln \left(\frac{m v^3}{2 Z_1 e^2 \nu} \right)$,

a result which differs from the previous one only by a factor of 2 in the log term; the difference could be eliminated by closer evaluation.

The Rutherford scattering law was derived on a classical basis, but later was found to be strictly true quantum-mechanically, for a Coulomb field. Hence, despite the conditions for the validity of the Bohr equation,

it was thought it might hold in the region of weak interaction, where $\kappa \ll 1$.

In 1930, however, Bethe[92] derived a somewhat different expression for dE/dx using Born's first approximation for the treatment of collision problems. The essential conditions for the validity of Born's approximation are:[91]

$$\text{(a)} \quad \lambda\!\!\!^{-}_{\text{de B}} \ll a$$

$$\text{(b)} \quad \kappa \ll 1 \qquad 7.4$$

The Bethe equation is[93]

$$-dE/dx = \frac{4\pi z_1^2 e^4}{m v^2} N B'_\varepsilon$$

where the "stopping number" $B'_\varepsilon = Z_2 \ln \frac{2 m v^2}{I}$

Bethe's equation differs from Bohr's only in the argument of the logarithm, which, in the Bohr equation, is $\frac{1}{\kappa}$ times that in the Bethe equation. $B_\varepsilon = B'_\varepsilon - Z_2 \ln \kappa$. Williams[91] has explained the reason for this discrepancy between Bohr's and Bethe's equations. Although the Rutherford scattering law is correct both classically and quantum-mechanically as to the distribution in θ, the regions which give scattering into the angle θ are different in the classical and in the Born derivation of it. In the classical case, we saw from momentum transfer, $Mv\theta = \frac{2 z_1 e^2}{b v}$, that is,

92. H. A. Bethe, Ann. d. Physik 5, 325 (1930).

93. M. S. Livingston and H. A. Bethe, Rev. Mod. Phys. 9, 245 (1937), p. 263.

scattering into the angle θ is from collisions with an impact parameter $b = \frac{2 Z_1 e^2}{M v^2 \theta}$. In the wave treatment, in which no impact parameter is defined, scattering into θ comes from the region $\frac{\hbar}{M v \theta}$. The ratio between the two is seen to be κ. Accordingly, we see that at $\kappa = 1$ the two treatments come together. (See also ref. 89, p. 77) Since the differing factor is in a logarithmic term, the divergence between the two is not rapid near $\kappa = 1$. However, the difference is detectable in its effect on the range of a particle, as Williams has shown.[94] Both Bohr's and Bethe's equations are to be regarded as good approximations justified by quantum mechanics in the region of their validity, respectively $\kappa \gg 1$ and $\kappa \ll 1$. As the application of either is extended beyond its domain, it gives too high an energy loss and, hence, a shorter range than is found experimentally. At $\kappa \approx 1$, both err on the high side in energy loss. Williams has studied from experimental data the optimum point for changing from one treatment to the other and finds it to be at about $\kappa = 1.2$ for our definition of κ. (Actually, Williams, and many other writers, use the criterion $\kappa' = \frac{\kappa}{2}$. However, κ as defined above is selected by Bohr (Ref. 89, p. 18) as appropriate.) What can we say now as to the range-energy law that should be fulfilled for carbon nuclei compared to lighter nuclei and compared to fission fragments? In this connection, consider other ways of writing κ. Since $\frac{e^2}{\hbar} = v_o$, the orbital velocity of the electron in the Bohr hydrogen atom, and $Z_1 \frac{e^2}{\hbar} = Z_1 v_o = v_K$, the

---

94. E. J. Williams, Proc. Roy. Soc., London, A 135, 108 (1932).

velocity of a K-electron around the incident nucleus, we have

$$\kappa = \frac{2 Z_1 e^2}{\hbar v} = 2 Z_1 \frac{v_o}{v} = 2 \frac{v_K}{v} \qquad 7.6$$

and at $\kappa = 1.2$, $v = 1.67\ v_K$. As noted earlier, when $v = v_K$, a nucleus begins to alternate capturing and losing the K-electron. Since fission fragments never lose their K-electrons, their velocity is always less than v_K and, hence, for them, the Bethe equation is invalid, the Bohr equation suitable (modified to have Z_1^* rather than Z_1). The table below shows the deviation of C^{12} nuclei from the lighter nuclei.

TABLE 7.1

Nucleus	At $v = 4.391 \times 10^9$ cm/sec			At $\kappa = 1.2$		v_K ($\frac{cm}{sec}$) x 10^{-9}	E(Mev) at $v = v_K$
	E(Mev)	Range (μ) in emulsion	κ	E(Mev)	Range (μ)		
C^{12}	120	194.	.598	29.83	25.7	1.310	10.73
α	40	561.8	.199	1.10	3.73	0.4368	0.398
d	20	1115.	.100	0.138	$\sim$2.	0.2184	0.0497
p	10	557.5	.100	0.069	$<$ 1.	0.2184	0.0248

The ranges for alphas and protons are those given by Wilkins[18] for Ilford nuclear emulsions of density 3.92 gm/cm^3. The ranges for carbon nuclei are those found experimentally in the present research. It is apparent that for alphas, deuterons and protons of the initial energy given by the the Crocker 60-inch Cyclotron, almost the whole range in emulsion is given by the Bethe equation. However, for carbon nuclei the Bohr equation gives

a better approximation at an appreciable residual range. It is to be understood that changing the type of stopping law will not greatly change the range of the carbon nuclei. The two laws are the same except in the logarithmic term and there they differ by the argument in the Bohr equation being $1/\kappa$ times that of the Bethe equation. This means that, in the valid domain of the Bohr equation, it gives a slightly smaller stopping than the Bethe equation and, hence, a longer range, which we expect to be realized experimentally.

It will be noticed in Table 7.1 that the velocity of the nucleus reaches the velocity of its K-electrons at a point not greatly lower than the cross-over point to the Bohr equation. The effect of the consequent electron pick-up (to be discussed later) will be a greater effect in extending the range than is the functional change in going from the Bethe to the Bohr equation.

It is well known that so long as we use a single functional relation for dE/dx, we may get a simple relation between the ranges of particles of various masses and charges (Ref 93, p. 269). The region where such a procedure is useful is only in the Bethe region, $\kappa \ll 1$.

$$-dE/dx = k_1 \frac{Z^2}{v^2} \ln k_2 v^2 = Z^2 f(v)$$

$$\int_{R_o}^{R} dx = \frac{1}{Z^2} \int_{v_o}^{v} \frac{dE}{f(v)}, \quad R_o \text{ being the residual range}$$

at which the function changes and v_o the corresponding velocity. Since the change is gradual, the relation will be more accurate, but less useful, the higher we take R_o. We need only one constant ; hence, we could

extrapolate the law down to $R_o = 0$ and calculate a corresponding v_o if we wish.

The integration gives: $R-R_o = \frac{M}{Z^2}(F_1(v) - F_1(v_o))$

$$F_1(v) = \frac{Z^2(R-R_o)}{M} + F_1(v_o) \quad \text{where } F_1(v_o) = \text{a constant, c.}$$

Inverting the function, we get

$$v = F_2\left(\frac{Z^2(R-R_o)}{M} + c\right)$$

or $$E/M = F\left(\frac{Z^2(R-R_o)}{M} + c\right) \qquad 7.7$$

If we absorb $\frac{Z^2R_o}{M}$ in c, we see that for stripped nuclei of different masses and charges, if $v_1 = v_2$, then

$$\left(\frac{E}{M}\right)_1 = \left(\frac{E}{M}\right)_2 \quad \text{which implies} \quad \left(\frac{Z^2\,R}{M}\right)_1 = \left(\frac{Z^2\,R}{M}\right)_2 + c. \qquad 7.8$$

Hence, an elegant way of plotting range-energy curves is to plot $\frac{Z^2\,R}{M}$ vs $\frac{E}{M}$. The curves in the region $\kappa \ll 1$ should differ by only an additive constant in their abscissae. The experimental range-energy curve for C^{12} nuclei will be compared to that of alphas and protons by this criterion.

In the original derivation of Bethe's equation, in order to have a weak enough interaction to permit use of Born's approximation, he assumed that the velocity of the incident nucleus was higher than that of any of

the electrons in the stopping material, a serious limitation on the use of the equation if the stopping material nuclei are heavier than the incident nucleus.

Mott[95] showed that the limitation could be remedied, since he proved that a quantum-mechanical solution of the problem in terms of impact parameter for $\kappa < 1$ and $\lambda\!\!\!^{-}_{de\,B} \ll a$ (eq. 7.3 (b)) gave the same answer as the Born wave approximation, and, hence, except for close slow collisions, the limitation of Born's method to fast collisions could be removed, down to the limit $\kappa \approx 1$. This permitted Bethe (Ref. 93, p. 265) to modify his equation, putting $B_\varepsilon = Z_2 \ln\left(\frac{2 m v^2}{I}\right) - c_K$ where c_K takes care of the diminished stopping, and consequent increased range, due to the fact that the incident nucleus is no longer able to knock out the K-electrons from the stopping material. c_K has been evaluated by Bethe. Similarly, a c_L could be defined, but it would be useful only for a light incident nucleus in a heavy target, since the use of the correction is based on the assumption that $\kappa < 1$, that is, that the incident nucleus has not gone into the Bohr region nor started to pick up electrons itself. Adding c_K has not affected the validity of the form (7.7) for the range-energy relation. Notice that for alphas in hydrogen or carbon nuclei in, say, beryllium, the c_K correction cannot be used; there will be a correction due to failure to excite the K-electrons, but before that time the incident nucleus will have started picking up electrons.

---

95. N. F. Mott, Proc. Camb. Phil. Soc. 27, 553 (1931).

2. dE/dx for $Z_1^* < Z_1$:

This is the region to which fission fragments are born, and the region any nucleus must enter when its velocity falls below $v \cong v_K$ (at $K \approx 2$, not far inside the Bohr region). The C^{12} nuclei enter the region at about 10.73 Mev, when they have a remaining range of about 9.2 microns. Alphas enter the region at about 0.4 Mev and protons at 0.025 Mev where their residual ranges are very small. Even so, the capture of electrons by the alpha is principally responsible for extending the alpha range beyond strict proportionality to that of protons, so that eq. (7.8) becomes:

$R_p(E) = 1.0069\ R_\alpha(3.973\ E) - 1.5\mu$ in emulsion.[18] In air the constant is about 0.2 cm. We must expect the electron pickup effect to be much larger in extending the range of carbon ions with respect to alphas and protons. For instance, the experimental deviation from proportionality is given by the equation below, which must not be used for carbon ions below about 40 Mev.

$$\left(\frac{Z^2\,R(v)}{M}\right)_{C^{12}} = \left(\frac{Z^2\,R(v)}{M}\right)_\alpha + 24.0\mu$$

or,

$$R_{C12}(E) = \left(\frac{1-0.00064}{3}\right) R_\alpha\left(\frac{1-0.00064}{3}E\right) + 8.0\mu \qquad 7.9$$

In comparison with the expression written for protons and alphas,

$$R_\alpha(E) = 3.00192\ R_{C12}(3.00192\ E) - 24.0\mu$$

Eq. (7.9) shows how nearly the relation is true that a C^{12} nucleus of the three times the energy of an alpha will have one- third the range.

For C^{13} nuclei as compared to C^{12}, the effect of electron pickup and of change over from the Bethe to the Bohr region will be exactly the same for identical velocities. Hence, we expect a strict proportionality at the same velocity (Ref. 93, p. 271):

$$\left(\frac{Z^2 R(v)}{M}\right)_{C^{13}} = \left(\frac{Z^2 R(v)}{M}\right)_{C^{12}}$$

$$R_{C13}\left(\frac{13.00428}{12.00060}\,E\right) = \frac{13.00428}{12.00060}\,R_{C12}(E) \qquad 7.10$$

From the residual range of 10 microns down, carbon ions might be expected to behave somewhat like fission fragments of small charge. Actually the comparison will be found to hold for a much shorter range of about 2.3 μ. A quick glance at the behavior of fission fragments will give a basis for comparison.[89]

Stopping by electron collision is by far predominant for fission fragments until their velocity falls to $v = v_o$, the velocity of the ground state electron in hydrogen. At that time they have covered about two-thirds of their range. The rate of energy loss through electronic collisions per unit path length varies as $(Z_1^*)^2/v^2$. Since a fission fragment from its origin has a full core of K and L electrons, and since the electronic stopping term cuts off at $v \approx v_o$, before all the valence

electrons are picked up, we are concerned only with intermediate shells where the Thomas-Fermi statistical description may be used (Ref. 89, p. 101 and 116) to give the estimate: $Z_1^* \sim Z_1^{1/3}\ v/v_o$, valid for the region $v_o < v < Z_1^{2/3}\ v_o$. Therefore, we see that dE/dx is roughly independent of the velocity, in marked contrast to the case of a particle of fixed charge, where the ionization increases rapidly as the particle slows down. Even for fission fragments, in case of the lighter group, the ionization may at first increase slightly as the velocity decreases.

In the case of carbon nuclei we cannot use the Thomas-Fermi statistical method to give Z_1^*. The carbon nucleus has a kinetic energy of 10.7 Mev when its velocity is that of the sixth electron. It picks up the two K electrons in this region. Then its charge will be fairly constant until it reaches the velocity of its fourth electron, at 1.4 Mev. In Fig. 41 are indicated the C^{12} kinetic energies corresponding to the velocities of its various electrons, with an approximate curve drawn for Z_1^*. We must not expect electrons to go from zero to full time occupancy of an electronic state at any well-determined point, nor is Z_1^* to be interpreted to correspond to the actual charge that exists, since the effective charge may be less in a stopping substance lighter than the incident particle than it is in a heavier (Ref. 89, p. 118).

We may think of the C^{12} ion as reducing its charge by two units in the neighborhood of $v = 6\ v_o$, but behaving then like a particle of fixed charge - for instance, its ionization loss per unit path increasing as $1/v^2$ - until the kinetic energy falls to the vicinity of 1.4 Mev and

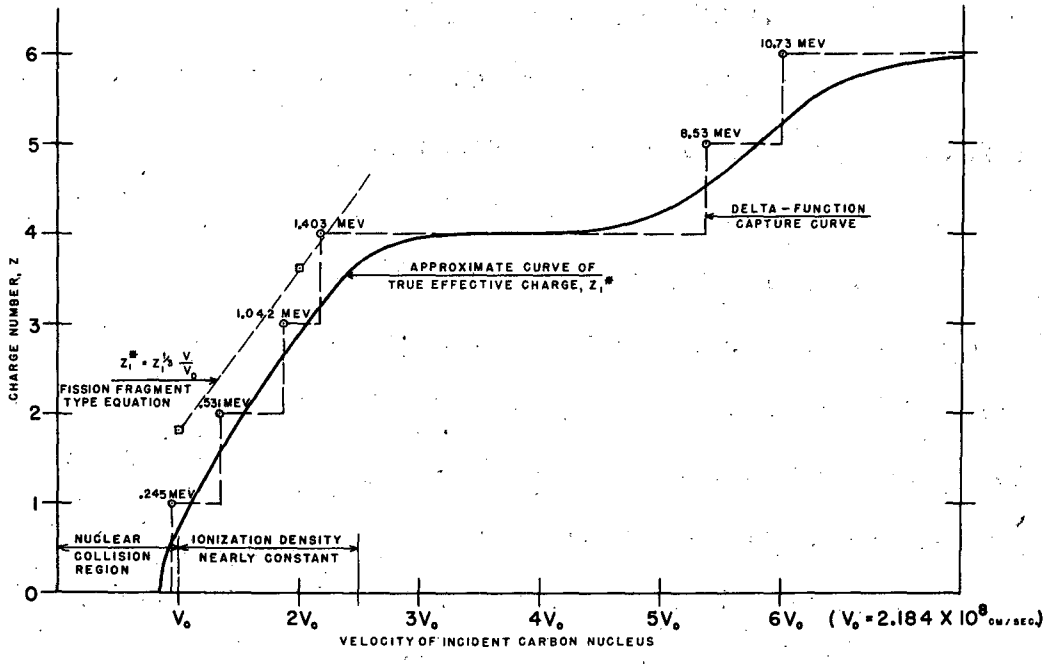

EFFECTIVE CHARGE OF CARBON IONS
IN REGION OF ELECTRON CAPTURE

MU3811

FIGURE 41

the ion begins to pick up L electrons. Here, possibly, we may use an expression like $Z_1^* = Z_1^{1/3} v/v_o$, if we limit it to the region: $v_o \ll v \ll 2.5\ v_o$. It has been sketched in on the graph to show how it fits. In this region it appears that the carbon ion should behave much like a fission fragment in that the ionization will not increase as the velocity decreases. In Ilford E-1 emulsion, it is noticeable that near its end the carbon track appears to thin down a little and, within 2 to 4 microns from the end, may even have a gap or two.

It is of passing interest to notice the effect of electron capture on the Bragg ionization curve for carbon nuclei compared to that for alphas. In the region of stripped nuclei, dE/dx for carbon nuclei is, according to the equation, nine times as high as for alphas of the same velocity (still almost true after entering the Bohr region, since the only change is entry of Z_1 under the long term). But at about 11 Mev the carbon nucleus begins to reduce its charge (at $v \cong 6v_o$, while the alpha does not reduce charge until $v \cong 2v_o$). From $v = 6v_o$ to approximately $2.5\ v_o$ the carbon ionization may increase, but not at the rate expected by $1/v^2$ since its charge has fallen from six to four. Indeed, at $v = 2\ v_o$, dE/dx for an alpha equals the value a carbon nucleus had at $v = 6\ v_o$. The increase in ionization from $6\ v_o$ to $2\ v_o$ is the only edge the carbon ion has on the alpha. In emulsion an alpha track a few microns from its end may become fairly comparable in density to a carbon track at the same point. A Bragg curve made by recording oscilloscope "pip" heights from an ionization chamber shows a wide low peak for carbon ions.

3. Nuclear Collision Region: $v \ll v_o$.

Loss of energy through electronic collisions is the important mode until $v = v_o$ quite closely. At that point Z_1^* decreases very rapidly because

of the pick-up of the valence electrons; therefore, electronic stopping becomes very small. If a new effect did not come in there would be a long tail added to the range. The new effect is nuclear collisions, which have been rare occurrences thus far. Now the factor M_2 in the denominator, which kept this stopping term small, is overbalanced by the decrease in velocity.

Of course, the nuclear collision region is an extremely small part of the range for a proton or alpha, and not much larger for a carbon nucleus (its energy is only 0.25 Mev when it enters the region). If we compare the nuclear collision term with the electron term for carbon ions and for fission fragments, we see that although it appears as the same function for each, namely, varying as $(Z_1/Z_1^*)^2$, this does not denote the same level of significance for carbon and fission fragments at a given velocity. At $v \cong v_o$, Z_1^* is not essentially different for the two particles, and decreases toward zero at about the same velocity, but Z_1 is, of course, of the order of six to nine times greater for a fission fragment. Hence, the nuclear stopping term is a relatively much larger effect for fission fragments, as is evidenced by the bending and branching of a fission fragment track in the latter half of its range. A carbon track will often be bent into a hook-shape at its very end but branching there is fairly rare. Further, the branching from nuclear collisions in the early part of the track is less frequent for carbon ions than for fission fragments since the cross section (Ref. 89, p 43) for nuclear collisions varies as Z_1^2. Correspondingly, it is noticeable in the emulsions containing C^{12} and alphas together that branching occurs much more frequently for carbons than for alphas. One further point to remark on is that when $M_1 > M_2$, the deflections of the incident particle are not large in nuclear

collisions, and the slowing-down process is comparable to that from electronic collisions. This is the usual case for fission fragments, the exception being for heavy stopping materials. But when $M_1 \leq M_2$, the elastic nuclear collisions produce large deflections and disperse the beam. This process accounts for the small hook-ends often observed on carbon tracks.

When the incident particle is deflected in a nuclear collision, the struck particle is also displaced, though often the displacement may not be sufficient that it could be detected as visible branching. Just as the Rutherford scattering law gives a forward-peaked maximum in the laboratory system for the incident particle, so it gives a peak towards 90 degrees for the struck particles. The displacement of atoms in the target materials is studied under the name of "radiation damage".[96] The much greater capacity of carbon ions, as compared to lighter ions, in producing radiation damage has stimulated interest in their use for this purpose.

4. Region of gas kinetic collisions.

The nuclear collision term in Eq. (7.1) holds for a considerable distance below v_o, but does not hold for $v \ll v_o$. The nuclear collisions continue, but a different type of equation must be used (Ref. 89, p. 136), and the collision cross sections become larger until, at the very end of its velocity, the particle is brought to rest or to equilibrium (in case the stopping substance is a gas) by gas kinetic collisions. This region is completely inconsequential for carbon ions in emulsion.

96. J. C. Slater, J. Appl. Phys. 22, 237 (1951).

5. Straggling in Range.

Since the stopping of a nucleus is almost entirely due to small energy losses in collisions, the statistical fluctuation in the number of these collisions per unit length will show up in a fluctuation of the energy lost per unit distance traveled and, hence, of the expected range beyond that interval. The total range to bring a particle to rest may fluctuate considerably. For particles as heavy as nuclei, we need not concern ourselves with range straggling from another source: curved paths from multiple scattering.

For small energy losses, the probability function for the energy loss for any given thickness will be closely gaussian; consequently, the mean square fluctuation in energy may be evaluated and transformed to mean square fluctuation of the range (Ref. 89, p. 127). For a particle traveling among nuclei heavier than itself, the resulting expression for straggling from electronic collisions is:

$$\frac{\sigma_\varepsilon\{R\}}{R} = \left(\frac{3\,m}{4\,M_1}\right)^{1/2}$$

where $\sigma_\varepsilon\{R\}$ is the standard deviation in range, M_1 is the mass of the incident particle, and m the mass of an electron. For alphas in emulsion this gives a range straggling compared to the total range of close to one percent; for carbon nuclei, 0.6 percent, for fission fragments, 0.1 percent.

Straggling from nuclear collisions may also be calculated. For alphas and carbons it is at most a few percent of the straggling from electronic

collisions, and, hence, is negligible. For fission fragments, however, there is a large contribution in the close neighborhood of v_o, where the residual range is about one-third of the total range. This may give a relative standard straggling of about 3 percent of the total range (Ref. 89, p. 138). For carbon the residual range at $v = v_o$ is so small that the contribution to the total range straggling would be extremely small, even if the carbon were in a medium lighter than itself rather than one heavier, which tends instead to scatter the carbon nucleus. In measuring the ranges of carbon nuclei in emulsions in this research, it was easy to straighten out visually the small end hocks to give a close measurement of the actual distance traveled.

B. EXPERIMENTAL EQUIPMENT AND RESULTS.

In designing apparatus to obtain a range-energy curve, the objective set was to get an "absolute" relation in the sense that the energy would be obtained from measurement of the curvature in a known magnetic field and the range of the same particles would be recorded in emulsion. At the same time it was desirable to obtain "relative" range-energy data, with the range and energy of the carbon ions compared directly to that of another type of particle. Relative sets of data may show up errors that would go undetected on an absolute measurement basis. Since alpha particles are accelerated along with the C^{12} ions, it was convenient to use them as a relative standard; the range-energy relation for them has been measured by many experimenters and cannot be far wrong. If C^{12} ions

were to be used, there was no necessity for making measurements on C^{13} ions. Direct proportionality should hold very closely.

An ideal way to measure the energy is by setting up three narrow slits in the nearly uniform magnetic field between the pole tips and to adjust these slits so that a few particles deflected up or down from the beam platter will pass through the slits. Hubbard and MacKenzie[97] have used this method to obtain precise range-energy data for protons. It was not practicable on the Crocker Laboratory sixty-inch cyclotron to set up the necessary apparatus inside the tank. However, the same principle could be used on the external beam without the necessity of scattering it out of the median plane. The accuracy of measurements would be limited principally by the size of the beam available but should be quite adequate.

The prerequisites for measuring the energy in the external magnetic field are that the field strength and the slit positions should be accurately known. The slits must, of course, be narrow, spaced as far apart as possible, and there must be a means of detecting when they are adjusted so that the maximum beam is passing through them.

The magnetic field is falling off rapidly in the region traveled by the external beam. Unless it were made nearly uniform, it would not be possible to measure it accurately and, also, there would be a large error in the calculated energy from any small error in measurement of the absolute position of the slits. Accordingly, steel plates to uniformize the field were designed* For symmetry the inner and outer edges were circular arcs

---

97. E. L. Hubbard and K. R. MacKenzie, Phys. Rev. 85, 107 (1952).

* I am indebted to Professor Wilson Powell for a discussion of the practical aspects of design of uniformizing plates. It was not possible to follow all his recommendations, e.g., that the beam be kept in the central portion only.

which were placed at the corresponding radii with respect to the center of the pole tips (Figure 42). The inner faces were made parallel and as close to each other as feasible (actually 9/16 inch). The outer surfaces were then tapered, with the amount of taper calculated on the engineering approximation that, considering the magnetic field above and below the plates as undisturbed, the magnetomotive force $\int \vec{H} \cdot d\vec{l}$ (measured along any field line) that originally was present in the region occupied by the plates would all be placed across the gap between the plates. The basis for the approximation is that H in the iron is very small: $\mu H_{iron} = H_{air}$. If t_1 and t_2 are the plate thicknesses at the inner and outer radii, one could be found in terms of the other by $H_1 (2t_1 + W) = H_2 (2t_2 + W)$ where W is the gap between the inner faces. For the inner arc at the 35-inch radius and the outer at the 47-inch radius, suitable thicknesses were one-half inch and two inches. For ease of machining, the taper was made uniform. Two-inch boiler plate was used. In Figure 46 is shown a composite of measurements of the magnetic field between the pole tips and of the field between the plates. The field beyond the plates was measured with them in position. Figure 43 is a photograph made during the measurement of the field between the plates. This measurement was made with a General Electric fluxmeter and a specially constructed small coil. Relative measurements of the field were taken along four radial lines, approximately at slits 1, 2 and 3, and at the center of the photographic chamber. Along each radial line, the field was measured at half-inch intervals. One absolute measurement was taken on each radial line. At the inner and outer edges, the field varied rapidly, but it was relatively uniform in the middle region.

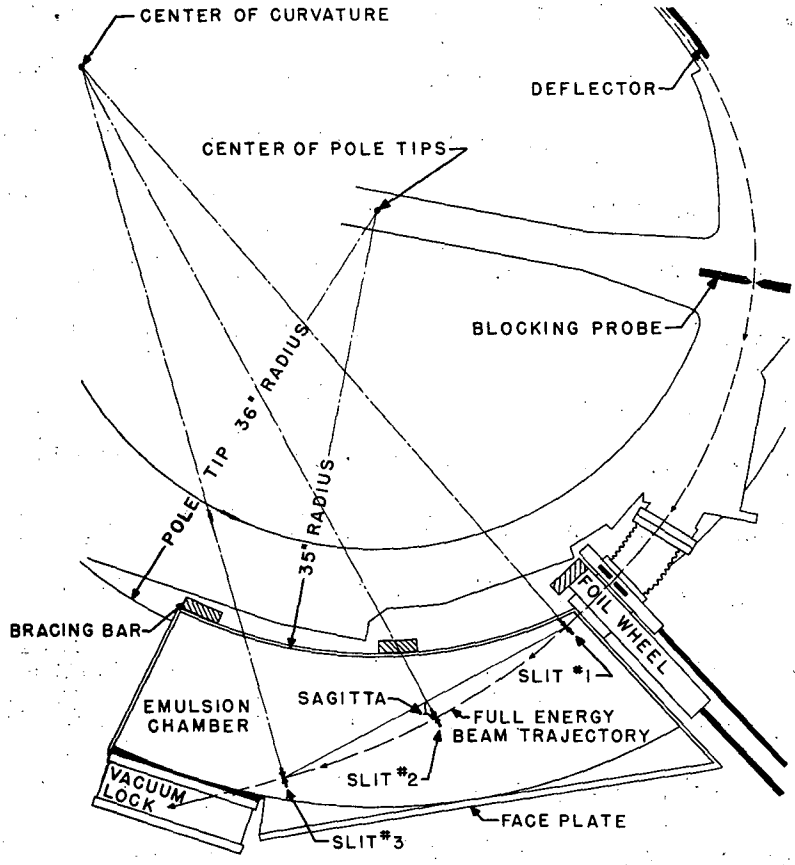

RANGE—ENERGY APPARATUS ON CYCLOTRON
(SHOWN WITH FULL ENERGY BEAM)

FIGURE 42

FIGURE 43.

The apparatus for obtaining range-energy is shown in position with the faceplate removed. Measurements of the magnetic field with the General Electric flux-meter are being made. The blocking probe is in the port at the extreme right of the picture.

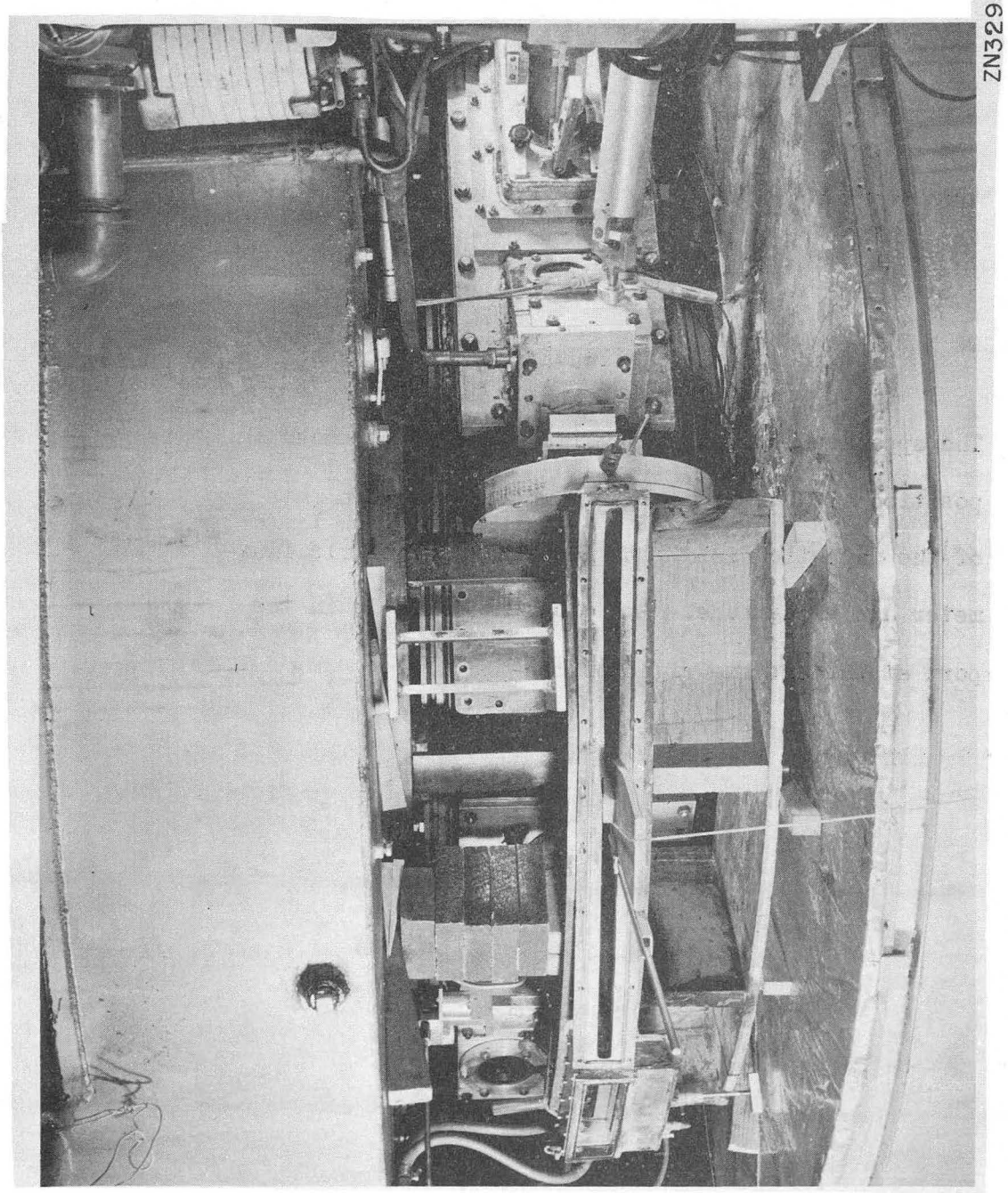

FIGURE 43

FIGURE 44

The sagitta-measuring arm with its three slits to measure the beam energy and the photographic plates to record the range are shown in their relative positions. The top guide plate for the center slit has been removed to expose the slit to view. The stainless steel micrometer which moves the center slit can be seen through the lucite window. Numbers 1 and 3 slits are fixed with respect to the arm. The pivots at these points for the adjusting rods are directly over the slits. Behind the third slit is the scintillator head in position. The light is transmitted down a lucite rod to the photomultiplier tube in the magnetic shield. Below it is its amplifier. After the beam is located, the scintillator is retracted enough to permit the beam to pass to the photographic plates.

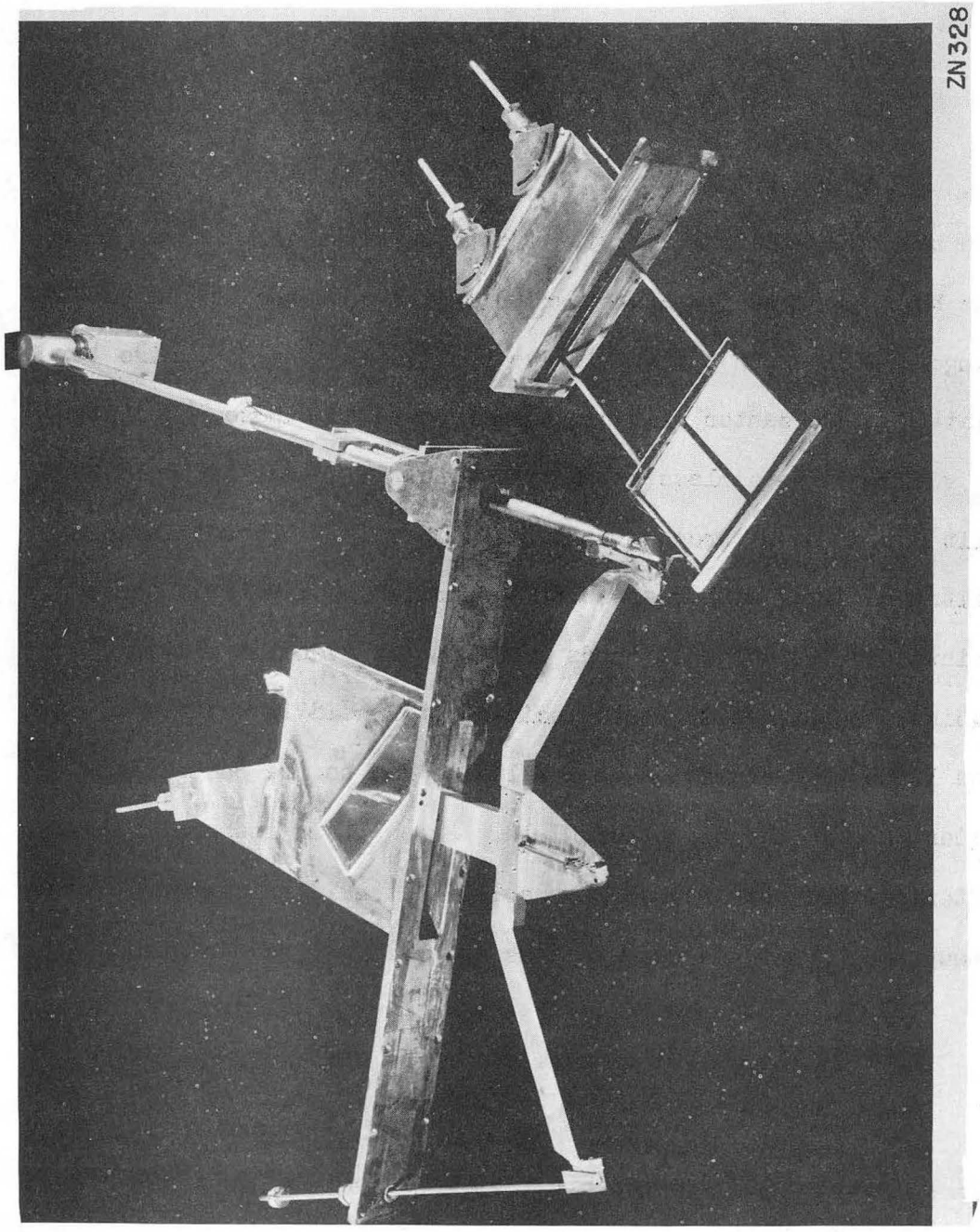

FIGURE 44

FIGURE 45

A combined blocking probe and ionization chamber are shown in this picture. The blocking probe was desirable to eliminate stray beam in off-center orbits from coming out between the dees. To use the blocking probe effectively, it was necessary to know where the maximum of the deflected beam lay; this was the function of the ionization chamber. After locating the beam, the probe was moved out the amount necessary to put the slit where the chamber window had been. Later a longer, more effective blocking probe was used, separate from the ionization chamber.

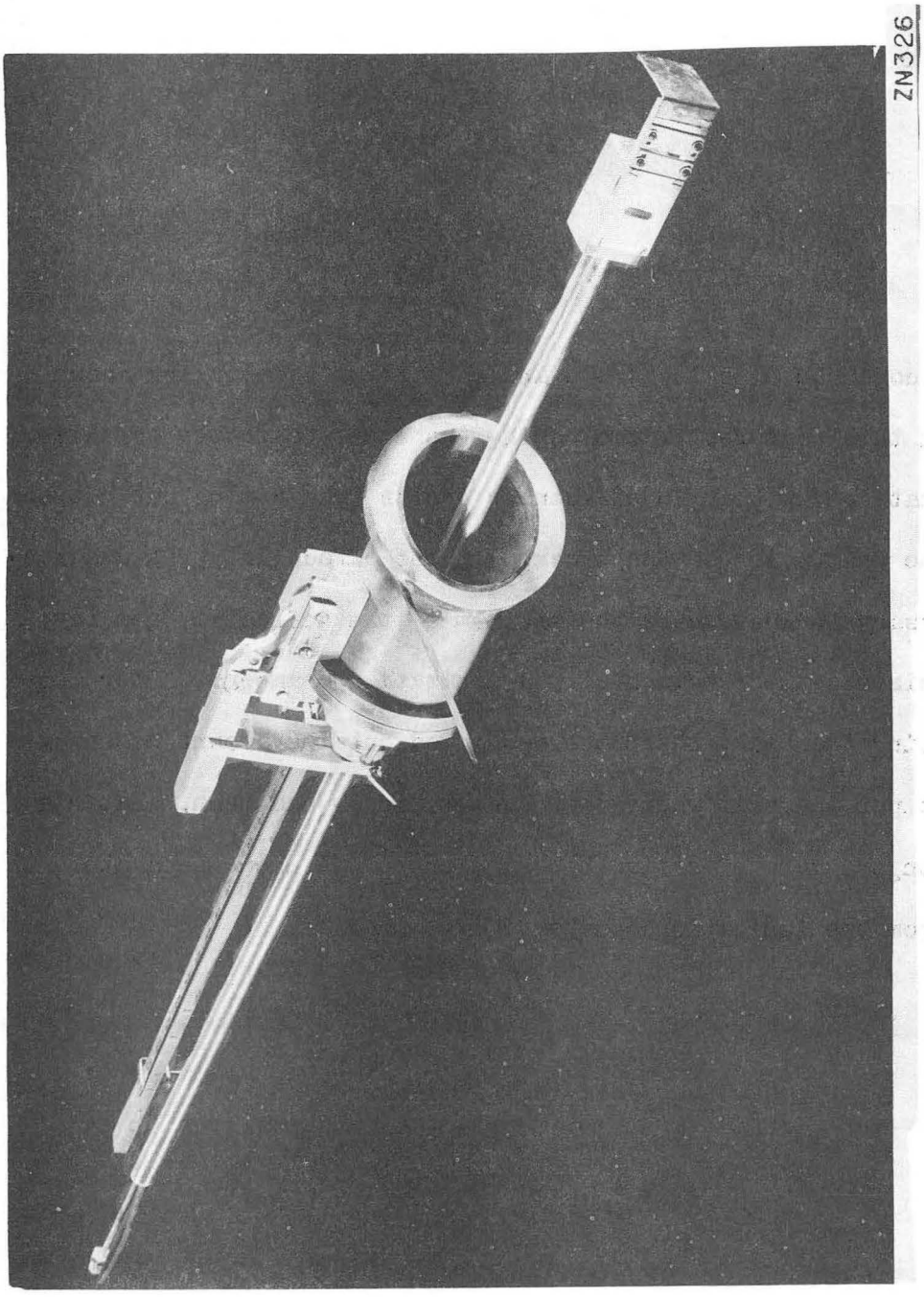

FIGURE 45

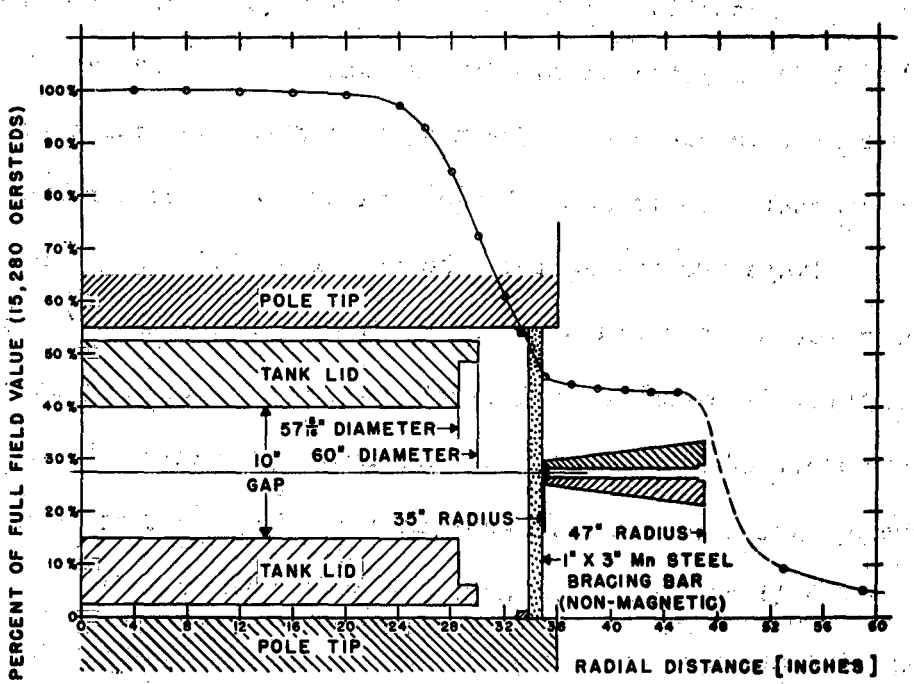

MAGNETIC FIELD USING PLATES,
SHOWN IN POSITION,
TO UNIFORMIZE THE FRINGING FIELD

FIGURE 46

In the area where the beam would be measured, the field was uniform within about three percent.

Since the field was relatively uniform, it was not necessary that the absolute position of each slit be measured with great precision. The only precise measurement required was the position of the middle slit with respect to the two outer slits. To satisfy these requirements, the beam arm, or sagitta-measuring arm shown in Fig. 44, was designed. The first and last slits are fixed on the arm, but the arm can be moved as desired by rods attached to bearing collars centered over these slits. The middle slit is centered between the other two and can move in and out in a channel. It is on a plunger loaded by a phosphor-bronze spring so that it always presses against the end of a stainless steel micrometer. The micrometer is adjusted by a rod leading through a Wilson seal. Its one-inch throw is extended by inserting gauge blocks. The setting of the micrometer, after the slits are adjusted for maximum beam, can be read through a lucite window. From this reading and a value previously found for the line of sight measurement of the three slits, the sagitta of a circular arc through the three slits can be obtained with an accuracy of approximately 0.001 inch. The non-uniformity of the field will cause a deviation from a circular arc, but the correction can be calculated with the circular arc as the first approximation.

The adjusting rod attached to the third slit is made of two tubes with a lucite rod inside. On the inner end of the rod, an anthracene crystal was cemented to give scintillations from particles coming through No. 3 slit. The lucite rod conducted the light pulses to where the

magnetic field was small enough that a 1P-21 photomultiplier tube could be shielded from it. After the beam was located, the inner stainless steel tube could be retracted a little more than an inch to permit the beam to pass to the photographic plates which then were shoved into place. In order for individual scintillation pulses to show clearly on an oscilloscope screen to permit adjusting to pick up the beam, a "pulse-stretcher" was added to the amplifier by K. D. Jenkins.

The photographic plates were brought up in a cassette, which was pumped down after positioning it on the apparatus. Then a wedge-action vacuum lock could be opened to permit shoving the plate holder into position. The plate holder could be maneuvered by two rods and located with respect to No. 3 slit by means of notches. The plates were inclined to the horizontal at an angle of $4^{\circ}45'$. An especially large plate holder was used, holding two plates 3-1/4 x 4-1/4 inches, in order to get a long trace of the beam pencil. The lowest energy for which the beam arm can be used is about 40 Mev. For range-energy data below 40 Mev, the beam of that energy could be passed through a thin foil which would give little dispersion, and the new energy could be measured by the curvature of the center line of the beam on the two plates.

In addition, the length of trace given by two plates was desired in order to experiment with the capture and loss of electrons by carbon ions out near the end of their range. When the first and second electrons began to be picked up, traces of C^{6}, C^{5}, and C^{4} beams should be seen. The separation of the traces would be adequate, at least on the second plate. A few accurate points on the capture and loss of electrons by

carbon nuclei would be of considerable interest for comparison with theory since the pick-up of the two inner electrons should be essentially different for carbon ions passing through a foil of greater atomic number, say aluminum or gold, compared to their passing through one of less atomic number, for example, beryllium (see reference 89, Chapter 4).

The entire region between the plates had to be in vacuum, with no other magnetic material than the two field-uniformizing plates. The sealing strip around the plate edges, the face-plate assembly, and the photographic chamber vacuum lock were made of brass. All these were hard-soldered to the steel plates. The high heat required and unequal shrinkage caused warping of the brass and cracking at soldered joints. Great difficulty was had in obtaining a vacuum tight system. Other than that, the apparatus functioned well.

The second difficulty was in getting a carbon beam intense enough that the three narrow slits could be brought into adjustment to pass it. The procedure was as follows: Nos. 1 and 2 slits were retracted. A moderately narrow beam entering the plates was obtained from either the blocking probe slit or the slit in front of the foil wheel. No. 3 slit was moved in or out to find the limits of the beam and its approximate maximum. Then No. 1 slit was moved into position with No. 2 still retracted. Finally, No. 2 was moved in until, first, the inner face of the slit cut out the beam, and then the beam reappeared through the slit. During adjustments of slits Nos. 1 and 2, the beam often faded into the background of random pulses. No points could be obtained with the slits open 0.010 inches. Two good points in the range-energy curve

were obtained with the slits open 0.020 inches, and two more with them open 0.040 inches. Even with the latter slit width, the center of the energy distribution is well determined, although the energy spread passed is higher than desired.

As a first approximation, the beam energy could be calculated from the measured sagitta under the assumption that the magnetic field was uniform. When the range-energy points based on this assumption were plotted, they were found to be uniformly of too low an energy for the range measured. This error could be seen from the points found for the alphas that came through the slits at the same time the carbon ions did. The error was large, corresponding to a magnetic field nine percent too low. The accuracy of the General Electric fluxmeter was expected to be within one-half percent. The only source of error seemed to be that the absolute field measurements may have been taken where the field was changing rapidly or that the area used for the coil was in error. The coil had been destroyed and measurements could not be repeated. However, check measurements were made with a Rawson-Lush rotating-coil Gaussmeter. The average of readings with it indicated the original absolute values were, as predicted, nine percent too low. However, the Rawson-Lush could not give individual readings of the field that were accurate enough to use. Its accuracy is only 2.5 percent of full scale (12,000 oersteds). Indeed, the motor rotating the coil could be heard slowing down as the probe was moved in beyond the center of the plates.

Absolute energy values for the measured ranges had to be foregone.

Fortunately, the relative alpha standard was always present, although the number of alphas that could be found on some of the plates was lower than desired. The data from these points, for both carbon ions and alphas, are given in Table 7.2.

The data of Table 7.2 do not specify what value of energy corresponds to the measured ranges. It is known that the momentum per unit charge was the same for the carbon and helium ions. Assuming that charges and masses are well established, we can calculate that the energy of the carbon ions was 3.00196 times that of the alphas. From that point on, the actual value of the carbon energy will be determined by the range-energy data assumed for the alpha. In the low energy part of the curve, calculated from knock-on protons, the energy will similarly depend on the proton range-energy data used. In the present work, the data given by Wilkins[18] (which is in agreement with that of Rotblat) has been used. The numerical values (plotted in Fig. 47) for the measurements made with the slits are:

$\bar{R} \pm \sigma\{\bar{R}\}$ (microns)	173.63±0.20	61.86±0.14	54.51±0.12	45.29±0.10
E (Mev)	112.02	56.52	52.20	45.43

Notice that it is $\sigma\{\bar{R}\}$, not $\sigma\{R\}$, which is of interest. The accuracy of the carbon ion curve in the region determined by the slits (from 45 Mev up) should be about that of the alpha curve, which is presumed to be of the order of one percent.

Because of the unknown magnetic field strength, the very low energy points could not be obtained by the proposed method, nor would it be

TABLE 7.2

COMPARATIVE RANGES (MICRONS) IN ILFORD E-1 EMULSION OF C^{12} AND He^4 IONS OF THE SAME MOMENTUM PER UNIT CHARGE

Run No. with Slit Opening	Particle	Number of Tracks Measured	Method of Measurement	$\bar{R}$	$\sigma\{R\}$	$\sigma\{\bar{R}\}$	True $\frac{Z^2}{M}\bar{R}$	$\Delta\left(\frac{Z^2}{M}\bar{R}\right)$	$\sigma\left\{\Delta\left(\frac{Z^2}{M}\bar{R}\right)\right\}$
RUN I 0.020" Slit	C^{12}	125	Superstage micrometer	173.63	2.20	0.20	520.87	21.59.	0.85
	Alpha	125	Superstage micrometer	499.62	6.70	0.60	499.28		
RUN II 0.040" Slit	C^{12}	100	Reticule	61.68	1.43	0.14	185.57	27.18	0.76
	Alpha	50	Superstage micrometer	158.39	4.54	0.64	158.28		
RUN III 0.040" Slit	C^{12}	100	Eyepiece reticule	54.51	1.16	0.12	163.52	24.45	0.77
	Alpha	44	Superstage micrometer	139.17	4.50	0.68	139.07		
RUN IV 0.020" Slit	C^{12}	100	a) Reticule b) Superstage micrometer	43.31 44.96	0.39 1.26	0.04 0.13			
	C^{12}	100	Calibrated eyepiece	45.29	0.98	0.10	135.87	24.70	0.61
	Alpha	11	Calibrated eyepiece	111.25	1.77	0.53	111.17		

The value used for the smooth curve through the data in Fig. 47 is as follows:

Weighted average $\Delta\left(\frac{Z^2}{M}\bar{R}\right) = \frac{2(21.59) + 27.18 + 24.45 + 24.70}{5} = 23.90 \pm \sim 0.75.$

True $(Z^2/M)_{\alpha} = 1 - 0.000692$

True $(Z^2/M)_{C12} = 3(1 - 0.000050)$

Under the columns headed σ, the values given are the estimate, s, of σ from the sample.

$$\sigma\{R\} \approx s = \sqrt{\frac{\Sigma(\bar{R} - R_i)^2}{n-1}} \cdot \sigma\{\bar{R}\} = \frac{s}{\sqrt{n}} \cdot \sigma\left\{\Delta\left(\frac{Z^2}{M}\bar{R}\right)\right\} = \sigma\left\{\left(\frac{Z^2}{M}\bar{R}\right)_{C12} - \left(\frac{Z^2}{M}\bar{R}\right)_{\alpha}\right\}$$

$$= \sqrt{\left(\frac{Z^2}{M}\right)^2_{C12} \sigma^2\{\bar{R}_{C12}\} + \left(\frac{Z^2}{M}\right)^2_{\alpha} \sigma^2\{\bar{R}_{\alpha}\}}.$$

possible to evaluate accurately any data on capture and loss of electrons. In addition, the near-zero beam through the slits prevented getting the desired data.

To obtain range-energy points below 45 Mev, a method somewhat similar to that used by Rotblat[98,99] was employed. By measuring the angle between the carbon ion and a knock-on proton, and from a knowledge of the energy of the proton based on a measurement of its range, the energy of the carbon ion after the collision can be calculated to plot against its range. The equation is:

$$E_C/\text{lab} = E_p/\text{lab}\,\frac{\left(1 - \frac{M_p}{M_c}\right)^2}{\frac{4M_p}{M_c}\cos^2(\theta+\varphi)}$$

$$\text{or}\quad E_c = E_p\,\frac{(2.49849)}{\cos^2(\theta+\varphi)},$$

where $\theta+\varphi$ is the angle between the proton and the carbon ion after the collision. In the original survey of plates exposed to study nuclear events, coordinates had been set down for many proton knock-ons. The most suitable of these near the end of the range were now analyzed. The resulting points are plotted as open triangles in Figure 47. Each point is from a single knock-on. The accuracy is not high compared to that of Rotblat; he used at least 800 tracks at each energy point. The values of the C^{12} range and energy calculated from the individual knock-on events are:

---

98. J. Rotblat, Nature 165, 387 (1950).

99. J. Rotblat, Nature 167, 550 (1951).

R(u)	E(Mev)	R(u)	E(Mev)	R(u)	E(Mev)
4.9	6.25	13.4	16.93	18.1	20.68
6.3	8.50	13.7	14.04	20.3	24.82
6.8	9.60	13.7	14.92	21.9	27.96
7.5	7.96	14.5	19.72	23.0	24.50
7.8	8.44	16.2	18.28	23.4	28.02
9.3	12.78	16.9	21.35	27.4	30.65
11.4	16.97	17.1	20.52	28.8	28.69

The C^{12} energies shown were calculated after calibrating the microscope vertical adjustment against a standard of depth obtained from the Film Group of the University of California Radiation Laboratory. Also the proper emulsion shrinkage factor of 2.3 was used. The dispersion of the individual points is probably due primarily to uncertainty in measuring the angle $\theta + \varphi$ between the C^{12} and the proton after the collision. If the angle is 60 degrees, an error of one degree will give about six percent error in energy. A judgment as to the true angle might be in error by as much as three degrees.

It will be noticed that the difference between the Z^2R/M for carbon ions and for alphas begins to decrease long before the expected pick-up of the innermost electron by carbon. This is the effect to be expected as the velocity enters the cross-over region from the Bethe equation as the velocity enters the cross-over region from the Bethe equation ($K<1$) to the Bohr equation ($K>1$). The optimum cross-over point, $K = 1.2$ is at 29.83 Mev. The divergence appears to begin slightly above that value, as is predicted.

As the curve enters the region of electron pick-up, a conceptual curve as to what the shape should be has been drawn in to give the best fit for the points.

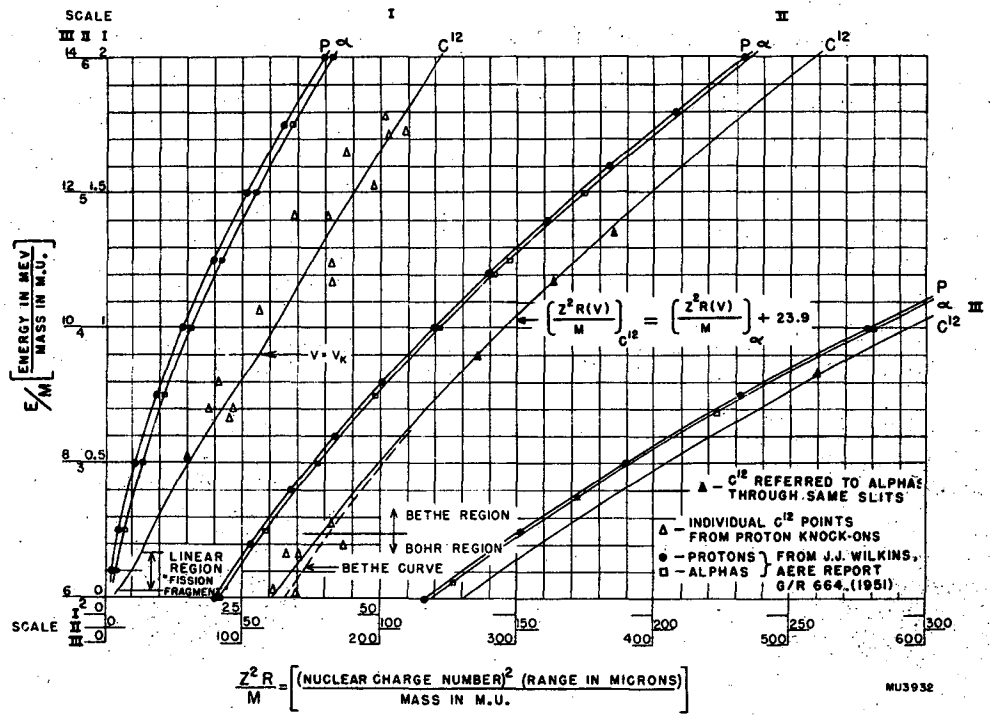

RANGE ENERGY CURVE FOR C^{12}

FIGURE 47

ACKNOWLEDGMENTS

It is a pleasure to acknowledge the interest and guidance of Professor E. M. McMillan, Professor A. C. Helmholz and Professor J. G. Hamilton throughout the course of this work. The development and study of the carbon ion beam under the stimulating encouragement and interest of Professor Hamilton has been a project in which all members of the sixty-inch cyclotron staff have taken a close part, giving willing assistance and helpful suggestions. In particular, thanks are due to Dr. T. M. Putnam and Mr. G. B. Rossi.

The discussions with Dr. W. H. Barkas on many points regarding the technique of emulsion studies and interpretation of observations have been very helpful. Especial thanks are due to Mr. A. J. Oliver who has contributed long hours of painstaking work in making the photographic mosaics in this work.

The assistance of Mrs. R. Gibbs in the survey of the plates was invaluable. Many of the most interesting stars were found by her and the tedious statistical measurements were made by her.

Miss H. Jones has assisted materially in the compilation and editing of this paper. Mr. R. Burton prepared all the drawings, with careful attention to the specified details. Mrs. B. Butler gave valuable assistance in preparing the copy.

This work was performed in part under the auspices of the Atomic Energy Commission.

REFERENCES

1. L. W. Alvarez, Phys. Rev. 58, 192 (1940).

2. C. A. Tobias, Ph.D. thesis, University of California, Berkeley (1942), Phys. Rev. 70, 89 (1946) and UCRL Report 1039 (1950).

3. R. I. Condit, Ph. D. thesis, University of California, Berkeley (1942), and Phys. Rev. 62, 301 (1942).

4. H. York, R. H. Hildebrand, T. M. Putnam and J. G. Hamilton, Phys. Rev. 70, 446 (1946).

5. J. F. Miller, J. G. Hamilton, T. M. Putnam, H. R. Haymond and G. B. Rossi, Phys. Rev. 80, 486 (1950).

6. A. Ghiorso, S. G. Thompson, K. Street, and G. T. Seaborg, Phys. Rev. 81, 154 (1951).

7. J. M. Hollander, UCRL Report 1396,(July, 1951).

8. J. O. Rasmussen, UCRL Report 1473 Rev. (December, 1951).

9. Atomic Energy Levels, Vol. 1, Sec. 1, Circular 467, Nat. Bur. Stds. (1949).

10. J. Mattauch and A. Flammersfeld: Isotopic Report. (1949) Tubingen.

11. R. R. Wilson, Phys. Rev. 56, 459 (1939).

12. E. O. Lawrence and M. S. Livingston, Phys. Rev. 40, 24 (1932).

13. B. B. Rossi and H. H. Staub: Ionization Chambers and Counters, McGraw-Hill Book Company, New York (1949).

14. P. C. Giles and W. H. Barkas, Phys. Rev. 85, 756 (1952).

15. S. O. C. Sorensen, Phil. Mag. 40, 947 (1949).

16. M. Blau, R. Rudin and S. Lindenbaum, Rev. Sci. Instr. 21, 978 (1950).

17. M. Blau, Phys. Rev. 75, 279 (1950).

18. J. J. Wilkins, A.E.R.E. Report G/R. 664, Harwell, England (1951).

19. A. J. Oliver, private communication.

20. H. Bradner, F. M. Smith, W. H. Barkas and A. S. Bishop, Phys. Rev. 77, 462 (1950).

21. J. M. McAlister and D. W. Keam, Proc. Phys. Soc., London, A64, 91 (1951).

22. N. Metropolis and G. Reitwiesner: Table of Atomic Masses. USAEC Report NP-1980 (1950).

23. L. J. Cook, E. M. McMillan, J. M. Peterson and D. C. Sewell, Phys. Rev. 75, 7 (1949).

24. S. Fernbach, R. Serber and T. B. Taylor, Phys. Rev. 75, 1352 (1949).

25. I. Perlman, A. Ghiorso and G. T. Seaborg, Phys. Rev. 77, 26 (1950).

26. N. Arley and K. R. Buch: Introduction to the Theory of Probability and Statistics, John Wiley & Sons, New York (1950).

27. G. Bernardini, E. T. Booth and S. J. Lindenbaum, Phys. Rev. 85, 826 (1952).

28. H. Fishman and A. M. Perry, Phys. Rev. 86, 167 (1952).

29. W. F. Hornyak, T. Lauritsen, P. Morrison and W. A. Fowler, Rev. Mod. Phys. 22, 291 (1950).

30. J. Heidmann and H. A. Bethe, Phys. Rev. 84, 274 (1951).

31. W. Horning and L. Baumhoff, Phys. Rev. 75, 370 (1949).

32. L. S. Germain, Phys. Rev. 82, 596 (1951).

33. E. Gardner and V. Peterson, Phys. Rev. 75, 364 (1949).

34. E. Gardner, Phys. Rev. 75, 379 (1949).

35. E. W. Titterton, Phil. Mag. 42, 109 (1951).

36. M. Blau and A. R. Oliver, Bull. Amer. Phys. Soc. 27, No. 3 (1952).

37. J. Frenkel, Phys. Zeits. Sowjetunion 9, 533 (1936). (In English).

38. V. F. Weisskopf, Phys. Rev. 52, 295 (1937).

39. V. F. Weisskopf and D. H. Ewing, Phys. Rev. 57, 472 (1940).

40. V. F. Weisskopf, Lecture Series in Nuclear Physics, (MDDC 1175) USAEC (1947) (Los Alamos Lecture Notes).

41. K. J. Le Couteur, Proc. Phys. Soc., London, A63, 259 (1950).

42. G. Parzen and L. I. Schiff, Phys. Rev. 74, 1564 (1948).

43. R. Jastrow, Phys. Rev. 81, 165 (1951).

44. N. Page, Proc. Phys. Soc., London, A63, 250 (1950).

45. D. H. Perkins, Phil. Mag. 40, 601 (1949).

46. M. A. Preston, Phys. Rev. 71, 865 (1947).

47. P. E. Hodgson, Phil. Mag. 43, 190 (1952).

48. W. L. Gardner, N. Knable and B. J. Moyer, Phys. Rev. 83, 1054 (1951).

49. L. W. Alvarez, Phys. Rev. 80, 519 (1950).

50. C. Franzinetti and R. M. Payne, Nature 161, 735 (1948).

51. F. L. Adelman and S. B. Jones, Science 111, 226 (1950).

52. E. W. Titterton, Phil. Mag. 42, 113 (1951).

53. S. C. Wright, Phys. Rev. 79, 838 (1950).

54. L. Marquez and I. Perlman, Phys. Rev. 81, 953 (1951).

55. R. E. Batzel and G. T. Seaborg, Phys. Rev. 82, 607 (1951).

56. G. Gamow and C. L. Critchfield, Theory of Atomic Nucleus and Nuclear Energy-Sources, Oxford: The Clarendon Press (1949).

57. D. Halliday, Introductory Nuclear Physics, John Wiley & Sons, New York (1950).

58. J. A. Wheeler, Phys. Rev. 52, 1083 and 1107 (1937).

59. L. R. Hafstad and E. Teller, Phys. Rev. 54, 681 (1938).

60. R. R. Haefner, Rev. Mod. Phys. 23, 228 (1951).

61. F. K. Goward, V. L. Telegdi and J. J. Wilkins, Proc. Phys. Soc., London, A63, 402 (1950).

62. J. J. Wilkins and F. K. Goward, Proc. Phys. Soc., London, A63, 1173 (1950).

63. J. J. Wilkins and F. K. Goward, Proc. Phys. Soc., London, A64, 201 (1951).

64. V. L. Telegdi and M. Verde, Helv. Phys. Acta 22, 380 (1949).

65. M. Eder and V. L. Telegdi, Helv. Phys. Acta 25, 55 (1952).

66. A. Hemmendinger, Phys. Rev. 73, 806 (1948) and revision, Phys. Rev. 75, 1267 (1949).

67. A. V. Tollestrup, W. Z. Fowler and C. C. Lauritsen, Phys. Rev. 76, 428 (1949).

68. H. A. Bethe, Rev. Mod. Phys. 9, 69 (1937).

69. C. H. Millar and A. G. W. Cameron, Phys. Rev. 81, 316 (1951).

70. J. J. Wilkins and F. K. Goward, Proc. Phys. Soc., London, A64, 849 (1951).

71. M. B. Stearns and B. D. McDaniel, Phys. Rev. 82, 450 (1951).

72. J. R. Oppenheimer, Phys. Rev. 47, 845 (1935).

73. C. F. v. Weiszacker, Zs. F. Phys. 88, 612 (1934).

74. E. J. Williams, Kgl. Danske Videnskabernes Selskab., (Math-fys. Meddelelser), 13, No. 4 (1935).

75. B. d'Espagnat, C. R. Acad. Sci. Paris, 230, 1268 (1950) and 231, 38 (1950).

76. S. M. Dancoff, Phys. Rev. 72, 1017 (1947).

77. E. J. Williams, Proc. Roy. Soc., London, A169, 531 (1939).

78. Fermi: Orear, Rosenfeld, Schluter, Nuclear Physics, University of Chicago Press (1950).

79. R. Serber, Phys. Rev. 72, 1008 (1947).

80. J. R. Oppenheimer and M. Phillips, Phys. Rev. 48, 500 (1935).

81. H. A. Bethe, Phys. Rev. 53, 39 (1938).

82. J. M. Blatt and V. F. Weisskopf, The Theory of Nuclear Reactions. (A forthcoming book, issued in part as ONR Technical Report No. 42, and as AEC Report NP-1587, Laboratory for Nuclear Science and Engineering, Massachusetts Institute of Technology, 1950).

83. J. Jungerman and S. C. Wright, Phys. Rev. 76, 1112 (1949).

84. R. H. Goeckermann and I. Perlman, Phys. Rev. 76, 628 (1949).

85. S. Frankel and N. Metropolis, Phys. Rev. 72, 914 (1947).

86. G. Farwell, E. Segrè and C. Wiegand, Phys. Rev. 71, 327 (1947).

87. L. Marshall, Phys. Rev. 75, 1339 (1949).

88. K. W. Allen and J. T. Dewan, Phys. Rev. 80, 181 (1950).

89. N. Bohr: The Penetration of Atomic Particles Through Matter. Kgl. Danske Videnskabernes Selskab., (Math-fys. Meddelelser) 18, No. 8(1948).

90. N. Bohr, Phil. Mag. (6) 25, 10 (1913).

91. E. J. Williams, Rev. Mod. Phys. 17, 217 (1945).

92. H. A. Bethe, Ann. d. Physik 5, 325 (1930).

93. M. S. Livingston and H. A. Bethe, Rev. Mod. Phys. 9, 245 (1937).

94. E. J. Williams, Proc. Roy. Soc., London, A135, 108 (1932).

95. N. F. Mott, Proc. Camb. Phil. Soc. 27, 553 (1931).

96. J. C. Slater, J. Appl. Phys. 22, 237 (1951).

97. E. L. Hubbard and K. R. MacKenzie, Phys. Rev. 85, 107 (1952).

98. J. Rotblat, Nature 165, 387 (1950).

99. J. Rotblat, Nature 167, 550 (1951).